

Chitosan as adjuvant and particle forming excipient in a nano-in-microparticulate dry powder for nasal and pulmonary vaccine delivery

Dissertation

submitted in fulfilment of the requirements for the degree of

Doctor in Natural Sciences

at

Kiel University, Germany

by

Simon-David Lennart Buske

Kiel 2014

Erster Gutachter:	Prof. Dr. Hartwig Steckel
Zweiter Gutachter:	Prof. Dr. Thomas Rades
Tag der mündlichen Prüfung:	24.03.2014
Zum Druck genehmigt:	24.03.2014

Gewidmet meinem Großvater Opa Herbie

Die eine Lehre, die wir daraus ziehen, ist die Notwendigkeit ständigen Erprobens. Keine Wunder. Kein Perfektionismus. Keine Endzeit.

Wir müssen einen skeptischen Glauben entwickeln, das Dogma meiden, gut zuhören und beobachten, versuchen, Ziele klarzustellen und zu bestimmen. Nur so können wir die richtigen Mittel wählen.

David Landes

Parts of this work have been published

R. Scherließ, S. Buske, Dry powder nanoparticulate formulations for mucosal vaccination, Nanoformulation, edited by Tiddy G, Tan RB. Singapore, RSC Publishing (2012) 104-112

R. Scherließ, S. Trows and S. Buske. Overcoming challenges of inhaled vaccines through intelligent particle engineering. Inhalation (2013) June, 8-14

R. Scherließ, M. Mönckedieck, K. Young, S. Trows, S. Buske and S. Hook. Evaluation of impact of nasal dry powder vaccine formulations on uptake and activation by dendritic cells. in Dalby, R.N. et al. (Ed.) Respiratory Drug Delivery Europe 2013 (2013) 279-283

R. Scherließ, S. Buske, K. Young, B. Weber, T. Rades and S. Hook, In vivo evaluation of chitosan as an adjuvant in subcutaneous vaccine formulations. Vaccine (2013), 31, 42, 4812-4819

Conference contributions

Buske, S. and Scherließ, R., Dry Powder Nanoparticulate Formulations for Mucosal Vaccination, ICMAT: NanoFormulation, Singapore (2011)

Buske, S. and Scherließ, R., Dispersion Behaviour of Dry Powder Nanoparticle-in-Microparticle Formulations for Nasal Vaccine Delivery, 8th World Meeting on Pharmaceutics, Biopharmaceutics and Pharmaceutical Technology, Istanbul, Turkey (2012)

Buske, S. and Scherließ, R., First steps in the development of a dry powder formulation for pulmonary vaccine delivery. Proceedings of DDL 23, Edinburgh, Scotland (2012) 353-356

Buske, S. and Scherließ, R., Nasal deposition analysis of a nano-in-microparticle vaccine formulation in children and adults using cast models. Proceedings of DDL 24, Edinburgh, Scotland (2013) 209-212

Lack of a specific mark or a reference to a trademark or a patent does not imply that this work or part of it can be used or copied without copyright permission.

Table of Contents

1	Introduction and Objectives	1
1.1	Introduction	1
1.2	Objectives	2
2	Theoretical Background	2
2.1	Achievements and Challenges of Vaccination and Immunisation	2
2.2	The Immune System.....	4
2.2.1	Mucosa Associated Lymphoid Tissue.....	5
2.2.2	Nose-Associated Lymphoid Tissue	7
2.2.3	Bronchus-Associated Lymphoid Tissue	8
2.3	Vaccine Administration Routes.....	8
2.3.1	Parenteral Route	8
2.3.2	Mucosal Route	9
2.4	Immunisation Strategies.....	11
2.5	Types of Vaccines	11
2.6	Vaccine Adjuvants	14
3	Materials	15
3.1	Antigens	15
3.1.1	Bovine Serum Albumin.....	15
3.1.2	Ovalbumin	17
3.2	Chitosan	18
3.3	Sodium Deoxycholate.....	21
3.4	Mannitol.....	22
3.5	Trehalose.....	23
3.6	Fluorescein Isothiocyanate.....	24
3.7	Devices	25
3.7.1	Nasal Powder Dispenser	25
3.7.2	Devices for Pulmonary Powder Administration.....	28
3.8	Animals	31

4	Methods.....	32
4.1	Static Light Scattering.....	32
4.2	H-Nuclear Magnetic Resonance Spectroscopy.....	33
4.3	Quantification of Water-Soluble-Protein-like-Contaminates in Chitosan.....	36
4.4	Endotoxins Level in Chitosan.....	37
4.5	Particle Size Distribution.....	37
4.5.1	Photon Correlation Spectroscopy.....	38
4.5.2	Laser Diffraction (HELOS).....	40
4.6	Scanning Electron Microscope.....	42
4.7	Bicinchoninic Acid Assay.....	42
4.8	Sodium Dodecyl Sulfate Polyacrylamide Gel Electrophoresis.....	44
4.9	Circular Dichroism.....	45
4.10	Drying.....	47
4.10.1	Spray Drying.....	47
4.10.2	Freeze Drying.....	48
4.11	Antigen Loading.....	49
4.12	Aerodynamic Characterisation.....	50
4.12.1	Uniformity of Delivered Mass.....	50
4.12.2	Intranasal Particle Deposition.....	51
4.12.3	Respirable Fraction.....	54
4.13	Cell Culture Experiments.....	56
4.13.1	Calu-3 Cells.....	56
4.13.2	Preparation of Bone Marrow-Derived Dendritic Cells.....	60
4.14	Fluorescence-Activated Cell Sorting.....	61
4.14.1	Sample Preparation for FACS analysis.....	62
4.14.2	Data Analysis of FACS Data.....	62
5	Experimental Section, Results and Discussion.....	63
5.1	Characterisation of Chitosan.....	63
5.1.1	Preparation of the Spray Dried Chitosan.....	63
5.1.2	Molecular Weight.....	63
5.1.3	Degree of Deacetylation.....	67
5.1.4	Transepithelial Electric Resistance.....	72

5.2	In Vivo Evaluation of Chitosan as an Adjuvant in Subcutaneous Vaccine Formulations	73
5.2.1	Preparation and Characterisation of Chitosan for the Adjuvant Study.....	74
5.2.2	Summarised Characteristics of the Chitosan for the Adjuvant Study	77
5.2.3	Animal Preparation and Vaccination Procedure	77
5.2.4	Results of the in vivo evaluation of the Adjuvant Effect	79
5.3	Nano-in-Microparticle Formulation Development	83
5.3.1	Ionic Gelation	84
5.3.2	Freeze Drying of the Nanosuspension	99
5.3.3	Spray Drying of the Nanosuspension	104
5.3.4	Preparations of Blends with the Dried Formulations	107
5.4	Aerodynamic Characterisation	108
5.4.1	Formulations for intranasal Delivery	108
5.4.2	Formulation for Lung Delivery	118
5.4.3	Preparation of the 1% Magnesium Stearate NiM Blend	125
5.5	Antigen Stability in the NiM Formulation	129
5.5.1	Sample Preparation	129
5.5.2	Results of the Antigen Stability	129
5.6	In Vitro and in Vivo Evaluation of Spray Dried Chitosan Nano-in-Microparticles as Vaccine Formulation	130
5.6.1	Preparation of the NiM Formulation for in Vivo Characterisation	131
5.6.2	Preparation of FITC-labelled Chitosan for in Vitro Cell Uptake.....	133
5.6.3	Protein Stability of the Formulation.....	135
5.6.4	MTT assay of the Spray Dried NiM Formulation	137
5.6.5	In Vitro Uptake into Bone Marrow-Derived Dendritic Cells	138
5.6.6	Study Design and Vaccination Scheme	139
5.6.7	Results of the in Vivo Evaluation of the Immune Response	140
6	Summary	148
7	Zusammenfassung der Arbeit	150
8	Appendix	152
8.1	List of Abbreviations	152
9	References	156

1 Introduction and Objectives

1.1 Introduction

“Few medical interventions compete with vaccines for their cumulative impact on health and well-being of entire populations”

(Schuchat, 2011).

The successes and the positive effects that vaccines had and have are outstanding and undoubtedly. The most popular one certainly is the eradication of smallpox announced by the World Health Organisation (WHO) on May, 8, 1980 in Geneva (Henderson, 2011). This shows the power that vaccines can have but, however, there are still many infectious diseases for which no vaccines are available and many people who have no access to existing vaccines. Therefore, the development of new and better vaccines is a very important issue that has to be associated with the implementation of modern vaccination campaigns (Vilella et al., 2004). Nowadays, most vaccines are given parentally and thus are formulated as solutions, suspensions or in a stabilised dried version (often lyophilisates) for reconstitution. The first two formulations are often critical with respect to stability issues because of the fragile structure of many antigens and thus need to be refrigerated during transport and storage. The third requires access to water for injection exactly at the facility where the vaccination takes place. For all three, it is necessary to have sterile materials and trained personnel locally. The development of vaccines using other routes of administration is an opportunity to avoid those problems as it is known from polio for which a vaccine that is administered orally is available and used in some “developing” countries like e.g. India and Nigeria. Other non-invasive routes are intranasal and pulmonary administration of vaccines. That would also promote a local immune response and thus lead to local protection at the place where many pathogens enter the body. Additionally, it can be assumed that with a vaccine formulated as a dry powder a high stability of the antigen and an increase in patient compliance will be achieved. When developing a vaccine that is to be delivered to mucosal surfaces it is neces-

sary to choose a “new” adjuvant which characteristics fulfil the immunological conditions of the target region better than those adjuvants that are nowadays used in vaccines (Kiyono, Fukuyama, 2004).

1.2 Objectives

The aim of this work is to identify a promising, innovative adjuvant suitable for mucosal vaccine delivery based on the current scientific literature and to characterise this adjuvant with respect to its chemical, physical and physiological properties. This adjuvant should be used to develop a nanoparticulate vaccine carrier system which, finally, should be formulated as a dry powder. This powder should also be suitable for intranasal and pulmonary delivery via nasal powder dispenser or dry powder inhaler, respectively. Subsequently, the developed formulation should be analysed with respect to its capability to stabilise and deliver the antigen after preparation, its dispersion behaviour and its deposition profile inside the nasal cavity as well as its respirable fraction. In addition, cell toxicity and cell uptake of the developed formulation is investigated. Finally, the developed formulation is tested in an *in vivo* study in mice upon intranasal administration.

2 Theoretical Background

2.1 Achievements and Challenges of Vaccination and Immunisation

The basic idea of vaccination was originally originated in Asia, more specifically in China, where children as early as AD 1000 already intranasally inhaled small amounts of a powder obtained from the skin lesions of patients who had recovered from smallpox (Gréco, 2001; Cao, 2008) to immunise them. Another method of active immunisation, called subcutaneous inoculation (also called variolation) was developed independently and applied in China, in some regions of Africa and India before the 16th century (Gross, Sepkowitz, 1998) and thus at least 200 years before Edward Jenner. For the inoculation also powder obtained from the skin

lesions was used. The powder was taken and applied to small wounds that were previously scratched into the skin of the person to be inoculated. This type of inoculation made its way from Asia passed through the Middle East to Turkey from where it was brought to Great Britain in, probably, 1721 (Dworetzky et al., 2003). Despite its successes, inoculation at that time was risky and fatal events were not uncommon (Riedel, 2005). That was surely one of the driving forces for Mr Jenner who had heard stories about dairy-maids who were protected against smallpox after having cowpox. He concluded that an infection with cowpox somehow, at that time the existence of microorganisms was not known yet, gives protection against smallpox. The crucial advantage that cowpox had was that an infection caused by cowpox was milder and the risk of dying from that disease was much lower compared to smallpox. Thus, the inoculation done with cowpox, named “vaccination” by Mr Jenner based on the Latin name for cow (*vacca*), was less risky and the fatality rate could be reduced dramatically.

In the 19th century, in particular, the works of Louis Pasteur and Robert Koch in the field of pathogens and microorganisms were responsible for major breakthroughs in the understanding of infectious diseases such as tuberculosis (Sakula, 1982) and the development of vaccines against these diseases. This development led to great success like the eradication of smallpox announced in 1980 by the WHO and the reduction in the prevalence of many other infectious diseases. But despite these successes, nowadays there are still about 3 million people dying every year from vaccine preventable diseases (Bloom et al., 2005). The development of new vaccines costs about US\$ 500 million per vaccine and often takes over a decade while the vaccine market has only a 2% share on the global pharmaceutical market (Kieny et al., 2004). That is why many pharmaceutical companies see vaccines as poor business and thus do not pay so much attention to it. Additionally, the number of people refusing vaccines increases continuously especially in the so-called “developed world” (Omer et al., 2009; Ehreth, 2003). But also in the “developing world” immunisation programs are partly under strong social, political and religious pressure (Streefland et al., 1999) e.g. in Nigeria where political and religious leaders boycotted the polio vaccination campaign in 2003 (Larson et al., 2011).

The use of new routes of administration like intranasal or pulmonary delivery has the capability to overcome some of these problems. It could ease the distribution by avoiding the need of medical trained personnel, sterile materials and working methods. This can lead to great successes as it was shown in the India campaign against polio (Bonu et al., 2003). If these new vaccines are formulated as dry powders an improved stability compared to liquid formulations can be assumed. That could help to avoid problems associated with the cold chain (Amorij et al., 2008) like freezing of vaccines (Matthias et al., 2007) or the presence of non-functioning refrigerators (Bloom et al., 2005) or no refrigerators at all. In addition, intranasal or pulmonary administration of vaccines will have also additional benefits from an immunological point of view (Alpar et al., 2005).

2.2 The Immune System

The human immune system is surely one of the most complex and impressive things that arose within the evolution. It has to be divided into two parts, the innate and the adaptive immunity. The innate immunity serves as first defence against pathogens. It is an unspecific protection against pathogens everyone is born with. The main effectors are macrophages, neutrophil granulocytes and natural killer cells (NK-cells) (Vollmar et al., 2013) and these cells are complemented by the complement system. The complement system is a complex enzymatic cascade system which consists of more than 35 soluble and cell bounded proteins (Janeway, 2002). If the elimination of the pathogen by the innate immunity failed the adaptive immunity takes over the control of the fight against the infection. Unlike the innate immunity, the adaptive immunity is antigen specific and thus it has to have a broad variety of specific surface antibodies for the recognition of the corresponding antigens and needs time to develop after the first antigen contact. The main actors are lymphocytes (especially B cells and T cells) which can activate systems to fight extracellular (e.g. many bacteria) or intracellular (e.g. viruses) pathogens. Antigens which penetrate into the body are noticed by antigen presenting cells (APCs) like dendritic cells (DCs). The DCs can take up the antigen and present it on their major histocompatibility complex I or II

(MHC-I and MHC-II). B cells have special B cell receptors (BCR) which can recognise antigens and after activation, mainly by Th2 (T helper 2) effector cells, B-cell differentiation takes place accompanied with the secretion of antibodies (humoral response). T cells also have special receptors (TCR) on their cell surface. Depending on the type of T cell these receptors can interact with MHC molecules on APCs or infected cells and as consequence they can secrete immune stimulatory agents (from CD4⁺ T helper cells), activate B cells or induce the apoptosis of the infected cells directly (CD8⁺ cytotoxic T cells) (Vollmar et al., 2013). Cytotoxic T cells are called CD8⁺ because in order to be able to bind to e.g. virus infected cells that are presenting an antigen on their MHC-I the TCR has to be accompanied by the glycoprotein CD8. After binding to the MHC-I the CD8⁺ cells induces the apoptosis of the infected cell.

T-helper cells are called CD4⁺ because in this case the TCR is accompanied by the glycoprotein CD4. These cells bind to the antigen presented on the MHC-II of APCs and then produce cytokines which propel the immune response.

2.2.1 Mucosa Associated Lymphoid Tissue

The mucosa associated lymphoid tissue (MALT) like the spleen belongs to the secondary lymphoid organs. It is a highly functional tissue that supplies antigen specific memory B and T cells to mucosal surfaces (Fujihashi, Kiyono, 2009). It is composed of follicles containing a variety of immune cells (Chadwick et al., 2010) which can be activated when needed. In addition, there are specialised epithelial cells located in the mucosal membranes which are called M-cells (microfold cells). These cells do not secrete any mucus, have short microvilli and they are able to take up particulate antigens via endo- or phagocytosis very effectively. M-cells are able to take up particles up to 10 μm in diameter (Tabata et al., 1996). But the uptake of particles in a nanometre scale up to 500 nm is preferred (Slütter et al., 2008) whereby smaller particles are taken up faster and to a higher extent (Kreuter, 1991). The captured material is transported through the cell in vesicles. On the basolateral side the cell is formed like a pocket where a high density of lymphocytes and APCs can be found (Janeway, 2002; Sharma et al., 2009). When the antigen is taken up by APCs, these cells then migrate to the local draining

lymph nodes where the antigen is processed and presented (Trows, 2012). T cells and plasma cells are generated. A peculiarity, which is a great advantage of the MALT, is that as a consequence of the immune response a special subtype of immunoglobulin A (IgA) which is called secretory IgA (sIgA) is produced. Subsequently, sIgA is secreted directly into the mucus (Figure 2.1) where it has the ability to entrap and neutralise pathogens before they are able to penetrate through the mucosal membranes. Secretory IgA is a dimeric form of IgA whereby both monomers are linked together by a polypeptide (J chain) (Miletic et al., 1996). Because of this structure these antibodies are resistant to degradation in the protease rich environment of the mucus (Neutra, Kozlowski, 2006).

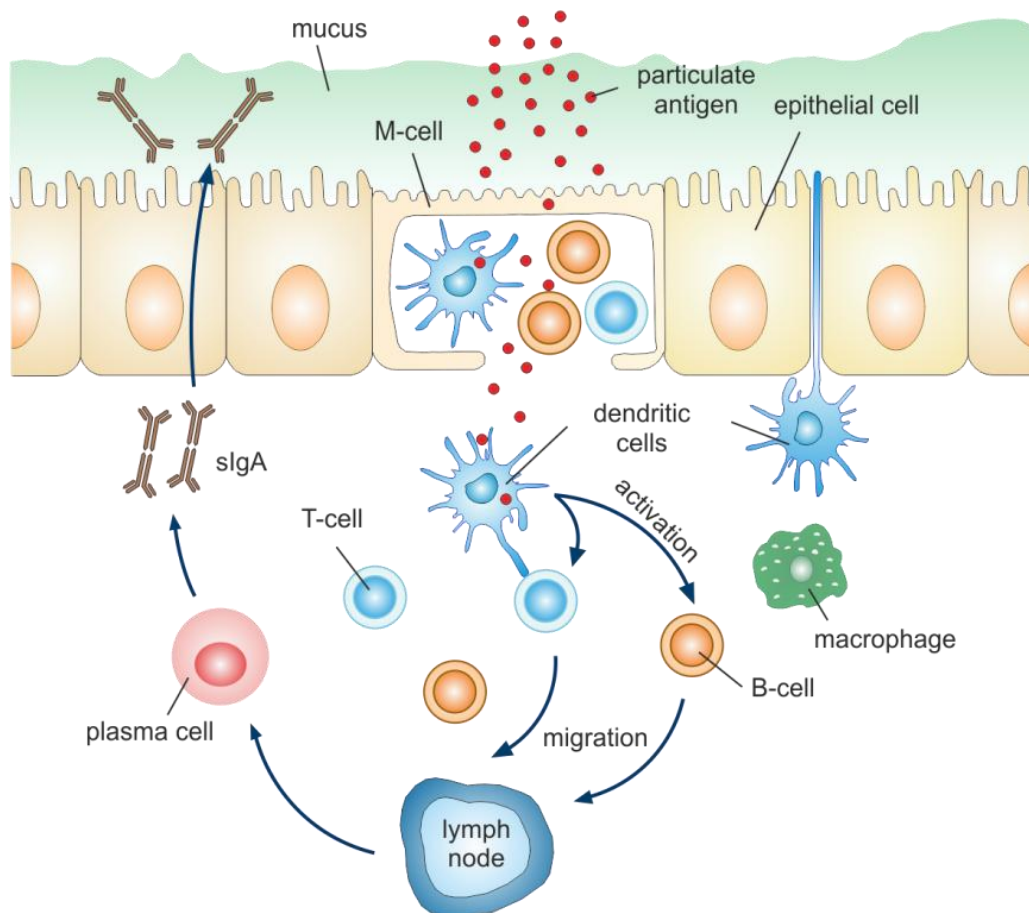


Figure 2.1 The activation and development of local immune response in the MALT by particulate antigens. Adapted from Neutra et al. (2006).

This means that antigen uptake via the mucous membranes leads to a strong systemic and in addition to that also to a local immune response which, in sum

gives a better protection (Amidi et al., 2010). It has to be mentioned that the production and secretion of sIgA not only occurs in the region where the antigen contact has taken place but on all mucosal surfaces (but to a different extent). This interaction between different mucosal surfaces that are not located nearby each other is termed the “common mucosal immune system” (Davis, 2001). This process can be used to develop intranasal or pulmonary vaccines which then give better protection because of the additional local immune response.

2.2.2 Nose-Associated Lymphoid Tissue

The nose-associated lymphoid tissue (NALT) is a subsidiary part of the MALT. It is located at the rear area of the nasal cavity and has an important role to play in the defence of mucosal surfaces but can also be used as target for effective vaccine delivery (Baudner et al., 2003). The lymphoid tissue of the nose is mainly formed by the tonsils nearby the nasopharynx and was first described in 1884 by Waldeyer and thus is called “Waldeyer ring” (Cocquyt et al., 2005). The “Waldeyer ring” is composed of the adenoid (also called nasopharyngeal tonsil), a pair of tubal tonsils and palatine tonsils and the lingual tonsil (Illum et al., 2001) as shown in Figure 2.2. An effective vaccination via the NALT will lead to both a strong systemic and a local immune protection as described afore (2.2.1).

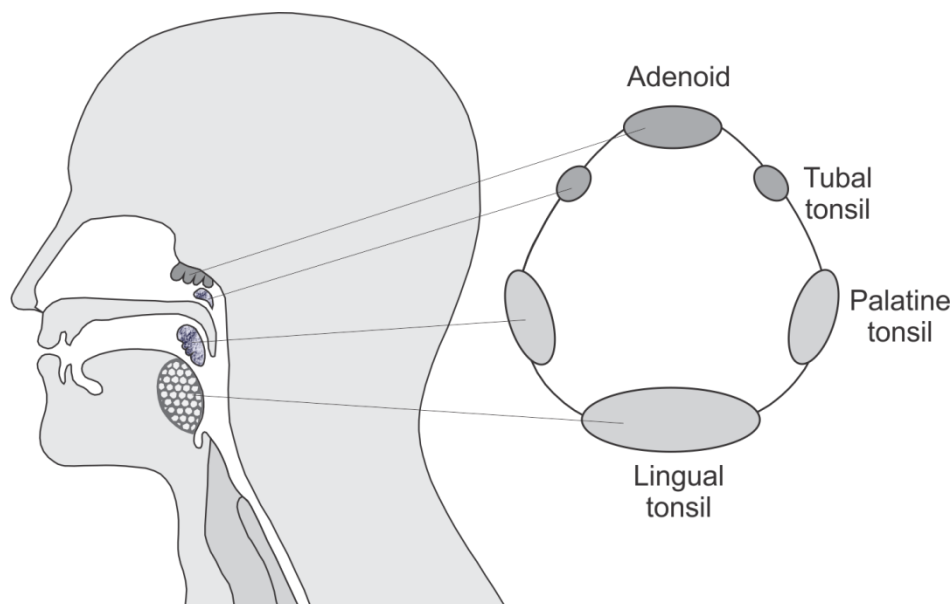


Figure 2.2 Lymphoid tissue of the "Waldeyer ring". Adapted from Perry and Whyte (1998).

2.2.3 Bronchus-Associated Lymphoid Tissue

Like the NALT, the bronchus-associated lymphoid tissue (BALT) is also a part of the MALT. The BALT which is located in the respiratory tract was first described as conglomerate of follicular aggregates in rabbits mainly found at branching sites of the bronchial tree in the bronchial wall (Bivas-Benita et al., 2005). It is a structure of organised lymphoid follicles. Nevertheless, it has to be mentioned that the BALT in humans is not a constitutive structure within the respiratory tract and that its structure and the size of the follicles are very age dependent and can differ greatly from person to person (Bivas-Benita et al., 2005). Like in the NALT M-cells with underlying APCs are present in the BALT and thus a vaccination with a particulate antigen formulation via the pulmonary route will also lead to a systemic as well as to a local immune protection after vaccination. Additionally, there is a highly developed network of DCs in the upper and lower respiratory tract which can also act as first line defence and activate the immune response (Holt et al., 1990).

2.3 Vaccine Administration Routes

There are different possible routes to deliver vaccines into patients. All of these routes have some advantages and some drawbacks compared to each other. Four of these routes are discussed in this section regarding their properties, the drawbacks they have and the advantages they offer.

2.3.1 Parenteral Route

Nowadays, most vaccines are still delivered parenterally through the skin via syringe and needle because this is the most effective way to bring an antigen into the human body. Additionally, the antigens used in vaccines often have low bioavailability and limited immunogenicity when they are administered by other non-parenteral routes (Amidi et al., 2010). On the other hand, the main drawbacks are that parenteral vaccine administration involves well-trained medical personnel and sterile utensils. Most of these vaccine products are formulated as

solutions or suspensions, which often causes problems regarding their stability and thus these vaccines have to be stored refrigerated during transport and storages. An inactivated influenza vaccine for example has to be kept in a very narrow temperature range from 2°C to 8°C the whole time (Amorij et al., 2008). Some of these problems can be solved by lyophilisation (Chung et al., 2012) and the production of vaccines which are reconstituted with water for injection just shortly before administration. But trained medical personnel and sterile materials cannot be avoided by such measures. The injection causes pain and is always associated with a residual risk of an infection. In addition, many people are afraid of syringe and needle and thus refuse vaccination (Szmuk et al., 2005).

2.3.2 Mucosal Route

The effective induction of a local immune protection as aforementioned (2.2.1) is the main reason for using the mucosal route of administration for vaccination (Borges et al., 2006). There are different approaches of which three will be discussed in the following subsections.

2.3.2.1 Nasal Route

For many pathogens the mucosal membranes of the nasal cavity are the site where they penetrate the human body. Therefore, the intranasal administration of vaccines against such pathogens is of great interest. The nasal delivery of drugs is very well accepted almost everywhere in the world by adults, children and even toddlers (Amorij et al., 2012). It is an easy way of administration that is coupled with a reduction of side effects and will also decrease the risk of spreading infections caused by contaminated materials (Baudner et al., 2003). In addition, the need of trained medical personnel and sterile materials would be also reduced (Chadwick et al., 2010). With respect to the mucosal administration of vaccines and the thereby generated antigen specific immune response it can be assumed that the intranasal administration offers some advantages compared to other delivery routes like the pulmonary one (Alpar et al., 2005). For example, it has been shown that nasal immunisation is more effective, requires lower doses

of antigen and less adjuvant compared to the oral immunisation (Fujihashi et al., 2002). But there are also some drawbacks. The most important one certainly is that the absorptive surface present within the nasal cavity is relatively small with only about 150 cm² (Amidi et al., 2010) compared to the 160 m² in the lungs (Deli, 2009) and the 200 m² of the intestine (Deli, 2009).

2.3.2.2 Pulmonary Route

Most of the drugs that are delivered to the lungs today are for the local treatment of lung diseases like chronic obstructive pulmonary disease (COPD) or asthma whereat a systemic API effect should be avoided. But also for vaccines the lung is a promising target and in different clinical studies in humans it was found out that the pulmonary vaccination was as effective as the parenteral route (Saluja et al., 2010). As already mentioned, one main advantage that the lung as delivery target would have is the large mucosal surface area of about 160 m² (Deli, 2009) and the very rapid transfer of the antigen into the blood stream for an immediate biological effect (Alpar et al., 2005). But there are also drawbacks, because an efficient deposition of vaccine into the lungs requires a formulation with particles with an aerodynamic diameter of less than 5 µm (Amidi et al., 2010). Milling is commonly used to obtain such small API (active pharmaceutical ingredient) particles as used in the treatment of COPD and asthma but these APIs are relatively stable and can overcome the stress that is caused by the milling process. Antigens are often proteins or other highly complex structures which are often not stable enough against heat and other stress factors which occur during the grinding process. Therefore, other methods like spray drying as it was used in this work have to be used to generate particles in the proper size range needed for an effective lung delivery.

2.3.2.3 Oral Route

The major advantage is that oral administration is probably the best accepted route by patients and that the intestine with about a total surface area of about 200 m² is a very large and effective absorption organ (Deli, 2009). The successes

achieved by the WHO vaccination campaign against polio (Ehreth, 2003) showed the acceptance of this route of administration. Probably the greatest drawback and thus the greatest challenge is the very aggressive environment in the stomach with a pH value of about 1 (Thews et al., 1999) and lots of enzymes. As said, many of the antigens used in vaccines are very sensitive and get easily harmed by such conditions. That is why, with a few exceptions like polio and typhus, there are no orally administered vaccines on the market.

2.4 Immunisation Strategies

Immunisation strategies can be roughly divided into three major strategies. Firstly, active immunisation, here a vaccine is applied which induces a strong immune response in consequence of which specific antibodies, specific T cells and memory B cells are generated. This leads to a long-term (in some cases a lifetime) immunisation of the person vaccinated. A second strategy, called passive immunisation, does not lead to a long-term immunisation because here specific antibodies are given to the patient in order to achieve a short-term protection against a specific invader. The applied antibodies are degraded in the human body within some weeks (Vollmar et al., 2013).

Therapeutic vaccination is a slightly different approach, because it is not a preventive vaccination. In therapeutic vaccination a disease that is already manifested is treated. The vaccines are produced out of the pathogens that are responsible for the disease or in cancer treatment from tumour cells of the patient in order to trigger the immune system to fight against these pathogenic structures. But until now, this kind of vaccination is still under investigation and it is not yet used in standard treatment of any disease (Vollmar et al., 2013).

2.5 Types of Vaccines

The vaccines that are currently available on the market can be divided into three different groups. The first are live attenuated vaccines which are obtained by repeated splitting of the pathogen in order to achieve a less virulent (attenuated)

pathogen strain. Subsequently, the most suitable strain will be cultivated in eggs or cell cultures and then will be used in the vaccine. Live attenuated vaccines are best and most reliable in inducing an appropriate immune response. The immunological protection caused by these types of vaccines often is life-long. But there are also risks because the pathogens are replication-competent and it cannot fully ruled out that the pathogen is becoming virulent again inside the host (Vollmar et al., 2013) and then will cause a serious infection. For example, a pregnancy is a contraindication to receive the live attenuated influenza vaccine but not to receive the inactivated one which is indeed recommended in such cases by the Centers of Disease Control and Prevention (CDC) (CDC, 2013).

Vaccines containing complete inactivated organisms and split preparations are produced from virulent strains of the virus or bacteria which are treated with heat or chemical agents (e.g. formaldehyde) or a combination of both. The pathogens in these types of vaccines are not replication-competent and thus those vaccines are less risky compared to live attenuated vaccines but they are also less effective in inducing an immune response (Vollmar et al., 2013).

Subunit vaccines contain specific surface antigens from virus or bacteria such as proteins or polysaccharides or in some cases subunits of the toxins produced by the bacteria (Table 2.1). These structures have the potential to trigger a sufficiently strong immune response that lead to an immunological protection. In general, these vaccines have fewer side effects compared to the two other types however, they are often also less effective (Vollmar et al., 2013). Therefore, these vaccines are usually given combined with adjuvants.

Some examples for the different types of vaccines are given in Table 2.1.

Table 2.1 Subdivision of the different classes of vaccines. Reproduced from Vollmar et al. (2013).

Category	Example	Characteristic
Live attenuated vaccines		
Viral	Rotavirus	Attenuated virus
	Influenza virus	Attenuated virus
Bacterial	Bacillus Calmette-Guérin (BCG)	Attenuated <i>mycobacterium bovis</i>
Inactivated organisms		
Viral	TBEV-virus	Formaldehyde inactivated
	Rabies virus	β -propiolactone inactivated
Bacterial	<i>Vibrio cholera</i>	Formaldehyde inactivated
Subunit vaccines		
Viral	Influenza virus	Influenza surface antigen
	HPV	L1-surfaceprotein
Bacterial	<i>Salmonella typhi</i>	Vi-polysaccharide strain Ty2
	<i>Vibrio cholera</i>	Recombinant toxin B subunit
Toxoids	<i>Corynebacterium diphtheria</i>	Formaldehyde treated toxin
	<i>Clostridium tetani</i>	Formaldehyde treated toxin

2.6 Vaccine Adjuvants

“Adjuvants are agents incorporated into vaccine formulations to enhance and increase the immune responses generated by the vaccine antigen”

(United States Pharmacopeial Convention)

Nowadays, a variety of vaccines are given in combination with an adjuvant. Alum was the first adjuvant and it is still widely used today. It was first described by Glenney et al. (Glenney et al., 1926) who precipitated diphtheria toxoids by adding potassium alum to it (Lindblad, 2004). This led to a significantly increased immune response. Nowadays, the antigen is most often adsorbed onto a pre-formulated alum gel (Lindblad, 2004). Despite the millions of doses of alum containing vaccines given every year to millions of people the fundamental mechanism is not yet completely understood (Tomljenovic, Shaw, 2011). It is assumed that the formation of a depot at the site of injection increases the dwell time of the vaccine and thus leads to an increased production of antibodies. Additionally, the induction of inflammation associated with the recruiting and activating of APCs is discussed (Lambrecht et al., 2009).

Another class are the immunostimulatory adjuvants like Monophosphoryl lipid A (MPL) which is derived from the lipopolysaccharide of Gram-negative bacteria mostly from *Salmonella Minnesota* (Singh, O'Hagan, 1999). Another immunostimulatory adjuvant is QS-21 which is gained from a highly purified fraction of Quil A. The main mechanism of action of both adjuvants is the induction of the release of Th1 cytokines, especially IL-2 and IFN- γ (Singh, O'Hagan, 2002).

In addition, there are submicron emulsions used as adjuvants like the squalene containing oil-in-water emulsion MF59 (Dupuis et al., 2001). MF59 is used in the Novartis influenza vaccine FLUAD and has shown to induce greater immunogenicity compared to the non-adjuvanted vaccine (Ansaldi et al., 2008). MF59 increases the antigen uptake into APCs (Wilson-Welder et al., 2009), promotes the Th1 mediated immune response and the release of a variety of cytokines (Dupuis et al., 1998).

But it has to be mentioned that all of these adjuvants which are very useful if the vaccines are administered parenterally, are not very promising with respect to mucosal vaccine delivery (Kiyono, Fukuyama, 2004; Lawson et al., 2011).

Therefore, an adjuvant which is better suited for mucosal vaccine delivery was selected in this work and thus the biopolymer chitosan was chosen because of its promising properties which are discussed in detail in section 3.2.

3 Materials

3.1 Antigens

An antigen is the most essential part of almost every vaccine by definition according to the USP 36 (United States Pharmacopeial Convention). It is the component recognised and processed by specialised cells of the immune system and therefore the main driver in the induction of an immune response. Because this work was aiming on a “proof of concept” manner and due to safety issues as well as for reasons of costs, no market-relevant model antigens were used in the formulation development.

3.1.1 Bovine Serum Albumin

Serum albumin is a globular protein. It is the most abundant protein in the circulatory system of animals and humans (Yang et al., 2008). With its high blood concentration of around 5 g per 100 mL serum, albumin is mainly responsible for maintaining the oncotic pressure and is the main modulator of fluid distribution between the body compartments (Fanali et al., 2012). It is also responsible for the transport of a wide range of endogenous and exogenous compounds such as amino acids or drugs (Carter et al., 1989). Bovine serum albumin (BSA; Figure 3.1) and human serum albumin (HSA) are very similar. Bovine serum albumin consists of 583 amino acids and has an isoelectric point (IEP) of 4.7 (Peng et al., 2004); human serum albumin is composed of 585 amino acids (Carter et al., 1989) and has its isoelectric point at pH 5.3 (Langer et al., 2003). They have an amino acid sequence homology of 76% (Huang et al., 2004c) and almost the same mo-

molecular weight of about 66,500 Da (Hirayama et al., 1990). Serum albumin consists of three domains, each composed of two subdomains containing three loops that are held together by disulphide bridges (Rothschild et al., 1988).

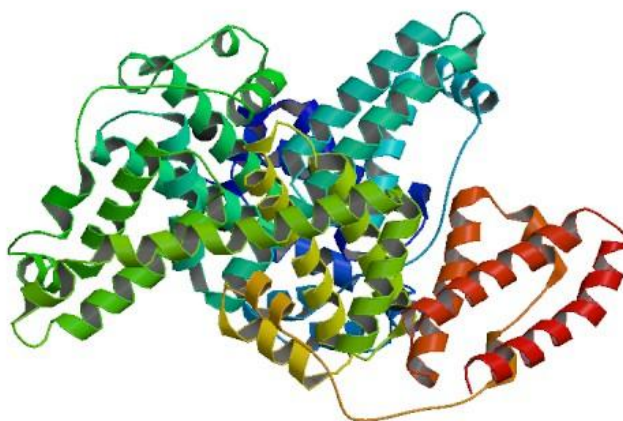


Figure 3.1 Structure of bovine serum albumin (from RCSB-data bank).

About 67% of BSA is organised in helical structures, 10% as turns and the remaining 23 % as extended chains. A reversible denaturation occurs when albumin is heated to temperatures between 42°C and 50° C which is caused by a structural change from α -helix to an intermolecular β -structure. At temperatures above 60°C the unfolding of α -helices becomes irreversible (Murayama, Tomida, 2004). Lyophilised Bovine serum albumin (albumin fraction V, protein content > 97%) used as model antigen in this work was obtained from Merck KGaA (Darmstadt, Germany).

3.1.2 Ovalbumin

Ovalbumin (OVA; Figure 3.2) is the most abundant protein in egg white, where it accounts for 60% to 65% of total protein content (Huntington, Stein, 2001).

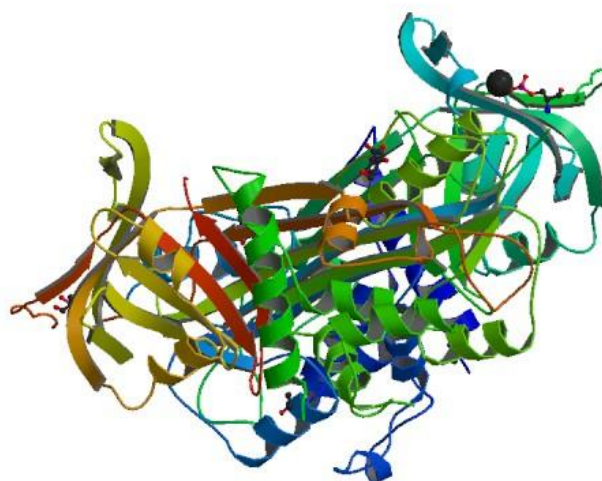


Figure 3.2 Structure of albumin from chicken egg (from RCSB-data bank).

Although belonging to the serpin family, ovalbumin does not show any protease inhibitory activity. It has been the subject of research for decades, but even today the physiological function of OVA is not completely resolved. It is presumed to be a storage protein (Gettins, 2002). Ovalbumin comprises 385 amino acids and this polypeptide chain has a molecular weight of 42,699 Da (Nisbet et al., 1981). These results are consistent with the reported m-RNA sequence (McReynolds et al., 1978). The ovalbumin monomeric phosphoglycoprotein has a molecular weight of 44,500 and an isoelectric point of 4.5 (Mine, 1995). Beside the native ovalbumin, there is a second formation called S-ovalbumin, which is more stable against higher temperatures and pH-values. Ovalbumin is transferred into S-ovalbumin at higher temperatures and pH-values (in vitro) or over storage of eggs (in vivo) (Smith, Back, 1965). The denaturation temperature of ovalbumin and S-ovalbumin at pH 8.8 is 84.5°C and 92.5°C (Donovan, Mapes, 1976), respectively. OVA is a well investigated and widely used model antigen in immunologi-

cal studies with C57BL/6 mice (Hänninen et al., 2001) but also with other mice like BALB/c (Larsen et al., 2001) or guinea pigs (Mauser et al., 1993). Ovalbumin from chicken egg white (A 7641) lyophilised powder grade VII from Sigma Aldrich (St. Louis, MO, USA) was used in this work.

3.2 Chitosan

Chitosan is a linear amino polysaccharide consisting of β -(1-4)-linked glucosamine and N-acetyl-glucosamine (Figure 3.3), it was discovered by the Frenchman Charles Rouget in 1859 (Le Roux, 2012) by boiling chitin in potassium hydroxide. The name chitosan was given to it by Hoppe-Seyler in 1894 (Baldrick, 2010).

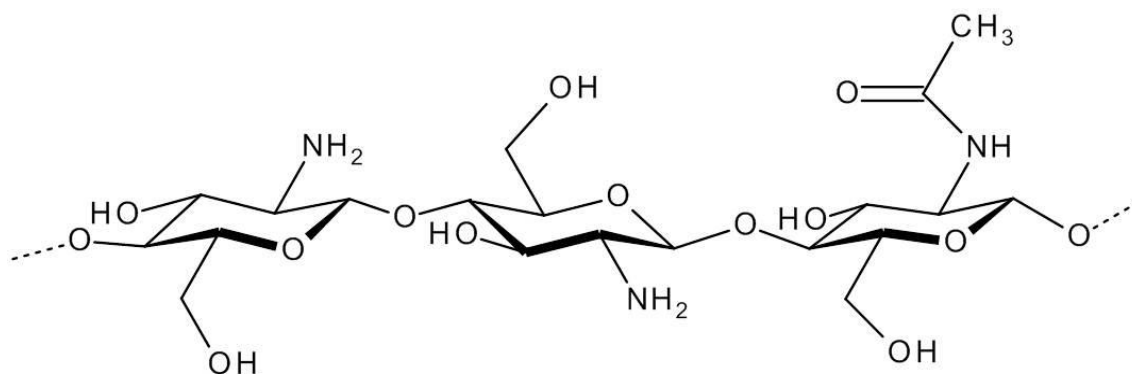


Figure 3.3 Structure of chitosan

After cellulose chitin is the most important and most abundant polysaccharide (Brugnerotto et al., 2001; Kumar, Majeti, 2000) in the world. Nowadays, chitosan is mainly obtained from chitin by partial deacetylation using sodium hydroxide. Although chitin occurs in nature in cell walls of fungi such as *aspergillus* and *mucor* (Qin et al., 2006), yeast and many other creatures like insects, to date the largest share of commercially used chitin is still gained from the shells of crustaceans (Rinaudo, 2006). Chitosan is biocompatible (Cadete et al., 2012), non-toxic, biodegradable (Huang et al., 2004b) and can be produced according to GMP guidelines (Zaharoff et al., 2007). Unlike chitin, chitosan is soluble in dilute organic acids like acetic acid and to a lower degree, in mineral acids such as hydrochloric acid due to its primary amino groups. The solubility of chitosan is strongly

dependent on the amount of free amino groups and thus on the degree of deacetylation (DDA) but also on the method of deacetylation that has been used in production (Pillai et al., 2009). The DDA is the proportion of glucosamine in a polymer chain but usually it is measured as a bulk average (Nguyen et al., 2009a). The viscosity of a chitosan solution is influenced by a variety of additional factors namely the molecular weight, pH value and ionic strength of the solvent, temperature and, of course, polymer concentration (Li et al., 1992). Chitosan is already widely used in cosmetics and food industry, for example as a chelating agent to clarify water (Illum, 1998) or beverages (Baldrick, 2010) and has been the subject of pharmaceutical research for more than three decades. It has been investigated as excipient in tablets in order to achieve a constant release profile, as xero gels for sustained release of poorly soluble drugs and in wound healing products (Illum, 1998). Chitosan is a promising excipient for mucosal vaccine formulations (van der Lubben et al., 2001; Illum et al., 2001; Prego et al., 2005) because of its mucoadhesive properties which are mainly caused by interactions between negatively charged sialic acid groups on the mucosal membranes with the positively charged amino groups of the chitosan (Bravo-Osuna et al., 2007; Vllasaliu et al., 2010). This leads to a decreased mucociliary clearance rate (Kang et al., 2009) and consequently to an increased dwell time of the applied formulation.

In addition, chitosan has the ability to interact and open tight junctions (Amidi et al., 2010; Vllasaliu et al., 2010; Aspden et al., 1997) which are located between the mucosal epithelia cells. This reversible effect leads to disruption of tight junctions and is caused by lysosomal degradation of the tight junction tetraspan protein claudin-4 (CLDN 4) but after chitosan is removed the tight junctions are rebuilt (Yeh et al., 2011) as shown in Figure 3.4.

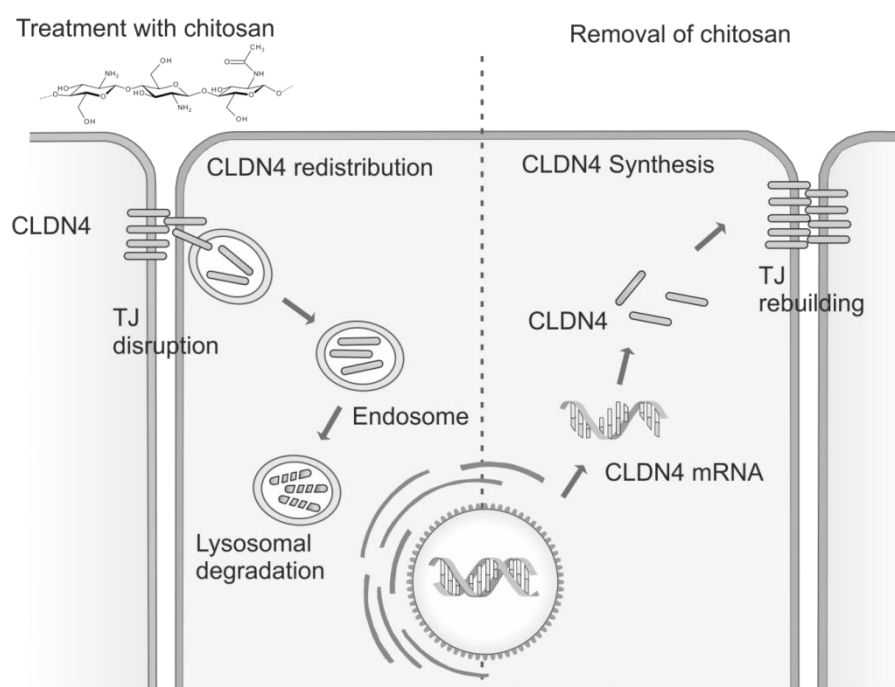


Figure 3.4 Mechanism of tight junction (TJ) opening by interaction of chitosan with CLDN4 and their reconstruction after chitosan removal. Adapted from H.-T. Yeh et al (2011).

Chitosan has already shown to increase specific humoral immunity after intramuscular co-administration with an inactivated Newcastle disease vaccine in chicken (Rauw et al., 2010) and a significantly increased immunogenicity after mucosal administration combined with modified diphtheria toxin compared to a chitosan free formulation (McNeela et al., 2000). In addition, studies have shown that chitosan microparticles loaded with antigen enhance both systemic and local immune responses after oral and nasal administration (Amidi et al., 2006). Chitosan is included in the National Formulary since edition USP35/NF30 and its hydrochloric salt is monographed in the Ph. Eur. since 2002 (Aranaz et al., 2009). In this work, five different chitosans with different properties have been charac-

terised and used for the formulation development while three of them were also tested *in vivo* with respect to their immunological properties. In this work, Chitopharm S, M, L (all Chitinor AS, Norway), ChitoClear FG 95 (Primex, Iceland) and a chitosan from Sigma Aldrich (St. Louis, MO, USA) were used.

3.3 Sodium Deoxycholate

Sodium deoxycholate (DCA; Figure 3.5) is the salt of the secondary bile acid deoxycholic acid. In the human body primary bile acids (cholic acid and chenodeoxycholic acid) are being secreted by the liver and then partially metabolised into secondary bile acids by bacteria. In concentrations up to 1% sodium deoxycholate showed no toxic effects (Cadete et al., 2012) and like other bile salts, sodium deoxycholate, as a surfactant is known to enhance nasal drug absorption.

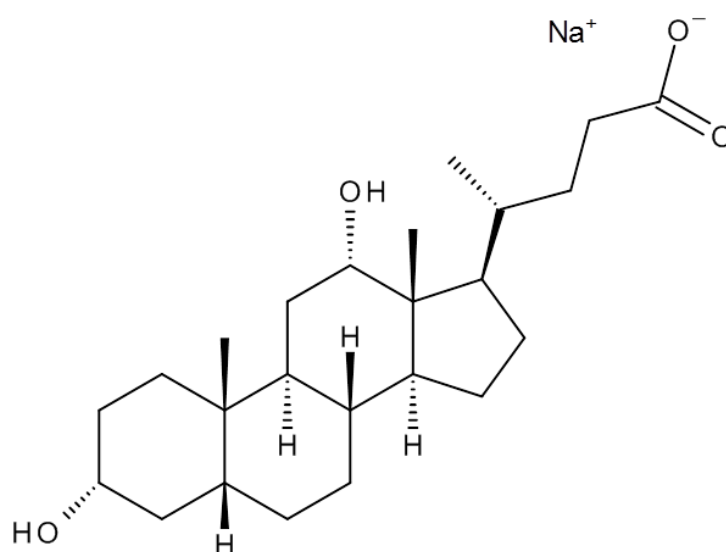


Figure 3.5 Structure of sodium deoxycholate ($C_{24}H_{39}NaO_4$, M_w : 414.64 $g \cdot mol^{-1}$)

DCA can not only increase the nasal absorption of proteins such as insulin (Gordon et al., 1985; Wheatley et al., 1988) but also inhibit the activity of proteolytic enzymes present in the mucus (Shinichiro et al., 1981). Due to its negative charge DCA is highly water soluble ($330 g \cdot L^{-1}$). These properties make DCA a very attractive and promising counter anion for nanoparticulate antigen carrier systems that are intended to be delivered onto mucosal surfaces. The DCA used

in this work was purchased from Carl Roth GmbH & Co KG (Karlsruhe, Germany).

3.4 Mannitol

Mannitol (Figure 3.6) is a non-reducing sugar alcohol or polyol consisting of a six-carbon chain. It frequently occurs in nature, for example in bacteria, fungi, plants and algae (Wisselink et al., 2002).

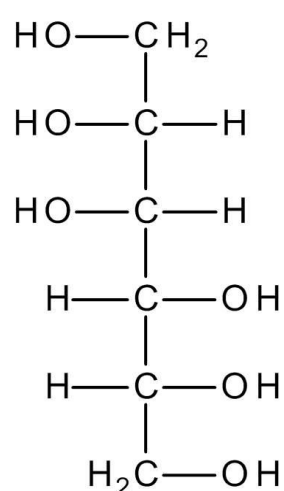


Figure 3.6 Structure of (D)-mannitol ($\text{C}_6\text{H}_{14}\text{O}_6$; M_w : $182.17 \text{ g}\cdot\text{mol}^{-1}$)

The manna ash tree *Fraxinus ornus* was the name giver of mannitol and had been the main source of mannitol until the nineteen-twenties (Soetaert, 1990). Today most of the mannitol is produced from fructose by catalytic hydrogenation using hydrogen gas, a nickel catalyst combined with high pressure and high temperature (Makkee et al., 1985) or by fermentation using microorganisms. Mannitol is an important substance for the food industry, among others because it is about half as sweet as sucrose (Debord et al., 1987), it does not induce hyperglycaemia (Helanto et al., 2005; Griffin, Lynch M. J., 1972) and is non-cariogenic. Pharmaceutically, mannitol is used as an osmotic laxative, as excipient in the preparation of tables and as filler for capsules. In this work, a spray dried mannitol grade (Pearlitol SD 200; Roquette, Lestream, France) was used as matrix excipient in spray and freeze drying and as carrier for the binary powder blends.

3.5 Trehalose

Trehalose (Figure 3.7) is a non-reducing, naturally occurring disaccharide consisting of two α , α' -1,1-glycosidic bonded glucose molecules (Birch, 1963). It can be found in a wide range of plants, fungi, insects (Behm, 1997) and some invertebrates (Fairbairn, 1958). In 1858 Berthelot extracted trehalose from a secretion insects use to build shells, called trehala manna and named it trehalose. In the same year trehalose was also isolated by Mitscherlich from mushrooms, who named the new substance mycose (Richards et al., 2002). Berthelots work contained more information (e.g. the molecular formula) about the new substance, thus the name trehalose prevailed. Trehalose has a unique high optical rotation of $[\alpha]_D^{25} + 178^\circ$ for the di- and $[\alpha]_D^{25} + 197.1^\circ$ for the anhydrate (Stanek, 1957), respectively. Trehalose is a well-known and widely used excipient in freeze drying (Kadoya et al., 2010) because of its properties as a lyoprotectant (Amorij et al., 2008). In research it has already been used to stabilise freeze-dried subunit influenza vaccine (Amorij et al., 2007) for reconstitution and a whole inactivated virus (WIV) vaccine formulated as a powder for nasal delivery (Huang et al., 2004a). Trehalose used in this work was obtained from British sugar PLC in Peterborough, UK.

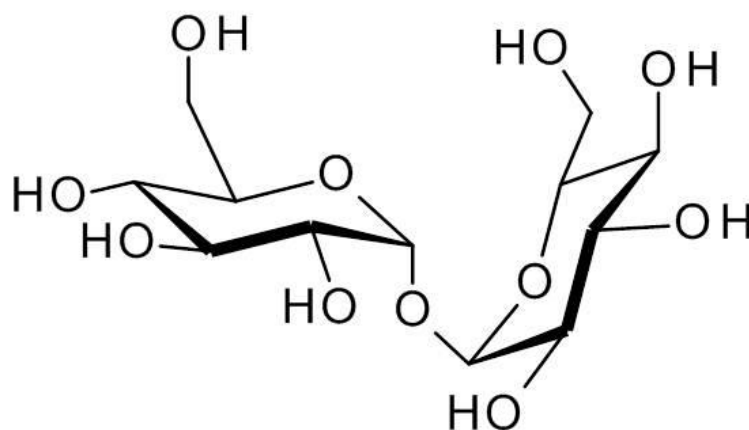


Figure 3.7 Structure of trehalose ($C_{12}H_{22}O_{11}$; M_w : $342.30 \text{ g}\cdot\text{mol}^{-1}$)

3.6 Fluorescein Isothiocyanate

Fluorescein isothiocyanate (FITC; Figure 3.8) is very suitable for the purpose of labelling chitosan because it shows a strong fluorescence and can be covalently connected with chitosan via the free amino group by a simple reaction in which the fluorescein thiocarbamoyl derivative accrues (Twining, 1984).

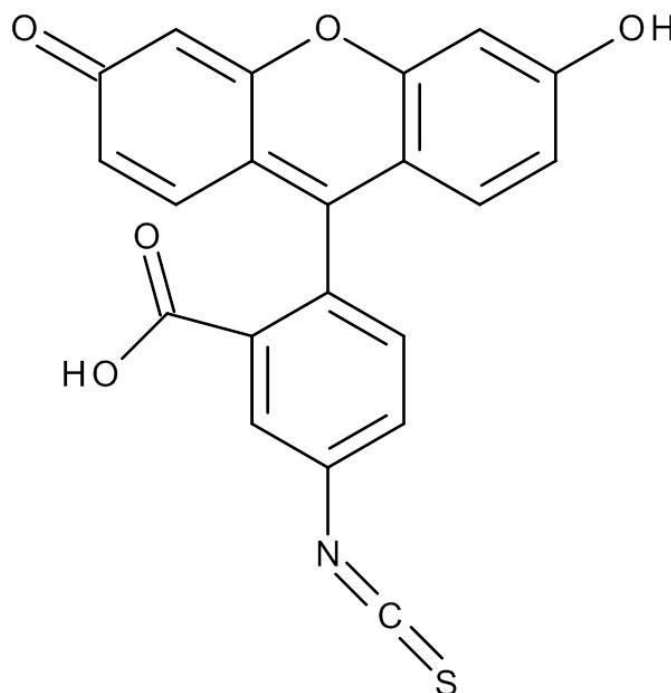


Figure 3.8 Structure of fluorescein isothiocyanate (FITC; $C_{21}H_{11}NO_5S$; M_w : $393.38 \text{ g}^*\text{mol}^{-1}$).

It is already extensively used in research for labelling proteins such as insulin (Martin et al., 2005), ovalbumin (Borges et al., 2006) or serum albumin (Amidi et al., 2006). FITC has an excitation maximum of 495 nm and an emission maximum of 519 nm. Also the labelling of chitosan with FITC is already described in literature (Vllasaliu et al., 2010; Huang et al., 2002). In this work, fluorescein isothiocyanate isomer I (F7250) from Sigma-Aldrich (St. Louis, MO, USA) was used for the purpose of labelling chitosan.

3.7 Devices

Depending on the therapeutic target, vaccine delivery into the nasal cavity could be favourable compared to lung drug delivery and vice versa. To test both approaches two nasal powder disperser and two dry powder inhalers (DPIs) were tested and analysed regarding their capability to deliver the developed formulation in a satisfactory way into the respective regions of interest.

3.7.1 Nasal Powder Dispenser

For a sophisticated vaccine product the combination of the powder formulation and the application device is a crucial issue. There are few different devices for intranasal drug powder delivery available and they can be roughly divided into three groups: multidose reservoir devices like the PowderJet, capsule based devices (e.g. Miat Nasal Insufflator) and single-dose devices for single use such as the Powder UDS. In this work, the PowderJet and the Powder UDS were used, tested and analysed for dispersion of the self-developed dry powder vaccine formulations.

3.7.1.1 PowderJet®

The PowderJet (Figure 3.9) is a multidose reservoir device for intranasal powder delivery. When the device is used, the air in the lower compartment (1) is compressed, at the same time the dip tube (2) in the reservoir chamber (3) is lowered and thereby a single dose of powder is metered. Shortly after the dip tube has reached the bottom of the reservoir chamber the pressure in the lower compartment is so high that the compressed air passes through a porous membrane (4) which connects both compartments directly above the dip tube. The compressed air expands through the membrane, entrains the metered powder dose, releases and disperses it at the end of the dip tube. The PowderJet is a generous item on loan from RPC Formatec (Mellrichstadt, Germany).

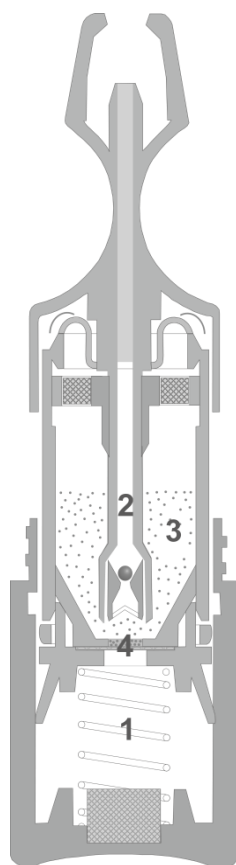


Figure 3.9 Schematic figure of the PowderJet with inner construction.

3.7.1.2 Powder UDS[®]

The Powder UDS is a single dose device which is designed for disposable use. A single powder dose is placed in the main container (1) which is sealed with a plastic ball (2) at the top. A plastic thorn (3) is placed into the container from the other side and then fixed with an assembling tool. Then this construction is fixed in the tube of the outer container as shown in Figure 3.10. When the device is used by the patient, it is pushed together, thereby the air in the entire system is compressed (4), the bar (5) pushes up the thorn, when the thorn reaches the ball at the top of the container, the ball is pushed upwards. At this moment the system is open, the compressed air expands through the main container and the powder is entrained. All devices were filled with about 25 mg of powder, manually using a highly accurate balance (Sartorius, WMC6014-d) and assembled using the specific assembling tool. All devices were stored at 23% relative humidity and room temperature prior to testing. The devices were a gift from Aptar Pharma (Louvenciennes, France).

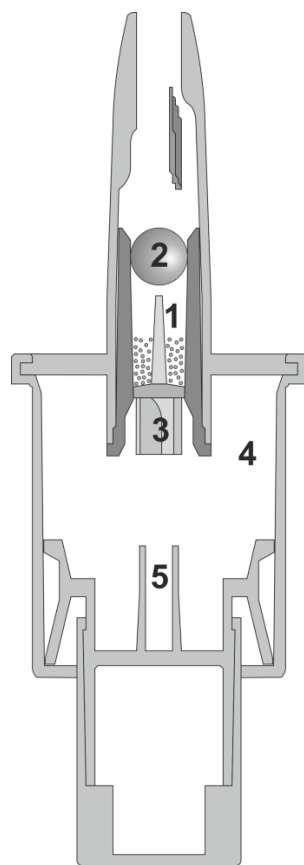


Figure 3.10 Schematic figure of the Powder UDS with inner construction.

3.7.2 Devices for Pulmonary Powder Administration

Dry powder inhalers (DPIs) which came up in the 1970s are powerful tools to deliver pulverised drugs into the lungs. Compared to pressurised metered dose inhalers (pMDIs) and nebulisers they are the preferred devices in the treatment of local pulmonary diseases like asthma and COPD. Because they are activated by the inhalation of the patient they overcome the need of coordination of inhalation and actuation (Islam, Gladki, 2008) like it is the case using pMDIs. Unlike nebulisers, DPIs are portable and the use of medication is not nearly that time-consuming as it is for nebulisers (Geller, 2005). Over the last 15 years the pulmonary administration in the treatment of systemic diseases, lung cancer or as alternative route for vaccines has become a new area of interest in research (Li-Calsi et al., 1999). In this work, two capsule based DPIs were used, tested and analysed regarding their particle size distribution (PSD) and respirable fraction when used with the developed dry powder vaccine formulation.

3.7.2.1 HandiHaler®

The HandiHaler® (Figure 3.11) from Boehringer Ingelheim Pharma GmbH & Co. KG (Ingelheim, Germany) is a capsule based breath activated dry powder inhaler. After the capsule is placed inside the aerosolisation chamber (4) it is pierced by two pins sideways at the top and the bottom of the capsule body using the piercing button (3). If air flows through the pierced capsule provided by the inhalation of the patient the capsule starts oscillating in a specific manner prescribed by the design of the aerosolisation chamber (Behara et al., 2011); the powder leaves the capsule and is released through the mouthpiece (2).

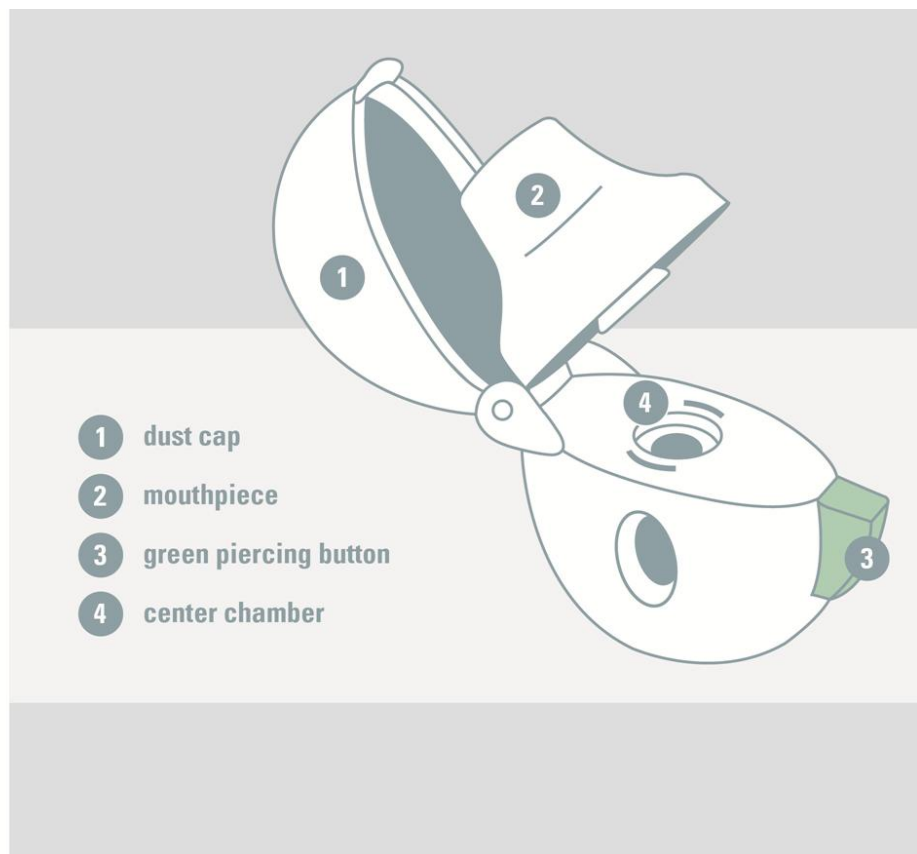


Figure 3.11 Design of the HandiHaler.

3.7.2.2 Aerolizer® (Cyclohaler)

Like the HandiHaler, the Aerolizer/Cyclohaler (Figure 3.12) is a capsule based breath activated DPI. The capsule is placed inside the appropriate indentation (2). For inhalation the capsule is pierced by four pins (3) at each end of the capsule body. When an air flow is provided upon inhalation the capsule is lifted up to the aerosolisation chamber where the pierced capsule starts rotating. The powder is pressed out of the capsule by the arising centrifugation forces and is delivered via the mouthpiece (1).

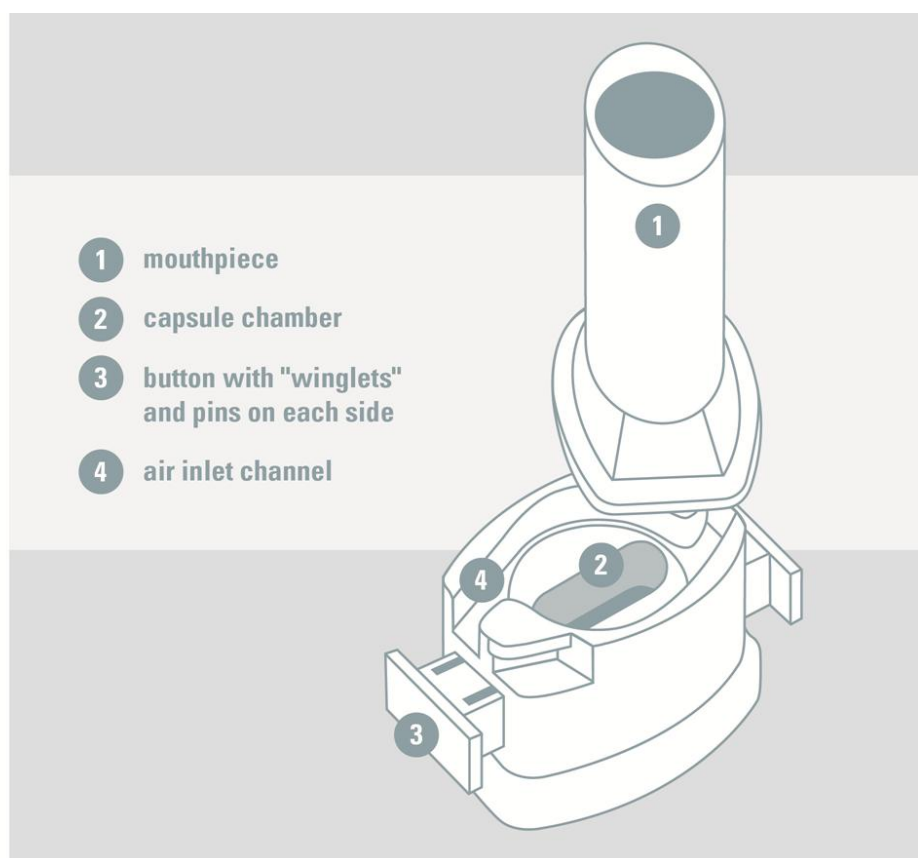


Figure 3.12 Design of the Aerolizer/Cyclohaler.

3.8 Animals

In this work, two *in vivo* studies (5.2; 5.6) were conducted and for both studies OT-I, OT-II transgenic (TG) and C57Bl/6J mice, aged 6-8 weeks, obtained from HTRU, University of Otago were used. All mice were bred and maintained under pathogen free conditions and had access to food and water *ad libitum*. OT-I and OT-II TG mice have modified genomes. OT-I mice express a significant percentage of CD8 T cells which carry a transgenic T cell receptor (TCR) specific for the MHC-class I (*major histocompatibility complex*) restricted OVA peptide aa 257-264 (Hänninen et al., 2001). While OT-II mice contain rearranged V α and V β genes (Pettini et al., 2009) making them express a significant percentage of CD4 T cells carrying a transgenic T cell receptor (TCR) which is specific for the MHC-class II restricted OVA peptide aa 323-339 (Barnden et al., 1998). All experiments were performed with the approval of the University of Otago Animal Ethics Committee.

4 Methods

4.1 Static Light Scattering

In this work, static light scattering (SLS) was used to determine the molecular weight of the chitosans which have been employed. Static light scattering is a widely used method to determine weight-average molecular weight (M_w) of polysaccharides (Wu, 2010) like chitosan. In SLS, a laser light is sent into the sample and the average scattering intensity is measured over a defined period of time (Wang et al., 2005). The intensity of scattered light is proportional to the molecular weight (weight-average) and the concentration of dissolved polymer. This proportionality is given by the reduced Rayleigh equation (Equation 4.1) (Malvern Instruments, 2003).

$$\frac{KC}{R_\theta} = \left(\frac{1}{M} + 2A_2C \right)$$

Equation 4.1 Reduced Rayleigh equation.

K is an optical constant, R_θ is the Rayleigh ratio, M is the weight-average molecular weight, A_2 is the second virial coefficient and C is the sample concentration. Using the Rayleigh equation a Debye plot, a linear fit of KC/R_θ versus C , can be generated where the intercept is equal to the inverse molecular weight and the resulting slope is twice the second virial coefficient. To determine the molecular weight, static light scattering measurements were performed using a ZetaSizer Nano ZS (Malvern Inc., Malvern, UK). The ZetaSizer Nano ZS is a single angle laser light scattering apparatus with an angle of 173° and a He-Ne laser (633 nm) as light source.

4.2 H-Nuclear Magnetic Resonance Spectroscopy

H-Nuclear Magnetic Resonance Spectroscopy ($^1\text{H-NMR}$) works by using the fact that the nucleus of the 1-hydrogen atom consists of one proton which can have two different spin conditions: $+\frac{1}{2}$ (\downarrow) and $-\frac{1}{2}$ (\uparrow). If no external magnetic field (B_0) is applied to the system both conditions are on the same energy level and thus equally likely, they are degenerated energy levels (Braun, 1998). If an external magnetic field is applied this situation is changing. Now, both conditions are on different energy levels (Figure 4.1) because of what is called the Zeeman Effect (Zeeman, 1897).

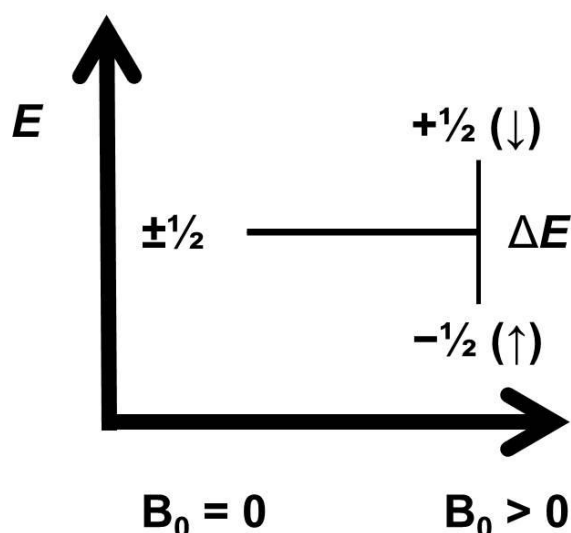


Figure 4.1 Schematic energy levels without and with an applied external magnetic field. Adapted from Braun (1998).

Although the difference (ΔE) is very small, because of the laws of physics, there are slightly more nuclei in lower energy level ($-\frac{1}{2}$). In the moment in which the externally applied energy, in the form of radio radiation, equals ΔE , the nuclei absorb this energy and are lifted to the higher energy level ($+\frac{1}{2}$). This radiation absorption is detected and plotted against the magnetic field strength in a $^1\text{H-NMR}$ spectrum (Rücker et al., 2001). A second important effect to disclose the molecular structure is the chemical shift. The chemical shift is the (relative) distance between one resonance signal of the sample and the signal of a chosen

standard e.g. TSP (deuterated sodium trimethylsilyl propionate) which is often used in aqueous systems, usually given in ppm. It occurs because an external magnetic field does not only affect the atomic nuclei, but also the spin of the electrons in the surrounding environment of the hydrogen nucleus. Here, according to Lenz's law (Lenz, 1834) the magnetic field can induce an electrical current which in turn induces another magnetic field that opposes the original magnetic field. Because these second magnetic field lines are running in closed paths, they can increase or decrease the magnetic field that is actually occurring at the atomic nucleus (effective magnetic field, B_{eff}). This leads to differences in the chemical shift and thus can disclose information about formation of hydrogen atoms in the molecule. The third important effect that is used to obtain structural information is the spin-spin coupling. Spin-spin coupling causes signal splitting in a ^1H -NMR spectrum. It mainly depends on the number of hydrogen atoms bonded to neighbouring carbon atoms. These hydrogen atoms generate a magnetic field that can increase or decrease B_{eff} of the hydrogen nucleus which is actually detected. For example, the signal of H_x is influenced by two hydrogen atoms H_A which are bonded to the neighbouring carbon atom (Figure 4.2).

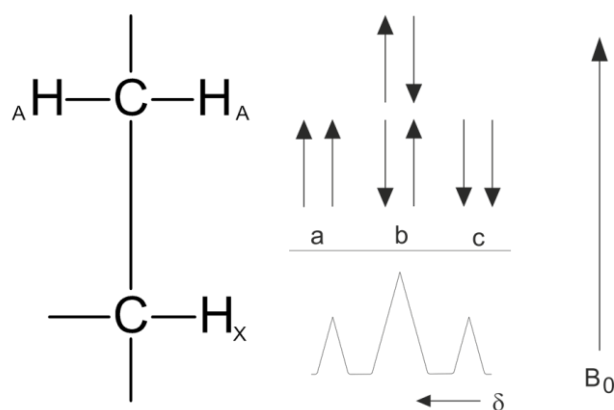


Figure 4.2 Spin-spin coupling of a hydrogen atom (H_x) with two neighbouring ones (H_A). Adapted from Rucker et al. (2001).

In one quarter of cases both atoms have the same spin direction ($\uparrow\uparrow$) to each other and increase the external field. In half of the cases their spin direction is oppositely ($\uparrow\downarrow$; $\downarrow\uparrow$) and their magnetic fields balance each other. And in the last quarter of cases, again both atoms have the same spin direction ($\downarrow\downarrow$) but this time in the

opposite direction compared with the external magnetic field (Rücker et al., 2001). In this case a triple splitting will be detected with an intensity distribution of 1:2:1. Intensity distribution of spin-spin couplings are following Pascal's triangle.

There are several techniques available to determine the degree of deacetylation, such as infrared spectroscopy (Baxter et al., 1992), Circular dichroism methods (Domard, 1987) and potentiometric methods (Qun, Ajun, 2006). In this work, ^1H -NMR spectroscopy was used to determine the DDA. ^1H -NMR spectroscopy is a widely used and well-established technique (Hirai et al., 1991; Brugnerotto et al., 2001) and it is the method required by the USP (United States Pharmacopeial Convention) to determine the DDA of chitosan. Measurements were performed on an ARX 300 (Bruker, Rheinstetten, Germany) spectrometer under a magnetic field of 300 MHz and a temperature of 80°C . Chemical shifts were expressed in parts per million (ppm) downfield from TSP which was used as external reference. The degree of deacetylation was calculated as ratio of the integrals of the H1 proton of the deacetylated form (H1D) to the sum of the integrals of H1D and the three protons of the acetyl group (AcH) in the acetylated form (Figure 4.3, Equation 4.2).

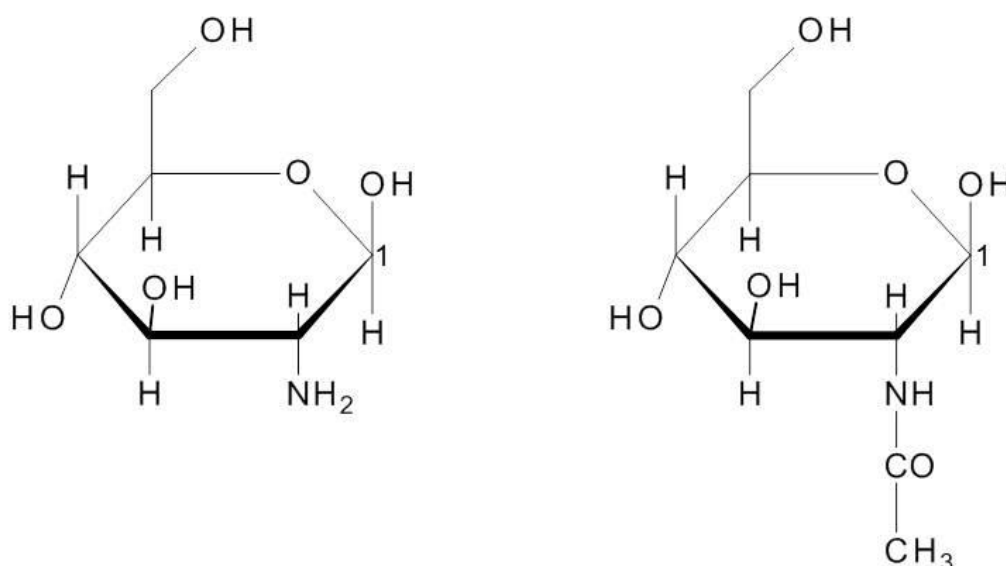


Figure 4.3 Deacetylated and acetylated glucosamine (chitosan monomers).

$$DDA(\%) = \left(\frac{H1D}{H1D + \frac{AcH}{3}} \right)$$

Equation 4.2 Equation used to calculate the DDA (Lavertu et al., 2003).

4.3 Quantification of Water-Soluble-Protein-like-Contaminates in Chitosan

Water soluble contaminates such as proteins have the capability to act as immune activating agents (Groot, Scott, 2007). Therefore, the water-soluble-protein-like-contaminates (WSC) were analysed using a self-developed extraction method. Then the WSC were quantified via BCA assay. For this, 5 g of each chitosan quality, used in the first *in vivo* study, were dispersed in 2 L ddH₂O and stirred for 72 h at 50°C. Subsequently, these suspensions were filtered through a paper filter (Whatman Schleicher & Schuell, Dassel, Germany) and the filtrates were transferred into a round-bottomed flask where the residual water was removed using a rotary evaporator (Heidolph Instruments GmbH, Schwabach, Germany) at a temperature of 65°C and pressure of 5 mbar. After the entire water was completely evaporated, the solid residues were redissolved in 5 mL ddH₂O and shaken for 5 h on a shaker (Edmund Bühler GmbH, Hechingen, Germany). Finally the content of contaminates was analysed as protein equivalents via a Micro BCA assay (Thermo Scientific, Rockford, IL, USA).

4.4 Endotoxins Level in Chitosan

An endotoxin is an almost ubiquitous agent with a strong proinflammatory potential (Trivedi et al., 2003). Endotoxin levels were determined using a semi-quantitative approach with limulus amoebocyte lysate (LAL). Chitosan was dispersed in sterile, endotoxin-free LAL water and extracted at 65 °C for 4 h. Afterwards, chitosan was removed and the supernatant was incubated in serial dilution with LAL reagent (Limusate, sensitivity 0.03 I.U.*ml⁻¹, Wako Chemicals USA, Inc, Richmond, VA, USA) to determine the endotoxin content which are given in I.U.*g⁻¹.

4.5 Particle Size Distribution

The knowledge of the particle size distribution (PSD) is very important because it affects many factors such as the rate of dissolution (Dokoumetzidis, Macheras, 2006; Bruner, St. Tolloczko, 1901), the powder flowability (Geldart et al., 2006) and aerodynamic behaviour (Hickey, Martonen, 1993) as well as the cell up-take (Huang et al., 2004b; Chadwick et al., 2010), the distribution in the human body (Gaumet et al., 2008), the immunogenicity (Kang et al., 2009) and toxicity (Karls-son et al., 2009). Basically, there are different methods to determine the particle size distribution, based on the intensity, on the mass or volume fraction or the number of particles in a grain size fraction. Because larger particles have a stronger effect onto the mass and volume fraction than smaller ones have, there are crucial differences in these kinds of distributions, even if the same group of particles is analysed. With light scattering methods, like laser diffraction and photon correlation spectroscopy a volume or intensity distribution is obtained. Mass distributions are obtained by sedimentation, sieve analysis and impaction and impingement determinations. A number distribution is obtained using microscopic and impedance methods such as coulter counter. In this work, photon correlation spectroscopy and laser diffraction were used to determine the particle size distribution of the nano- and microparticles, respectively.

4.5.1 Photon Correlation Spectroscopy

Photon correlation spectroscopy (PCS; also known as DLS - dynamic light scattering) is a user-friendly, quick and reliable method to determine the particle size distribution in the nanometre scale. The measuring principle is based on the Brownian motion. The Brownian motion is the random movement of very small particles of less than $5\ \mu\text{m}$ (in diameter); but this is also depending on their density; in a liquid caused by the bombardment of molecules surrounding them (Leuenberger, 2002). Smaller particles become faster than larger ones when they are hit by molecules because of their lower mass and the principles of momentum. Moreover, they undergo less resistance from the dispersion media due to their size. Because their “random walk” (Kac, 1947) is faster, the fluctuation of scattered light is higher. To determine the velocity of the particles the intensity of scattered light is detected at different time points (t , $t+\delta t$, $t+2\delta t$), where δt is in the range of nano or micro seconds. Then a correlation between those time points is calculated. With progressive time ($t+\infty\delta t$) the correlation will inevitably decrease - for smaller particles faster than for larger ones - and will reach zero at $t+\infty\delta t$ (Malvern Instruments, 2003). This is shown exemplarily in Figure 4.4

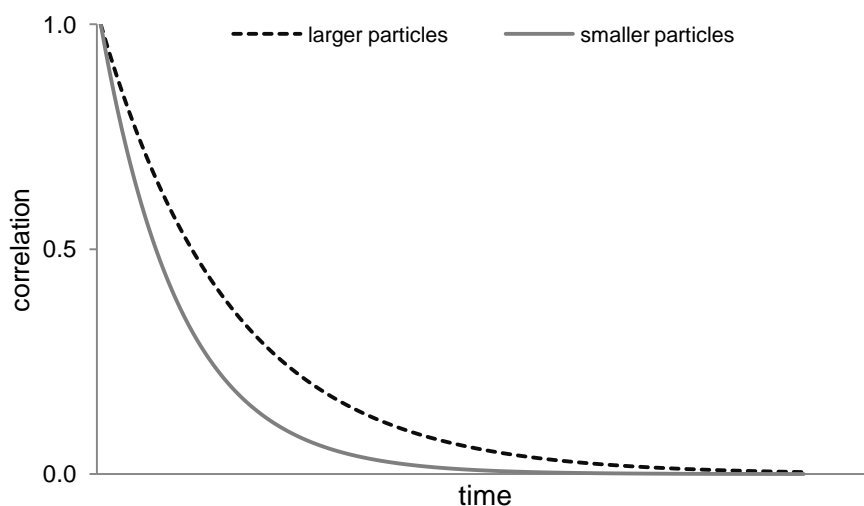


Figure 4.4 Exemplary correlation functions of smaller and larger particles.

The relationship between the velocity of particles and their size is defined by the Stokes-Einstein-Equation.

$$d(H) = \frac{kT}{3\pi\eta D_{t,avg}}$$

$d(H)$ = hydrodynamic diameter, m; target value

D = translational diffusion coefficient, $m^2 \cdot s^{-1}$; determined by PCS

η = viscosity of the dispersion media, $J \cdot m^{-3} \cdot s$; known

k = Boltzmann constant, $J \cdot K^{-1}$; known

T = absolute temperature, K; known

Equation 4.3 Stokes-Einstein-Equation.

The initial result is the hydrodynamic diameter (Equation 4.3), which is the diameter of a hypothetical hard sphere having the same diffusion behaviour than the particle that is actually measured. The result is a distribution by intensity, which is converted into a volume or mass distribution via Mie-theory (Malvern Instruments, 2011). In this work, measurements were performed using the Malvern ZetaSizer Nano ZS (Malvern, UK) which is able to determine particles in a size range from 0.6 nm to 6 μm . As Equation 4.3 indicates, the knowledge of the viscosity is necessary for a correct determination of the particle size, therefore the viscosity of each sample was determined prior to every PCS measurement using the vibro viscometer SV-10 (A & D Company, Tokyo, Japan). Fresh nano-suspensions were directly measured after preparation without any further treatment. While the spray and the freeze dried products were redispersed in double distilled water (ddH₂O) or PBS buffer and filtered through a 1 μm glass fibre membrane filter (Acrodisc[®], PALL Corp., Port Washington, NY, USA) before they were analysed. A manual measurement method had been used where the temperature was set to 20°C. The data were calculated via ZetaSizer software from Malvern. Besides the cumulants mean (z-average) which is an intensity based harmonic mean (Thomas, 1987), the polydispersity index (PDI; calculation according to ISO Standard 13321:1996) was determined. The polydispersity index

is a measure of the width of the particle size distribution in which a perfect monomodal group of particles would have a PDI of zero. On the other side, the highest value the PDI can become is 1. It is worth noting that the z-average is only comparable with other techniques if the sample is monomodal (Malvern Instruments, 2011). Up to a PDI of 0.5 the z-average is a reliable value for comparative purposes. When the PDI is between 0.5 and 0.7 the z-average should not be used, but peak means can be analysed directly from the distribution curves (Malvern Instruments, 2003). If the PDI is higher than 0.7 it indicates that the particle size distribution of the sample is very broad and that PCS is probably not a suitable technique (Malvern Instruments, 2011) for this sample. In addition, for two measurements photon cross correlation spectroscopy (PCCS) was used. By PCCS a second laser beam is sent into the sample leading to a unique scattering geometry and thus the cross correlation of the scattered light allows a clear distinction between single and multiple scattered fractions. For PCCS the Nanophox from Sympatec GmbH (Clausthal-Zellerfeld, Germany) was used.

4.5.2 Laser Diffraction (HELOS)

Laser diffraction was used to determine the particle size distribution of the produced dry powder formulations. The sample is brought in the measuring zone using a suitable dispersing unit. Inside the measuring zone is a monochromatic, coherent, parallel laser beam (Witt, Röthele, 1995) which is diffracted, deflected and reflected at the surface of the particles. As a result, a characteristic, angle dependent diffraction pattern of concentric circles accrues and is detected by a semicircular-ring-element which integrates of a 180° angle (Witt, Röthele, 1995). The first minimum of monodisperse particles occurs at r_0 (Equation 4.4). It can be seen that the size range in which the laser diffraction apparatus can measure is also depending on the wavelength λ and the focal distance f .

$$r_0 \cong 1.22 \frac{\lambda * f}{x}$$

Equation 4.4 Relation between r_0 , the wavelength of the light source and the focal distance.

If all these information are put together they can be converted via Mie or Fraunhofer-theory into a particle size distribution, such as the cumulative volume distribution $Q_3(x)$. In this work, a HELOS laser diffraction apparatus with different dispersing units from Sympatec GmbH (Clausthal Zellerfeld, Germany) was used. It has a Helium-Neon (HeNe) laser with a wavelength of 632.8 nm as light source. And has the ability to work with different focal distances which makes it possible to measure in a size range from 0.1 μm to 8,750 μm . In this work, standardly the x_{50} value (particle diameter at $Q_3=50\%$) calculated by Fraunhofer equation is given.

4.5.2.1 RODOS

The RODOS unit is a compressed air dispersing unit. The powder sample is placed in a hopper and is then dispersed by compressed air into the measuring zone. In this work, 3 bar dispersion pressure was standardly used. It was assumed that with 3 bar dispersion pressure all agglomerates were destroyed so that the particle size distribution of the individual, primary particles can be determined using this method.

4.5.2.2 Sprayer Module

The Sprayer unit is an adapter to measure particle size distributions produced by pump-sprays (like most nasal sprays are) and propellant based devices such as pMDIs directly upon device actuation. The device is triggered by a force actuator. The Sprayer unit was used for measuring the PSD upon powder release using the Powder UDS. The actuation force was set to 60 N and the end of the device was placed 10 cm ahead of the measuring zone. Measurements using the Sprayer module were performed at a spray angle of 70°.

4.5.2.3 Inhaler Module

The Inhaler unit is an adapter to measure particle size distributions produced by dry powder inhalers (DPIs) and nebulisers. An air flow can be applied to mimic the inhalation of a patient. The inhaler unit was used for measuring the PSD af-

ter powder release out of the HandiHaler and the Aerolizer. Measurements were performed with an applied airflow of $60 \text{ L}\cdot\text{min}^{-1}$ for both devices to have the same conditions as the Ph. Eur. requires for the Twin Stage Impinger, and additionally with $50 \text{ L}\cdot\text{min}^{-1}$ for the HandiHaler and $100 \text{ L}\cdot\text{min}^{-1}$ for the Aerolizer to achieve a pressure drop of 4 kPa over the device according to the Ph. Eur. and USP for physical tests of DPIs when using the Next Generation Pharmaceutical Impactor (European Directorate for the Quality of Medicines, 2013; United States Pharmacopeial Convention). The end of mouthpiece of the device was placed 12.5 cm ahead of the measuring zone.

4.6 Scanning Electron Microscope

In order to obtain additional information of the spray and freeze dried particles such as their shape and surface structure scanning electron microscope (SEM) pictures were taken. Prior to the imaging, the samples were placed on a self-adhesive, conductive polycarbonate film (Leit-Tabs, Plano GmbH, Wetzlar, Germany). This film was glued to an aluminium sample holder (Agar Scientific Ltd., Stansted, UK). Subsequently, the material was sputtered with gold using a Sputter-Coater (SCD 005, Bal-Tec AG, Vaduz, Liechtenstein) with 50 mA for 65 s. The prepared samples were rasterised with an accelerating voltage of 15-20 kV. Two scanning electron microscopes were used; the Smart SEMTM Supra55VP with SmartSEM V5.00 software and the Zeiss DSM 940 both from Carl Zeiss AG (Oberkochen, Germany) with Orion 6 software (Orion Microscopy, Labuissière, Belgium).

4.7 Bicinchoninic Acid Assay

The bicinchoninic acid (BCA) assay is a biochemical method to determine the total amount of dissolved protein in solutions or suspensions. The BCA assay was developed and first described by Smith et al. (Smith et al., 1985) thus it is sometimes called *Smith-assay*. As sodium salt, as it is present in the assay, BCA is a stable, sensitive and highly specific reagent for Cu^{1+} ions, Smith et al. suggested

that if protein is placed in an alkaline system containing Cu^{2+} ions, the copper is reduced from Cu^{2+} to Cu^{1+} . Subsequently, BCA is forming a 2:1-complex (Figure 4.5) with the generated Cu^{1+} leading to a colour change from green to purple. The resulting complex is stable and has an absorbance maximum at 562 nm. The colour intensity is proportional to the amount of formed complex and is therefore proportional to the amount of protein.

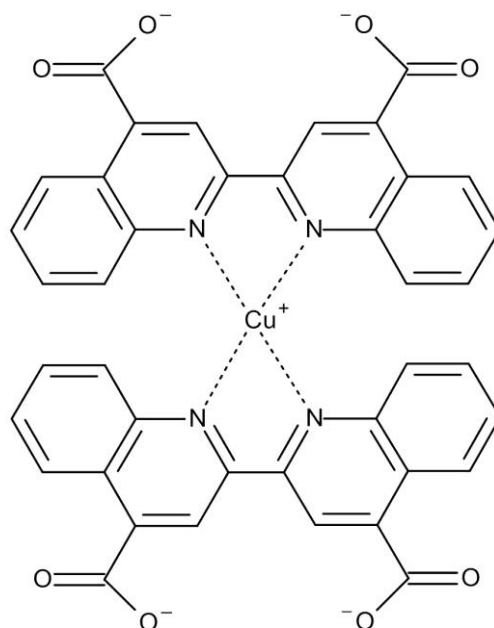


Figure 4.5 Structure of the purple complex of BCA with copper ion in the centre.

Compared to the Lowry-assay the BCA assay has some key advantages, namely it is more sensitive, more specific, the working reagent is more stable and the assay is less interfered by surfactants, often used to solubilise proteins. In this work, the Micro-BCA™ Protein Assay Kit (Thermo Scientific, Rockford, IL, USA) with a detection limit of $2 \mu\text{g}\cdot\text{mL}^{-1}$ was used. Measurements were performed according to the manufacturers' instructions for microplate procedure. Briefly, $150 \mu\text{L}$ of the sample were placed into the microplate well then $150 \mu\text{L}$ of working reagent were added. Then the sample was incubated for 2 h at 37°C , subsequently sample absorbance was measured at 562 nm using a Thermo Spectra III Reader 96-well plate reader (Tecan Group Ltd., Männedorf, Switzerland) with easy WIN fitting V6.00a software. Absorbance data were converted into protein

content by using a calibration curve of the reference protein (BSA or OVA) and a best-fit polynomial curve fitting.

4.8 Sodium Dodecyl Sulfate Polyacrylamide Gel Electrophoresis

Sodium dodecyl sulfate polyacrylamide gel electrophoresis (SDS-PAGE) is a method to analyse the molecular weight of proteins by separating them according to their electrophoretic mobility. Because the electrophoretic mobility is not only dependent on the molecular weight but also on the shape and charge of the proteins, sodium dodecyl sulphate (SDS) is used as anionic detergent. SDS imparts the protein a negative charge which is in proportion to its molecular weight. In combination with heat, SDS leads to a denaturation that linearises the proteins. In addition to that, reducing agents, like 2-mercaptoethanol or dithiothreitol (DTT; also known as Cleland's reagent (Cleland, 1964)) are used to cleave intramolecular disulphide bridges. After the polyacrylamide gel is polymerised it is placed into an electrolyte buffer. Then the samples are placed into a pocket at the top of the polyacrylamide gel. An electric field is applied to the system which causes migration of the negatively charged SDS-protein-complex towards the cathode. The migration of the proteins is held back by the tangled network of polyacrylamide in the gel. Because of their size, smaller proteins can travel faster through that network than larger ones. In this work, SDS-PAGE was used as an analytical tool to verify whether the production procedure of the nano-in-microparticles harms the antigen (OVA or BSA). A loading buffer containing SDS and 2-mercaptoethanol was added to the dissolved samples and protein references of OVA and BSA, respectively. Then they were heated at 95 °C for 5 min and transferred into the pockets. A discontinuous set up was used where the samples first travelled through a stacking gel with a pH value of 6.8 and 6% polyacrylamide to get concentrated. After they had passed the stacking gel, they went into a running gel with a pH value of 8.8 and 10% polyacrylamide (Rodbard, Chrambach, 1970). The system was started with an electrical potential of 120 V for 6 min. Then the potential was increased to 200 V and the SDS-PAGE was run for 50 min. Finally the gels were stained with Coomassie Brilliant Blue G 250 (Carl

Roth GmbH, Karlsruhe, Germany) to visualise the protein bands. SDS-PAGE was performed using a Mini Protean Tetra Cell System (BIO-RAD Laboratories Inc, Hercules, CA, USA) and a PageRuler Prestained Protein Ladder (Thermo Scientific, Waltham, MA, USA) as a molecular weight marker.

4.9 Circular Dichroism

Circular dichroism (CD) spectroscopy is a technique able to disclose important information about the conformation and structure of proteins (Sreerama, Woody, 2004), especially about the secondary structure (Bannister, Bannister, 1974; Sreerama, Woody, 2000). A plane polarised light ray can be divided into two circularly polarised elements, one rotating counter-clockwise (left), one rotating clockwise (right) but with the same frequency, phase and amplitude. If those two rays pass through a sample in which they are absorbed differently elliptical polarisation is induced into the resulting radiation (Equation 4.5). If $A_L > A_R$ the circular dichroism is positive and vice versa.

$$\Delta A = A_L - A_R$$

Equation 4.5 Resulting absorption difference in CD active sample.

A spectropolarimeter detects this absorption difference in relation to the wavelength and converts it into ellipticity (θ) value. If there are two light vectors (E_R and E_L) that are absorbed differently due to the structure of the sample (e.g. chiral carbons in peptide bonds)(Bloemendal, Jiskoot, 2005) the resulting vector sum (E) describes an elliptical path (Figure 4.6, left). The ellipticity (θ) corresponds to the arc of the ellipse and is described by the tangent of the ratio of short to long axis as described in Equation 4.6 (Rücker et al., 2001) and shown in Figure 4.6.

$$\theta = \arctan\left(\frac{E_L - E_R}{E_L + E_R}\right)$$

Equation 4.6 Relation between the absorption difference and the ellipticity.

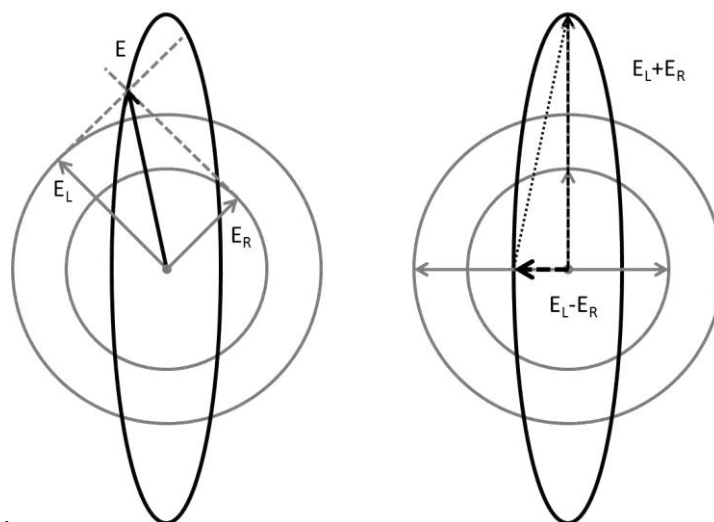


Figure 4.6 Light vectors E_L and E_R , the resulting vector sum E and the paths which they describe (left). Short and long axis, that are used to calculate the ellipticity (right).

Regarding proteins there are three main regions of interest in a CD spectra, namely the peptide bond with an absorption below 204 nm, absorption of aromatic amino acid side chains between 260 to 320 nm and weaker but broad absorption bands around 260 nm of the disulphide bridges (Kelly et al., 2005). In this work, circular dichroism spectroscopy was used to investigate the integrity of the secondary structure of OVA after the spray drying process. Measurements were performed in a wavelength range from 190 to 250 nm (Chang et al., 1978) in a quartz glass cuvette (0.05 cm in diameter) at room temperature. Chitosan can interfere in CD measurements (Domard, 1987) therefore it was removed by precipitation with sodium hydroxide and centrifugation for 15 min at 6,000 rcf (8,452 rpm) prior to the measurements. Nanoparticles were also removed by centrifugation for 5 min at 14,000 rcf (12,910 rpm). A J-720 spectropolarimeter (Jasco Inc., Easton, MD, USA) was used to obtain the CD spectra.

4.10 Drying

Drying is one of the most frequently used operations in the production process of drug products but at the same time it is one of the most critical ones especially when working with thermo-sensitive APIs like proteins. In this work, freeze and spray drying were examined in order to convert a nanosuspension into a dry powder. When working with nanosuspensions, drying becomes even more difficult because the successful drying of a nanosuspension, which readily reverts back to its original shape regarding size and distribution after reconstitution, is a pretty tricky and challenging task (Chung et al., 2012).

4.10.1 Spray Drying

Spray drying is an effective and efficient method of drying solutions or suspensions containing proteins in order to achieve a good-to-handle powder suitable for pulmonary (Maury et al., 2005; Lee, 2002) or nasal drug delivery but also for many other purposes. Because the drying process is fast the protein can be stabilised within the matrix without structural damage. For spray drying the intermediate (solution or suspension) is atomised by a nozzle or a rotary atomiser. When the generated droplets impinge upon the heated gas flow in the spraying tower, the solvent evaporates from the out- to the inside. This process leads to the characteristic shape of hollow spheres sometimes with holes or dimples. The holes are formed when solvent in the inside of a particle is evaporating, expanding and thereby breaking through the thin outer shell that has already been formed. Dimples are formed when the outer shell is not destroyed by the expanding solvent but is pulled together because of the occurring vacuum inside the particle after solvent expansion. In some cases this effect can lead to a total collapse of some of the particles (Maa et al., 1997). The dry particles are separated from the air flow in a cyclone. In this work, a BÜCHI Mini Spray Dryer B290 (BÜCHI Labortechnik AG, Flawil, Switzerland) with a 2.20 mm nozzle for the intranasal and a 1.50 mm nozzle for the pulmonary drug delivery approach was used, respectively. Different process temperatures were examined in order to optimise the powder properties like size and dispersibility (4.10.1).

4.10.2 Freeze Drying

Freeze drying is probably the most gentle drying method available (Franks, 1998) and therefore frequently used in the pharmaceutical industry, especially in the processing of thermo-labile APIs (Wolff et al., 2008) such as proteins (Kadoya et al., 2010). A frozen aqueous (protein) solution still has a low, but significant vapour pressure. If the ambient pressure is constantly held below this pressure the frozen water that is contained in the sample sublimates. A simple lyophilisation process consists of three parts: first, complete freezing of the sample at normal pressure; second, primary drying by sublimation in frozen condition at significant reduced pressure; third, secondary drying at moderate temperature at very low pressure. In this work, a Christ alpha 1-4 freeze dryer (Martin Christ GmbH, Osterode am Harz, Germany) was used for lyophilisation. Different lyophilisation excipients were examined for freeze drying the nanosuspension (5.3.2).

4.11 Antigen Loading

Regarding the antigen loading of the nanoparticles, there are two main parameters of interest. One is the loading efficiency (LE, Equation 4.7) which is the percentage of antigen that is associated with the prepared particles based on the amount of antigen originally used in the process.

$$LE, \% = 1 - \left(\frac{B}{A_w} \right)$$

Equation 4.7 Equation to calculate the loading efficiency. *B* is the amount of antigen determined in the supernatant. *A_w* is the total amount of antigen in the process.

In literature this value is sometimes called encapsulation efficiency (EE) although this often is an inaccurate term because mostly the value is calculated by using the API content in the supernatant and thus it cannot be distinguished between API encapsulated inside the particles and API adsorbed on the surface of the particles. The second parameter of interest is the loading capacity (LC; Equation 4.8) which is the mass of antigen associated to the particles in relation to the overall mass of the particles expressed as percentage.

$$LC, \% = \left(\frac{A_w - B}{C} \right)$$

Equation 4.8 Equation to calculate the loading capacity. *B* is the amount of antigen determined in the supernatant after particles forming. *A_w* is the total amount of antigen in the process and *C* the mass of the nanoparticles.

In this work, it was focused on the loading efficiency which was examined as a function of the pH value (5.3.1.6) and the antigen concentration (5.3.1.7). In order to determine the loading efficiency the corresponding nanosuspensions were diluted in a 1 to 10 ratio with ddH₂O. Diluted samples were transferred into 1.5 mL centrifugation tubes. Residual chitosan was precipitated with 50 μL sodium hydroxide (1N). Subsequently, samples were centrifuged at 14,000 rpm for

10 minutes. Afterwards, the protein content in the supernatant was analysed via BCA assay (4.7).

4.12 Aerodynamic Characterisation

When drug products like vaccines should be delivered into the nasal cavity or to the lungs, aerodynamic studies of the developed formulation can help to optimise the formulation and to get a deeper understanding of the interplay between powder formulation, application device and target regions. Therefore, different methods of aerodynamic characterisation were performed in this work. The formulations which were developed for intranasal delivery were characterised in two different nasal cast models (adult and child) and those for pulmonary delivery were investigated using the Twin Stage Glass Impinger (TSI).

4.12.1 *Uniformity of Delivered Mass*

In order to identify the most suitable combination of nasal device and dry powder formulation the uniformity of the mass delivered from the nasal powder disperser was determined. A modified test based on the USP 36 (United States Pharmacopeial Convention) method Delivered Dose Uniformity and Spray Content Uniformity method (FDA 2002) which was named Delivered Mass Uniformity (DMU) was conducted (5.4.1.1). For this, 20 doses were emitted and the individual mass per dose was determined by reweighing the devices. Boundaries of 125% and 75%, as well as 120% and 80% of the average delivered mass were set as limits according to the USP 36 testing for nasal sprays. For the Powder UDS 20 individual devices were analysed, while for the PowderJet 20 successive single doses were released, after the device was primed by releasing 5 shots. Acceptance criteria was that not more than 2 of the 20 doses were outside the range 80% to 120% of the mean, and none were outside the range of 75% to 125% of the mean, referring to the USP 36 testing for nasal sprays (<601> United States Pharmacopeial Convention).

4.12.2 Intranasal Particle Deposition

When developing a nasal powder formulation nasal deposition analysis is a very useful tool to characterise and optimise the formulation in order to deliver the drug product to the desired regions inside the nasal cavity. There are different methods to determine the nasal deposition of liquids and powders. For *in vivo* studies in apes or humans but also in most other animals, a radioactive tracer like Technetium-99m (^{99m}Tc) (Bacon et al., 2012; Hughes et al., 1993) which can be detected via gamma cameras can be used. But, because they are costly, very time-consuming and because of the radiation exposure such studies are neither suitable as routine method nor usable in early stage formulation development. To avoid the radiation exposure and the other mentioned drawbacks, replicas of the human nasal airways (nasal cast models) can be used to determine and analyse the deposition pattern upon drug release (Cheng et al., 2001). Such replicas from humans can be achieved as cadaver cast (Zamankhan et al., 2006), by magnetic resonance imaging (MRI) (Guilmette, Gagliano, 1994) or x-ray computed tomography (x-ray CT). Replicas are easier to handle and can be used multiple times. Another relatively new way to calculate the deposition of different particle groups at different air flows inside the nasal cavity is via computational fluid dynamics (CFD) (Li et al., 2012). This technique requires a relatively high initial effort but then parameters e.g. particle size can be easily changed and the resulting effects can be calculated.

4.12.2.1 *Nasal Cast Models*

In this work, two different nasal cast models, achieved from CT scan data, were used. Both models were obtained from healthy volunteers. One was representing an adult male and the other a five year old boy (Figure 4.8). Both casts were divided into five regions of interest:

1. nostrils
2. nasal vestibule
3. lower turbinates
4. middle and upper turbinates
5. nasopharynx

representing different regions of the human nasal cavity (Figure 4.7).

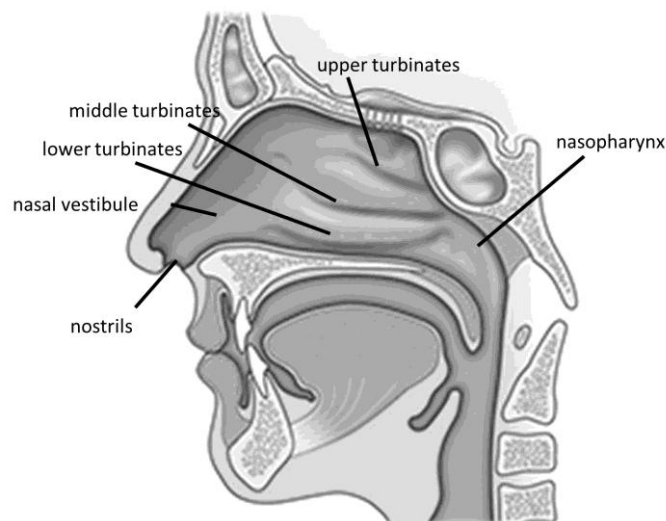


Figure 4.7 Regions of interest inside the human nasal cavity. Modified from Mosby's Physical Examination Handbook 7th edition (2003).

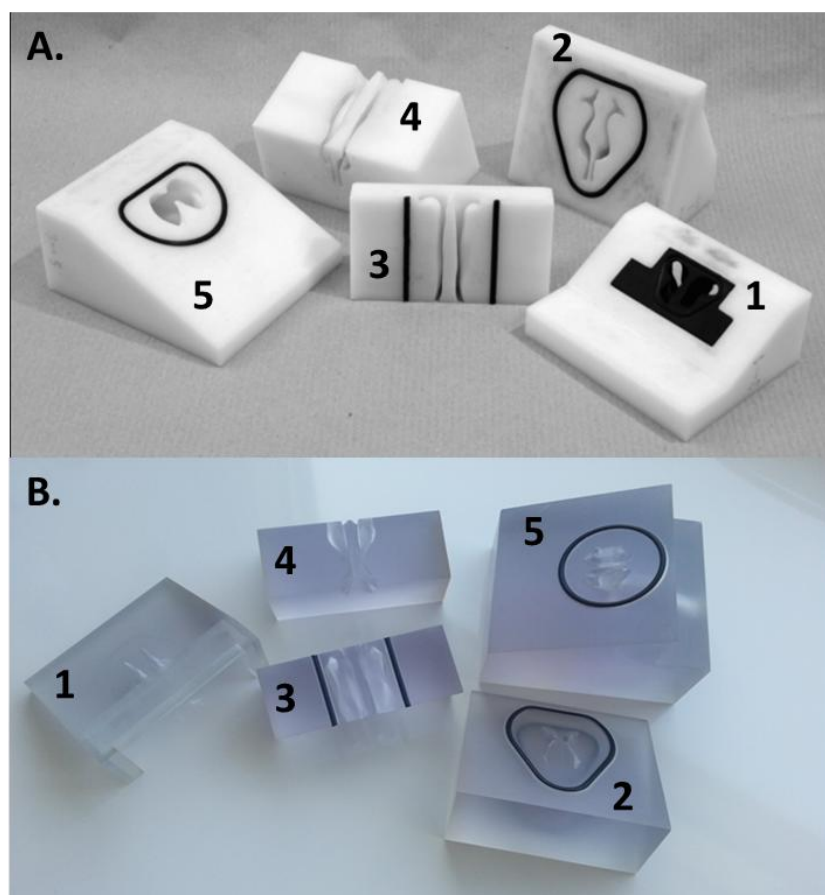


Figure 4.8 Segments of the adult cast (A.) and the child cast model (B.). Numbers give the regions in the nasal cavity which they represent.

Both cast models have an opening at the rear end (behind the nasopharynx) to allow collection of the post-nasal fraction and for simulating an inspiration air flow by attaching a regulated vacuum pump. Both were items on loan from Boehringer Ingelheim (Ingelheim, Germany).

4.12.2.2 *Nasal Deposition Analysis*

To analyse the powder deposition inside the nasal cast models all five segments were moisturised with double distilled water to mimic the moist environment in the nasal cavity. Then the device was placed at the entrance of the nostrils and was actuated. Determination was only performed with the most suitable device. For determination, ten devices, each filled with about 25 mg of the powder formulation were used for one run. Experiments were performed without air flow ($0 \text{ L}\cdot\text{min}^{-1}$) to mimic a breath holding patient and with moderate air flow of $15 \text{ L}\cdot\text{min}^{-1}$ and $10 \text{ L}\cdot\text{min}^{-1}$ for the adult and the child model (Bennett et al.,

2007), respectively, representing a normal nasal breathing. Subsequently, all segments were rinsed separately with ddH₂O using 5 mL and 2.5 mL per segment for the adult and the child cast model, respectively. In order to determine the deposition profile the antigen content in each segment and in the post-nasal fraction was analysed via BCA assay (4.7). All experiments were performed in a triplicate. Results were compared to a calculated ideal deposition profile. The ideal profile was calculated as an equal amount of vaccine formulation (based on the antigen content) per surface area in each segment with the exception of the nostrils. Powder that is deposited in the nostrils can be removed unwantedly and easily by sneezing or cleaning the nose. Therefore, deposition in this region is unwanted. However, dendritic cells as the target cells can be found throughout the complete inner surface of the nasal cavity. Hence, it is reasonable to make use of the complete surface. Further, the clearance of particles being deposited in the turbinates will take longer than the clearance of particles from the nasopharynx so that there is a certain depot effect.

4.12.3 Respirable Fraction

In order to determine the respirable fraction of the developed formulations the Twin Stage Glass Impinger (TSI) was used to analyse the aerodynamic behaviour of the formulations. A vacuum pump was connected downstream to the TSI to generate an air flow through the entire system. Ten capsules with about 3.5 mg powder formulation were used for each run, standardly three runs were analysed to gain the respirable fraction. Filled capsules were stored at 23% relative humidity and room temperature prior to testing. Because of the low drug loading in the final formulation analytical issues prevented to use another method which would provide even more aerodynamic information e.g. the Next Generation Impactor (NGI).

4.12.3.1 Capsule Filling

Quali-V® HPMC capsules size 3 (Qualicaps Europe S.A., Madrid, Spain) were used for testing. Capsules were filled manually using a highly accurate balance (Sartorius, WMC6014-d).

4.12.3.2 Twin Stage Glass Impinger

In order to investigate the aerodynamic behaviour and to determine the respirable fraction the Twin Stage Glass Impinger (Figure 4.9; Ph.Eur.7.4., 2.9.18, Apparatus A; TSI, Copley Scientific, Nottingham, UK) was used.

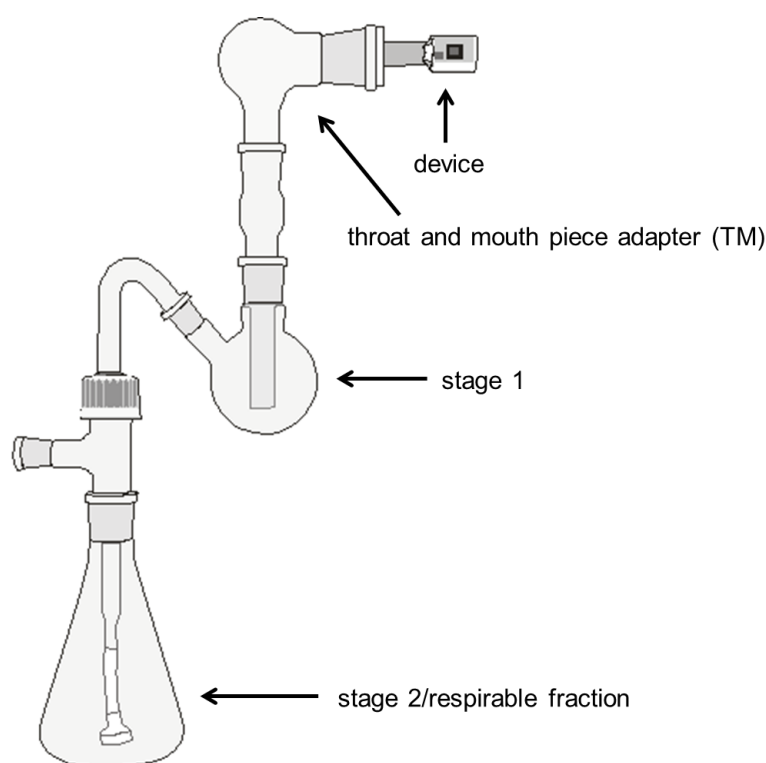


Figure 4.9 Figure of the TSI with fraction names and connected to a device (Aerolizer).

All measurements were performed using a flow rate of $60 \text{ L} \cdot \text{min}^{-1}$ according to the European Pharmacopeia (European Directorate for the Quality of Medicines, 2013). This leads to a (aerodynamic) cut-off diameter of $6.4 \mu\text{m}$, with smaller particles reaching the second stage which then represents the respirable fraction. Prior to testing 7 mL double distilled water were dispensed in the upper impingement chamber (stage 1) and 30 mL in the lower one (stage 2). DPIs were connected to the TSI via silicon mouth piece adapters. Flow was started and held

on to the system for five seconds. Afterwards, the amount of protein in both chambers (stage 1, stage 2) was determined by BCA assay (4.7). Additionally, the amount of protein in the throat and mouth piece adapter was analysed. The device and capsule retention was calculated as difference between total and delivered dose.

4.13 Cell Culture Experiments

Cell culture experiments can be very helpful to obtain important information such as the cell toxicity, the influence onto the cell layer integrity or the cell uptake of formulated particles, of raw materials that had been used and of the formulations that were developed. In this work, Calu-3 and bone marrow-derived dendritic cells (BMDCs) were used for *in vitro* investigations.

4.13.1 Calu-3 Cells

Calu-3 cells are human epithelial cells obtained from lung adenocarcinoma tissue. They have to be handled according to the biosafety level 1 and are one of the few *in vitro* cell lines representing the human airway epithelial (Stentebjerg-Andersen et al., 2011). Calu-3 cells have been used for the testing of drug delivery systems and particle toxicity for approximately twenty years (Grenha et al., 2007).

Unlike other human airway cell lines, such as NCI-H292 or A549, Calu-3 cells express functional tight junctions and also express functional desmosomes and zonulae adherents (Winton et al., 1998). Minimum Essential Medium (MEM) with Earle's salts supplemented with 10% (V/V) foetal bovine serum (FBS), 1% (V/V) non-essential amino acids (100x) and 1% sodium pyruvate (100mM) (all Biochrome AG, Berlin, Germany) was used as growth media. Cells were cultivated at 37°C, 95% relative humidity and 5% CO₂. For subcultivation, the cells were grown in cell culture flasks with a 75 cm² bottom (Greiner bio-one, Frickenhausen, Germany), from where they were trypsinated (trypsin/ EDTA, 0.25%/ 0.02%) when needed. In this work, Calu-3 cells which were obtained from ATCC

have been used for transepithelial electric resistance (TEER) and cell toxicity measurements.

4.13.1.1 *Transepithelial Electric Resistance*

All Transepithelial Electric Resistance measurements were performed by using the “classical” liquid-covered culture method (LCC) where both sides of the cells are covered with medium. The cells were seeded on 12 polyethylene terephthalate (PET; USP class VI certified) micro porous membranes with a pore diameter of 0.4 μm (Greiner Bio-One GmbH, Frickenhausen, Germany) and a cell density of $2.65 \times 10^5 \text{ cell} \cdot \text{cm}^{-2}$. A volume of 0.5 mL cell suspension was added to the apical and 1.5 mL pure growth media to the basolateral compartment, respectively (Figure 4.10).

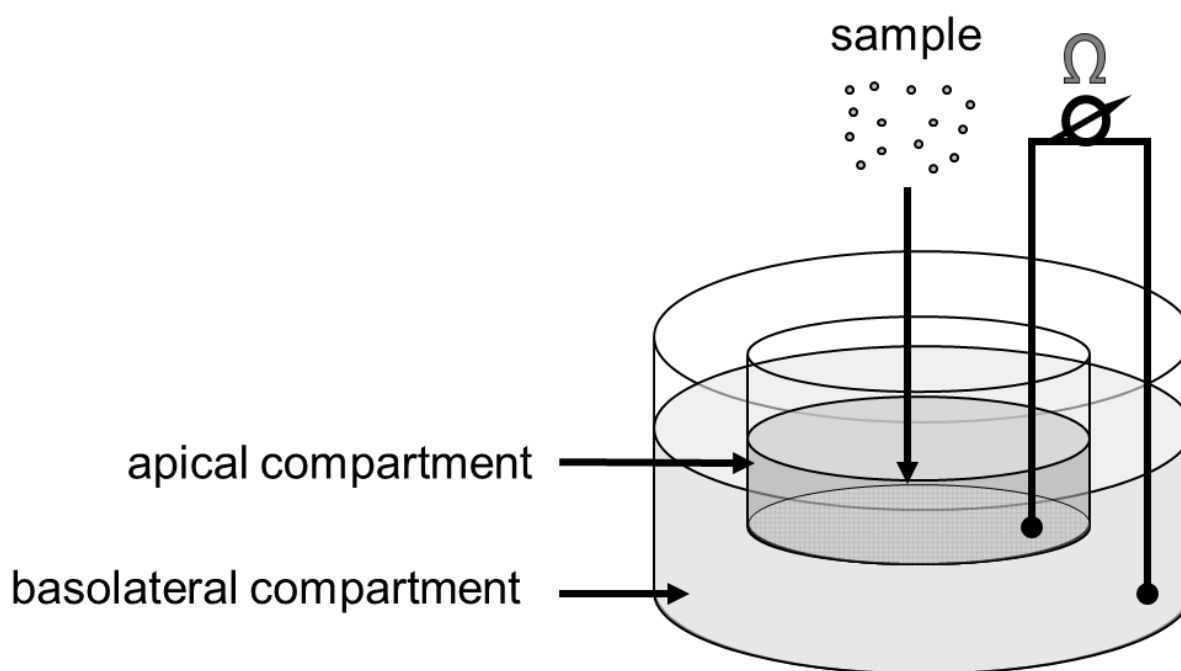


Figure 4.10 Experimental set up for TEER measurements.

The cells were cultivated at 37°C, 95% relative humidity and 5% CO₂ and were allowed to grow until their TEER value was at least 800 Ω (Kotzé et al., 1999). First of all, the initial TEER value was measured; subsequently the sample was added to the apical side. After that the TEER value was measured after 1 h, 5 h and 8 h, subsequently the apical chamber was removed and rinsed thrice with

5 mL sterile PBS-Buffer (pH 7.4) in order to remove the sample and then refilled with fresh growth medium. Medium from the basolateral side was also removed, rinsed once with 5 mL PBS and refilled with fresh growth medium. After 24 h (related to the start of the experiment) the TEER value was measured again. The electrical resistance was measured using a WPI EVOMX (World Precision Instruments, Sarasota, FL, USA) device with a chopstick electrode.

4.13.1.2 Thiazolyl Blue Tetrazolium Bromide Cell Toxicity Assay

In 1963 Slater et al. discovered that Thiazolyl Blue tetrazolium bromide (MTT; (3-(4,5-Dimethyl-2-thiazolyl)-2,5-diphenyl-2H-tetrazolium bromide) can be used to measure the activity of various dehydrogenase enzymes (Slater et al., 1963). Twenty years later Tim Mosmann used that knowledge to develop the MTT cell activity assay (Mosmann, 1983). Since then the test has been modified several times (Denizot, Lang, 1986; Hansen et al., 1989). Nowadays, the MTT assay is a well-established, well-known technique to determine cell toxicity. It detects living, but not dead cells while the intensity of the signal is depending on the mitochondrial cell activity. MTT is reduced into a dark blue formazan product when it is incubated with live cells. The cleavage of the tetrazolium ring (Figure 4.11) that causes the colour change from yellow to dark blue is mediated by succinate dehydrogenase in the cell mitochondria (Fotakis, Timbrell, 2006) and thus can only occur in living cells.

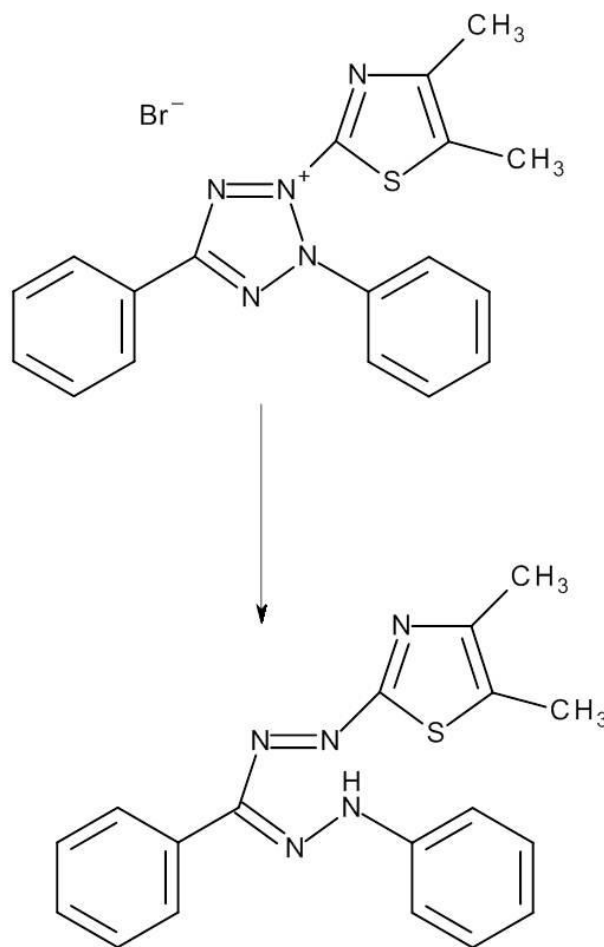


Figure 4.11 Ring cleavage of MTT in active mitochondria of living cells.

The MTT assay shows a linearity from about 200 to 50 000 cells per well even at a concentration of 10^6 cells \cdot mL $^{-1}$ the actual cells show no absorption (Mosmann, 1983). The MTT assay is widely used to determine the cell toxicity of nanoparticles (Grenha et al., 2007; Huang et al., 2004b; Cadete et al., 2012). In this work, Calu-3 cells and MTT assay were used to analyse the cell toxicity of spray dried chitosans and the nano-in-microparticle formulation. For testing, cells were seeded on a 96-well-plate (Biochrome AG, Berlin, Germany) at a cell number of $1.5 \cdot 10^5$ cells \cdot mL $^{-1}$. 200 μ L of the cell suspension were pipetted into each well resulting in a cell number of $3 \cdot 10^4$ cells per well. The cells were allowed to form a monolayer within three days before the toxicity test was performed. All samples were dissolved in HBSS+HEPES buffer (Biochrome AG, Berlin, Germany) and then appropriately diluted via dilution series. After the MEM was removed, 200 μ L of sample solutions was pipetted into each well (quadruple determina-

tion). After that the cells were incubated for 4 h at 37°C and 5% CO₂ with the samples. Afterwards, the sample solutions were removed and 25 µL of a MTT solution (5 mg*mL⁻¹ in HBSS+HEPES) were added into each well and incubated for 2 h at 37°C and 5% CO₂. Subsequently, all cells were lysed by adding 100 µL of 5% SDS in a mixture of DMF (dimethyl formamide) and water in a ratio of 1 plus 1 with a pH-value of 4.7 (using acetic acid) into each well. Then the plate was shaken for half an hour before the absorptions were measured at a wavelength of 570 nm. Detection was performed by a multi-well plate reader (Thermo Spectra III Reader, easy WIN fitting V6.0a, Tecan, Austria). The gained absorption data were transferred into viability data via two point calibration using MS Excel (Microsoft Corp., Redmond, USA). A four parameter sigmoidal curve fit with SigmaPlot (Systat Software Inc., San Jose, USA) was performed in order to calculate the LC₅₀-values. LC stands for Lethal Concentration. The LC₅₀ is the concentration of a substance that kills 50% of the test cells (Calu-3) during the observation period (4 h). A solution of 5 mM SDS (1.4419 mg*mL⁻¹, sodium dodecyl sulphate, Fluka Chemie GmbH) in HBSS+HEPES buffer and pure HBSS+HEPES buffer were used as positive (0% viability) and negative control (100% viability), respectively.

4.13.2 Preparation of Bone Marrow-Derived Dendritic Cells

Bone marrow-derived dendritic cells (BMDCs) that were used for the *in vitro* cell uptake experiments were gained from male C57BL/6 mice (3.8). Animals were sacrificed by cervical dislocation and then the hind limbs were removed, femur and tibia were cut off and the bone marrow was washed out using a needle and sterile complete Iscove's modified dulbecco's medium (cIMDM). Through a cell strainer the bone marrow was transferred into a 50 mL falcon tube, then the cells were washed using cIMDM and centrifuged for 8 min at 12,000 rpm. Subsequently, the cell sediment was resuspended and the red blood cells were lysed by adding sterile red blood cell lysis buffer and incubated for 10 min. Then cells were washed and centrifuged again. Cells were counted using trypan blue staining and the total cell number was calculated. Finally, the cells were suspended in cIMDM containing 20 ng*mL⁻¹ granulocyte macrophage colony stimulating factor

(GM-CSF) as differentiation activator in a concentration of 10^6 cells \cdot mL $^{-1}$. Cell suspension was divided and 5 mL per well were transferred into a six well tissue culture plate. Cells were incubated at 37°C with 5% CO $_2$ to mature into BMDCs. After four days of maturation 3 mL of the supernatant were removed and replaced by cIDMD containing 10 ng \cdot mL $^{-1}$ GM-CSF. The cells were incubated for two more days. At day six cells were harvested by rinsing the wells using PBS. Then the cells were again centrifuged and finally suspended in cIMDM containing 20 μ g \cdot mL $^{-1}$ GM-CSF at a concentration of 10^6 cells per mL. Details of the uptake experiment are described in the appropriate section (5.6.5).

4.14 Fluorescence-Activated Cell Sorting

Fluorescence-activated cell sorting (FACS) is a relatively new technique invented in the late 1960s (Herzenberg et al., 2002). It is a laser-based technique which enables the user to count and sort viable cells according to different properties. The cell suspension which is to be analysed is hydrodynamically focused so that single cells pass through the laser beam in the measuring zone. When cells pass through, the light is scattered and if the cells were previously stained a fluorescence signal can be detected. There are several detectors to detect these interactions. One of them is in a line with the laser beam and detects the forward scatter (FSC), another one in a 90° angle detects the side scatter (SSC) of the cells. The extent of light scattering is depending on the structure of the cells. Cells with a smooth surface (e.g. T cells) scatter the light much less than cells with a rough surface e.g. granulocytes. The FSC gives information about the volume of the cell while the SSC is a measure of the complexity of the cell content. In addition, there are one or more detectors to measure the fluorescence. Lasers with different wavelengths can be used to analyse multiple fluorescence staining in one step. Fluorescent dyes like propidium iodide (PI) which is able to enter and stain dead cells (but not living ones) can be used to distinguish between dead and viable cells. Labelled antibodies which bind to specific surface structures like certain clusters of differentiation (CD), are used to generate detailed information of the cell population that is investigated. For example, FACS can be used for cell

counting, immunophenotyping, ploidy analysis and green fluorescent protein (GFP)-expression (Cormack et al., 1996). In this work, FACS analysis was used to look at T cell number and activation to gather information about the adjuvant activity of different chitosans upon s.c. administration and of the immunisation potential of a chitosan nanoparticle formulation being administered intranasally. For this, obtained samples were labelled for CD4⁺ and CD8⁺ TG cells. Furthermore, it has been used in the evaluation of the BMDC uptake assay to detect formulation-positive cells and cell activation. The FACS analysis was performed on a BD FACS Canto II instrument (BD Biosciences) and the achieved data were analysed using Kaluza software (Version 1.1, Beckman Coulter; Pasadena, CA, USA).

4.14.1 Sample Preparation for FACS analysis

In both *in vivo* studies mice were euthanised by an intraperitoneal overdose of anaesthetic on day 31. Subsequently, axial, brachial and mesenteric lymph nodes and spleen were harvested and cell suspensions of 2×10^6 cells per mL in cIMDM were prepared. For FACS analysis 1 mL of the purified cells was washed twice with FACS buffer (PBS-buffer pH 7.4 containing $10 \text{ g} \cdot \text{L}^{-1}$ BSA) and blocked with antiCD16/32 to avoid unspecific staining. Cells were stained for CD4 and CD8 positive T cells as well as for V α 2 and V β 5 positive cells (transgenic, antigen-specific cells). All antibodies used were obtained from BD Biosciences. To distinguish between viable and dead cells propidium iodide was used. (Mönckedieck, 2013)

4.14.2 Data Analysis of FACS Data

Statistical analysis was performed by one way ANOVA analysis or when the assumption of normality was violated by one way ANOVA on ranks using Sigma Plot (Version 11.0 and 12.5, Systat Software Inc., San Jose, CA, USA). The experiment-wise error rate ($\alpha < 0.05$) was controlled using Bonferroni's adjustment for the one way ANOVA or Dunn's method when one way ANOVA on ranks was used. Data was log-transformed prior to statistical analysis.

5 Experimental Section, Results and Discussion

5.1 Characterisation of Chitosan

In this work, five different chitosan qualities (Chitopharm S, M, L, Chitosan from Sigma, ChitoClear FG 95) were used for different purposes. All chitosans were analysed with respect to their molecular weight and their degree of deacetylation. For a first *in vivo* study (adjuvant study) three chitosans (Chitopharm S, Chitosan from Sigma, ChitoClear FG 95) were tested with respect to their adjuvant activity. For this study two of them (Chitopharm S and Chitosan from Sigma) were transferred into the hydrochloride by spray drying. Both spray dried qualities were evaluated regarding their cell toxicity via MTT assay. ChitoClear FG 95, Chitopharm S and Chitosan from Sigma which were used in the adjuvant *in vivo* study were additionally characterised with respect to their endotoxin level, their content of water-soluble-protein-like-contaminates and their particle size distribution via laser diffraction. In addition, Chitopharm S, which was used in most particle forming experiments, was also characterised regarding its effect onto the cell layer integrity of Calu-3 cells via TEER measurements.

5.1.1 Preparation of the Spray Dried Chitosan

For spray drying Chitopharm S and Chitosan from Sigma were dissolved in 0.025 N HCl and spray dried using the BÜCHI Mini Spray Dryer B290 (BÜCHI Labortechnik AG, Flawil, Switzerland) with an inlet temperature of 90°C and an outlet temperature of 45°C. A 1.5 mm two-fluid nozzle was used.

5.1.2 Molecular Weight

The molecular weight is one of the most important characteristics of chitosan (Mao et al., 2007) but it is also very difficult to determine (Nguyen et al., 2009b). The molecular weight has a strong influence on many important properties of chitosan such as the ability to enhance the permeation across membranes (Hagesaether, 2011) and the extent of mucoadhesion (Takeuchi et al., 2005). Therefore,

the knowledge of the average-molecular weight is fundamental when working with chitosan. Static light scattering (4.1) was used to determine the molecular weight of all chitosans that were used in this work.

5.1.2.1 Sample Preparation for Static Light Scattering

Prior to every sample measurement background light intensity was determined and the backscattering of toluene as scattering standard with a Rayleigh ratio of $1.35 \times 10^{-5} \text{ cm}^{-1}$ was measured. All samples were dissolved in 0.02 M sodium acetate and 0.1 M sodium chloride at a pH-value of 4.5 and a refraction index increment (dn/dc) of $0.192 \text{ mL} \cdot \text{g}^{-1}$ of chitosan was assumed (Nguyen et al., 2009a). Five different sample concentrations in the range from 0.25 to $1.00 \text{ g} \cdot \text{L}^{-1}$ were prepared and measured in a series starting with the highest. Prior to each measurement samples were filtered through a $0.45 \text{ }\mu\text{m}$ PTFE filter into a square glass cuvette. All measurements were performed at a temperature of 20°C . The obtained data were analysed via the Debye plot method (4.1).

5.1.2.2 Results of the Static Light Scattering

The determined molecular weights are summarised in Table 5.1. It can be seen that the spray drying process did not influence the molecular weight.

Table 5.1 *Molecular weights of native and spray dried chitosans determined by SLS. (n=3; SD=spray dried; sd=standard deviation)*

Chitosan Quality	Weight-Average Molecular Weight, kDa (\pm sd)
Chitopharm S	79.4 (\pm 4.50)
Chitopharm S SD	78.1 (\pm 0.69)
Chitopharm M	123.4 (\pm 15.3)
Chitopharm L	135.2 (\pm 10.1)
ChitoClear FG 95	101.8 (\pm 4.99)
Chitosan from Sigma	148.5 (\pm 6.60)
Chitosan from Sigma SD	149.1 (\pm 6.46)

The obtained data points were analysed by a linear fit to achieve the y-axis interception. The molecular weight was determined by calculating the reciprocal of the y-axis interception according to the Debye plot. Data were accepted for calculation when the coefficient of determination was $R^2 \geq 0.85$, as advised by the manufacturer of the ZetaSizer (Malvern Inc.). The Debye plots generated from SLS measurements of Chitopharm S, M and L which were used to investigate the dependence of the molecular weight on the resulting particle size of nanoparticles (5.3.1.4) are shown in Figure 5.1.

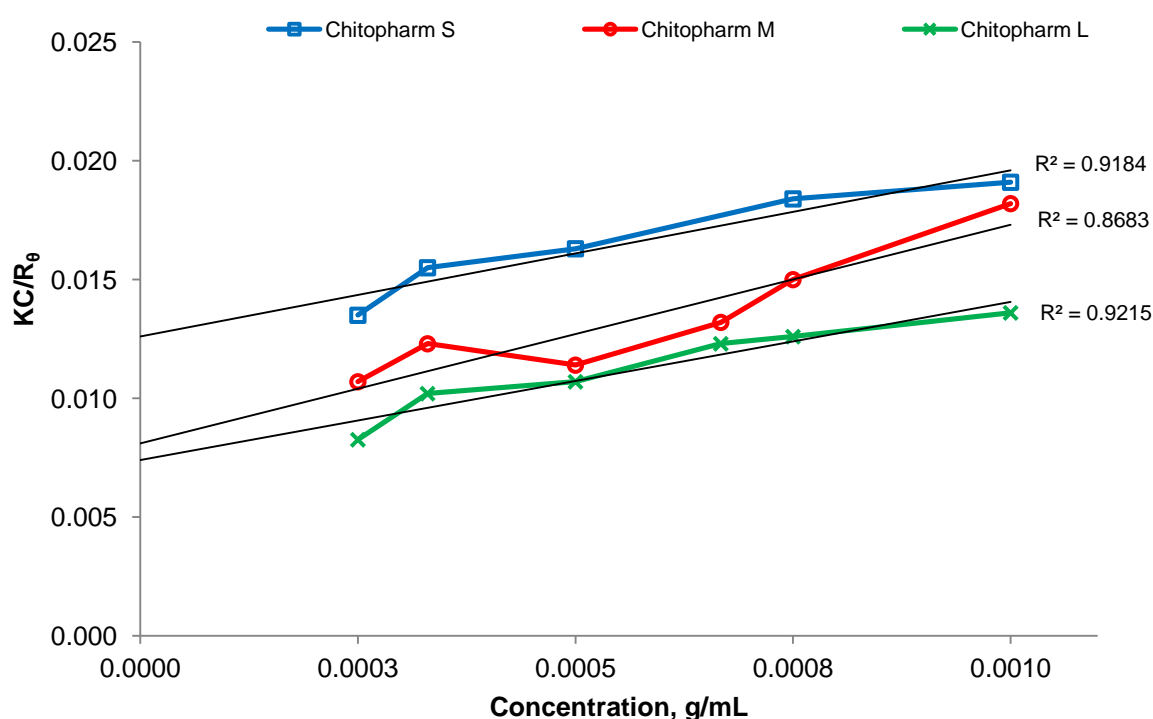


Figure 5.1 Debye plots obtained by static light scattering data of Chitopharm S, Chitopharm M and Chitopharm L with linear fit and corresponding coefficient of determination.

The Debye plots generated from SLS measurements of the native and spray dried chitosan qualities used in the adjuvant *in vivo* study are displayed in Figure 5.2.

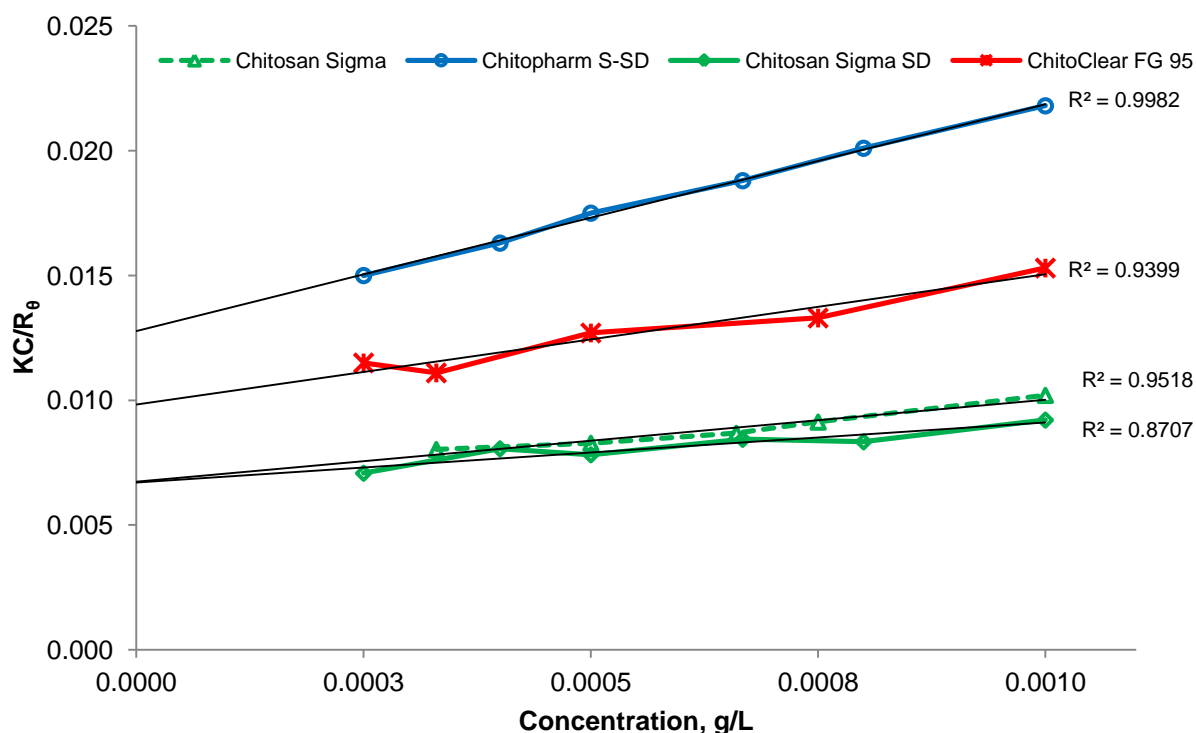


Figure 5.2 Debye plots obtained by static light scattering data of Chitopharm S SD, Chitosan from Sigma native and spray dried as well as native ChitoClear FG 95 with linear fit and corresponding coefficient of determination.

The results show that the spray drying process used does not induce any changes in the molecular weight of the employed chitosans. The monomers within the chitosan chain are linked together via β -(1-4) glycosidic bonds where the oxygen is integrated in an acetal structure (Figure 3.3 Structure of chitosan). Acetals are known to be stable against lower pH values and heat. During the preparation process these two parameters act upon the chitosan but in a relatively moderate extent using 0.025 N hydrochloric acid and inlet temperature of 90°C and thus the observation that the molecular weight is not influenced by the spray drying process was expected.

5.1.3 Degree of Deacetylation

The degree of deacetylation (DDA) is the percentage of glucosamine molecules in the chitosan chain. It is a highly interesting characteristic because it influences not only physical properties, such as solubility and chemical characteristics, like the acid dissociation constant of chitosan but also physiological ones. A higher DDA leads to slower lysozymic degradation (Aiba, 1992) and a higher cellular uptake even when the polymer is formulated as nanoparticles (Huang et al., 2004b). In this work, ^1H -nuclear magnetic resonance spectroscopy (4.2) was applied in order to determine the DDA of all chitosans that were used.

5.1.3.1 Sample Preparation for ^1H -NMR Spectroscopy

Prior to each measurement about 5 mg of every sample were dissolved in 1 mL 2% CD_3COOD (Acetic acid D4, 99.5% Atom%D, Carl Roth GmbH & Co KG, Karlsruhe, Germany) in D_2O (Deuterium oxide 100 Atom%D, Carl Roth GmbH & Co KG, Karlsruhe, Germany). Spray dried samples had to be pre-treated because a direct H-NMR analysis of those samples was not suitable. For this, about 500 mg of each spray dried chitosan was dissolved in 25 mL double distilled water. Subsequently, the free base was achieved by precipitation using 1N NaOH whereby the pH value was increased to 10. Precipitated samples were centrifuged by 7,830 rpm for 7.5 min at a temperature of 20°C. After that, the supernatant was removed and the sediment was washed with double distilled water and again centrifuged. This procedure was repeated until the supernatant had the same pH-value as the pure dispersion medium (ddH_2O). Subsequently, the achieved chitosan was filtered through a paper filter and dried for 72 h at a temperature of 65°C and a pressure of 200 mbar using a vacuum dryer (Heraeus Vacutherm, Thermo Scientific, USA). The chitosan thus obtained was treated as mentioned above for the ^1H -NMR measurements.

5.1.3.2 Results of $^1\text{H-NMR}$ Spectroscopy Measurements

The determined degrees of deacetylation of all chitosan qualities and spray dried hydrochlorides that were used in this work are given in Table 5.2.

Table 5.2 Degree of deacetylation of native and spray dried chitosans. (*SD=spray dried*)

Chitosan	Degree of Deacetylation
Chitopharm S	81.1%
Chitopharm M	82.0%
Chitopharm L	73.5%
ChitoClear FG 95	81.3%
Chitosan from Sigma	75.8%
Chitopharm S SD	81.3%
Chitosan from Sigma SD	78.7%

$^1\text{H-NMR}$ spectra of Chitopharm S, M, L are shown in Figure 5.3, those of Chitosan Sigma and ChitoClear FG 95 in Figure 5.4 and of the spray dried and reprecipitated chitosans in Figure 5.5. The integrals on which the DDA was calculated are labelled in the figures. The integral of the H1D proton was calibrated to 1.00. The AcH peak is caused by the three protons of the acetyl group and therefore the integral has to be divided by three for the calculation of the DDA (Equation 4.2).

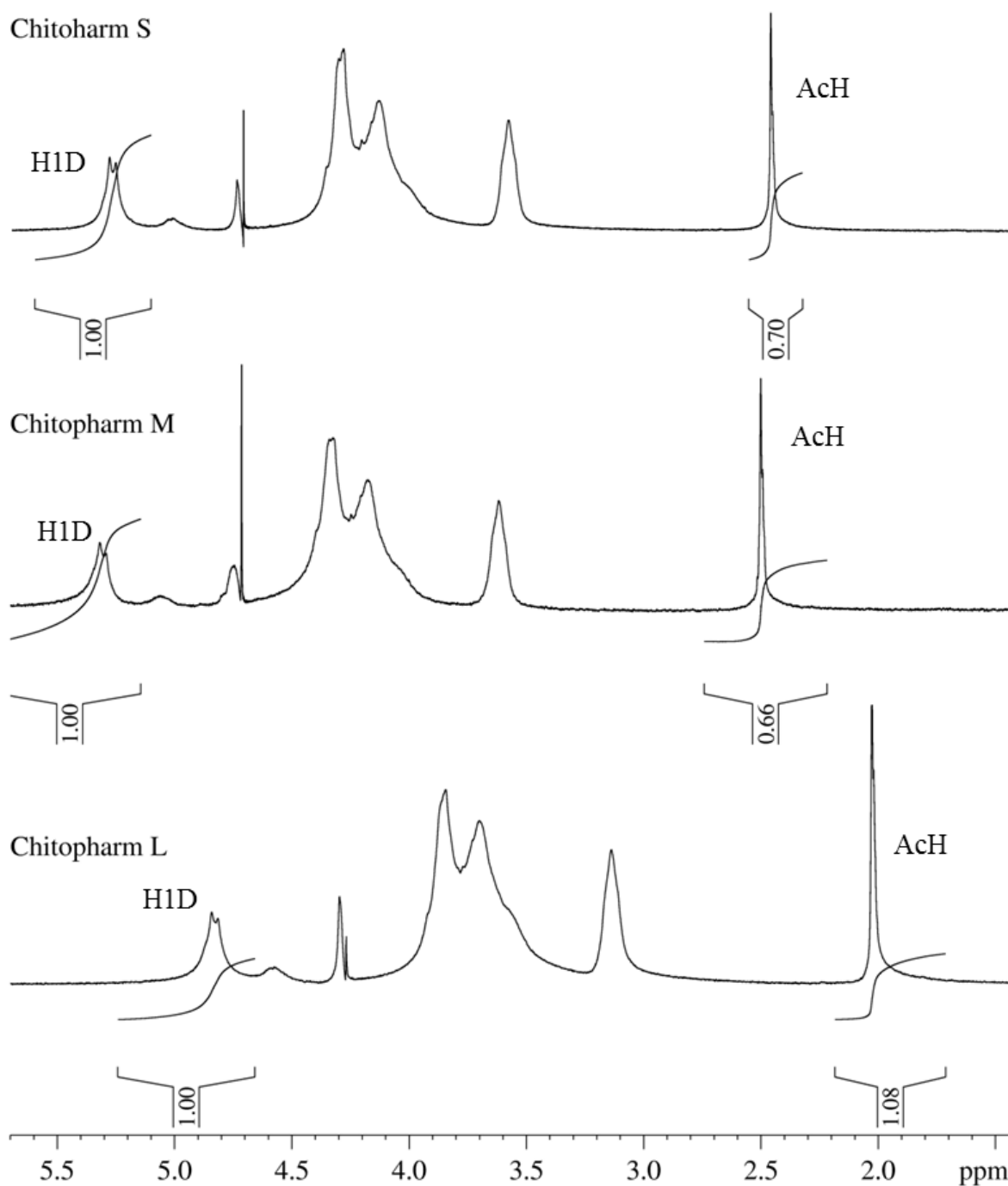


Figure 5.3 $^1\text{H-NMR}$ spectra of Chitopharm S, M, L recorded at 80°C in 2% CD_3COOD with integrals used to calculate the DDA.

It can be seen that Chitopharm S and M have nearly the same DDA, namely 81.1% and 82.0% while Chitopharm L has a distinct lower one of 73.5%.

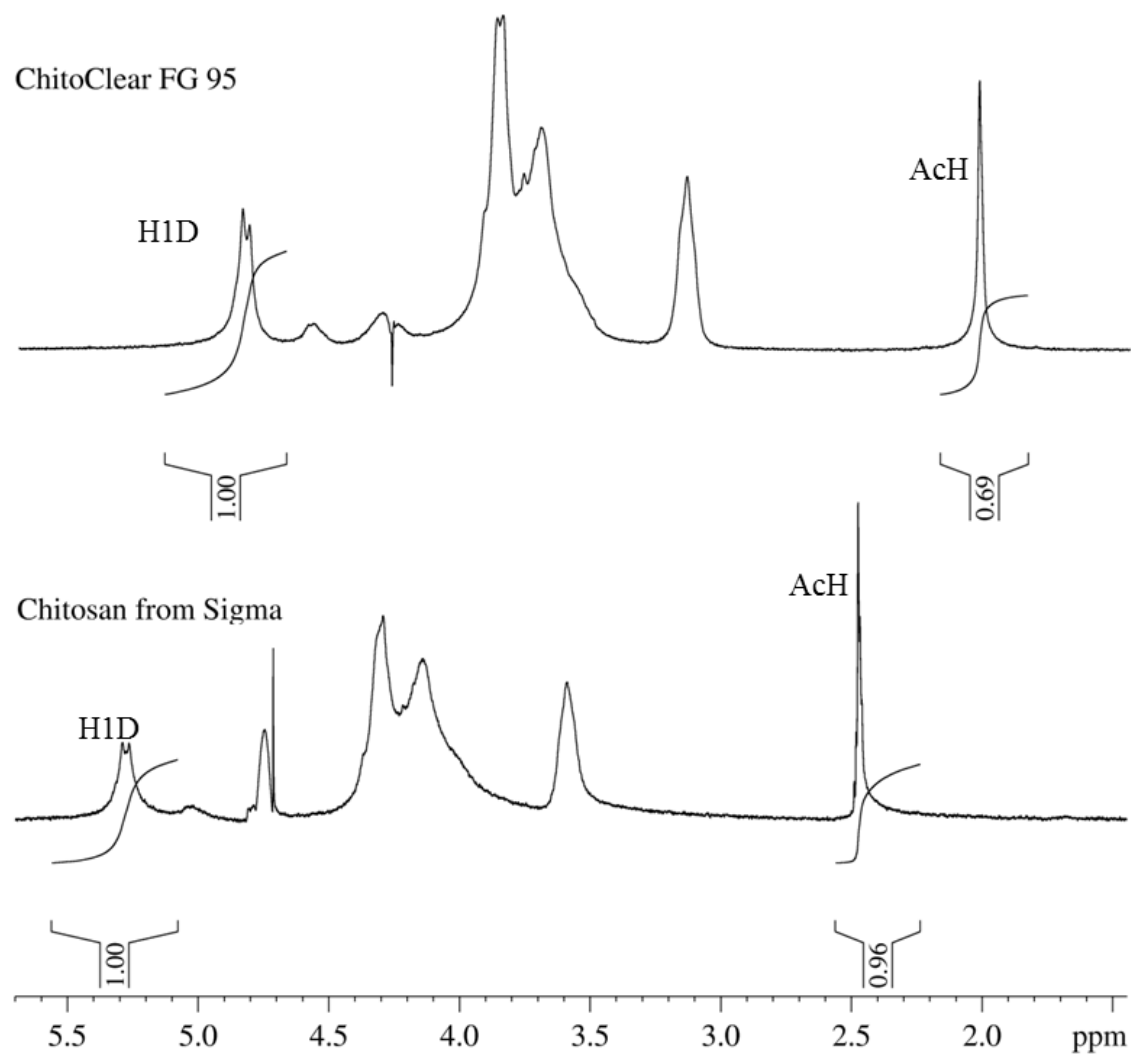


Figure 5.4 $^1\text{H-NMR}$ spectra of ChitoClear FG 95 and Chitosan from Sigma recorded at 80°C in 2% CD_3COOD with integrals used to calculate the DDA.

Based on the spectra the calculated values of ChitoClear FG 95 and Chitosan from Sigma were 81.3% and 75.8%, respectively.

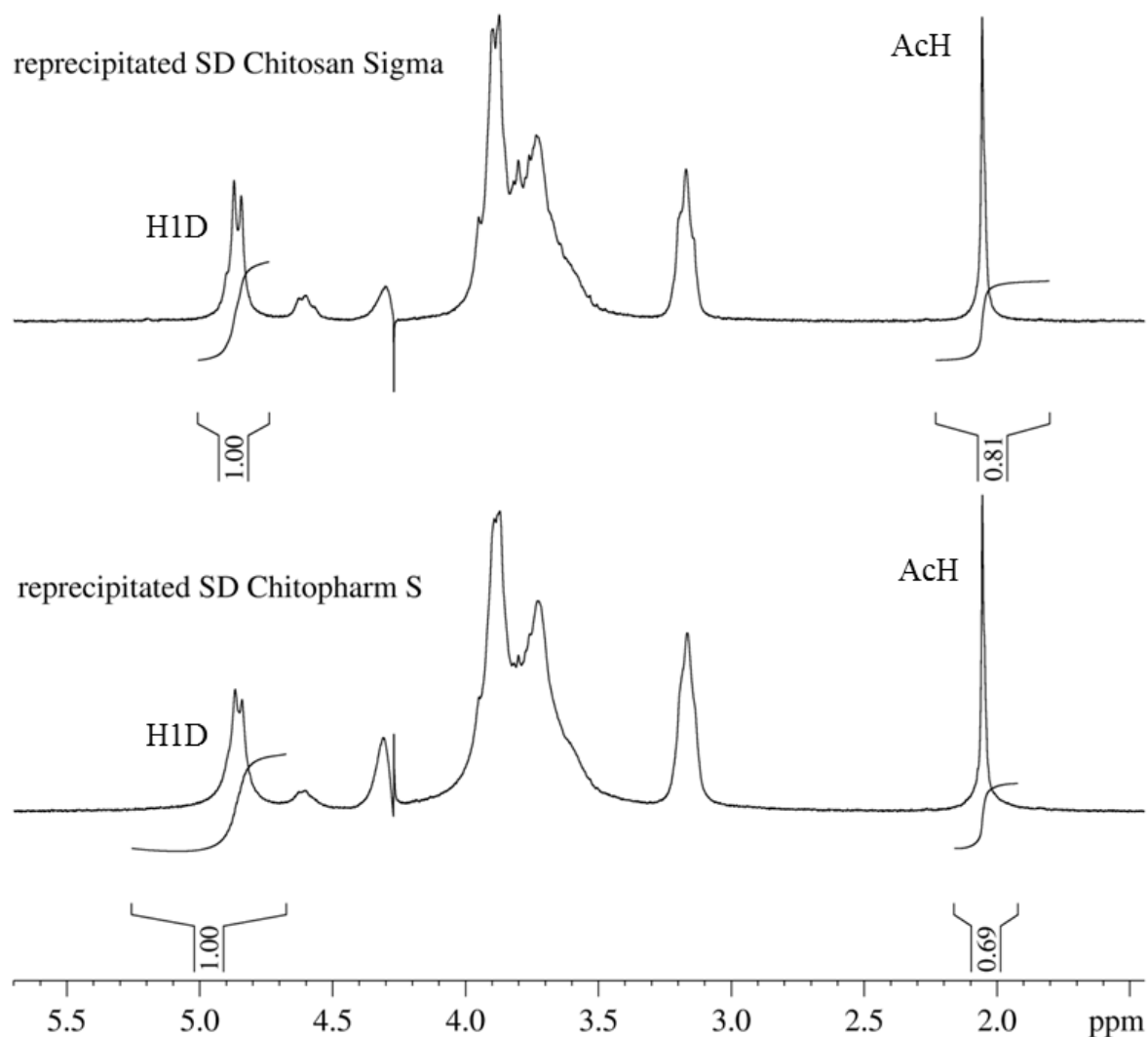


Figure 5.5 $^1\text{H-NMR}$ spectra of the spray dried and reprecipitated chitosan recorded at 80°C in 2% CD_3COOD with integrals used to calculate the DDA.

Regarding Chitopharm S there is, as expected, no change in the DDA after spray drying and reprecipitation. The marginal difference of 81.1% to 81.3% is within the method variability. Looking at Chitosan from Sigma, a little but unexpected increase from 75.8% to 78.7% was observed. It is assumed that this increase is more likely to be an artefact caused by the treatment with sodium hydroxide during the sample preparation than due to the spray drying process. Sodium hydroxide (about 40%) combined with heat is commonly used to obtain highly deacetylated chitosan (Domard, Rinaudo, 1983). The fact that a change in the DDA only occurs for Chitosan from Sigma is probably because it has a lower original DDA

than Chitopharm S. Therefore, Chitosan from Sigma is more accessible to the deacetylation reaction.

5.1.4 Transepithelial Electric Resistance

Transepithelial electric resistance (TEER) was used to investigate whether Chitopharm S affects the cohesion between the Calu-3 cells within the cell layer and if it does to what extent. Transepithelial electrical resistance is a method to measure the paracellular ion flux and thus a measure of the cell layer integrity and the cell network (Deli, 2009). For Caco-2 cells it is already described that chitosan interacts with those cell junctions which lead to a reduced TEER value (Smith et al., 2005). The opening of the tight junctions can increase the amount of antigen that is taken up via the paracellular pathway (Hagesaether, 2011). For testing, 10 mg of Chitopharm S were suspended in 0.5 mL of the cell medium in the apical compartment. Measurements were performed as described in section 4.13.1.1. The obtained results are shown in Figure 5.6.

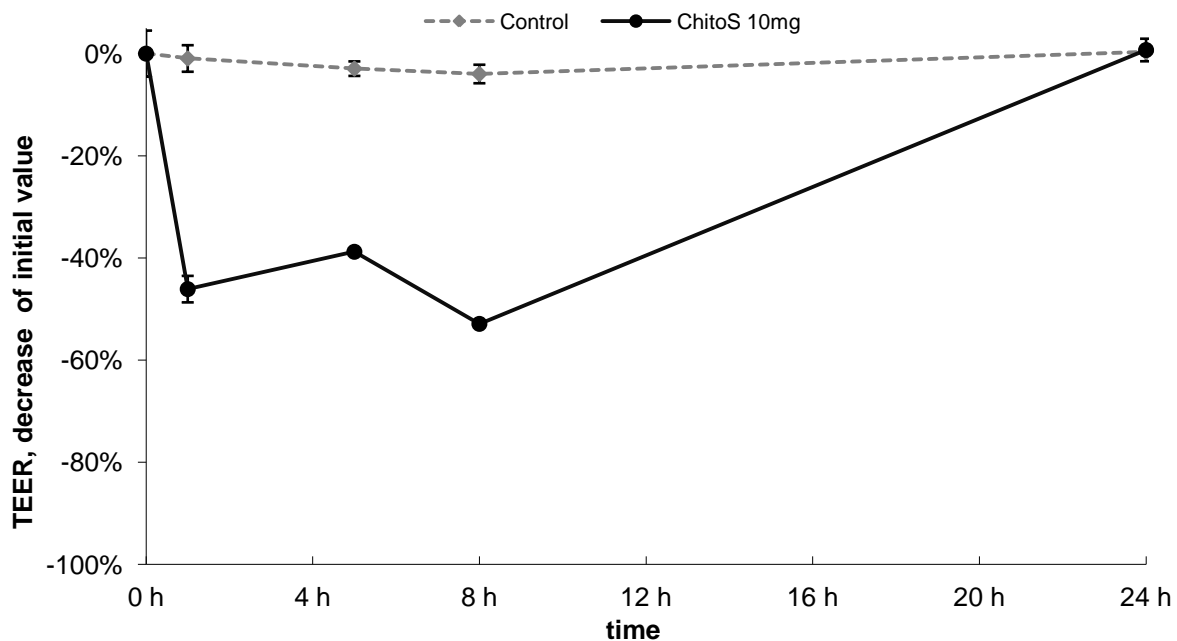


Figure 5.6 TEER measurements of Chitopharm S (black) compared to growth medium control (grey). After 8 h the sample was removed by rinsing. (Error bars show the standard deviation of three TEER measurements)

The measurements show clearly that the cell layer integrity is noticeably affected by the chitosan. This is reflected by the decrease of the TEER value after adding (t=0 h) the chitosan into apical compartment, whereas the cells in medium control were virtually unaffected. After eight hours the sample was removed by rinsing off. Subsequently, both compartments were refilled with fresh medium. As data show, after the sample was removed, the cells recovered. Finally, after 24 h the cell layer integrity is completely restored. Although particles larger than 50 nm cannot simply pass through the opened tight junctions (Jung et al., 2000) the free antigen which is contained in the developed NiM formulation (5.3) can pass and thus enter the human body through the paracellular pathway. This effect will increase the amount of antigen that will be taken up by the body. A quick recovery, as seen in the experiment, is, of course, important in order to obtain full mucosal protection back as soon as possible to avoid the penetration of pathogens or other antigens than those needed for the vaccination.

5.2 In Vivo Evaluation of Chitosan as an Adjuvant in Subcutaneous Vaccine Formulations

As mentioned earlier (3.2), chitosan is known to have adjuvant properties and is seen as a promising future adjuvant by many researchers and immunologists (Zaharoff et al., 2007; Rauw et al., 2010). In order to investigate this effect and to identify the chitosan quality with the highest adjuvant activity an *in vivo* study was conducted. In this study, three chitosans with different properties (summarised in Table 5.3) were characterised (5.1) and then combined with ovalbumin (3.1.2) acting as model antigen for subcutaneous administration (5.2.1). The final formulations were administered subcutaneously via syringe and needle to the neck of C57Bl/6J mice (3.8). Finally, the immunological effect was analysed. For this, the expressions of antigen specific CD4⁺ and CD8⁺ TG T cells in the lymph nodes and the spleen were determined via FACS analysis (4.14). The experimental part of this *in vivo* study was performed at the University of Otago, School of Pharmacy in Dunedin, New Zealand in cooperation with Sarah Hook.

5.2.1 Preparation and Characterisation of Chitosan for the Adjuvant Study

Two out of the three chitosans that were used were modified via spray drying prior to testing. ChitoClear FG 95 was used as received and applied as a suspension while Chitopharm S and Chitosan from Sigma were applied as solutions in PBS. In order to make them accessible for administration via syringe and needle and soluble in physiological PBS both were spray dried as previously described (5.1.1). Viscosities of all three samples were determined (Table 5.3) using the Vibro Viscometer SV-10 (A&D Company Limited, Tokyo, Japan). Cell toxicity of both spray dried samples was analysed via MTT assay (4.13.1.2).

5.2.1.1 Particle Size Distribution of Chitosan and Spray Dried Chitosans

Particle size distributions of all three samples were analysed by laser diffraction using the Helos RODOS system. In addition, a SEM picture of the spray dried Chitopharm S sample which is pictured in Figure 5.7 was made.

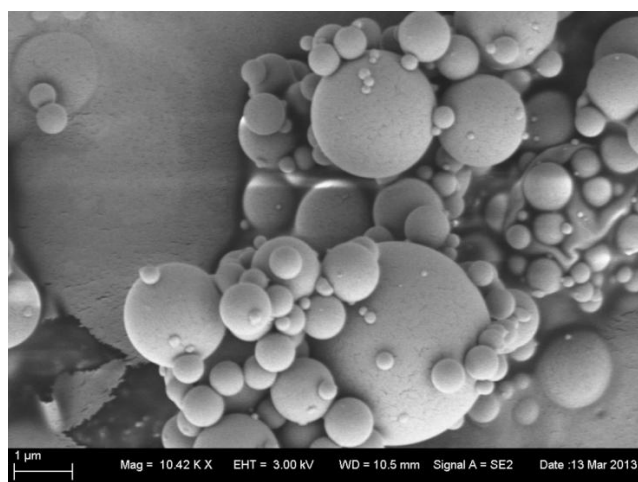


Figure 5.7 SEM picture of spray dried Chitopharm S.

X_{50} -values determined via laser diffraction were 4.06 μm for Chitopharm S SD, 2.19 μm for Chitosan from Sigma SD and 20.84 μm ChitoClear FG 95 (see also Table 5.3). Regarding both spray dried chitosan samples the particle size and the distribution are of minor importance because both were administered as solutions dissolved in PBS. This is important, because it can be assumed that the partially soluble chitosan can be transported to lymph nodes nearby the site of

injection (SOI) or even to the spleen relatively fast and easier than large non soluble particles such as those from ChitoClear FG 95 which was given as suspension. Because of their size the administered chitosan particles will, probably, not be transported away from the SOI or if only to a much smaller extent than the dissolved chitosans. These differences in formulation can lead to differences in the immune response because if the chitosan is transported to the spleen this can lead to a direct interplay between the adjuvant and the immune cells there. Additionally, it is known from literature that chitosan as adjuvant, formulated in a soluble form and administered s.c. can lead to significantly higher values of CD4⁺ cells (Zaharoff et al., 2007) while the s.c. administration of a chitosan suspension is known to be rather ineffective (Marcinkiewicz et al., 1991).

5.2.1.2 Results of the MTT Cytotoxicity Assay

The MTT assay which is described in section 4.13.1.2 was performed in order to analyse the cell toxicity of both spray dried chitosan qualities that were administered subcutaneously in the adjuvant *in vivo* study. ChitoClear FG 95, which was used as received, is insoluble in each of those buffers that can be used for MTT assay and thus it was not accessible for testing. The results of both spray dried chitosan samples are displayed in Figure 5.8. The LC_{50} values were calculated via a four parametric sigmoidal plot and turned out to be 0.3260% for Chitopharm S SD and 0.3031% Chitosan from Sigma SD.

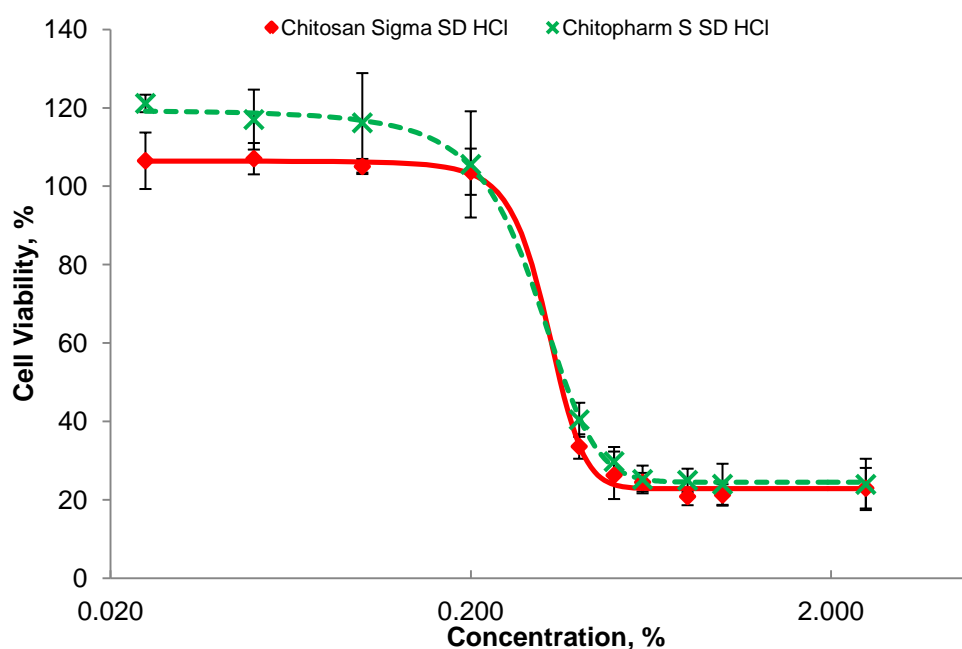


Figure 5.8 MTT toxicity data of spray dried Chitopharm S and Chitosan from Sigma. Error bars represent the standard deviation of the quadruple analysis.

5.2.2 Summarised Characteristics of the Chitosan for the Adjuvant Study

All results of the characterisation of all chitosans that were used in the adjuvant study are summarised in Table 5.3.

Table 5.3 *Parameters of interest of the chitosans used for the in vivo study for subcutaneous vaccine administration. (SD=spray dried sample; WSC=Water-Soluble-Protein-like-Contaminates; n.d.=not determined)*

	Chitopharm S SD	Chitosan Sigma SD	ChitoClear FG 95
M_w, kDA	78.1 (±0.69)	149.1 (±6.46)	101.8 (±4.99)
DDA, %	81.3	78.7	81.0
Endotoxin level, IU*g⁻¹	3.1	1.5	46.8
WSC, %	0.0124	0.0483	0.0392
rel. WSC ratio	1	3.9	3.2
pH of a 1% sol. in water	3.55	3.32	n.d.
Viscosity of 1% sol. in PBS 7.4, mPas	4.27	3.78	1.04 (suspended)
LC₅₀ in Calu-3, %	0.3260	0.3031	n.d.
X₅₀-value, μm	4.06	2.19	20.84

5.2.3 Animal Preparation and Vaccination Procedure

The adoptive transfer method (Pettini et al., 2009) was used to study antigen specific primary T cell response after immunisation. For this, suspensions of single OT-I and OT-II lymphocytes (4×10^6 cells) obtained from the lymph nodes and spleens of the OT-I/II mice were injected into the tail vein of the C57BL/6 mice. Animals were divided into seven groups with three animals per group. On the next day, all mice received a subcutaneous immunisation into a dorsal skin fold of 10 μg OVA formulated in either 200 μL alum gel (Alu-Gel-S, Serva, Germany) (group 1) or with 1 mg of spray dried Chitopharm S (group 2), ChitoClear FG 95 (group 3) or spray dried Chitosan from Sigma (group 4), dissolved and suspended, respectively, in 200 μL sterile PBS. The groups 5, 6, and 7 received 1 mg of spray

dried Chitopharm S, ChitoClear FG 95 or spray dried Chitosan from Sigma in 200 μ L sterile PBS without antigen. Vaccinations were repeated at day 28. Samples were harvested on day 31. Obtained cells were prepared as described before (4.14.1).

Table 5.4 *Vaccine groups and the formulations they received.*

	Received Formulation
Group 1	OVA+alum
Group 2	OVA+Chitopharm S SD
Group 3	OVA+ChitoClear FG 95
Group 4	OVA+Chitosan from Sigma SD
Group 5	Chitopharm S SD
Group 6	ChitoClear FG 95
Group 7	Chitosan from Sigma SD

5.2.4 Results of the *in vivo* evaluation of the Adjuvant Effect

The obtained FACS data were analysed with respect to total number and percentages of CD4⁺ and of CD8⁺ transgenic (TG) cells as shown below. It can be seen that the spray dried Chitosan from Sigma combined with OVA (group 4) led to a significant increase in CD4⁺ TG cells in total number compared to all three antigen-free formulations (group 5, 6, 7). Compared to the other antigen-containing formulations (group 1, 2, 3) the obtained differences in the mean values are not significant (Figure 5.9).

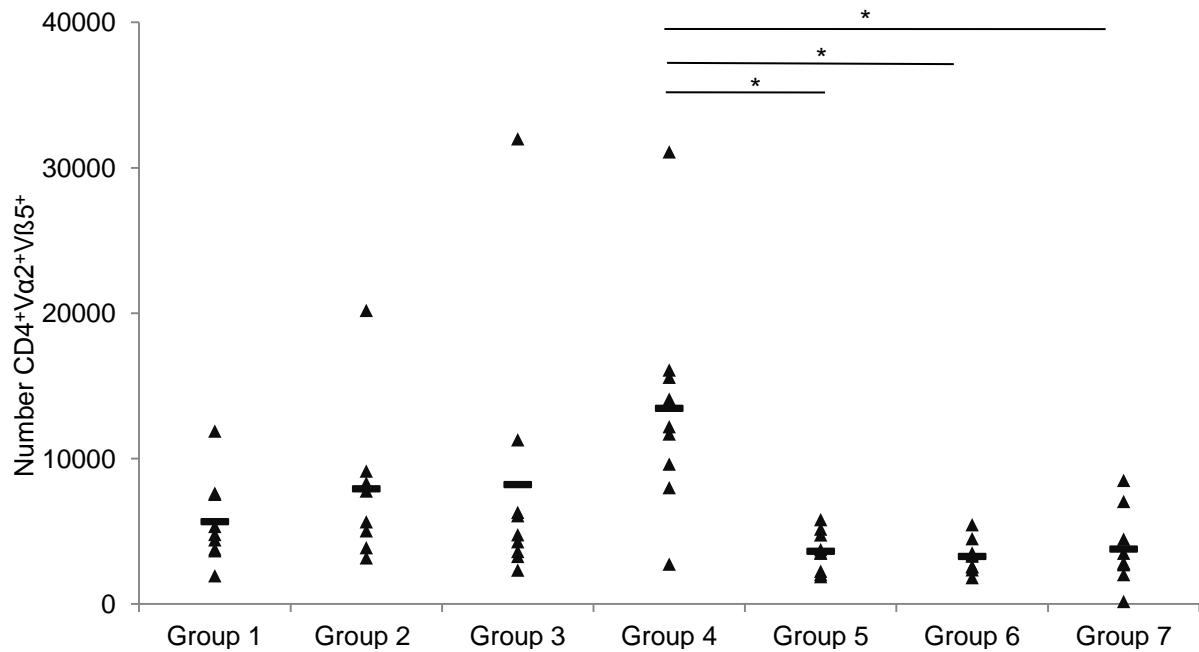


Figure 5.9 Total number of CD4⁺ TG cells from the lymph nodes (LN). Data from each Animal (triangle) and the mean group values (black bar). (* $p \leq 0.05$; One way ANOVA on ranks, Dunn's method)

When looking at the percentage of CD4⁺ TG cells it can be seen that the suspended ChitoClear FG 95 formulation with antigen (group 3) showed a significant increase in CD4⁺ TG cells compared to the three antigen-free formulations (group 5, 6, 7) but not compared to other antigen-containing formulations (groups 1, 2, 3; Figure 5.10). However, the variability within this group was by far the highest.

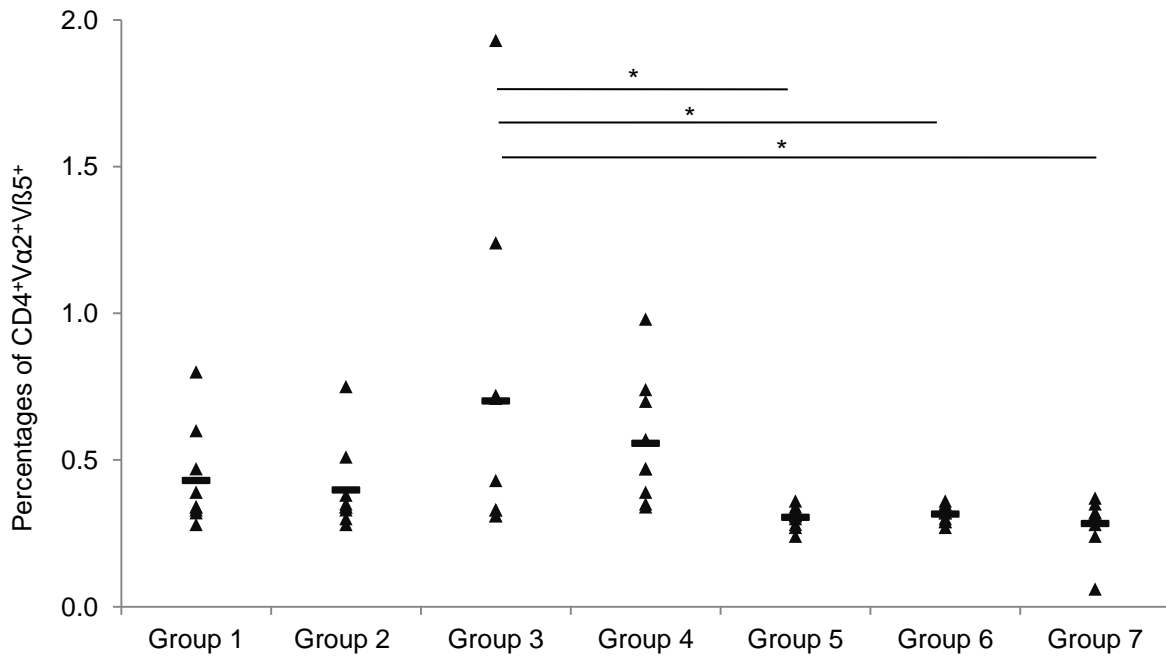


Figure 5.10 Percentage of CD4⁺ TG cells from the lymph nodes (LN). Data from each Animal (triangle) and the mean group values (black bar). (*p ≤ 0.05; One way ANOVA on ranks, Dunn's method)

Regarding the CD8⁺ TG cells it can be seen that the spray dried Chitosan from Sigma (with OVA; group 4) showed the best performance. Regarding the total number of CD8⁺ TG cells (Figure 5.11) it led to a significantly increased mean value compared to all antigen-free formulations (group 5, 6, 7) and also when it is compared with the control group (OVA+alum; group 1). Regarding the spray dried Chitopharm S it can be seen that the antigen-containing formulation (group 2) led to a significantly increased total number of CD8⁺ TG cells compared the antigen-free formulation of Chitopharm S (group 5).

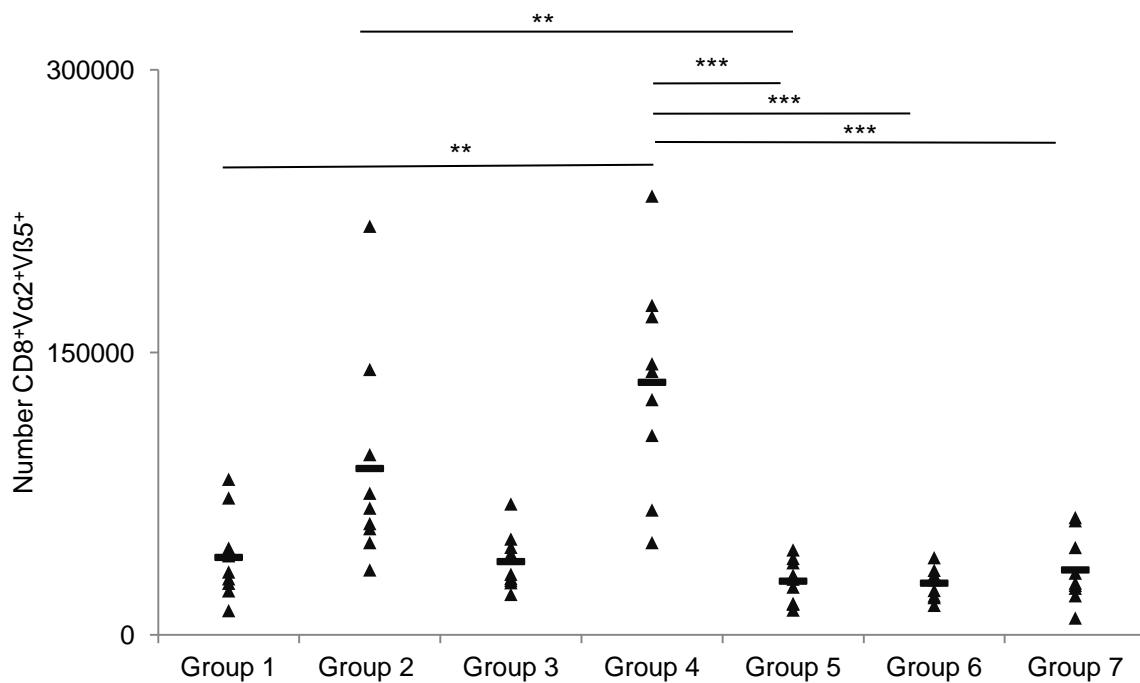


Figure 5.11 Total number of CD8⁺ TG cells from the lymph nodes (LN). Data from each Animal (triangle) and the mean group values (black bar). (* $p \leq 0.05$, ** $p \leq 0.01$, *** $p \leq 0.001$; One way ANOVA)

Regarding the percentage of CD8⁺ TG cells (Figure 5.12), again the spray dried Chitosan from Sigma with OVA (group 4) led to a significantly increased mean value compared to the antigen-free formulations (group 5, 6, 7). And again spray dried Chitopharm S with antigen (group 2) led to significantly higher values compared to its antigen-free formulation (group 5).

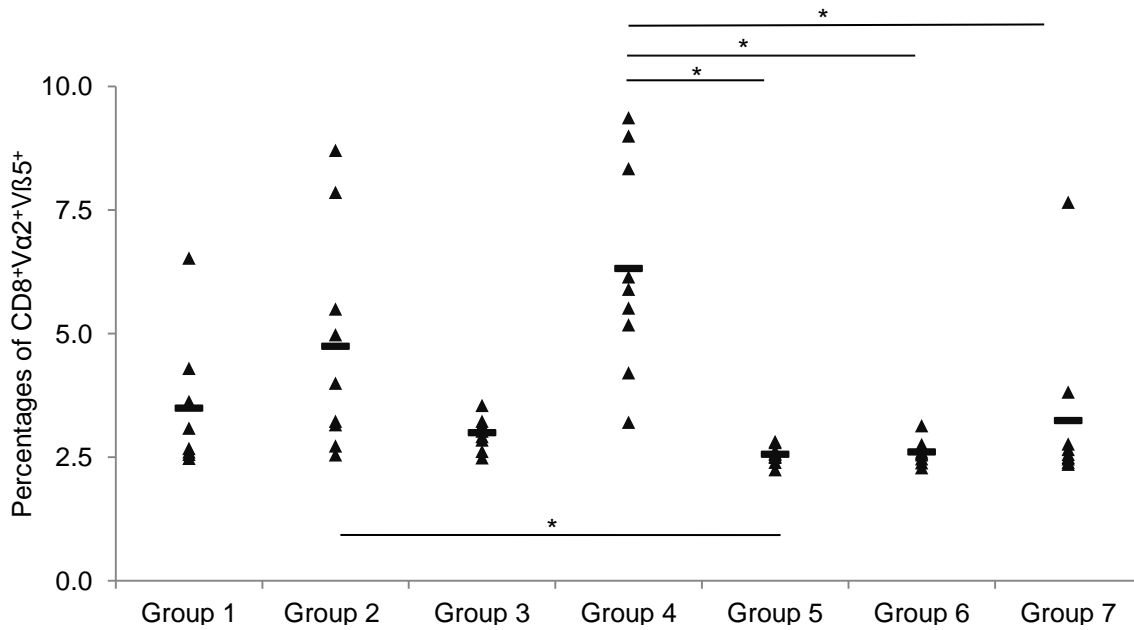


Figure 5.12 Percentage of CD8⁺ TG cells from the lymph nodes (LN). Data from each Animal (triangle) and the mean group values (black bar). (* $p \leq 0.05$; One way ANOVA on ranks, Dunn's method)

In sum, it can be concluded that chitosan administered with antigen led to an increase in CD4⁺ and CD8⁺ transgenic cells compared with chitosan given without antigen as it was shown for Chitosan from Sigma and in some cases for Chitopharm S. It can be stated that chitosan alone did not lead to unspecific proliferation of CD4⁺ and CD8⁺ TG because an increase in the expression of these cells was not detected when chitosan was administered without the antigen. It is noteworthy that Chitosan from Sigma with OVA (group 4) led to significantly higher values regarding total number of CD4⁺ TG cells as well as the total number and the percentage of CD8⁺ TG cells compared to all three antigen-free chitosan formulations. Chitosan from Sigma with OVA (group 4) also showed a significant increase in total number of CD8⁺ TG cells compared to the positive control of

OVA and alum (group 1). This indicates that this combination partly led to a significantly stronger cell-mediated immune response. The FACS data obtained from the spleen preparations are not shown because for all statistic comparisons no significant differences were observed, thus, it can be concluded that the adjuvant effect of chitosan mainly occurs in the lymph nodes nearby the SOI, even for the partially soluble samples. The data show that Chitosan from Sigma triggered the highest cell-mediated immune response. Chitosan from Sigma had the highest molecular weight of the three chitosans that were tested. It is assumed that a higher molecular weight leads to a slower diffusion of the antigen away from the SOI. This effect may extend the interaction between the antigen and APCs located at the SOI and thus increases the expression of, mainly, CD8⁺ TG cells. The formation of a depot at the SOI is a known mechanism of action for adjuvants (Ribeiro, Schijns, 2010). Based on the obtained results, Chitosan from Sigma was identified as the chitosan with the highest adjuvant activity. Next, a nano-in-microparticle formulation production method was developed. Finally, Chitosan from Sigma was formulated as a nano-in-microparticle (NiM) formulation and was tested in a second *in vivo* study (immunisation study).

5.3 Nano-in-Microparticle Formulation Development

The aim was to develop a dry powder model vaccine formulation which should be administered into the nasal cavity or the lungs. The following formulation properties were set as requirements: the primary antigen carrier should be a nanoparticulate system with primary particles about 200 to 300 nm in diameter so that these particles can be taken up by the specialised M-cells (2.2.1) (Sharma et al., 2009). The primary nanoparticles should be based on the biopolymer chitosan (3.2). By drying these primary particles should be transferred into a dry powder formulation which can be administered intranasally and pulmonary via nasal powder dispersers or dry powder inhalers to the desired target regions inside the nasal cavity or the lungs. Within the entire process the antigen has to be unaffected reading its structure, integrity and bioactivity. To meet these requirements a nano-in-microparticle (NiM) formulation was developed by a very

gentle two-step process composed of the preparation of primary nanoparticles consisting of chitosan and DCA associated with the antigen (BSA or OVA) via ionic gelation and a drying step for which spray and freeze drying with mannitol and trehalose were explored and optimised. The nanosuspension obtained in the interim stage was analysed with respect to its particle size distribution and antigen loading efficiency of the particles. Additionally, the resulting particle size of the nanoparticles was analysed in dependence of different parameters such as pH value, the antigen concentration and molecular weight of the chitosan. After drying the particle size distribution of the primary nanoparticles was verified and the final formulations were analysed with respect to their aerodynamic characteristics such as particle size distribution after air dispersion, dispersion behaviour after device actuation, nasal deposition profile and respirable fraction as well as their cell toxicity and cell uptake. Finally, in a second *in vivo* study (immunisation study) the developed dry powder nano-in-microparticulate formulation was administered intranasally to mice in order to evaluate its immunogenicity.

5.3.1 Ionic Gelation

In the case of ionic gelation two oppositely charged particles wherein one of them usually is a polymer (e.g. chitosan) were brought together. The opposite charges equalise each other and an insoluble system is generated. Because this process is very fast the resulting particles are often in a micrometre or nanometre scale. On the one hand ionic gelation is a very attractive way to produce micro-or nanoparticles with chitosan because the equipment expense is relatively manageable and the stress exposed on the product is low compared to other techniques such as milling. Usually toxic agents or organic solvents are not required and the gelation process can be performed at room temperature, just using stirring (Boonsongrit et al., 2006). But on the other hand finding the right conditions regarding polymer and counter ion concentrations is a challenging task, because nanoparticles are only formed in a specific combination of both (Xu, Du, 2003). In addition, the pH value and ionic strength in the surrounding medium have to be adjusted carefully to achieve stable nanosuspensions (Deng et al., 2009). In this work, an

ionic gelation method was developed to prepare chitosan-desoxycholate nanoscale particles of about 220-280 nm in diameter. During the particle forming process the model antigens, BSA or OVA, were partially associated with those nanoparticles. First, a standard preparation method was developed by trying different concentrations and ratios of the chitosan and the counter anion solution. Subsequently, it was investigated how different molecular weights and pH values affect the size and distribution of the resulting particles. Three chitosans (Chitopharm S, M, L) were used, in order to assess the influence of different molecular weights to the resulting mean particle size. Nanoparticles out of five saline buffered Chitopharm S solutions with different pH values were prepared and analysed in order to evaluate the influence of the pH value on the particle size and the antigen loading efficiency. Finally, nanoparticles from counter ion solutions with different antigen concentrations were prepared and analysed with respect to the resulting antigen loading efficiency. All these investigations were performed in order to gain a fundamental understanding of the gelation process. Later, the knowledge generated from these experiments was brought together with the results obtained from the adjuvant *in vivo* study (5.2) and applied to prepare tailored nanoparticles for the immunisation *in vivo* study (5.6).

5.3.1.1 Formation of Nanoparticles of Chitosan and DCA by Ionic Gelation

The development of a method which led to reproducible preparation of antigen containing Chitosan-DCA nanoparticles was started by testing different concentrations of Chitopharm S (1%, 0.5%, 0.2%, 0.1%) dissolved in 1% acetic acid combined with different concentrations of DCA (0.8%, 0.2%, 0.1%) dissolved in ddH₂O together with 5 mg*mL⁻¹ BSA. These solutions were also combined in different ratios to each other but in the following only some results obtained by a two (chitosan solution) plus one (DCA solution) ratio are shown. First, all substances were dissolved to the appropriate concentrations then the DCA solution was added to the chitosan solution under stirring at 650 rpm. The preparation procedure was performed at room temperature in 25 mL or 50 mL snap-cap glass vessels using four-way PTFE magnetic stirrer. Visual appraisal of results unsurprisingly showed that a higher concentration of chitosan and DCA led to a stronger

turbidity (Figure 5.13; Figure 5.14). This indicates that at higher concentrations more insoluble chitosan-DCA particles were formed.



Figure 5.13 0.1% (-007), 0.2% (-006) and 0.8% (-005) DCA solutions added to a 1% Chitopharm S solution (dissolved in 1% acetic acid). Control (C) is the 1% chitosan solution.

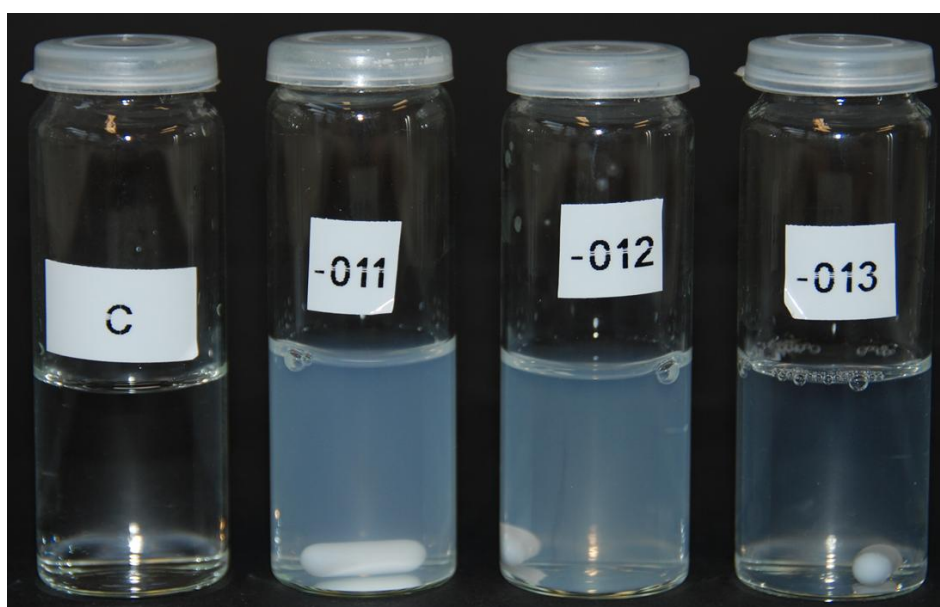


Figure 5.14 0.1% (-013), 0.2% (-012) and 0.8% (-011) DCA solutions added to 0.1% Chitopharm S solution (dissolved in 1% acetic acid). Control (C) is a 0.1% chitosan solution.

It can be seen that the use of a 1% chitosan solution led to monomodal distributed micro- but not nanoparticles (Figure 5.15). By reducing the chitosan concentration to 0.1% a group of particles of about 100 to 300 nm (first peak red line; Figure 5.16) was obtained but the particle size distribution was bimodal. In addition, these particles showed a distinct agglomeration tendency over time (from the red over the blue to the green curve; time period 10 min) as displayed in Figure 5.16. Therefore, it has to be stated that the produced nanoparticles were unstable over time and did not stay in their original shape.

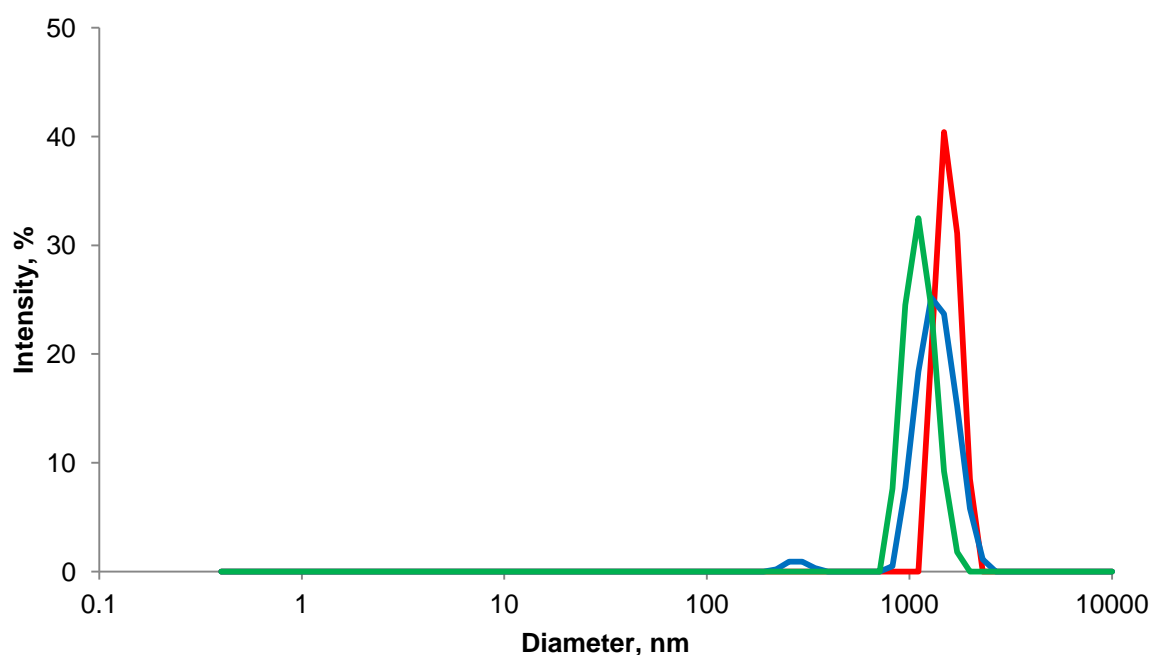


Figure 5.15 PCS data of a 1% Chitopharm S solution precipitated with 0.8% (green), 0.2% (red) and 0.1% (blue) DCA solutions, respectively. (All curves represent the mean of three independent measurements)

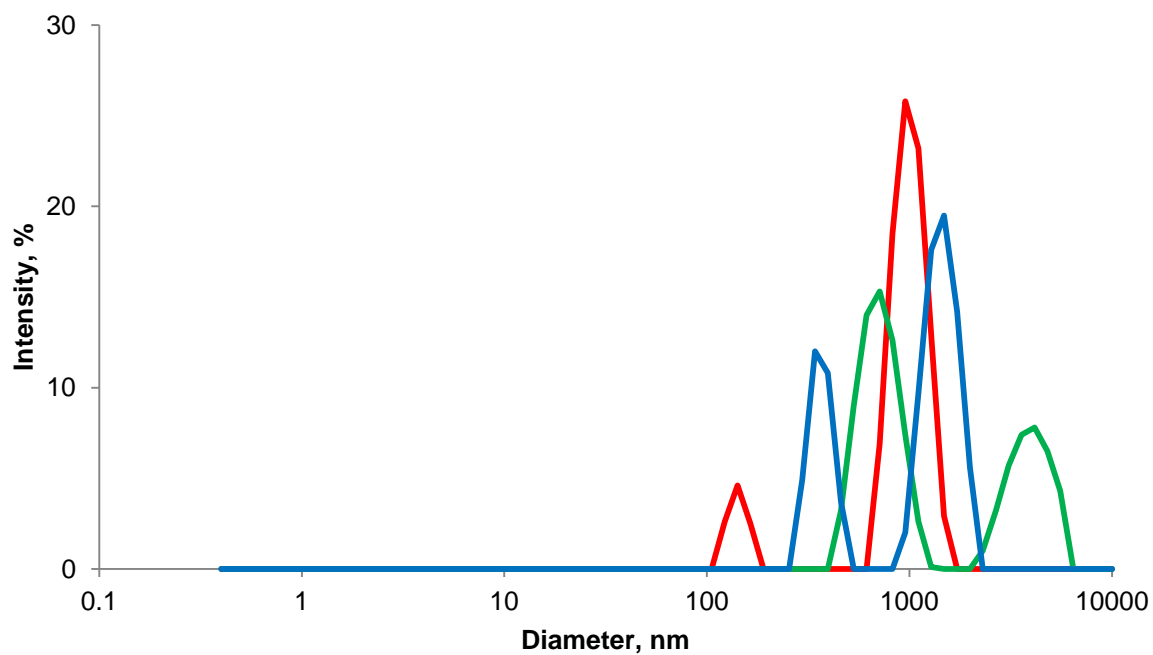


Figure 5.16 PCS data of particles obtained from a 0.1% Chitopharm S solution precipitated with a 0.2% aqueous DCA solution. Particle growth over time (from red to blue to green) was observed. (n=3; every curve represents one independent measurement)

5.3.1.2 Adding PBS for stabilising the Particles

It is known that the ionic strength of the surrounding medium has a strong influence on the stability of nanoparticles (Fan et al., 2012) and thus they can be stabilised by using buffers. Therefore, different volumes of PBS buffer pH 7.4 were added to the chitosan solution before the particle forming process was induced in order to stabilise the generated particles. This modification was combined with a pH adjustment and led best results regarding the size, distribution and stability of the nanoparticles and thus was adopted as standard method (5.3.1.3). Twenty-four hours after preparation the particles were still stable, monodispers distributed and in nanometre scale but it has to be mentioned that a slight increase in their z-average value from 254 nm to 325 nm was observed which is shown in Figure 5.17 and Figure 5.18. This observation is most likely to be caused by swelling of the hydrophilic particles in the aqueous dispersion medium surrounding them. The polydispersity indices (4.5.1) were 0.176 and 0.251 for the nanosuspension directly and 24 hours after preparation, respectively.

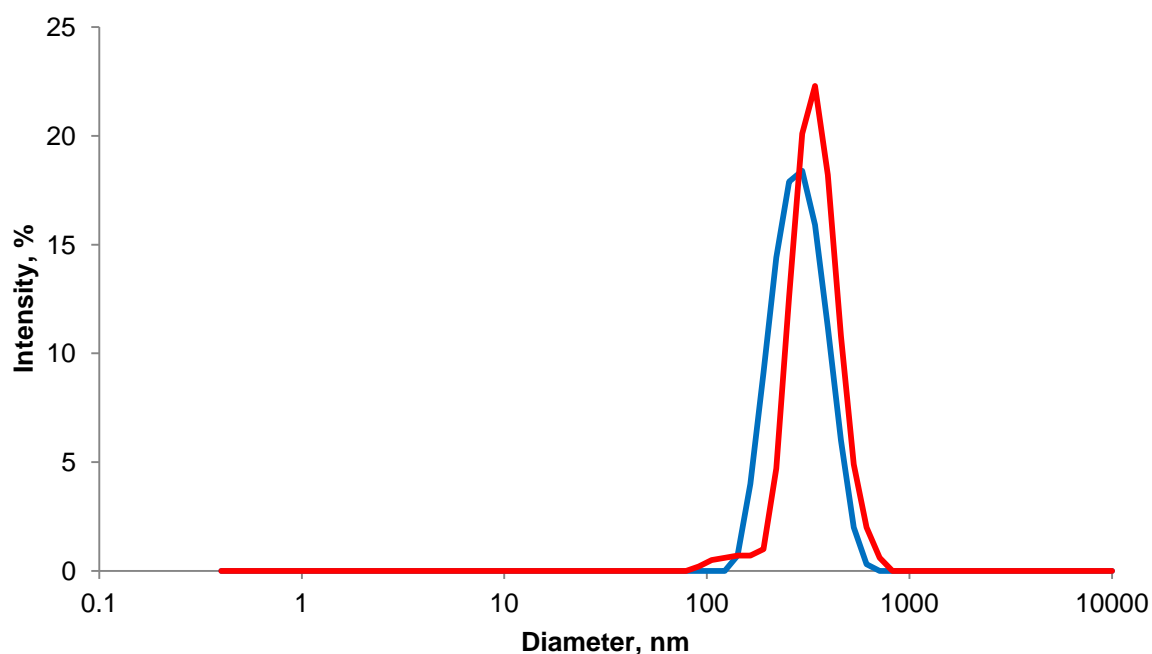


Figure 5.17 Particle size distribution of nanoparticles directly (blue) and 24 hours (red) after preparation.

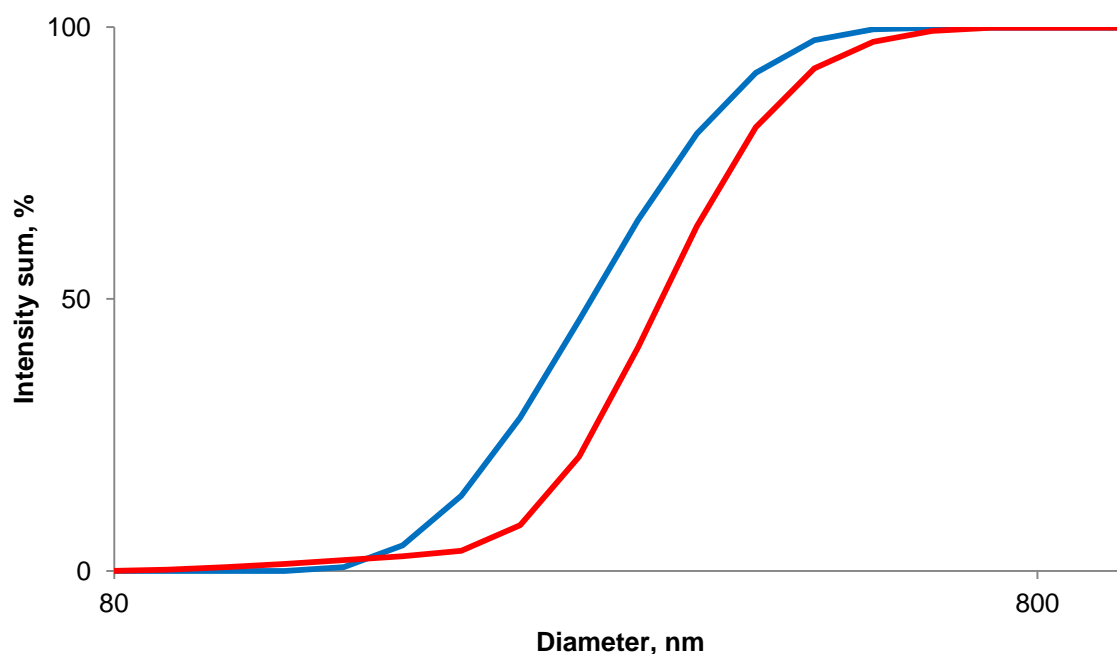


Figure 5.18 Particle size distribution of nanoparticles directly (blue) and 24 hours (red) after preparation.

For visual verification of the measured particle size, an SEM picture of the vacuum dried nanosuspension with size specification was taken and is shown in Figure 5.19. The picture shows an agglomerate of many nanoparticles. It can be seen that the two particles that were measured had a diameter of 104 nm and 163 nm, respectively. The fact that these values were lower than those obtained via PCS is due to two reasons, first larger particles within the agglomerate can also be seen on the SEM picture but the z-average obtained from the PCS measurements is a mean value. Second, with PCS the hydrodynamic diameter is determined and this value for hydrophilic particles suspended in aqueous medium is known to be larger than the diameter of the same particles after drying when water was removed.

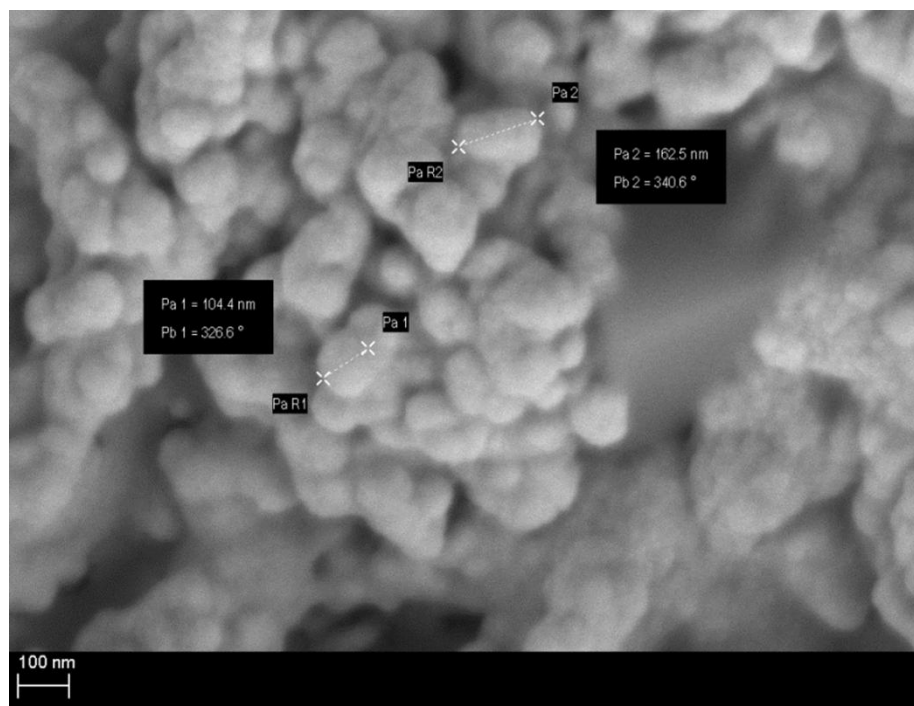


Figure 5.19 SEM picture of the vacuum dried nanosuspension. (Magnification of 64,090x)

5.3.1.3 Final Standard Method

Finally, based on the obtained results best nanoparticles were achieved by using a 0.1% chitosan dissolved in 1% acetic acid. Subsequently, 2.5 parts PBS buffer pH 7.4 and 7.5 parts ddH₂O were added to 10 parts of this chitosan solution. The pH value of the solution was adjusted to 5.5 using 1 N NaOH and subsequently 5 parts of a 0.2% aqueous sodium deoxycholate solution (containing 5 mg*mL⁻¹ antigen) were added under stirring with 650 rpm. This preparation procedure was used as standard method in this work.

5.3.1.4 Influence of the Molecular Weight on the Particle Size.

In order to evaluate the influence of the molecular weight on the resulting particle size of the chitosan-DCA nanoparticles three chitosan qualities with different molecular weights were used for preparation. The molecular weight was determined via static light scattering (4.1), samples were prepared as mentioned above (5.1.2.1). For clarity, molecular weights of those chitosans used in this experiment are again summarised in Table 5.5.

Table 5.5 *Chitosans that were used and their weight-average molecular weight (M_w). (Determined via SLS)*

	Chitopharm S	Chitopharm M	Chitopharm L
M_w , kDA	79.4	123.4	135.2

Chitosan solutions were prepared according to the standard method, chitosan was dissolved in 1 % acetic acid to a concentration of 0.1% then PBS buffer and ddH₂O were added and the pH value was adjusted. Nanoparticles were generated by adding a 0.2% BSA containing aqueous DCA solution under stirring. Obtained nanoparticles were analysed via PCS method (4.5.1).

The influence that different molecular weights of chitosan have on the resulting particle size is shown in Figure 5.20, corresponding PCS data are shown in Figure 5.21 and Figure 5.22. It can be seen that higher molecular weights of chitosan led to an increase in the resulting particle size ($R^2=0.8281$).

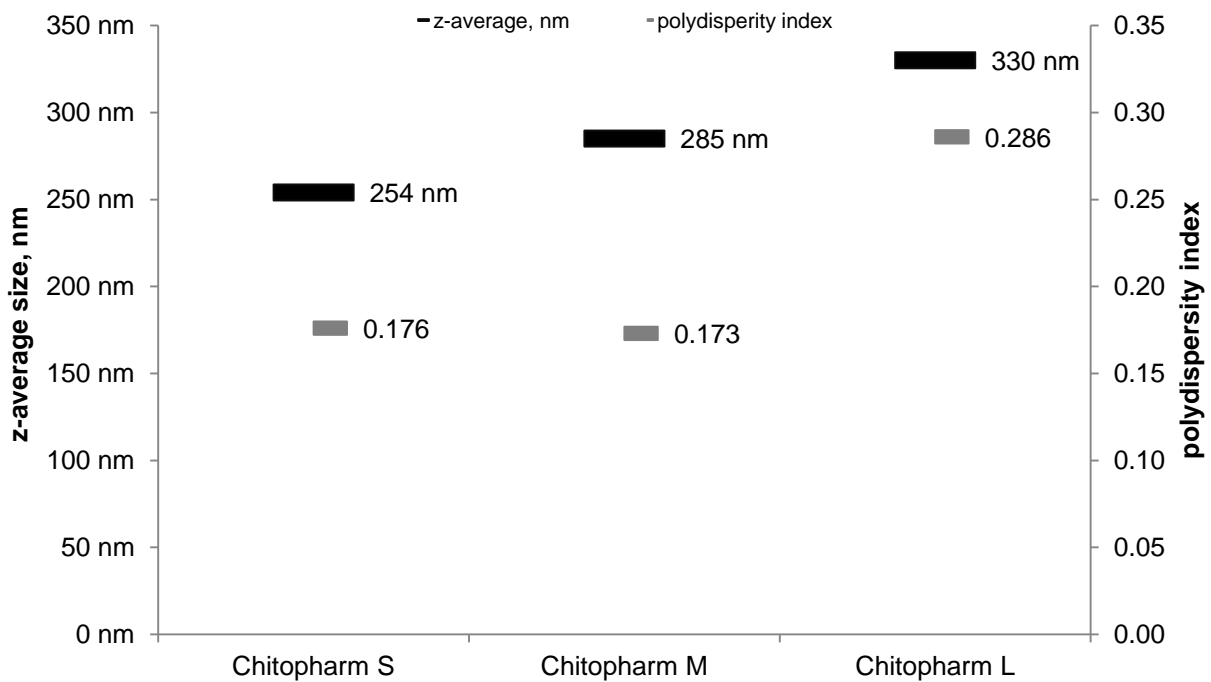


Figure 5.20 Resulting mean particle sizes and polydispersity indices of nanoparticles obtained by using chitosans with different molecular weights.

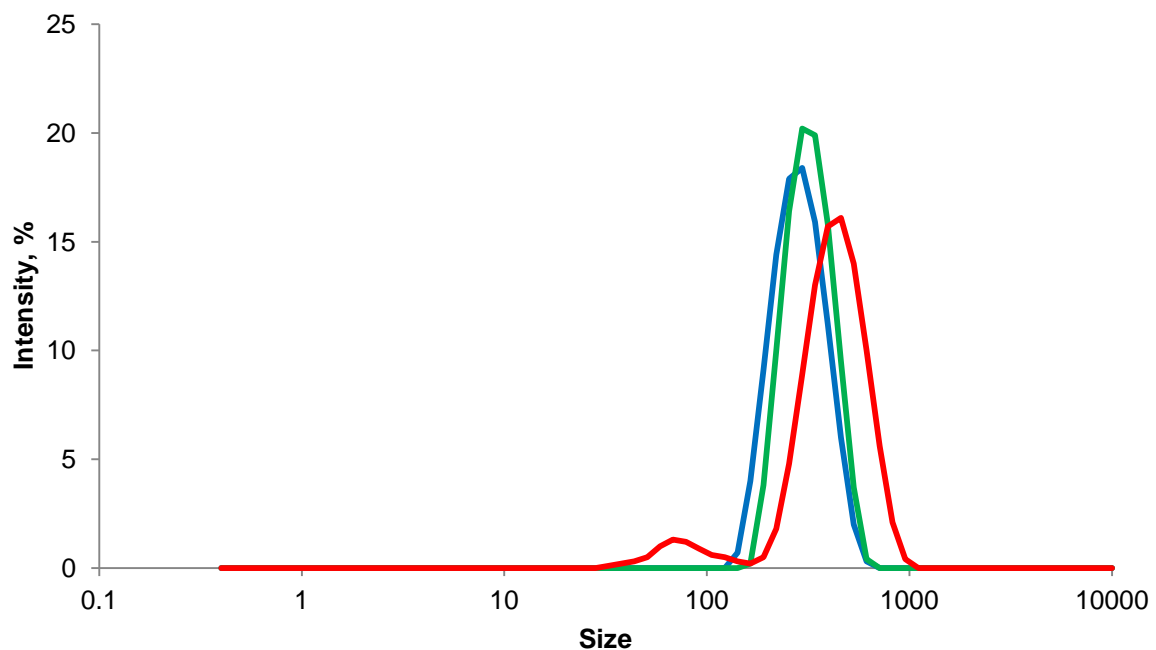


Figure 5.21 Particle size distribution of nanoparticles achieved using low M_w chitosan (blue), medium M_w chitosan (green), high M_w chitosan (red). ($n=3$; each curve represents the mean of three measurements)

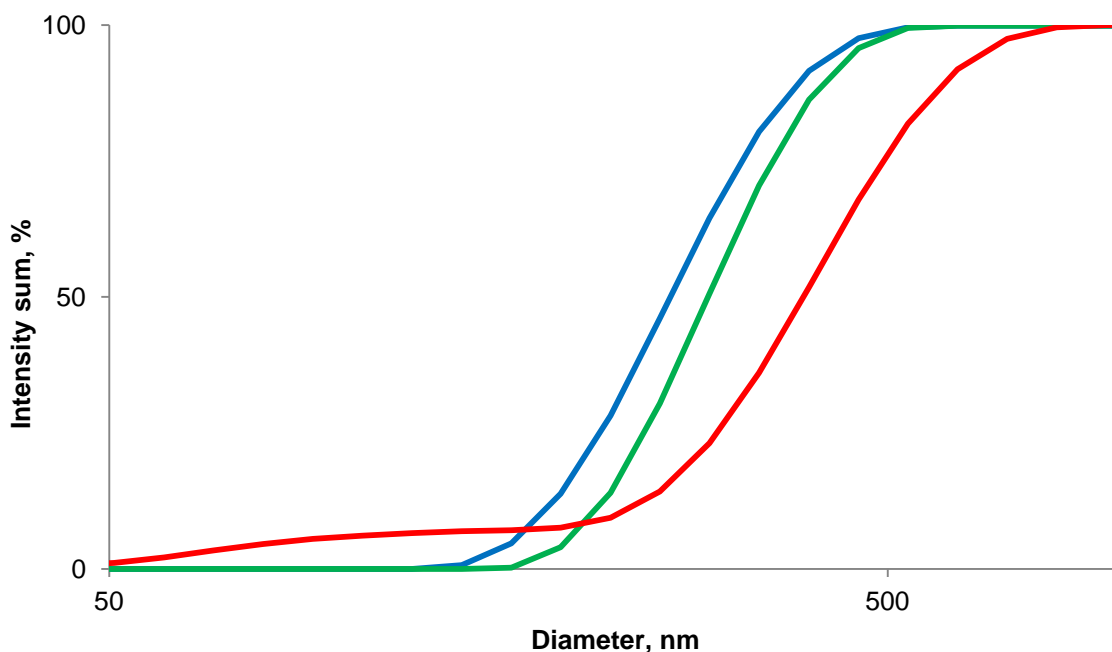


Figure 5.22 Particle size distribution of nanoparticles obtained using low M_w chitosan (blue), medium M_w chitosan (green), high M_w chitosan (red). ($n=3$; each curve represents the mean of three measurements)

The observation that a higher molecular weight of the polymer leads to larger particles has already been described in literature for chitosan with other counter ions (Huang et al., 2004b). Because the target size of the nanoparticles was set to 250 nm it was decided to use Chitopharm S for the following investigations.

5.3.1.5 Influence of the pH value on the Particle Size

In a second experiment the influence of the pH value on the particle size and the loading efficiency was investigated. It is described in literature that a higher DDA of chitosan at otherwise identical conditions leads to more compact particles (statement based on API release data) because of the higher number of reaction sites (Xu, Du, 2003). Because these particles were more compact, it was assumed that a lower pH value will also lead to more compact and thus to smaller particles because at a lower pH values more amino groups are positively charged. For testing, the pH value of the PBS buffered chitosan (Chitopharm S) solution was adjusted to 4.5, 5.5, 5.7, 6.1 and 6.4, respectively, before nanoparticles were generated by adding a 0.2% DCA solution (containing $5 \text{ mg} \cdot \text{mL}^{-1}$ BSA). The obtained particles were analysed regarding their particle size distribution via PCS.

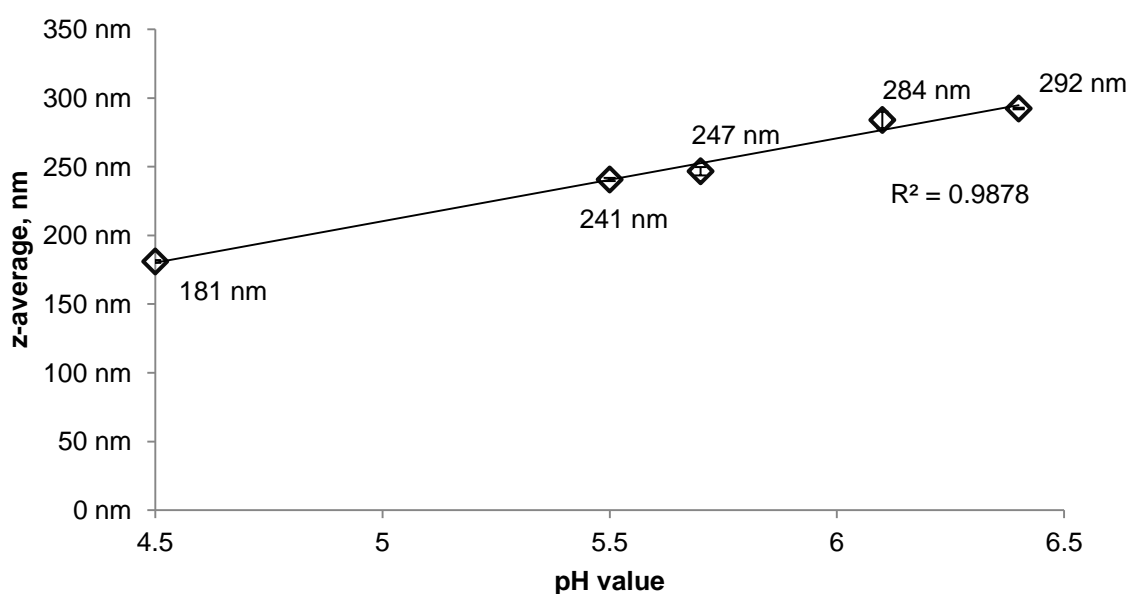


Figure 5.23 Mean particle size as a function of the pH values using Chitopharm S with linear regression line. Error bars represent the standard deviation of the triplicate.

In Figure 5.23 it can be seen that an increase in the pH value is accompanied by an increase in the size of the resulting nanoparticles. It is assumed that this happens because at lower pH values there are more deacetylated amino groups positively charged which thus participate in the reaction and were gelled with the counter ion. The resulting nanoparticles were smaller and, probably more compact (Xu, Du, 2003), because they had less loops in the polymer chain compared to preparation at higher pH values with more uncharged groups which do not participate in the reaction. As shown in Figure 5.23 a very good linear correlation between the pH value and the resulting particle size could be found, proven by the high coefficient of determination of 0.9878.

5.3.1.6 Influence of the pH value on the Loading Efficiency of the Particles

The loading efficiency of chitosan nanoparticles depends on a variety of factors; one is the antigen which is to be encapsulated. Vila et al. showed that for insulin a loading efficiency of over 90% can be achieved while for tetanus toxin the loading efficiency was only 33% when using an otherwise identical preparation method (Vila et al., 2002). Xu et al. have intensively studied the influence of dif-

ferent factors like antigen (BSA) concentration, degree of deacetylation, molecular weight on the loading efficiency (they call it encapsulation efficiency). They found that a higher degree of deacetylation (75.2%; 85.5%; 92%) and a higher molecular weight (ranged from 10 kDa to 210 kDa) tested independently of each other, both led to higher “encapsulation” efficiencies. While an increased antigen concentration (ranged from 1.0 to 3.0 mg*mL⁻¹) resulted in a decreased “encapsulation” efficiency. And interestingly, higher chitosan concentrations are associated by lower “encapsulation” efficiency (Xu, Du, 2003). This effect can be explained by the higher viscosity of the higher concentrated polymer solution which hinders the antigen to participate in the particle forming process (Vandenberg et al., 2001). In this work, it was focused on the loading efficiency which was examined as a function of the pH value and the antigen concentration. The loading efficiency (LE) was analysed at three different pH values, namely 4.5, 5.5 and 6.1. Loading efficiency was determined and calculated as described in section 4.11 using Equation 4.7. Results regarding the loading efficiency at different pH values are shown in Figure 5.24

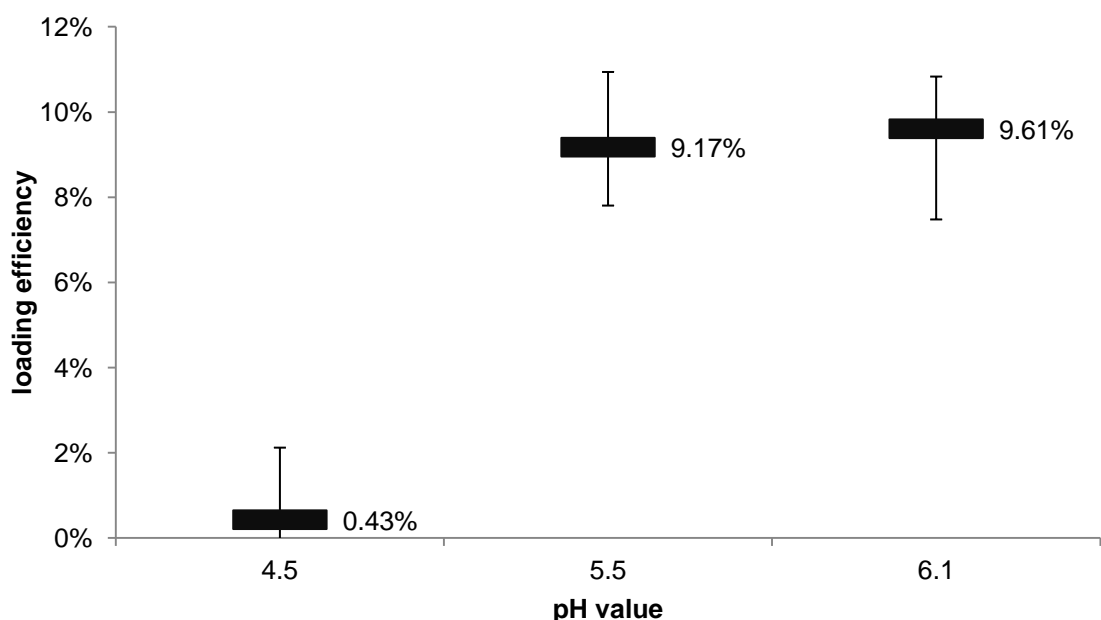


Figure 5.24 Relation between the pH value and the resulting loading efficiency. Error bars represent min and max values of the triplicate. ($R^2=0.8902$)

It can be seen that there are actually no difference in the LE at pH values of 6.1 and 5.5, but there is a sharp decrease in the LE when reducing the pH value to 4.5. The isoelectric point (IEP) of BSA is at pH 4.7 (3.1.1) which means that twice the pH value of the chitosan solution was above (pH 6.1, LE: 9.61%; pH 5.5., LE: 9.17%) and once below (pH 4.5; LE: 0.43%) the IEP of BSA. Above the IEP BSA is, in sum negatively charged and thus it is attracted by the positively charged ammonium groups at the chitosan polymer chain during the particle forming process and probably also on the surface of the nanoparticles after gelation. Below the IEP BSA has, in sum a positive charge and thus is rejected by the like charged ammonium groups so that it is excluded from the particle forming process and also from the particle surface because of electrostatic expulsion and thus it is not associated with the prepared nanoparticles. Results are summarised in Table 5.6.

Table 5.6 *Mean particle sizes, polydispersity indices and LE values for the nanoparticles obtained from PBS buffered chitosan solutions with different pH values. (n= 3; \pm sd; n.d.=not determined)*

pH value	z-Average, nm	Polydispersity Index	Loading Efficiency, %
4.5	181 (\pm 1)	0.254	0.43 (\pm 1.47)
5.5	241 (\pm 1)	0.244	9.17 (\pm 1.61)
5.7	247 (\pm 3)	0.196	n.d.
6.1	284 (\pm 6)	0.273	9.61 (\pm 1.85)
6.4	292 (\pm 1)	0.299	n.d.

5.3.1.7 Influence of the Antigen Concentration on the Loading Efficiency

Beside the influence of the molecular weight and the pH value, the relation between the antigen concentration in the counter ion solution and the resulting loading efficiency was examined. For this purpose, particles were prepared according to the standard production procedure (pH 5.5) with the exception that this time four DCA solutions with different BSA concentrations, namely $10.0 \text{ mg}\cdot\text{mL}^{-1}$, $7.5 \text{ mg}\cdot\text{mL}^{-1}$, $5.0 \text{ mg}\cdot\text{mL}^{-1}$ and $0.5 \text{ mg}\cdot\text{mL}^{-1}$ were used. The total concentration of BSA in the final suspension was thus $2.0 \text{ mg}\cdot\text{mL}^{-1}$, $1.5 \text{ mg}\cdot\text{mL}^{-1}$, $1.0 \text{ mg}\cdot\text{mL}^{-1}$ and $0.1 \text{ mg}\cdot\text{mL}^{-1}$, respectively. Results of this experiment are displayed in Figure 5.25.

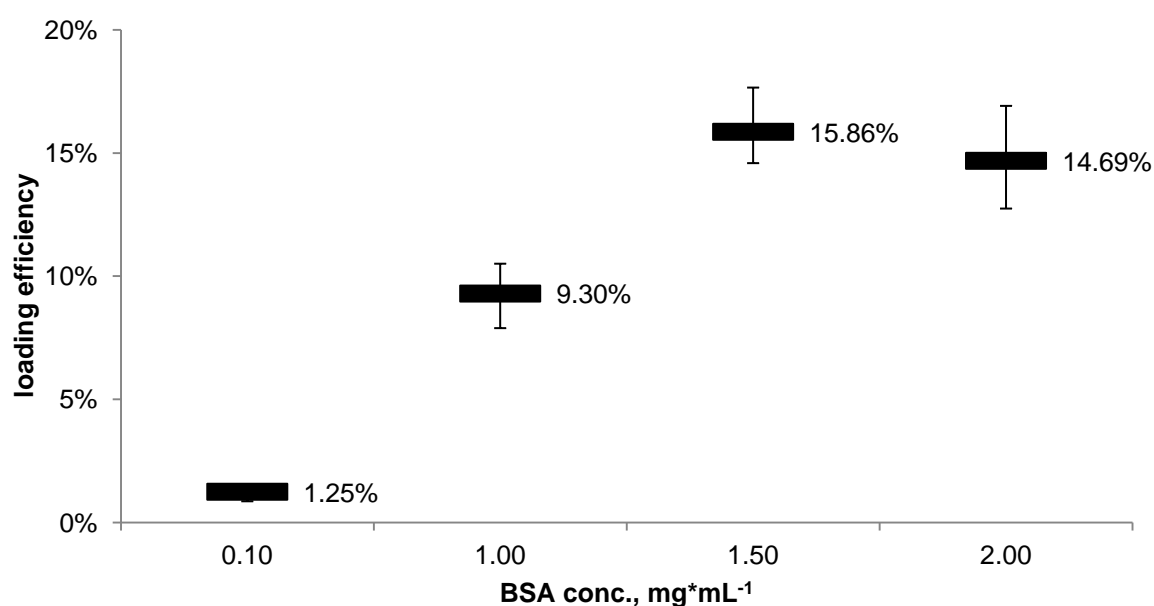


Figure 5.25 Relation between the BSA concentration in the final nanosuspension and the resulting loading efficiency. Error bars represent min and max values of the triplicate. ($R^2=0.8964$)

The results show that at a very low BSA concentration the loading efficiency was close to zero while increasing the concentration of BSA was associated with an increased loading efficiency reaching a maximum value of 15.9% at a concentration of $1.5 \text{ mg}\cdot\text{mL}^{-1}$. A further increase in antigen concentration was no longer coupled with an increasing loading efficiency. The observation that a higher BSA concentration leads to a higher loading efficiency is also described in literature by

Gan et al. (Gan, Wang, 2007) and Berthold et al. (Berthold et al., 1996) for chitosan nano- and microparticles gelled with tripolyphosphate and sodium sulphate, respectively. While a study by Xu and Du (Xu, Du, 2003) indicates the exact opposite also using chitosan and tripolyphosphate. It has to be summarised that the fundamental mechanism is not yet elucidated and there are contradictory data available in literature. At low BSA concentrations there are only very few BSA molecules present compared to the high quantity of DCA counter ions which then very quick saturate the positively charged ammonium groups of the chitosan. After the system is discharged the BSA molecules are no more attracted and thus they are excluded from the particle forming process. At high concentration ($2 \text{ mg} \cdot \text{mL}^{-1}$) the LE decreases again because at constant pH values the quantity of positively charged amino groups is also constant and thus saturated at a given concentration and then the additional BSA molecules cannot participate in the reaction.

5.3.2 Freeze Drying of the Nanosuspension

Lyophilisates prepared in this work were obtained by adding one part of one of those aqueous excipient solutions displayed in Table 5.7 to one part of the previously prepared nanosuspension (standard method 5.3.1.3).

Table 5.7 *Excipient solutions and their concentrations that were used for freeze-drying.*

Excipient	Concentration, %
	5
Mannitol	10
	15
	20
	20
Trehalose	30
	40

All samples were frozen in liquid nitrogen at a temperature of -196°C to avoid the appearance of regions with high salt concentration which may harm the protein (Franks, 1998). Additionally, it is known that the faster the freezing rate the better the redispersibility of the primary nanoparticles which were stabilised inside the lyophilised product (Chung et al., 2012). Subsequently, the frozen samples were transferred into a pre-cooled freeze dryer (Martin Christ GmbH, Osterode am Harz, Germany) at -20°C . After two hours of product acclimatisation the primary drying was started for 12 h at -20°C and a pressure of 1.037 mbar. This step was followed by the secondary drying for 12 h at 20°C and 0.001 mbar. Subsequently, the final freeze dried products were rated visually. It was found that the combination of nanosuspension with a 10% mannitol solution led to the best cake structure. Therefore, this product was further analysed, SEM pictures were taken of which one is shown in Figure 5.26.

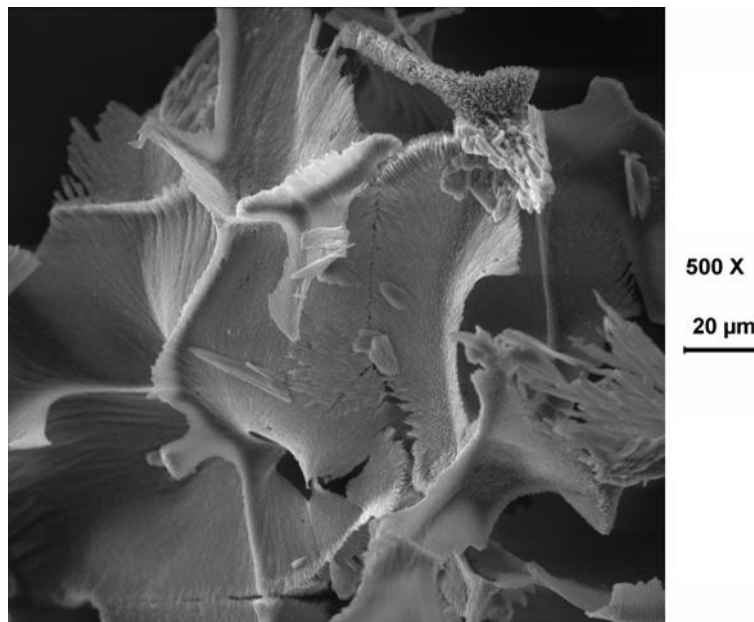


Figure 5.26 SEM picture of a freeze dried product. Nanosuspension plus 10% mannitol solution (Magnification: 500x)

The final composition of the freeze dried formulation with mannitol is shown in Table 5.8.

Table 5.8 Composition of the freeze dried formulation. (Calculated values)

Component	Amount
Chitosan	0.4%
Na-Deoxycholate	0.4%
Antigen (BSA)	1%
PBS salts	1%
Mannitol	97.2%

The particle size distribution of the primary nanoparticles prior to and after freeze drying was analysed via PCCS (4.5.1) using the Sympatec Nanophox. The freeze dried sample was reconstituted in ddH₂O and directly measured. Results are summarised in Table 5.9, PCCS data before and after freeze drying are shown Figure 5.27 and Figure 5.28, respectively. The final product was stored at 0% relative humidity and room temperature prior to measurement.

Table 5.9 Mean particle size before and after spray drying.

Sample	x ₅₀ Diameter
Nanosuspension	282 nm
Freeze Dried Product, reconstituted	185 nm

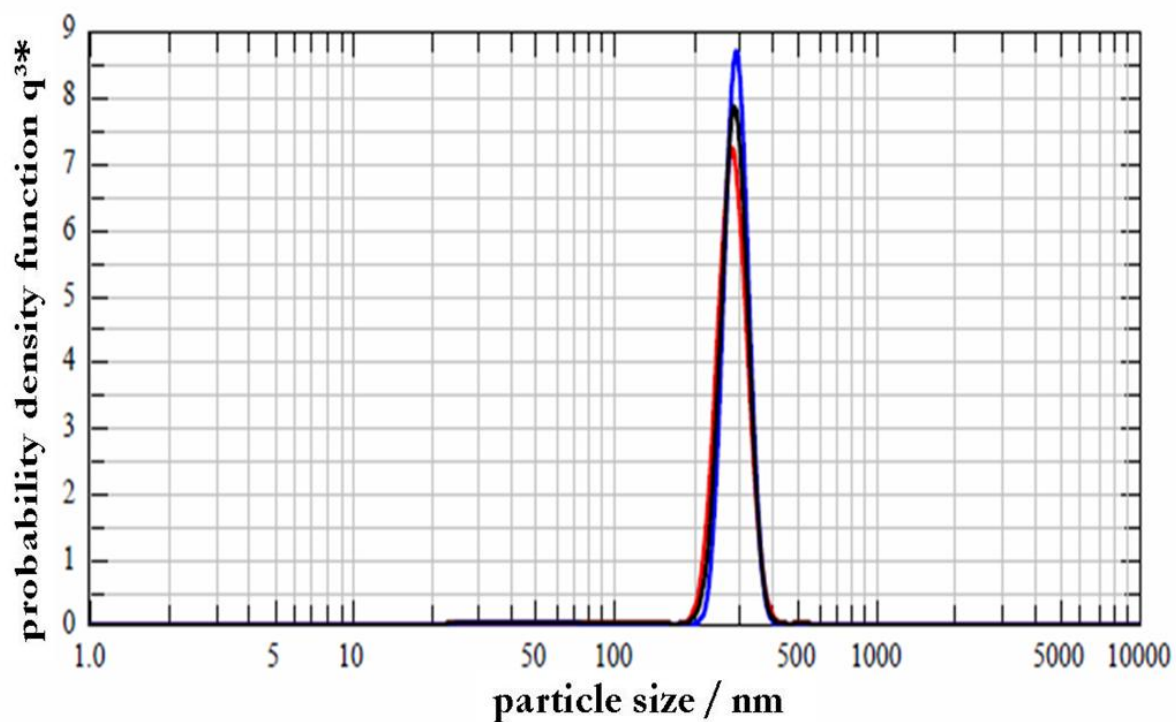


Figure 5.27 Particle size distribution of the nanosuspension (with mannitol) prior to the freeze drying measured by PCCS. (x_{50} -value of the triplicate: 282 nm)

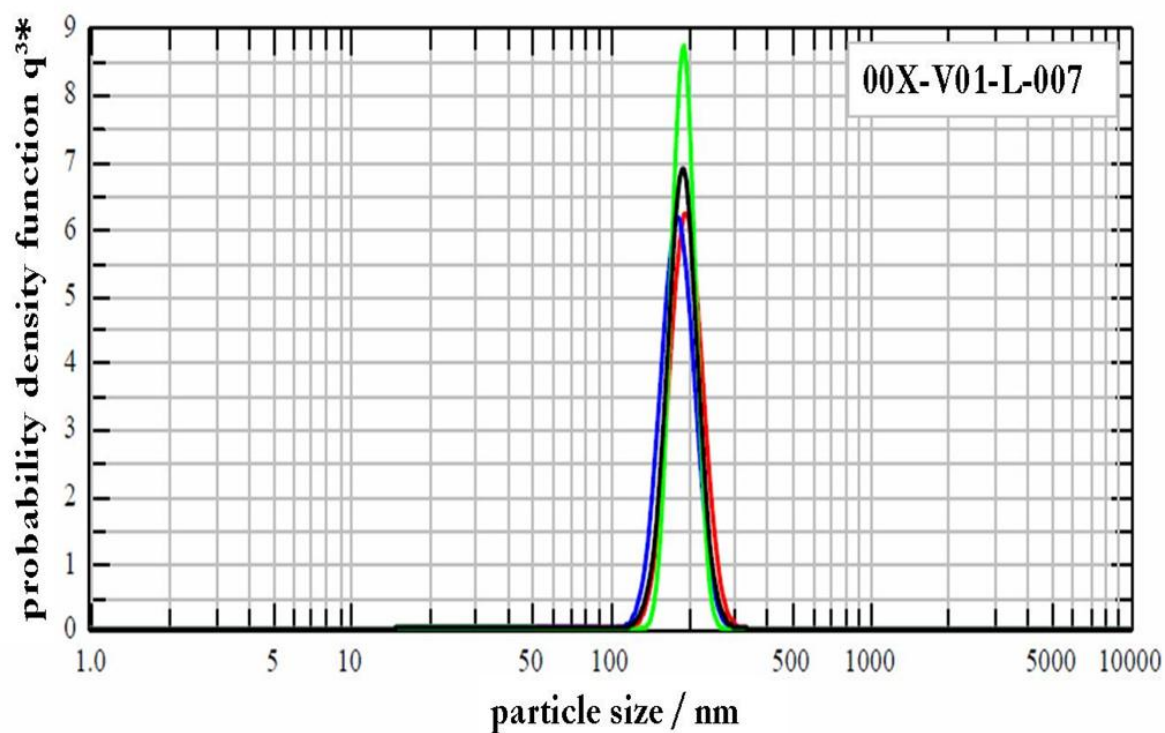


Figure 5.28 Particle size distribution of the reconstituted freeze dried sample measured by PCCS. (x_{50} -value of the triplicate: 185 nm)

The determined mean particle sizes were 282 nm and 185 nm for the nanosuspension (with mannitol) and the reconstituted freeze dried sample, respectively. The particle size distribution after freeze drying was still monomodal with particles in a nanometre scale. Because of the mannitol the viscosity of the nanosuspension with excipient was higher than those of the reconstituted freeze dried sample. It has to be mentioned that falsely the same viscosity was taken for the very dilute reconstituted freeze dried sample during the PCCS measurement. This is one reason explaining why the mean particle size for the freeze dried sample was so much smaller. In addition, it is likely that the drying process itself causes some shrinking of the particles. By using PCCS the hydrodynamic diameter is determined, directly after the ionic gelation process the particles are hydrous and gel-like and thus have a large hydrodynamic size. During the drying process water is removed and the particles shrink. When nanoparticles were reconstituted they were measured directly after the mannitol matrix was dissolved so that the particles had no time to re-hydrate and swell. Although no definitive statement can be made about the mean particle size after freeze drying and reconstitution, because of the unclear actual viscosity, the PCCS data show that the primary nanoparticles remain individually in a nanometre size and that their distribution is also not changing. Therefore, the freeze dried product was further investigated with respect to its dispersion behaviour using the PowderJet (5.4.1.1.1).

5.3.3 Spray Drying of the Nanosuspension

Additionally, dried nano-in-micro particulate powders were produced via spray drying using, again, mannitol as matrix agent. For this, different pump rates, process temperatures and mannitol concentrations were tested. Finally, it turned out that a 10% (w/v) mannitol solution added to the prepared nanosuspension in a one plus one ratio led to the most satisfactory results regarding the process yield as well as the powder properties. The BÜCHI Mini Spray Dryer B290 was used for spray drying. The final process parameters are displayed in Table 5.10.

Table 5.10 Parameters and values used in the final spray drying process.

Parameters	Value
Inlet temperature	110-115°C
Outlet temperature	35-45°C
Aspirator	35 m ³ *h ⁻¹
Spray air rate	670 m ³ *h ⁻¹
Pump rate	6.0-7.5 mL*min ⁻¹

Two two-fluid nozzles were used, for the nasal delivery approach one with an inner diameter of 2.2 mm and for the pulmonary delivery approach one with an inner diameter of 1.5 mm. The obtained powders showed only a small difference in their particle size distribution as displayed in Figure 5.29. The x₅₀-values were 3.82 µm and 3.07 µm using the 2.2 mm and 1.5 mm nozzle, respectively.

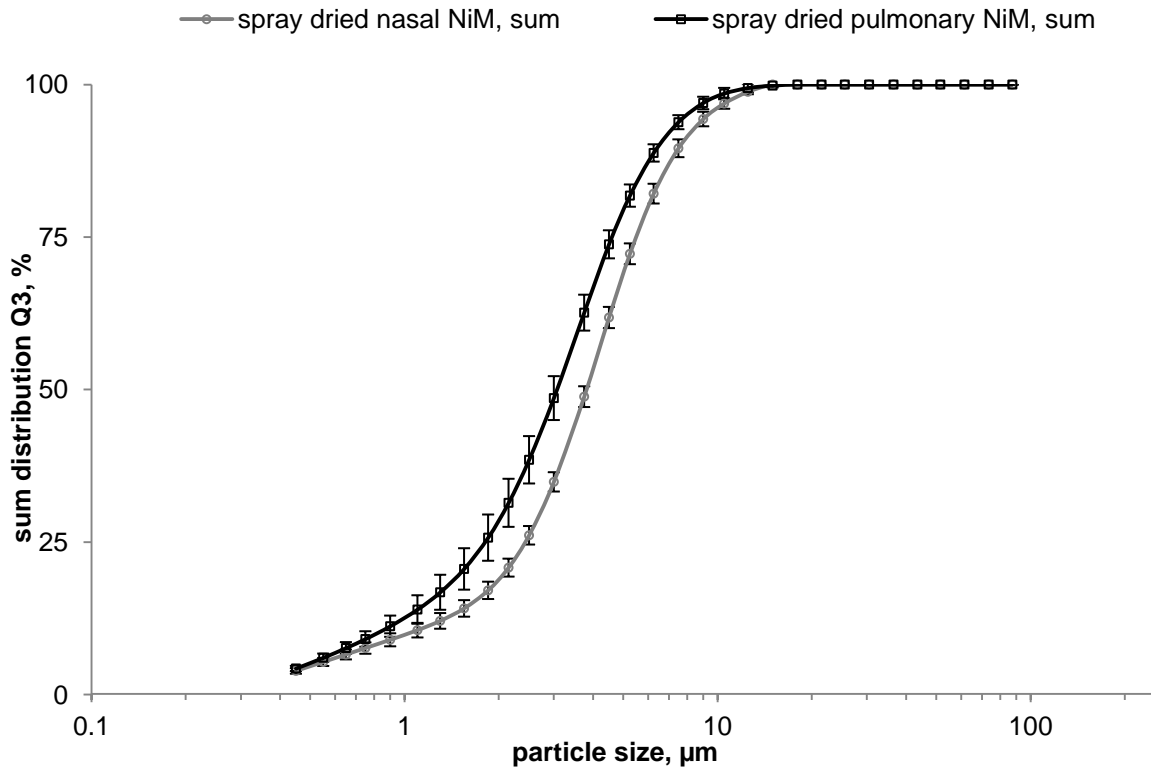


Figure 5.29 Comparison of the particle size distribution of the spray dried nano-in-microparticles for intranasal (2.2 mm nozzle) and pulmonary (1.5 mm nozzle) vaccine delivery. (n=3, error bars represent standard deviation)

The morphology of the spray dried particles (2.2 mm nozzle) is shown in Figure 5.30 where an agglomerate of many smaller particles can be seen. The shape of the single particles was spherical while they vary little in size. Their surface was not smooth and most of them had some fissures on it (so that they look like a ball of wool). Nevertheless, according to the scale displayed on the SEM picture the particle size was consistent with the data obtained by laser diffraction.

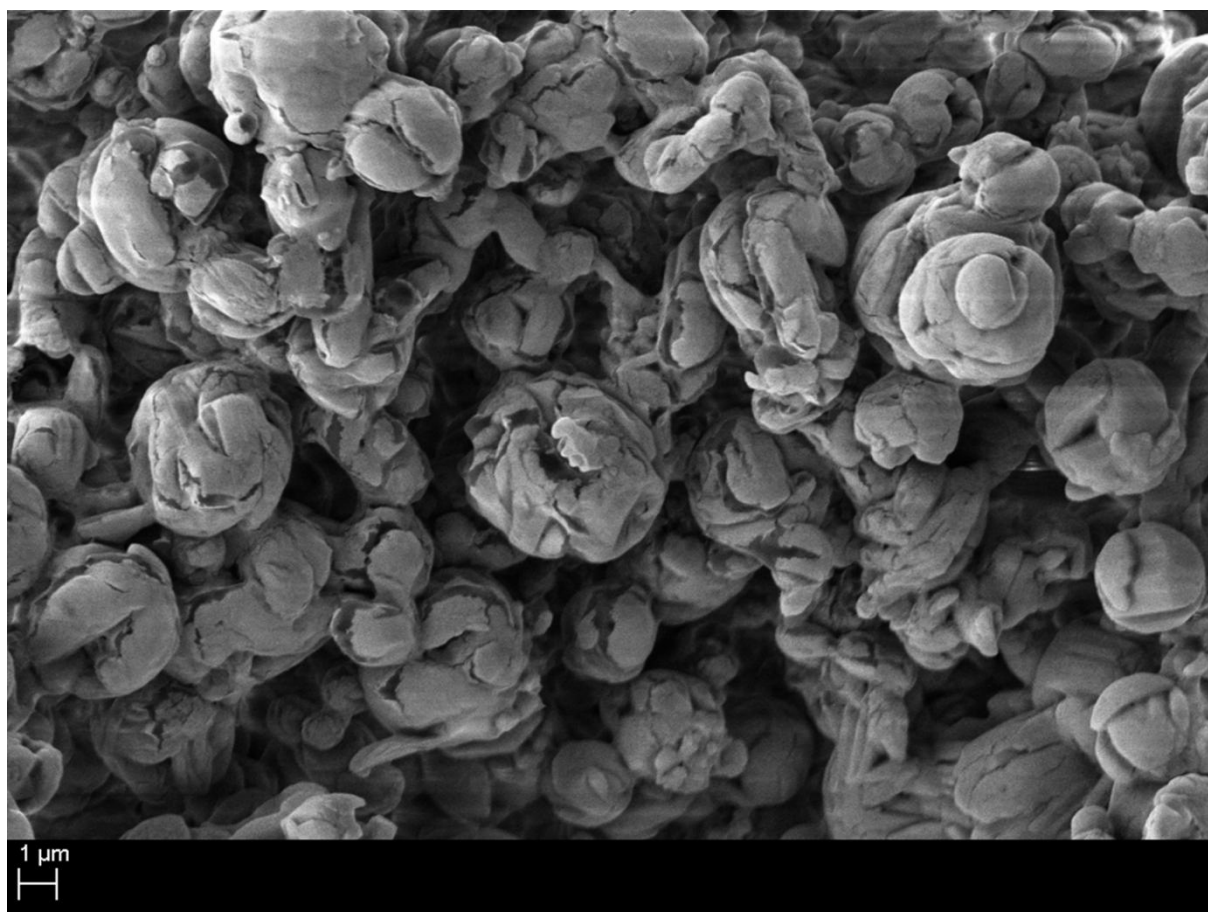


Figure 5.30 SEM picture of the spray dried nano-in-microparticles using a 2.2 mm nozzle. (Magnification: 3530x)

The final composition of the spray dried formulation is shown in Table 5.11.

Table 5.11 *Composition of the spray dried NiM formulation. *(Protein content determined via BCA assay n=3; ±sd)*

Component	Amount
Chitosan	0.4%
Na-Deoxycholate	0.4%
Antigen (BSA)	1% *(0.93% ± 0.016%)
PBS salts	1%
Mannitol	97.2%

Regarding the influence of the spray drying process on the particle size distribution of the nanoparticles, PCS data show very clearly that the process did not

harm the nanoparticles and the mean size and the distribution of the particles were not affected by the drying process as it is shown in Figure 5.31. The z-average of the nanosuspension prior to spray drying was 255 nm with a polydispersity index of 0.169, after spray drying and reconstitution of the formulation the z-average decreased negligibly to 246 nm while the polydispersity index increased to 0.218.

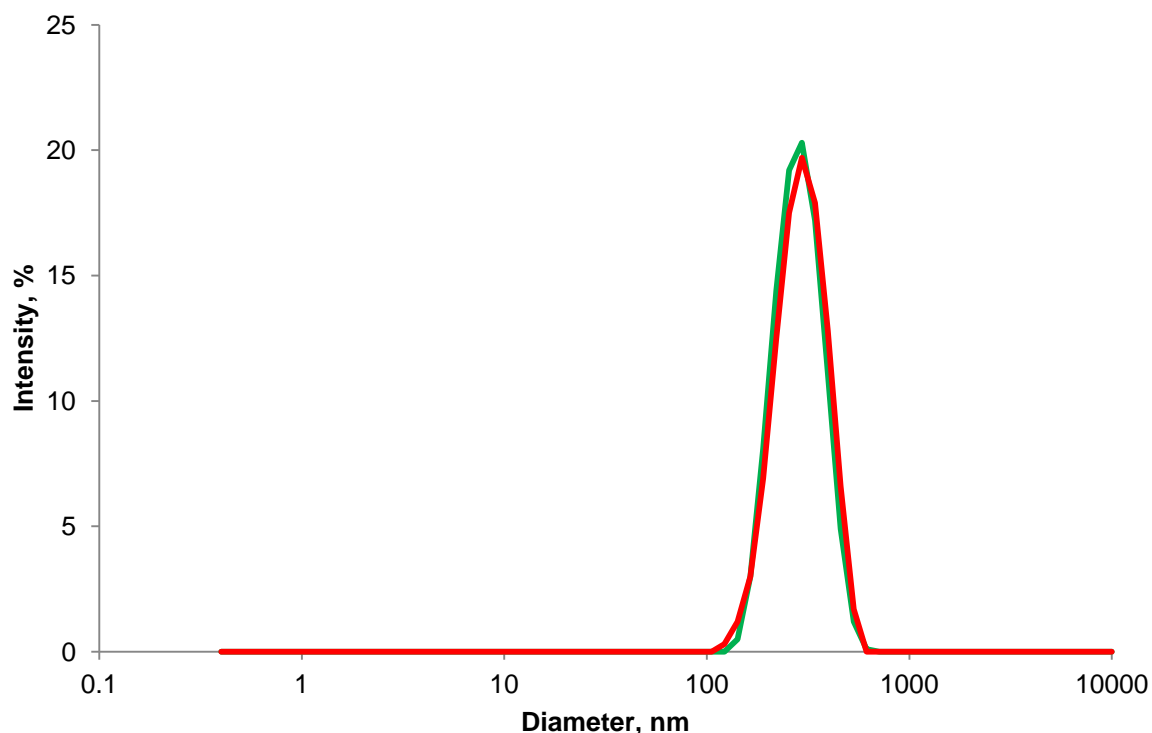


Figure 5.31 PCS data of the nanosuspension (green; z-average: 255 nm, PDI: 0.169) and of the reconstituted spray dried product (red; z-average: 246 nm, PDI: 0.218). Both curves represent the mean of a triplicate.

The final products were stored at a relative humidity of 23% and at room temperature prior to further testing.

5.3.4 Preparations of Blends with the Dried Formulations

In addition to the pure spray and freeze dried products, blends of each approach with Pearlitol SD 200 (sieve fraction 45-90 μm) were prepared in order to improve the flow properties of the formulations. All components were weighted and then mixed for 10 min using the Turbula mixer (Willy A.

Bachofen AG, Basel, Switzerland) at 42 rpm. For the spray dried product a blend containing 15% (w/w) of the spray dried powder with mannitol was prepared. For the freeze dried product a blend containing 5% (w/w) of the freeze dried product with mannitol was prepared. For this, the freeze dried cakes were carefully sieved and the fraction 45-90 μm was merged with mannitol and blended. The prepared blends were analysed regarding their Delivered-Mass Uniformity using the PowderJet and the Powder UDS.

5.4 Aerodynamic Characterisation

Shot weight analyses for the freeze and spray dried formulations for intranasal delivery and the blends of them were performed using the PowderJet and the Powder UDS. Based on the obtained results, a combination of formulation and device was chosen and used in the further investigations in which the intranasal deposition profile within the child and the adult nasal cast models were examined. In addition, the produced formulations for both, intranasal and pulmonary delivery were investigated and analysed with respect to their particle size distribution after air dispersion using the Helos RODOS and after device actuation using the Sprayer and Inhaler module, respectively. The NiM formulation for pulmonary drug delivery was then further investigated regarding its respirable fraction using the Twin Stage Glass Impinger.

5.4.1 Formulations for intranasal Delivery

5.4.1.1 Delivered Mass Uniformity

A modified testing procedure that was named Delivered Mass Uniformity (4.12.1) was performed for the freeze- and spray dried products and blends. The freeze dried products were tested combined with the PowderJet and the spray dried products with both devices. For testing, 20 shots (PowderJet) or 20 devices (Powder UDS) were actuated and the mass of the emitted dose was determined. In the resulting diagrams boundaries of 125% and 75% (solid black), 120% and 80% (dashed grey) of the mean (dotted black) are given.

5.4.1.1.1 Freeze Dried Formulations

The results of the pure freeze dried product (sieve fraction 45-90 μm) and the 5% mixture with Pearlitol SD 200 (sieve fraction 45-90 μm) using the PowderJet are shown in Figure 5.32 and Figure 5.33, respectively.

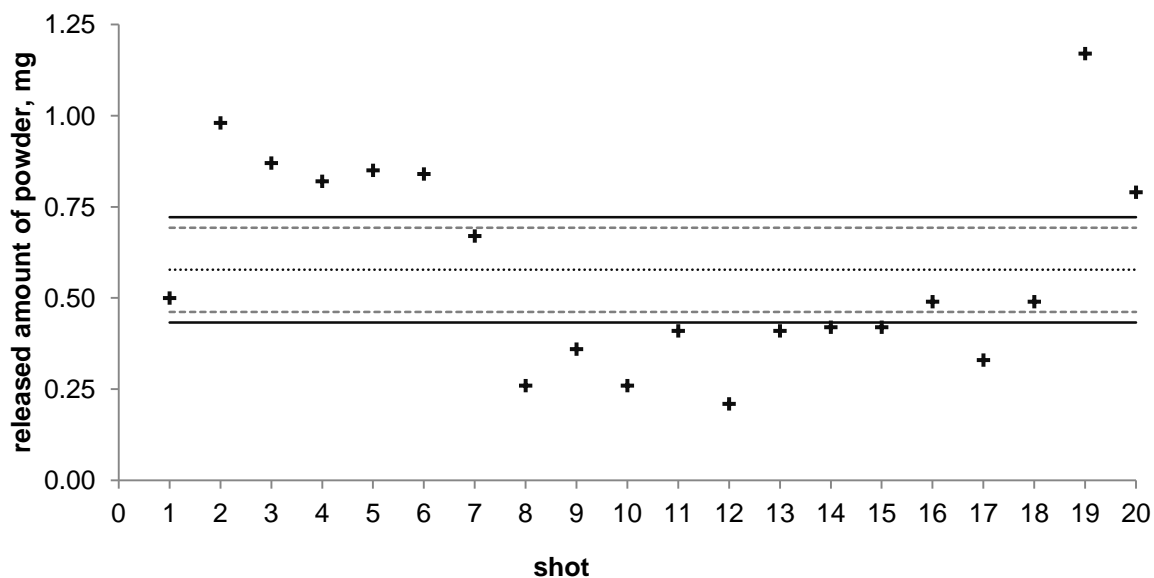


Figure 5.32 Delivered Mass Uniformity data of the pure sieved freeze dried formulation using the PowderJet device.

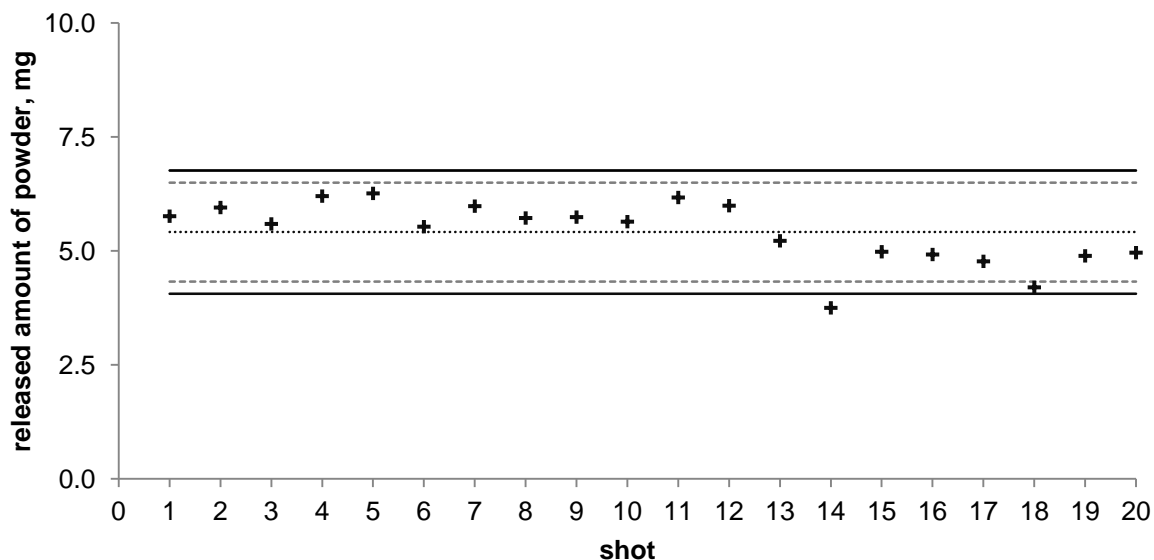


Figure 5.33 Delivered Mass Uniformity data of a 5% mixture of the freeze dried formulation with Pearlitol SD 200 using the PowderJet device.

For the pure freeze dried formulation, 16 shots out of 20 were out of the 75% to 125% boundaries while the mean delivered mass was only 0.58 mg. For the 5% mixture the mean value was 5.41 mg with only 2 shots outside the 80% to 120% and one outside the 75% to 125% limits. It is obvious that the combination of the pure freeze dried product and the PowderJet device was not suitable for a reproducible drug delivery into the nose and that the performance of the blended formulation was much better and fulfilled the requirements adopted from the Delivered Dose Uniformity according to the USP 36.

5.4.1.1.2 Spray Dried Formulations

From the beginning, the spray dried NiM formulation showed better flow and handling properties compared to the freeze dried one. Therefore, the pure spray dried product and the blend with Pearlitol SD 200 were analysed with respect to its Delivered Mass Uniformity using both devices. The results obtained from pure spray dried product and blended formulation using the PowderJet are shown in Figure 5.34 and Figure 5.35, respectively.

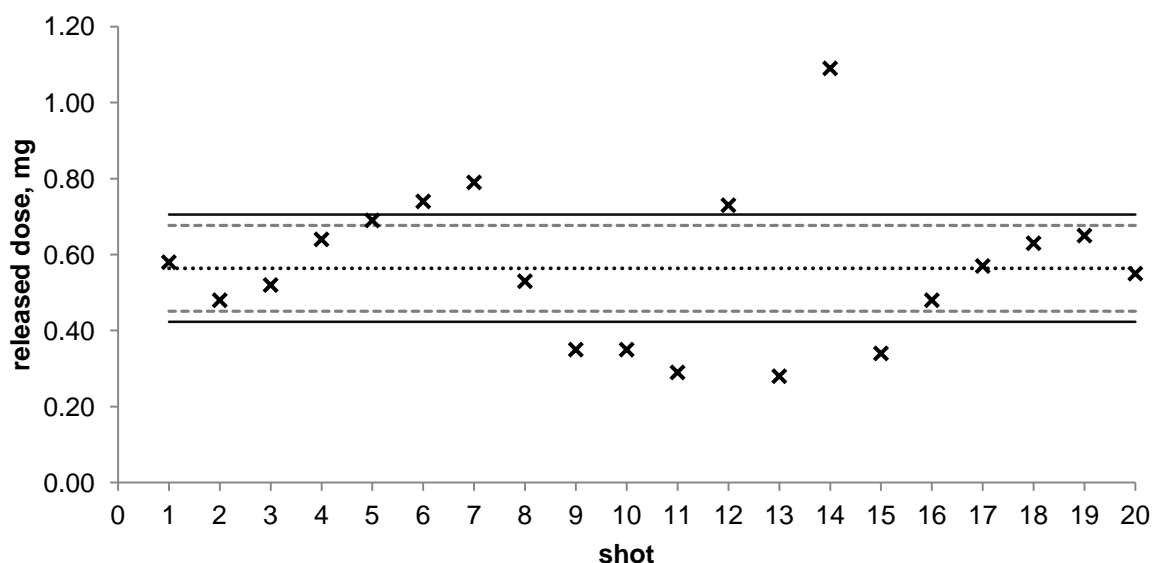


Figure 5.34 Delivered Mass Uniformity data of the pure spray dried NiM formulation using the PowderJet device.

Regarding the pure spray dried product the mean delivered mass was only 0.56 mg and there were nine and eight values outside the limits of 80% to 120% and 75% to 125%, respectively. Therefore this combination does not meet the requirements.

Regarding the combination of the PowderJet and the 15% blend all values were inside the 80% to 120% limits and the mean value was 4.70 mg.

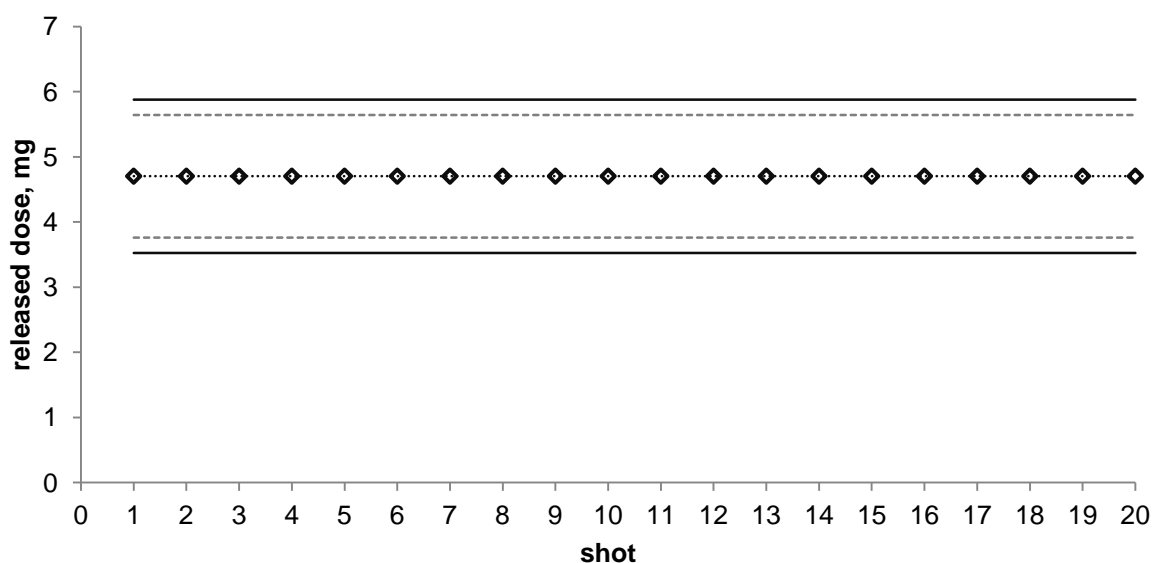


Figure 5.35 Delivered Mass Uniformity data of the 15% blend of spray dried NiM formulation with Pearlitol SD 200 using the PowderJet device.

It can be concluded that the pure spray dried product showed only poor dispersion behaviour when administered with the PowderJet. This problem was solved by preparing a 15% blend with Pearlitol SD 200.

Results for pure product and the blend using the Powder UDS are displayed in Figure 5.36 and Figure 5.37.

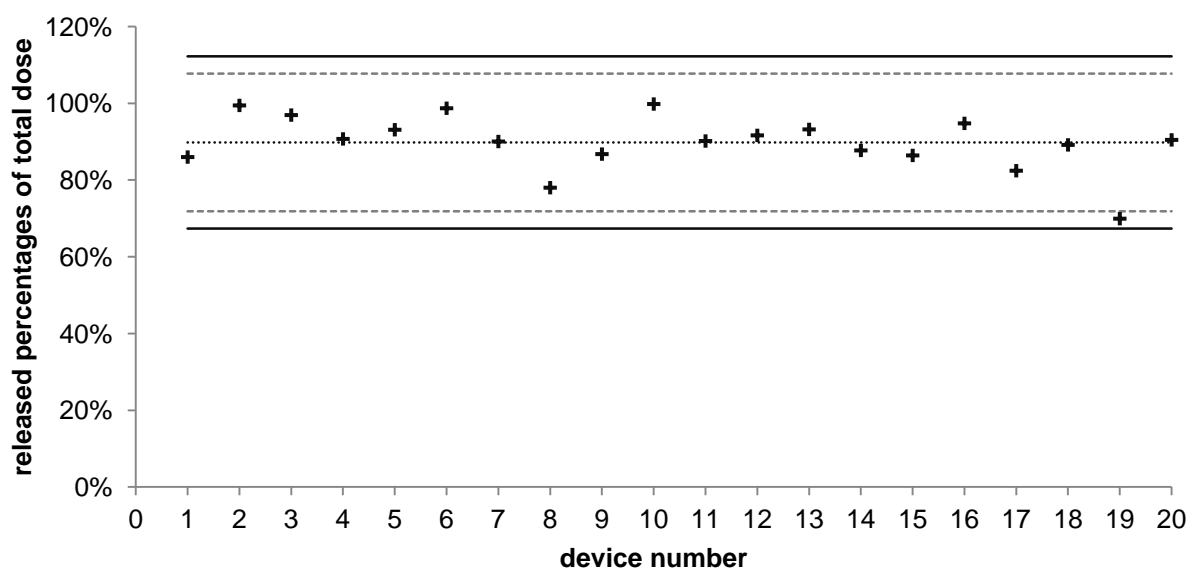


Figure 5.36 Delivered Mass Uniformity data of a pure spray dried NiM formulation using the Powder UDS device.

Regarding the Powder UDS with the pure spray dried product the mean delivered mass was 89.78% of the actually weighed product and one value (device no. 19) was below the 80% limit and no value was outside the 75% to 125% boundaries. Therefore the combination fulfilled the requirements of the test.

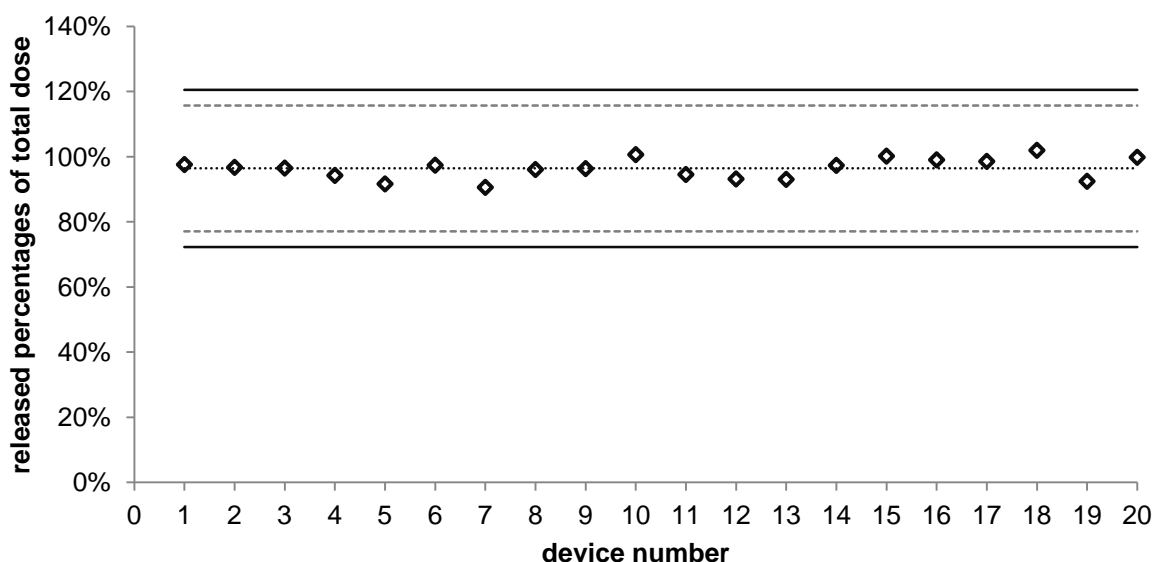


Figure 5.37 Delivered Mass Uniformity data of 15 % of the spray dried NiM formulation blended with Pearlitol SD 200 using the Powder UDS device.

For the 15% blend of the spray dried NiM formulation with Pearlitol SD 200 all emitted doses were inside the limits of 80% to 120%. The mean delivered mass value was 96.40% and thus this combination fulfilled the requirements of the test.

To conclude, the performances of the blends were better than those of the pure products but, especially for the pure spray dried product administered using the PowderJet a better performance was expected. The fact that the results obtained with the pure spray dried powder administered with the Powder UDS are significantly better than those obtained when using the PowderJet is due to the very different modes of operation which are explained in detail in section 3.7.1. Briefly, the PowderJet is the much more complex device. It is a multidose device in which the single dose is metered out of the powder reservoir prior to every actuation. This causes mechanical stress on the powder in the reservoir and can lead to processes such as compaction which, of course, then have a negative influ-

ence onto the powder dispersibility. The results suggest that the pure freeze and spray dried formulations are much more influenced by this mechanism of dose metering than the spray dried mannitol that was used as drug carrier. Although, it is obvious that the delivered mass is more uniform using a blended product, it was decided to use the Powder UDS combined with the pure spray dried NiM formulation in all nasal deposition studies and further investigations due to vast problems in achieving homogeneous blends and the low antigen content in these blends.

5.4.1.2 Laser Diffraction

The pure spray dried NiM formulation was further investigated with respect to its particle size distribution after device (Powder UDS) actuation using the Sprayer module at a spray angle of 70°. The comparison of these results with those obtained using RODOS module is given in Figure 5.38.

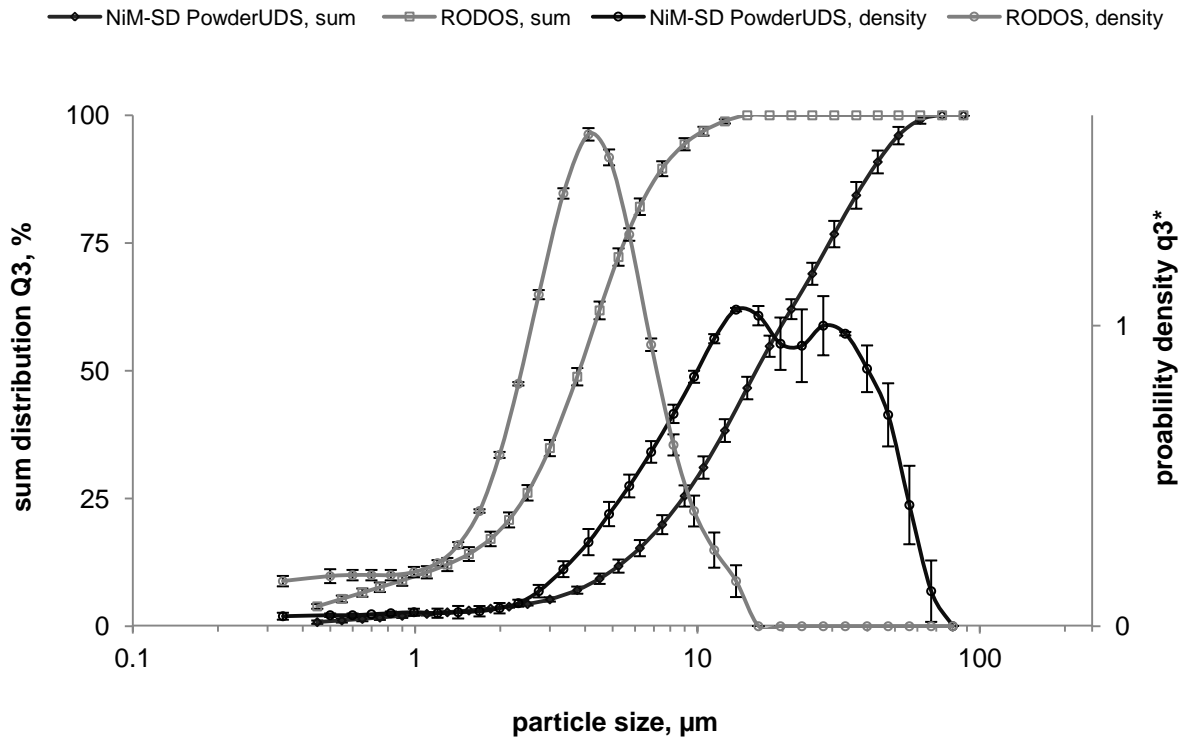


Figure 5.38 Comparison of particle size distribution of the spray dried nano-in-microparticle formulation after 3 bar air dispersion (grey) and dispersion with the Powder UDS device at a spray angle of 70°. (n=3, error bars represent standard deviation)

The x_{50} -value of the NiM formulation after 3 bar air dispersion was 3.82 μm and the distribution was monomodal. When using the Powder UDS the x_{50} -value increases to 16.23 μm while the size distribution becomes bimodal. The dispersion mechanism of the Powder UDS was not able to destroy the agglomerates of primary particles entirely and thus the measured particles still occur mainly as agglomerates and thus having a larger size. Regarding the nasal deposition of the formulation this effect is probably positive, because larger particles are more likely to be deposited inside the nasal cavity than smaller ones, especially when an air flow is applied.

5.4.1.3 Intranasal Deposition Analysis

The combination of pure spray dried NiM formulation and Powder UDS was investigated with respect to its deposition profile inside the nasal cavity using both cast models (4.12.2.1). The deposition profiles with and without applied airflow were determined and compared to the ideal profile. Once again, the ideal profile was calculated as an equal amount of formulation in all segments with exception of the nostrils.

The results of the nasal deposition in the adult and child cast models without and with applied air flow are displayed in Figure 5.39 and Figure 5.40, respectively.

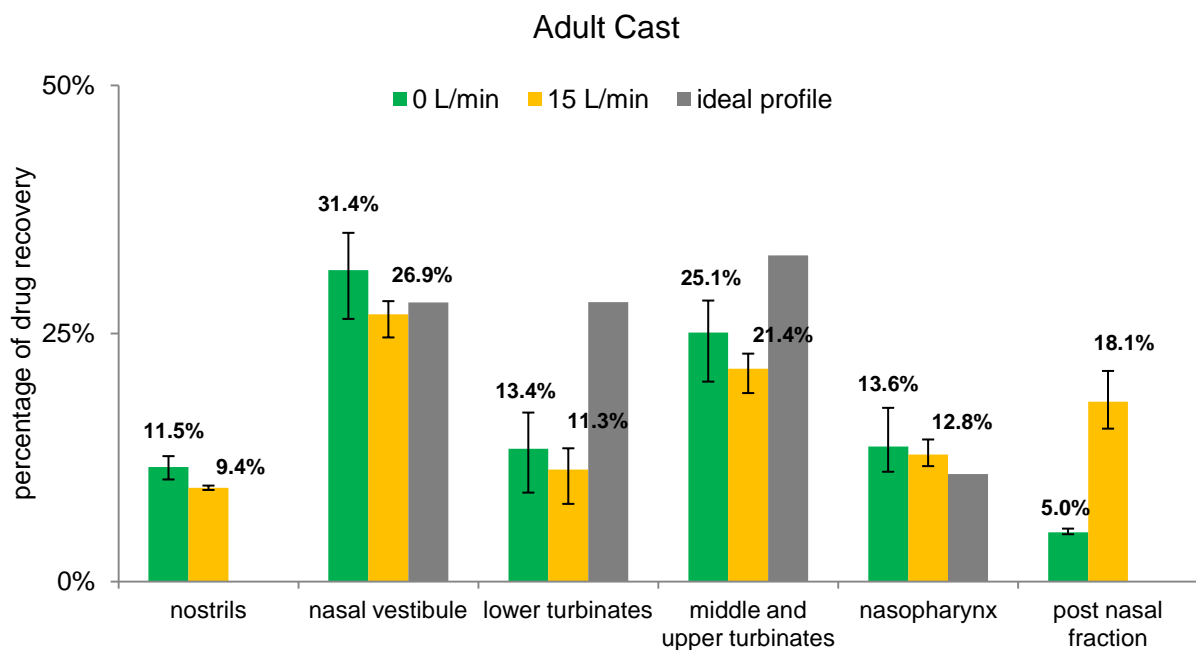


Figure 5.39 Nasal deposition of protein in the adult cast model with (yellow) and without (green) air flow compared to the ideal profile (grey). Error bars represent the min and max values of the triplicate.

Looking at the results obtained with the adult cast model it can be seen that regarding the nasal vestibule, the middle and upper turbinates and the nasopharynx the obtained deposition profile, with and without air flow was quite close to the ideal one. This did not apply for the lower turbinates where in both cases, with and without air flow the amount of NiM formulation was significantly lower than desired. The lower turbinates are located at the underside of the central region of the nasal cavity. As the NiM formulation was administered in an upward

direction with high velocity, it impacted more likely in the upper parts of the nasal cavity. This effect is already known from pMDIs used for intranasal administration (Cheng et al., 2001). When applying an air flow this led to a slight decrease in deposition in every region of the nasal cavity and a shift towards the rear parts of the nasal cavity as well as to a sharp increase in the post-nasal fraction which rose from 5% to 18.1%. Thus, the total amount of vaccine deposited in the nasal cavity declined from 83.5% to 72.4% of the delivered dose.

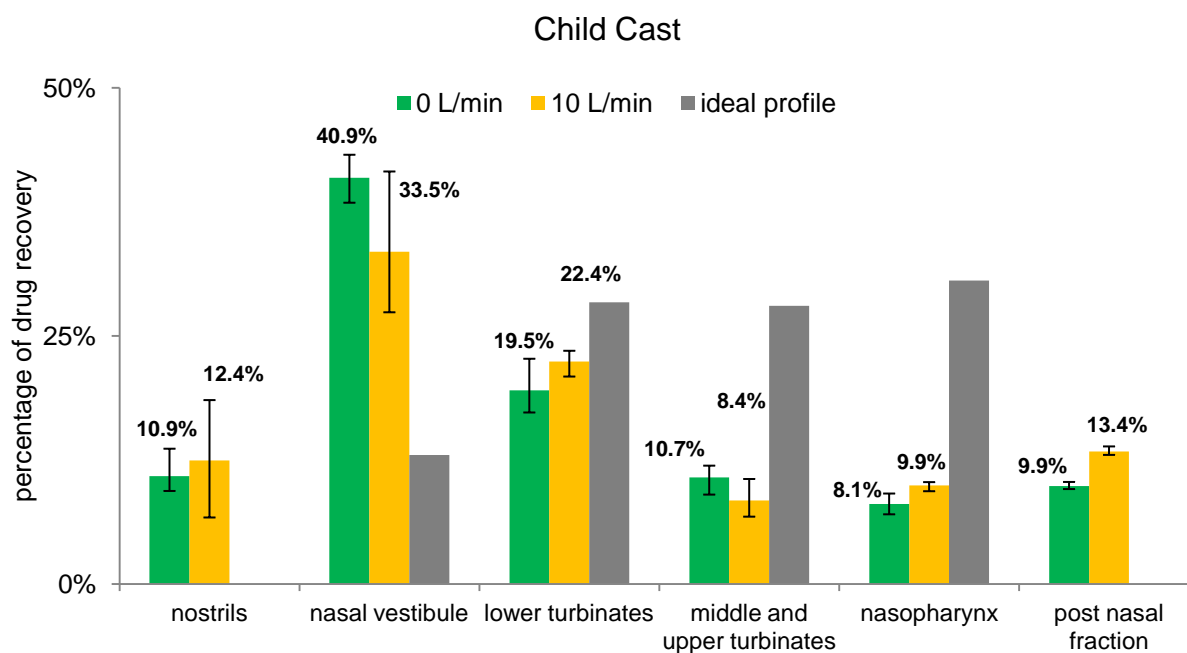


Figure 5.40 Nasal deposition of protein in the child cast model with (yellow) and without (green) air flow compared to the ideal profile (grey). Error bars represent the min and max values of the triplicate.

Regarding the deposition in the child cast model it can be seen that even more of the NiM formulation was deposited in the nasal vestibule, especially without but also with applied airflow compared to the adult cast model. The nasal vestibule in a child's nasal cavity is a region with very narrow airways of less than 1.5 mm (cast model) in diameter which are difficult to pass with a nasal formulation and thus a high amount of formulation is deposited here. Nevertheless, it can be assumed that the formulation deposited in the anterior regions will be transported to the posterior regions over time via the nasal clearance. Applying an air flow did not alter the deposition profile remarkably but the variability increased particularly in the anterior regions (nostrils and nasal vestibule). Unlike the adult

model, applying an air flow to the child model only led to a moderate increase in the post-nasal fraction from 9.9% to 13.4%, because the airways of a child are much narrower than those of an adult the powder was not able to follow the air stream to the same extent and thus it impacted in those narrow air paths. Nevertheless, the small increase in the post-nasal fraction also led to a slight decrease in the amount of formulation deposited within the desired regions of the nasal cavity from 79.5% to 74.2%.

It can be concluded that for both models the amount of NiM formulation deposited in the anterior region is relatively high because the airways in these regions are narrow and difficult to pass through. This observation is also described in literature for liquid nasal sprays (Shah et al., 2013). Regarding the adult cast it can be stated that administration should be performed while holding breath to maximise the amount being deposited in the nasal cavity and at the same time minimising the post-nasal fraction. With respect to the child cast model, the developed NiM formulation is not suitable, because the ideal profile is missed clearly. If the NiM formulation should be administered to children further formulation optimisation would be necessary, this may also include the search for a different device. Moreover, the studies showed that one has to distinguish very clearly between children and adults even in early stage formulation development, especially when the final product should be administered intranasally because of the huge age depending anatomical differences. The same is probably true regarding the gender, especially in adults but was not investigated in this work.

5.4.2 Formulation for Lung Delivery

The NiM formulation which was developed for pulmonary delivery was examined using two dry powder inhalers with respect to its particle distribution after pressurised air dispersion, after device release and regarding its respirable fraction using the Twin Stage Glass Impinger (4.12.3). Based on the obtained data the NiM formulation was developed further in order to reduce the unsatisfactorily high device and capsule retention observed when using the original spray dried NiM formulation.

5.4.2.1 Particle Size Distribution of the Formulation via Laser Diffraction

The particle size distribution of the spray dried powder was determined via laser diffraction using the RODOS module as well as the Inhaler module. When the RODOS module was used a dispersion pressure of 3 bar was applied to the powder. The Inhaler module was used with both devices, the Aerolizer and the Handihaler and at two different flow rates for each device. For the Aerolizer, flow rates of $60 \text{ L}\cdot\text{min}^{-1}$ and $100 \text{ L}\cdot\text{min}^{-1}$ were applied in order to have the same conditions as for the TSI testing and a pressure drop of 4 kPa through the device, respectively. Thus, when the HandiHaler was tested flow rates of $60 \text{ L}\cdot\text{min}^{-1}$ and $50 \text{ L}\cdot\text{min}^{-1}$ were applied, respectively. The particle size distribution of the spray dried product under pressurised air dispersion is shown in Figure 5.41.

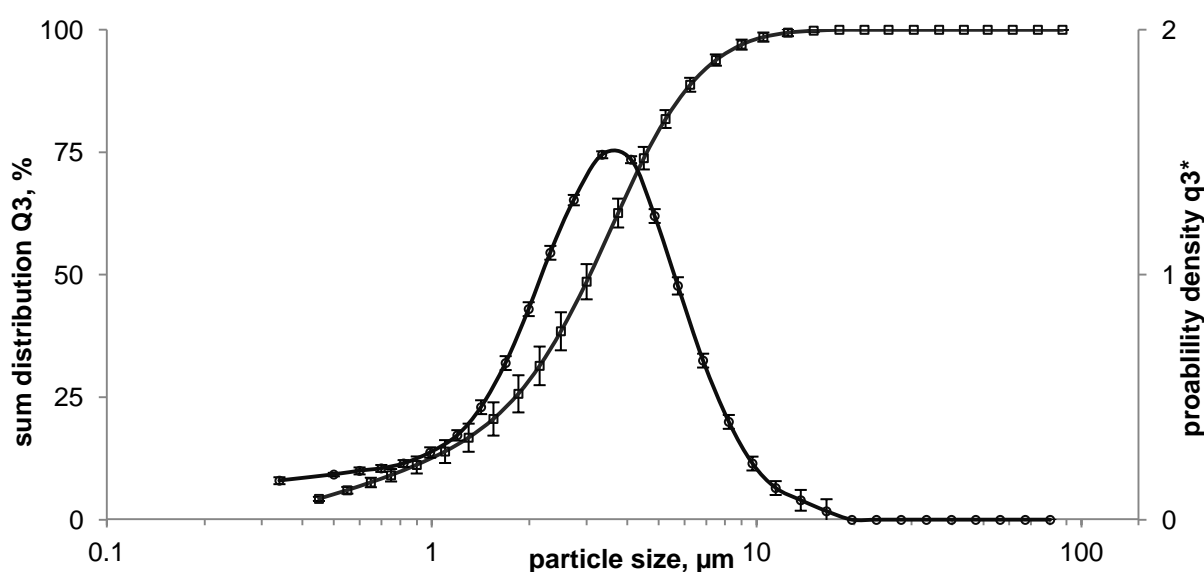


Figure 5.41 Particle size distribution of the spray dried nano-in-microparticles for pulmonary drug delivery with 3 bar dispersion pressure using the Helos RODOS module. (n=3, error bars represent the standard deviation)

The x_{50} -value of the NiM formulation was $3.07 \mu\text{m}$ and thus slightly lower than the value obtained for the NiM formulation for intranasal delivery ($x_{50} = 3.82 \mu\text{m}$; Figure 5.38). The particle size distribution was monomodal. The smaller x_{50} -value was due to the smaller nozzle that was used during spray drying. In principle, with an x_{50} -value below $5 \mu\text{m}$ the NiM formulation should be suitable for lung delivery.

The x_{50} -values of the powder released from the Aerolizer were $4.13\ \mu\text{m}$ and $5.32\ \mu\text{m}$ when applying an air flow of $100\ \text{L}\cdot\text{min}^{-1}$ and $60\ \text{L}\cdot\text{min}^{-1}$, respectively, to the device. The obtained particle size distributions are shown in Figure 5.42 and Figure 5.43 for $100\ \text{L}\cdot\text{min}^{-1}$ and $60\ \text{L}\cdot\text{min}^{-1}$, respectively.

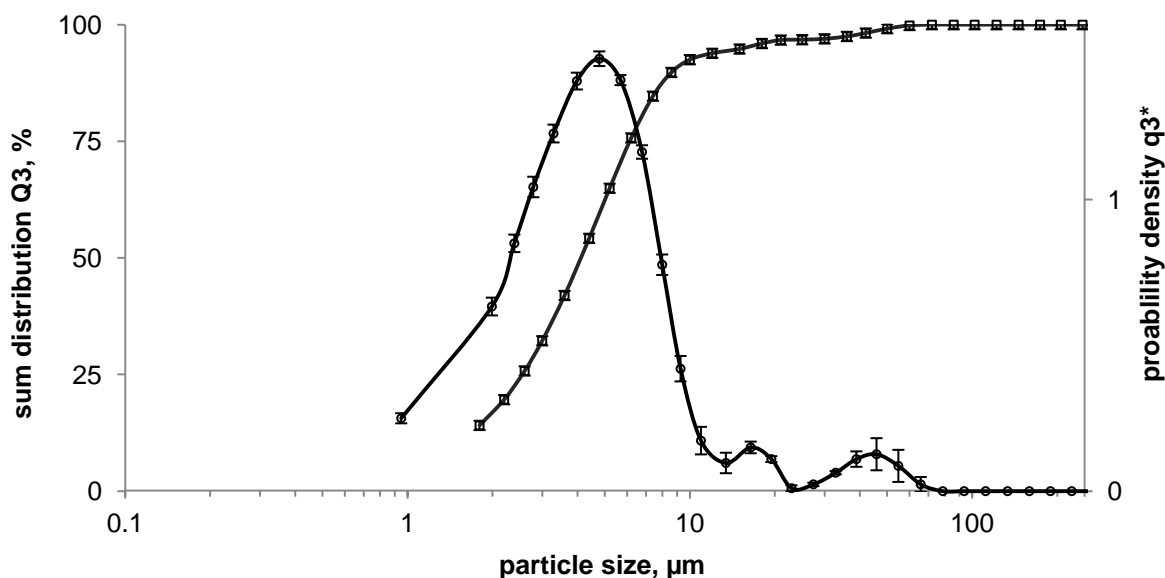


Figure 5.42 Particle size distribution of the spray dried nano-in-microparticles released from the Aerolizer using the Helos Inhaler module at an applied airflow of $100\ \text{L}\cdot\text{min}^{-1}$. X_{50} value of $4.13\ \mu\text{m}$ ($n=3$, error bars represent the standard deviation)

The distribution obtained by $100\ \text{L}\cdot\text{min}^{-1}$ air flow showed a second small peak at about $16\ \mu\text{m}$ and again another even smaller one at $45\ \mu\text{m}$. Thus it can be assumed that the de-agglomeration mechanism within the device was not able to destroy all the powder agglomerates.

The particle size distribution obtained at $60 \text{ L}\cdot\text{min}^{-1}$ showed a slightly higher x_{50} -value of $5.32 \mu\text{m}$ and also a second smaller peak at about $39 \mu\text{m}$.

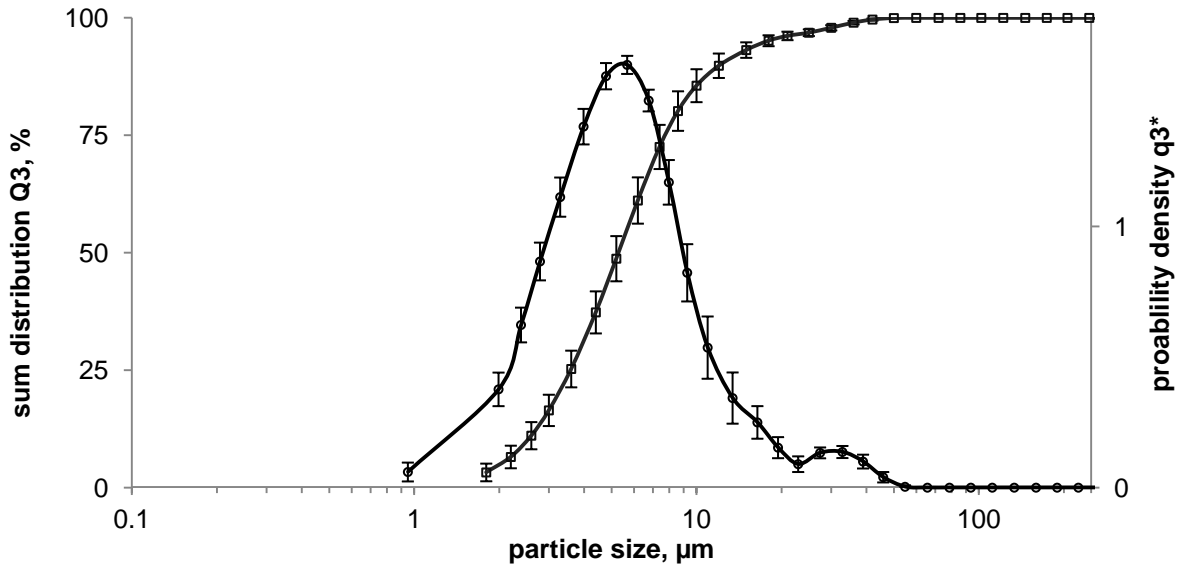


Figure 5.43 Particle size distribution of the spray dried nano-in-microparticles released from the Aerolizer device using the Helos Inhaler module with an applied airflow of $60 \text{ L}\cdot\text{min}^{-1}$. X_{50} value of $5.32 \mu\text{m}$ ($n=3$, error bars represent the standard deviation)

These results suggest that for both flow rates a respirable fraction around 50% can be expected.

The particle size distributions obtained using the HandiHaler with applied flow rates of 50 and 60 L*min⁻¹ are shown in Figure 5.44 and Figure 5.45.

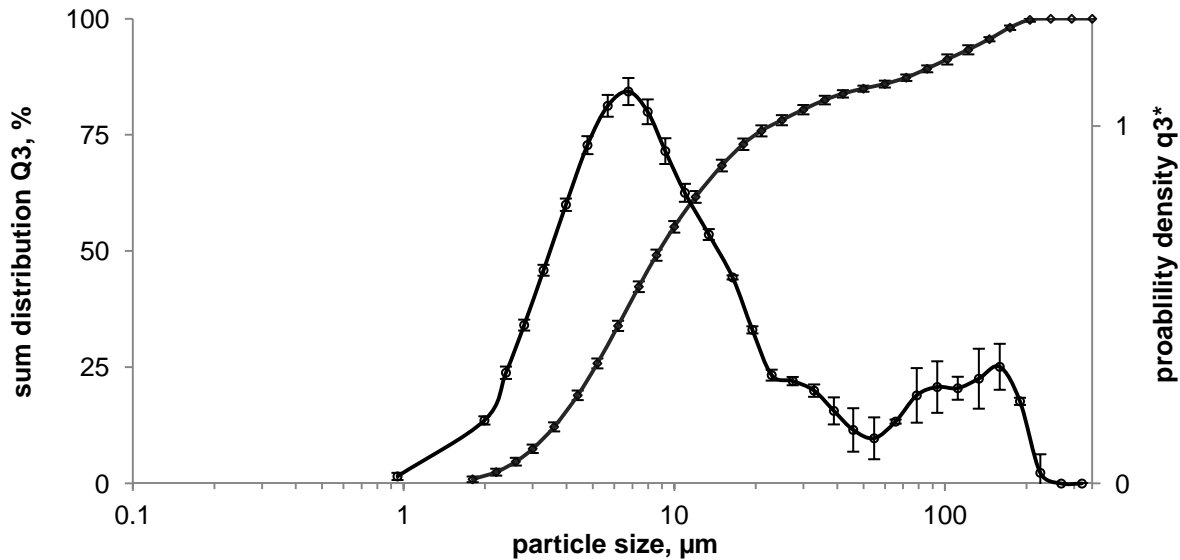


Figure 5.44 Particle size distribution of the spray dried nano-in-microparticles released from the HandiHaler device using the Helos Inhaler module with an applied airflow of 50 L*min⁻¹. X₅₀ value of 8.80 μm (n=3, error bars represent standard deviation)

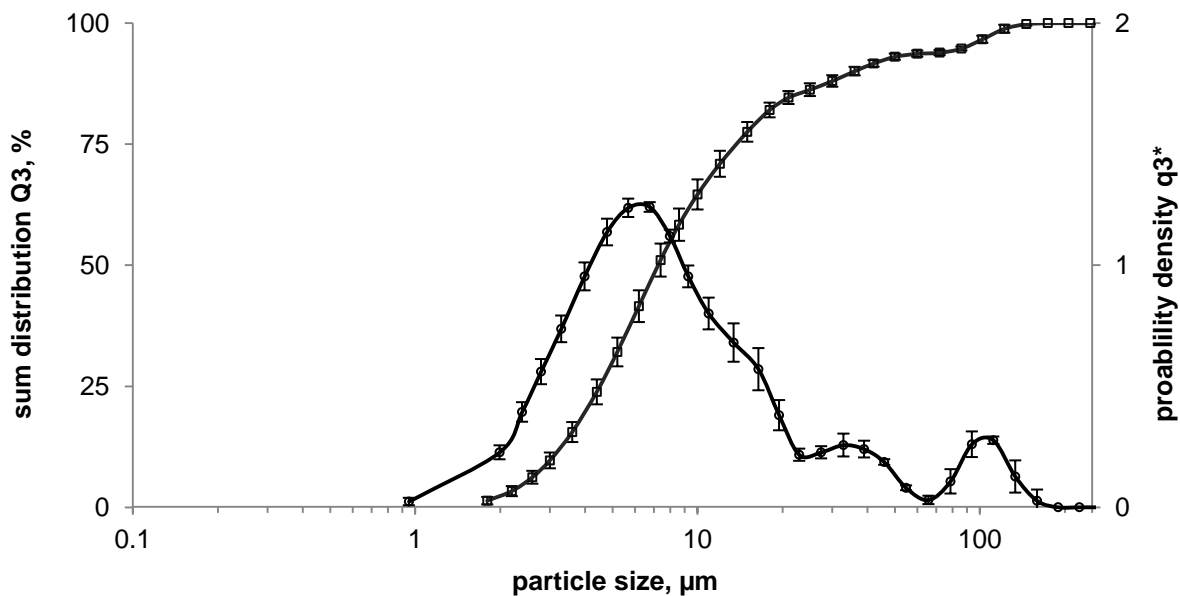


Figure 5.45 Particle size distribution of the spray dried nano-in-microparticles released from the HandiHaler device using the Helos Inhaler module with an applied airflow of 60 L*min⁻¹. X₅₀ value of 7.30 μm (n=3, error bars represent standard deviation).

The x₅₀-values were quite similar with values of 8.80 μm and 7.30 μm, respectively. Increasing the applied air flow up from 50 to 60 L*min⁻¹ led to a left shift

of the distribution whereas the structure of the distribution itself remains the same. Both distributions showed one dominant main peak followed by a second much smaller one which partly occurs at a shoulder of the first one, especially by $50 \text{ L}\cdot\text{min}^{-1}$ applied air flow, and a third one at a much larger size above $100 \mu\text{m}$. Laser diffraction data show that the forces applied on the powder within the dry powder inhalers during “inhalation” are not strong enough to destroy all agglomerates in order to deliver the spray dried particles individually. Nevertheless, flow rate and device differences could be observed where a higher flow rate led to a better de-agglomeration and thus lower x_{50} -values. With respect to both devices that were used it can be stated the x_{50} -values obtained using the HandiHaler were higher than those obtained with the Aerolizer. In addition, the data obtained using the Aerolizer showed a more regular distribution. All in all, data suggest that pulmonary powder administration will result in a higher respirable fraction when using the Aerolizer compared to the HandiHaler. But the observed differences were not of a great extent. To evaluate how these differences are related to the aerodynamic performance, both devices were tested and analysed with respect to their respirable fraction using the Twin Stage Glass Impinger.

5.4.2.2 Respirable Fraction of the Spray Dried NiM Formulation

The Twin Stage Glass Impinger, Apparatus A, Ph.Eur. 7.4 (TSI, Copley Scientific, Nottingham, UK) was used in order to determine the respirable fraction and to generate knowledge about the aerodynamic behaviour of the developed spray dried NiM formulation. Testing was performed as described in section 4.12.3.1 in accordance to the Ph. Eur 7.4 (European Directorate for the Quality of Medicines, 2013). First, both dry powder inhalers were tested with the pure spray dried NiM formulation. The results are given in Figure 5.46.

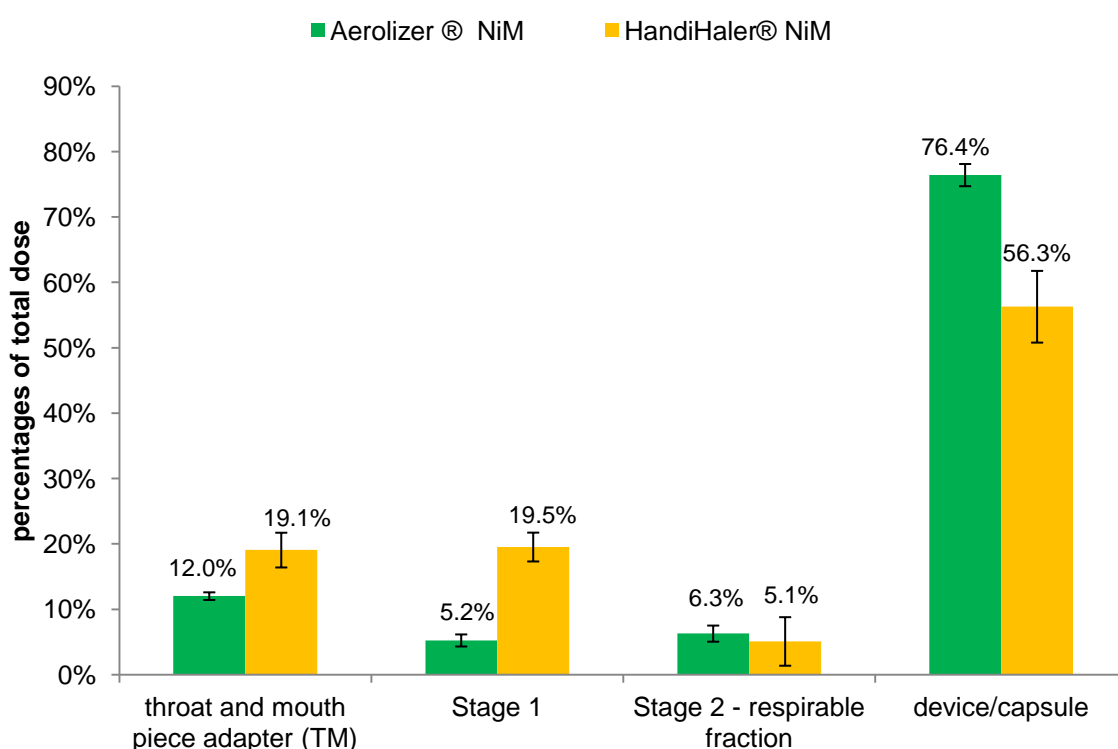


Figure 5.46 NiM formulation deposition within the TSI for the HandiHaler (yellow) and the Aerolizer (green) obtained using the spray dried NiM formulation. (n=3, error bars represent standard deviation)

Data show that the respirable fraction for both devices was only 5.1% (HandiHaler) and 6.4% (Aerolizer) of the total dose and that the percentage of formulation which is retained in the capsule and the device was very high, 56.3% and 76.4% for the HandiHaler and the Aerolizer, respectively. Based on these results the NiM formulation was developed further in order to reduce the capsule and

device retention. This was done by adding 1% magnesium stearate to the original spray dried NiM formulation.

5.4.3 Preparation of the 1% Magnesium Stearate NiM Blend

The 1% magnesium stearate (MgSt; $x_{50} = 9.29 \mu\text{m}$; via laser diffraction) containing NiM formulation (NiM+1%MgSt) was prepared by blending using the turbula mixer. A 1 g batch was prepared in a 25 mL glass vessel which was placed into a metal container secured with cotton cloths. Then the sample was blended for 3 h (Tay et al., 2010) at a speed of 42 rpm. Subsequently, the new formulation was stored at 23% relative humidity and room temperature until it was tested. The laser diffraction data of the blended formulation compared to the unblended one are shown in Figure 5.47.

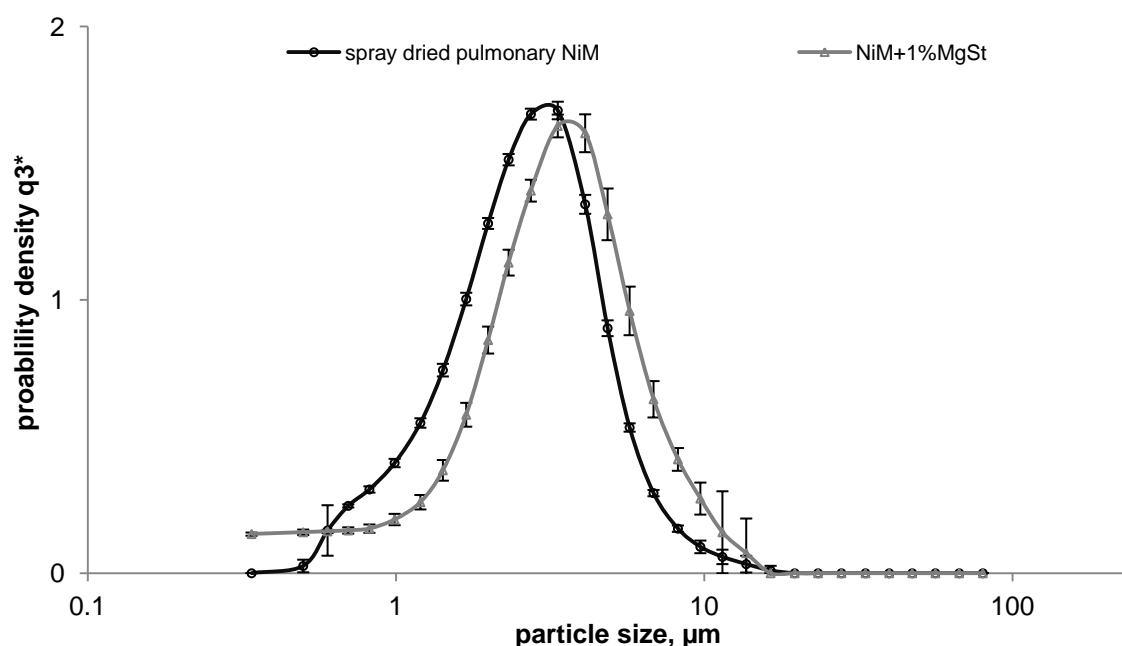


Figure 5.47 Particle size distributions of the NiM formulation and the NiM+1% MgSt formulation. X_{50} -values were 3.07 and 3.32 μm . ($n=3$, error bars represent standard deviation)

Regarding the PSD a slight increase in the x_{50} -value from 3.07 μm for the unblended to 3.32 μm for the blended sample was observed. This observation is explained by magnesium stearate covering the surface of the spray dried product during the unusually long blending process. Because the distribution after blend-

ing was still monomodal it can be assumed that the magnesium stearate was completely placed on the surface of the spray dried NiM particles.

5.4.3.1 Respirable Fraction of the Spray Dried NiM+1%MgSt Blend

The new NiM+1%MgSt formulation was also analysed using the TSI under the same conditions as the unblended NiM formulation was tested. The obtained results are shown, as a comparison to the unblended NiM formulation, in Figure 5.48 and Figure 5.49 for the HandiHaler and the Aerolizer, respectively.

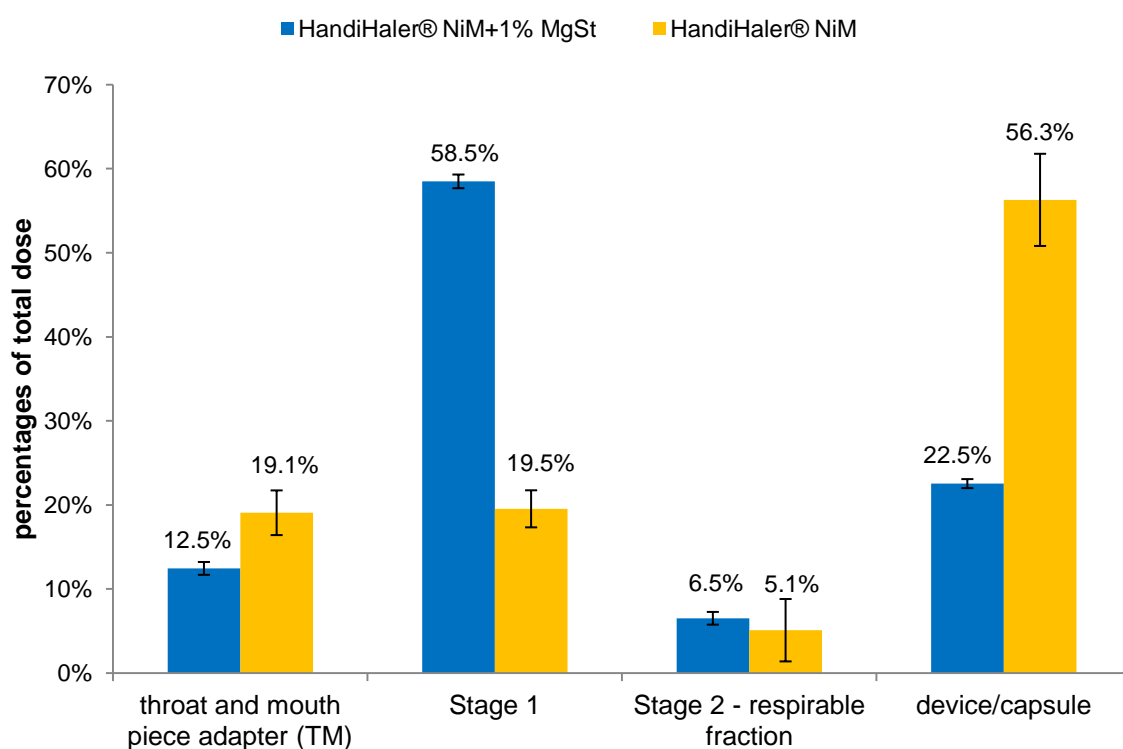


Figure 5.48 Formulation deposition within the TSI for the NiM formulation (yellow) and the NiM+1%MgSt formulation (blue) using the HandiHaler device. (n=3, error bars represent standard deviation)

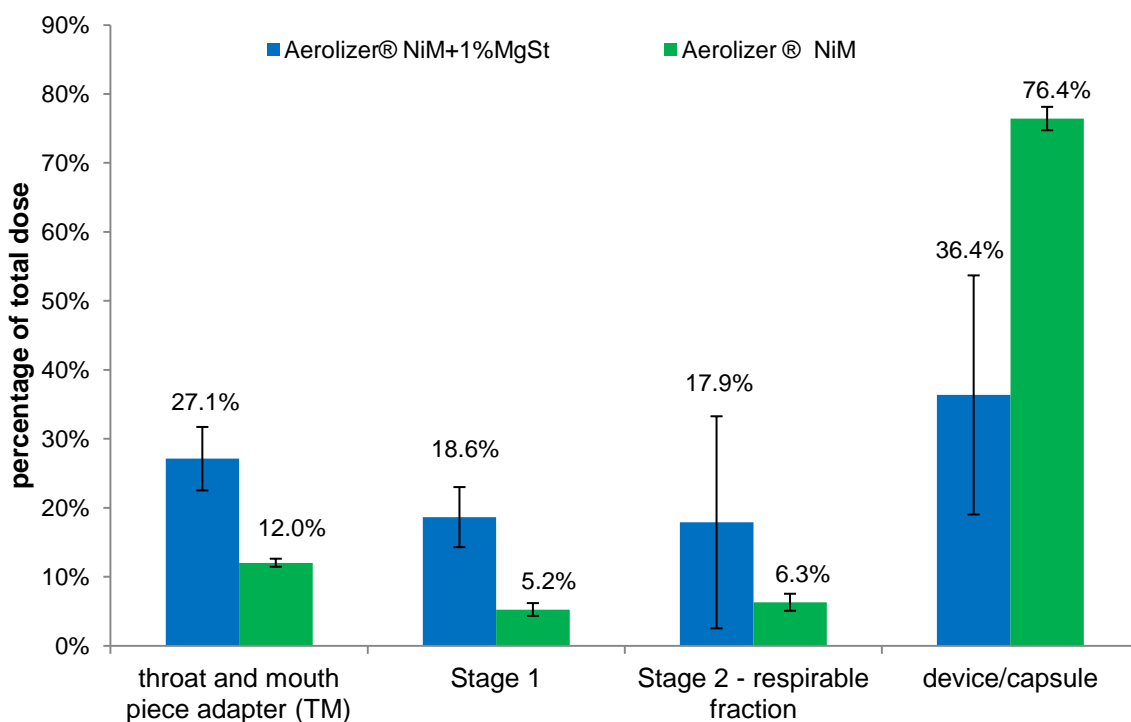


Figure 5.49 Formulation deposition within the TSI for the NiM formulation (green) and the NiM+1%MgSt formulation (blue) using the Aerolizer device. (n=3, error bars represent standard deviation)

For both devices it can be stated that adding magnesium stearate had a very positive effect and led to a significant decrease in the capsule and device retention (CD-retention). In numbers, for the HandiHaler and the Aerolizer the CD-retention decreased by 33.8 and 40.0 percentages points, respectively. But this is, especially, regarding the HandiHaler not associated with a notable increase in the respirable fraction which only rose from 5.1% to 6.5% because the formulation which then was additionally delivered was nearly completely deposited in stage 1 which thus increased from 19.5% to 58.5% of the total dose. There was also a decrease in the TM fraction but this percentage of the formulation was also mainly deposited in stage 1. Thus, regarding the HandiHaler it can be concluded that the blending process led to significant improvement in the amount of formulation that is actually delivered from device but not to a notable increase in the respirable fraction. Therefore, it is assumed that the blending step with MgSt reduces the adhesion forces between the powder particles and the capsule as well

as between powder particles and the device and thus led to a higher delivered dose. Because the respirable fraction did not change it is assumed that the cohesion forces between the particles were not or only to a small extent affected by blending procedure and that the de-agglomeration mechanism of the HandiHaler still was not strong enough to destroy these agglomerates.

Regarding the Aerolizer a strong decrease in the CD-retention was also observed but additionally a notable increase in the respirable fraction which increased from 6.3% to 17.9%. It has to be emphasised that this increase was accompanied by a dramatic rise in the variability in formulation deposition on both stages of the TSI but especially in the respirable fraction.

In summary, when the unblended NiM formulation was administered a very high capsule and device retention was observed. This problem was solved by adding 1% magnesium stearate to the NiM formulation and blending both components together for 3 hours. The new NiM-1%MgSt formulation showed a much lower capsule and device retention for both devices. Regarding the HandiHaler no notable improvement in the respirable fraction could be detected. However, for the Aerolizer a rise in the respirable fraction but associated by a dramatic increase in the deposition variability was observed. All deposition data are once again summarised in Table 5.12

Table 5.12 *Formulation deposition of the NiM and the NiM-1%MgSt formulations for both devices using the TSI as percentage calculated based on the total dose. (n=3; ±sd)*

Device	Formulation	Device/Capsule	TM	Stage 1	Stage 2
HandiHaler	NiM	56.3% (±5.48)	19.1% (±2.66)	19.5% (±2.20)	5.1% (±3.71)
	NiM-1%MgSt	22.5% (±0.54)	12.5% (±0.77)	58.5% (±0.81)	6.5% (±0.76)
Aerolizer	NiM	76.4% (±1.70)	12.0% (±0.58)	5.2% (±0.93)	6.3% (±1.23)
	NiM-1%MgSt	36.4% (±17.33)	27.1% (±4.60)	18.6% (±4.36)	17.9% (±15.7)

In conclusion, the high CD-retention of the pure spray dried NiM formulation could be reduced dramatically by adding 1% MgSt and blending. Because the respirable fraction of this new formulation was not significantly higher further optimisation would be necessary. Finding a way of reducing the cohesion between

the particles would have to be the next task in this direction but because of the prioritisation and the opportunity to perform a second *in vivo* and *in vitro* study this approach was not pursued further.

5.5 Antigen Stability in the NiM Formulation

Because of the performance in the aerodynamic studies (5.4) only the spray dried formulation was investigated with respect to the antigen stability. Although the integrity of the antigen that is used is not always an indispensability to trigger an immune response, this parameter can be used to review whether the most important component of the formulation is affected by the preparation process. In order to verify this, SDS-PAGE of BSA containing spray dried particles was performed as described in section 4.8.

5.5.1 Sample Preparation

The obtained spray dried NiM formulation was redispersed under stirring in PBS buffer pH 7.4 for 3 h in order to extract the entire protein. Then the sample was centrifuged (Centrifuge 5430 R, Eppendorf AG, Hamburg, Germany) for 30 min at 10,000 rcf (10,911 rpm) to separate the nanoparticles, the supernatant was subsequently ultra-filtrated using Vivaspin 6 tubes with a MW cut off of 5,000 dalton (Sartorius stedim biotech GmbH, Göttingen, Germany) at 4,000 rcf (6,901 rpm) for 30 min to concentrate the protein. 40 μL of loading buffer (consisting of sodium dodecyl sulfate, glycerine, bromophenol blue, β -mercaptoethanol and double distilled water) were added to 20 μL of the sample. In addition, as reference a sample containing 1.2 $\text{mg}\cdot\text{mL}^{-1}$ BSA in PBS buffer pH 7.4 (BSA), a sample with 1.2 $\text{mg}\cdot\text{mL}^{-1}$ BSA dissolved in 1 N NaOH (BSA-NaOH) and the molecular weight marker (MW) were loaded on the gel.

5.5.2 Results of the Antigen Stability

The results of the SDS-PAGE are shown in Figure 5.50 and it can be seen that the molecular weight of the protein in the formulation did not change during the

formulation process, because the bands of the samples (NPs) correspond to the band on the reference (BSA). Thus, it can be assumed that the protein retained its immunological activity. In addition, it can be seen that when BSA is heated in 1N NaOH for 1 h (BSA-NaOH) the structure of the protein was destroyed.

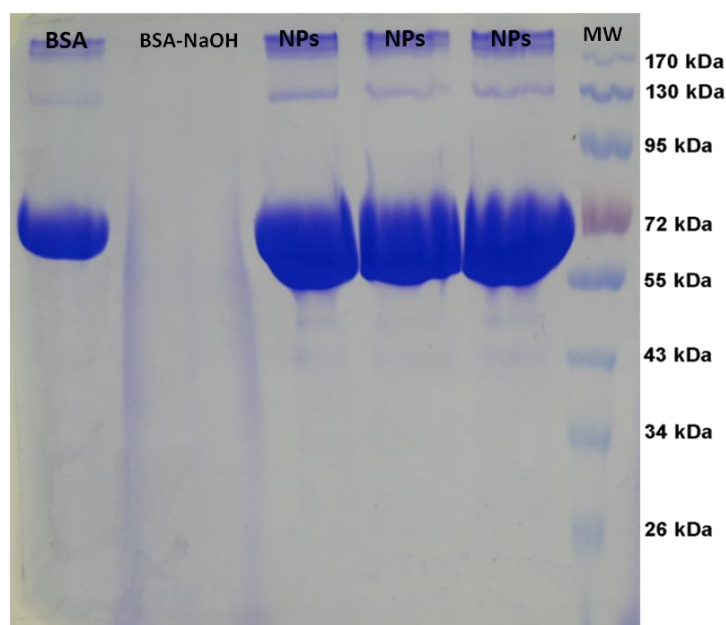


Figure 5.50 SDS-PAGE gel of the BSA containing nano-in-microparticle formulation with BSA reference and molecular weight marker.

5.6 In Vitro and in Vivo Evaluation of Spray Dried Chitosan Nano-in-Microparticles as Vaccine Formulation

Finally, a second *in vivo* study (immunisation study) was conducted in which the developed spray dried nano-in-microparticle formulation was evaluated with respect to its capacity to induce antigen specific (OVA) CD4⁺ and CD8⁺ T cell response after intranasal administration. In addition, *in vitro* experiments were performed in which the cellular uptake in bone-marrow dendritic cells (BMDC) and the cell toxicity in Calu-3 cells of the NiM formulation were investigated. In these studies the findings achieved in the first one (5.2) were brought together with the knowledge acquired from the nanoparticle forming and drying experiments (5.3). Because in the first *in vivo* study (5.2) Chitosan from Sigma showed the highest adjuvant activity in mice it was chosen to be used in this study as

adjuvant and particle forming excipient. The developed dry powder nano-in-microparticle formulation was produced and then administered to the animals using a nasal insufflator for rodents. In addition, FITC-labelled chitosan nano-in-microparticles were prepared and investigated in the *in vitro* experiments to examine their uptake in bone-marrow dendritic cells. The BMDC cell uptake and the *in vivo* experiments were performed in cooperation with Sarah Hook at the University of Otago, School of Pharmacy in Dunedin, New Zealand.

5.6.1 Preparation of the NiM Formulation for in Vivo Characterisation

Chitosan from Sigma was dissolved in 1% acetic acid to a concentration of 0.1% then 2.5 parts of PBS buffer pH 7.4 and 7.5 parts of ddH₂O were added to 10 parts of the chitosan solution. Subsequently, the pH value was adjusted and an OVA (5 mg*mL⁻¹) containing 0.2% DCA solution was added under stirring (650 rpm) to obtain the nanoparticle suspension. A 10% mannitol solution was added to this suspension in a one plus one ratio. The dry powder formulation was obtained by spray drying with an inlet temperature of 115°C and an outlet temperature of 60°C, respectively, using the 1.5 mm nozzle due to administration to mice. The particle size distributions of the primary nanosuspension and of the spray dried product after reconstitution were determined using PCS.

The results are shown in Figure 5.51. Z-average values were 242 nm (polydispersity index: 0.270) and 266 nm (0.244) for the nanoparticles before and after spray drying, respectively. Therefore, it can be stated that the nanoparticles actually had not changed in size and distribution during the spray drying process. Looking at the PCS data it can be seen that there is a small group of smaller particles below 100 nm. It is assumed that this is, somehow, due to the molecular weight (148.5 kDa) or the DDA (75.8%) because the same effect was observed for the preparation of nanoparticles using Chitopharm L (M_w : 135.2 kDa, DDA: 73.5%; Figure 5.21) but not for Chitopharm S and M. Nevertheless, the fundamental mechanism for this observation could not be clarified in this work.

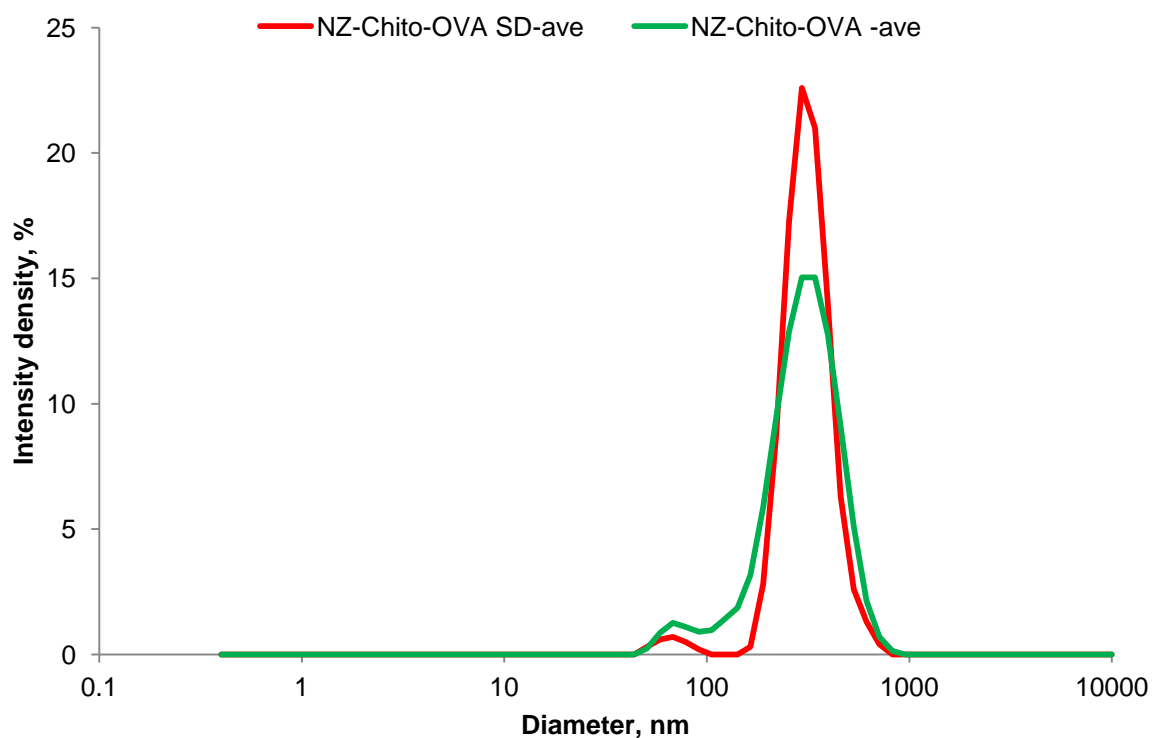


Figure 5.51 Particle size distribution of the nanosuspension (green) and the in water reconstituted spray dried NiM formulation (red). Curves represent a mean of three measurements. Nanosuspension 242 nm (PDI 0.270); spray dried NiM formulation 266 nm (PDI 0.244)

The final composition of the spray dried NiM formulation for this *in vivo* study is displayed in Table 5.13.

*Table 5.13 Composition of the spray dried NiM formulation for in vivo testing. *(Protein content determined via BCA assay)*

Component	Amount
Chitosan	0.4%
Na-Deoxycholate	0.4%
Antigen (OVA)	1% *(0.91%)
PBS salts	1%
Mannitol	97.2%

5.6.2 Preparation of FITC-labelled Chitosan for in Vitro Cell Uptake

For labelling chitosan with FITC a method described by Colonna et al (Colonna et al., 2008) was used. For this, 15 mL of methanol were mixed with 15 mL chitosan solution (1% chitosan in 0.1 N acetic acid). Subsequently, 7.5 mL of a 2 mg*mL⁻¹ FITC containing methanol solution were added to the chitosan solution to start the reaction. The reaction was run for 3 h in the dark at room temperature. Afterwards, the labelled chitosan was precipitated using 1 N sodium hydroxide at a pH value of 10. To collect the labelled chitosan the suspension was centrifuged at 7,800 rpm for 20 min at 30°C. The elevated temperature was selected to ease the sedimentation of the chitosan. Subsequently, the supernatant was removed and the sediment was rinsed with a water/methanol (30:70 v/v) mixture. A second centrifugation was performed with the same settings regarding the duration and rotation velocity but with a reduced temperature of 15°C. This procedure was repeated 10 times until the supernatant showed no fluorescence. The centrifuged chitosan was dissolved in 1% acetic acid and dialysed in the dark against water for two days using a Micro Float-A-Lyzer from Spectrum Europe B.V. (Brede, Netherlands) with a cellulose ester membrane and a molecular weight cut-off (MWCO) of 1 kD in order to remove FITC which was not bound to chitosan. Finally, the samples were transferred into a pre-cooled freeze dryer at -30°C. After 12 h of acclimatisation primary drying was started for 24 h at a temperature of -

20°C and a pressure of 1.030 mbar. Secondary drying was performed for 48 h at 20°C and a vacuum pressure of 0.001 mbar. The obtained freeze dried product was stored over P₂O₅ until it was used. Chitosan from Sigma was labelled. The labelled chitosan was used to prepare nanoparticles which then were spray dried to achieve a FITC stained NiM formulation to make the formulation accessible for intracellular detection. The particles were produced using the standard gelation method (5.3.1.3) and the established parameters in the spray drying process (5.3.3). Particle size distribution of the primary nanoparticles before and after spray drying is shown in Figure 5.52. The z-average values of the nanosuspensions before and after drying were 287 nm with a polydispersity index of 0.258 and 268 nm also with a polydispersity index of 0.258, respectively. Therefore, it can be stated that actually no change in size and distribution occurred during the spray drying process.

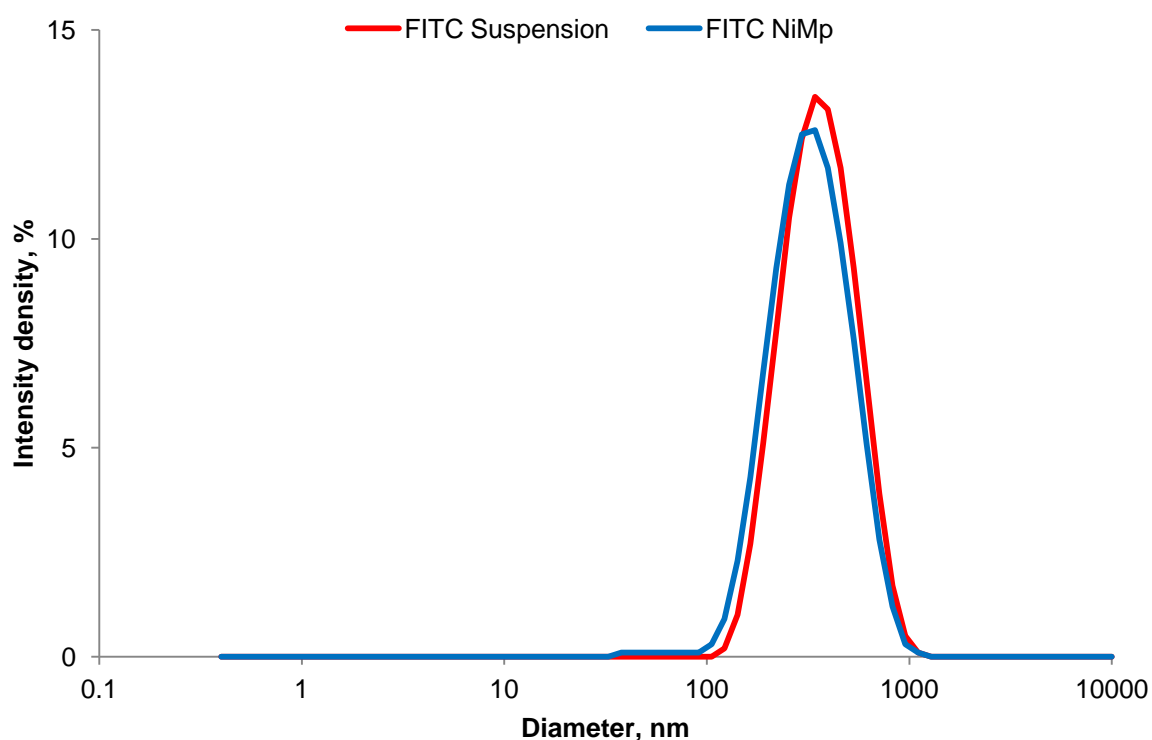


Figure 5.52 Particle size distribution by PCS of the FITC stained nanoparticles as suspension (red) and formulated as NiM powder after reconstitution in water (blue). Curves represent the mean values of three measurements.

5.6.3 Protein Stability of the Formulation

In order to ensure that the antigen (OVA) was not harmed by the production process SDS-PAGE and CD spectra of the final formulation were recorded.

5.6.3.1 SDS-PAGE of the NiM Formulation

The unstained spray dried NiM formulation was redispersed under stirring in PBS buffer pH 7.4 for 3 h. Then the sample was centrifuged (Centrifuge 5430 R, Eppendorf AG, Hamburg, Germany) for 30 min at 10,000 rcf (10,911 rpm) to separate the nanoparticles. 40 μ L of the loading buffer were added to 20 μ L of the supernatant. An OVA reference and a molecular weight marker were also applied. As displayed in Figure 5.53 it can be seen that the OVA processed in the NiM particles was not affected by that process regarding its molecular weight. The bands obtained from the NiM formulation (NPs) were on the same height as that one of the OVA reference. Therefore, it can be stated that the preparation process did not influence the OVA regarding its molecular weight.

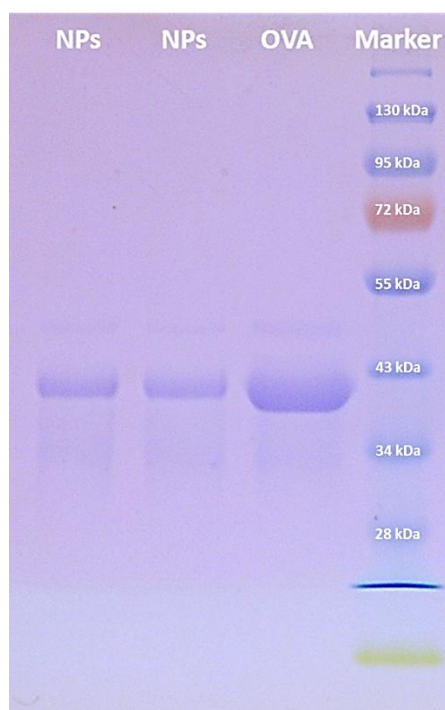


Figure 5.53 SDS-PAGE gel obtained from the OVA containing nano-in-microparticle formulation (NPs = NiM formulation), the protein (OVA) reference and the molecular weight marker.

5.6.3.2 Circular Dichroism of the NiM formulation

The CD spectrum (Figure 5.54) gives more information about the secondary structure of the protein and possible changes during the preparation process. For this, protein being extracted from the final NiM formulation was compared to an OVA reference. It can be seen that the two spectra are very similar and thus it can be stated that no significant structural changes occurred and that secondary structure of the OVA was actually unaffected.

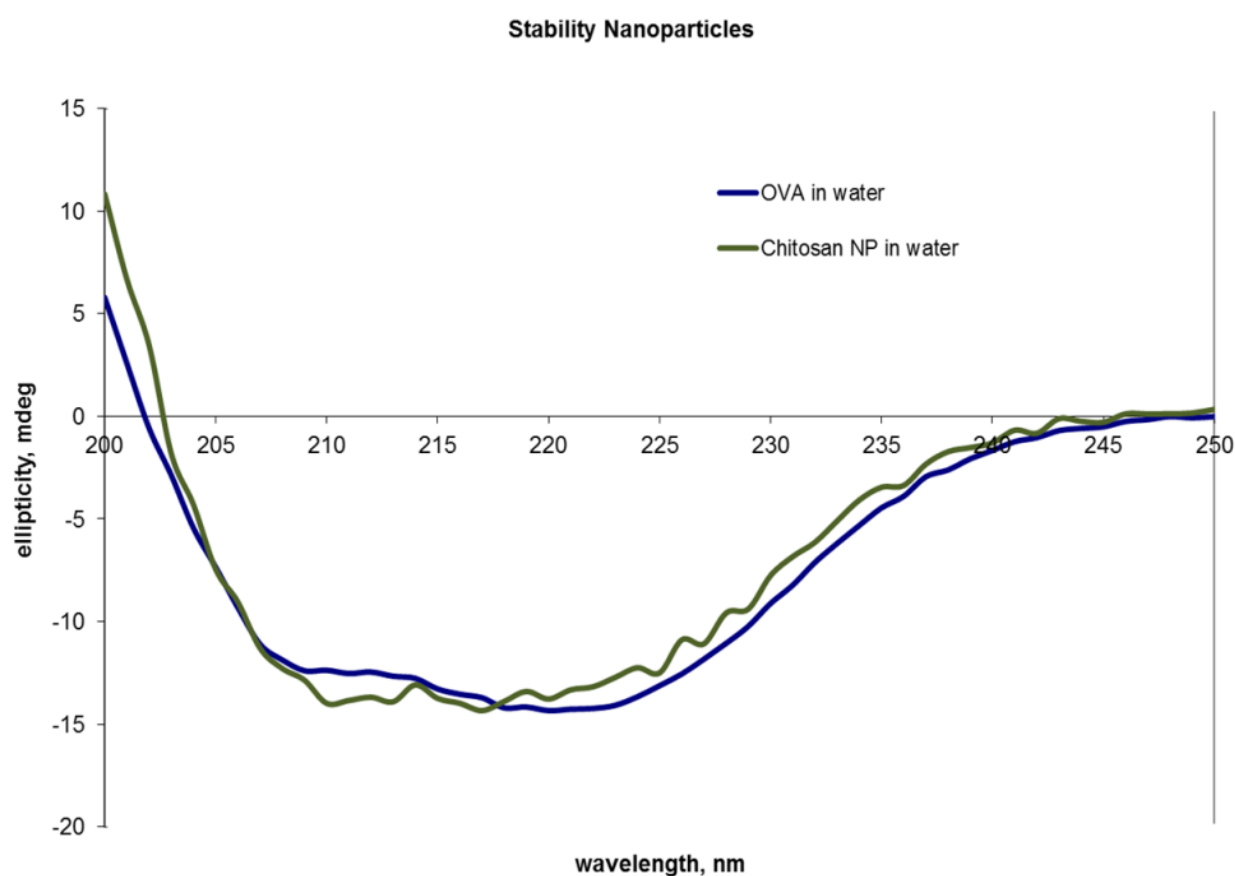


Figure 5.54 CD spectra of the OVA containing nano-in-microparticle formulation (dark green) and the OVA reference (blue).

5.6.4 MTT assay of the Spray Dried NiM Formulation

Like both spray dried chitosan formulations which were used in the first *in vivo* study the spray dried nano-in-microparticle formulation was tested regarding its cell toxicity using the MTT assay with Calu-3 cells, as described in section 4.13.1.2. Results of the NiM formulation compared to its main component mannitol (about 97.2% of the formulation) are displayed in Figure 5.55. The LC_{50} -value was calculated based on a four parameter sigmoidal plot and turned out to be 2.1855% for the NiM formulation.

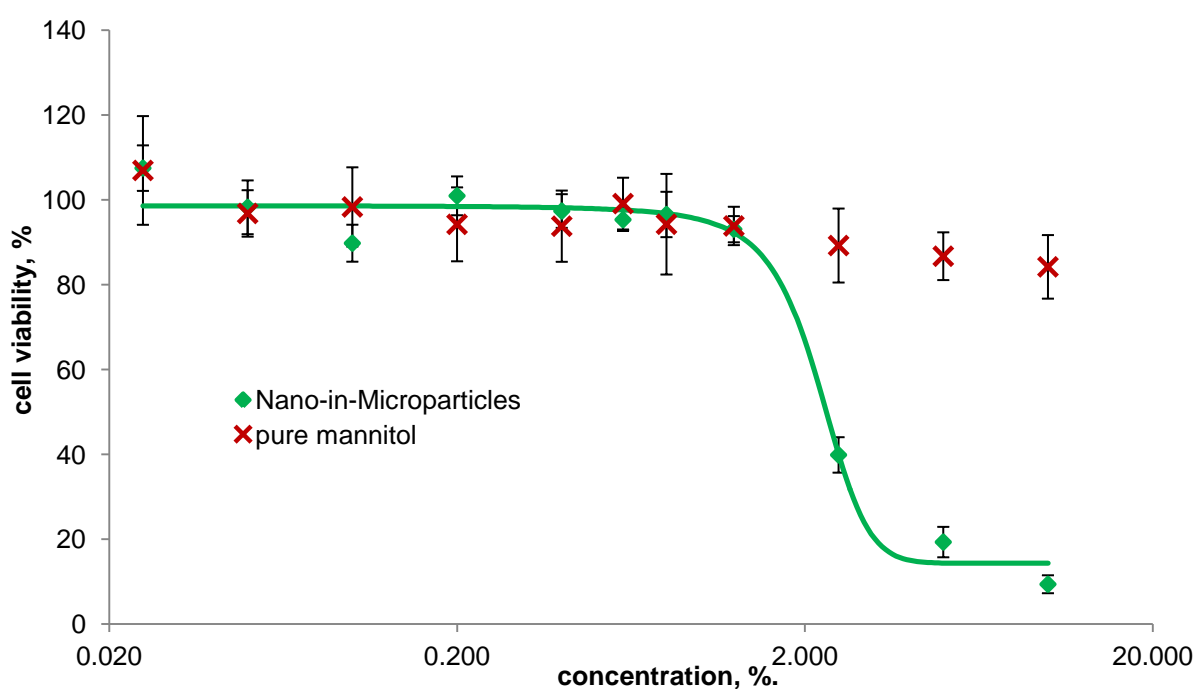


Figure 5.55 Toxicity data of spray dried Nano-in-Microparticles and pure mannitol (Pearlitol SD 200). Error bars show the standard deviation of the quadruple analysis.

5.6.5 *In Vitro Uptake into Bone Marrow-Derived Dendritic Cells*

In order to examine the cellular uptake by bone marrow-derived dendritic cells (BMDCs; 4.13.2) the FITC stained NiM formulation (5.6.2) was suspended in sterile PBS buffer pH 7.4 in three different concentrations. Then 500 μL of each suspension was added to 500 μL of the cell suspension so that a polymer concentration of 5, 10 and 50 μg per well resulted. The system was incubated for 24 h prior to FACS analysis. In order to determine the population of DCs data were analysed via FACS analysis by sorting for the CD11⁺ which is a specific DC surface marker. Subsequently, this population was gated for FITC positive cells to identify the percentage of DCs that had taken up the FITC stained NiM formulation. The results of the cell uptake experiment are shown in Figure 5.56. It can be seen that the NiM formulation is taken up by the DCs to a relatively high extent, additionally it can be stated that the extent of the uptake is not so much concentration dependent. An increase in NiM formulation concentration from 10 to 50 μg polymer per well only led to a slight but not significant increase in uptake.

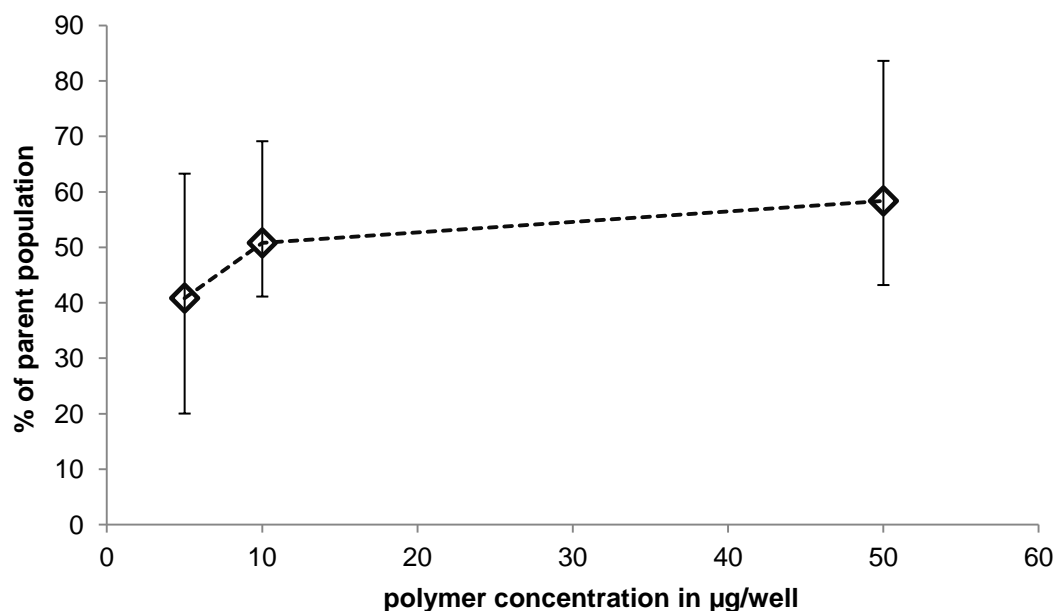


Figure 5.56 NiM formulation uptake in DCs as percentage of all living DCs as a function of the amount of formulation/polymer per well. (n=3, error bars represent the min and max values)

5.6.6 Study Design and Vaccination Scheme

The *in vivo* Study was designed three animals per group and three independent replicates were conducted. It was focused on four different groups which are displayed in Table 5.14. The adoptive transfer of transgenic OVA specific T cells was performed at day -1 and was done as described earlier (5.2.3). The same types of animals (OT-I, OT-II transgenic and C57Bl/6J mice; 3.8) used in the adjuvant study were used in this study. Animals received an initial immunisation at day 0 and two boost immunisations at day 14 and 28, respectively. At day 31 mice were sacrificed and the samples were harvested and prepared for FACS analysis as described earlier (4.14.1).

For intranasal administration of the dry powder (group 1, 2) and the solution (group 3) a dry powder insufflator (Model DP-4M, PennCentury, Wyndmoor, PA, USA) and an eppendorf pipette (Eppendorf AG, Hamburg, Germany) were used, respectively. Animals were anaesthetised via i.p. injection of a combination of ketamine, xylazine and atropine prior to intranasal administration of powder or solution. Regarding the verum NiM formulation (group 1) the delivered powder dose comprised 10 μg of antigen (OVA). For the placebo NiM formulation (group 2) antigen was substituted by the matrix (mannitol).

Table 5.14 *Groups and the formulations they received in the second in vivo study. (i.n.: intranasal administration; s.c.: subcutaneous administration)*

Group No.	Formulation
1	Chitosan-DCA NiM with OVA (i.n.)
2	Chitosan-DCA NiM without OVA (i.n.)
3	sterile PBS with OVA (10 μg in 50 μL ; i.n.)
4	Alum with OVA (50 μg in 200 μL ; s.c.)

5.6.7 Results of the *in Vivo* Evaluation of the Immune Response

In order to evaluate the immune response after immunisation the mediastinal and the cervical lymph nodes of the animals were harvested. The mediastinal lymph nodes belong to the intrathoracic lymph nodes (van den Broeck et al., 2006). They are situated in the mediastinum between the lungs. The cervical lymph nodes are located in the head and neck region, and they belong to the peripheral nodes (van den Broeck et al., 2006).

Samples were analysed via FACS with respect to the expression of CD4⁺ and CD8⁺ transgenic (TG) cells. The obtained data are shown and discussed the following sections. Data were analysed as described before (4.14.2).

5.6.7.1 FACS Data obtained from the Mediastinal Lymph Nodes

The total number of CD4⁺ TG cells obtained from the mediastinal lymph node is shown in Figure 5.57.

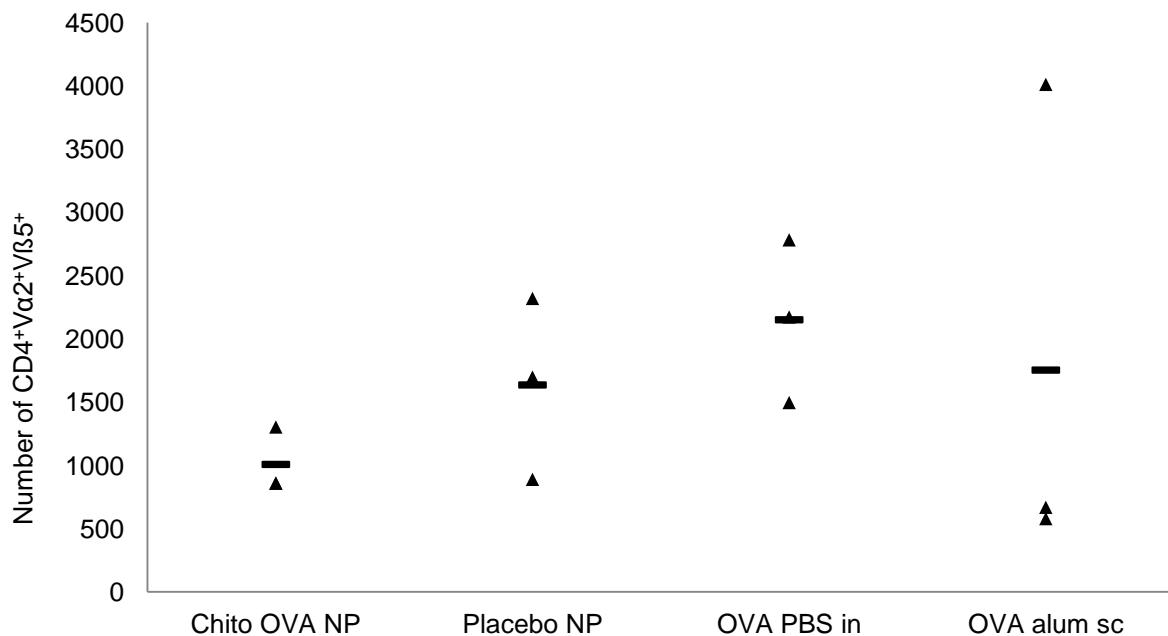


Figure 5.57 Total number of CD4⁺ TG cells from the mediastinal lymph node. Data from each animal (triangle) and the mean group values (black bar). No significant differences between the groups (One way ANOVA).

First, it has to be said that no significant differences between the groups were detected. Group 3 which received OVA in PBS buffer intranasally showed the

highest mean cell count but this value is only slightly higher than those of the other three groups. Regarding group 4 (OVA plus alum s.c.) it has to be stated that a very high variability within the group was observed. Nevertheless, the cell number also depends on the sample preparation which is an explanation for the high variability that was observed for some groups. This makes an interpretation difficult, because of the small group size of only three animals and the fact that only one lymph node was culled per animal.

The same is true when looking at the percentage of CD4⁺ TG cells of the parent population (Figure 5.58), where again a very high variability within group 4 was observed.

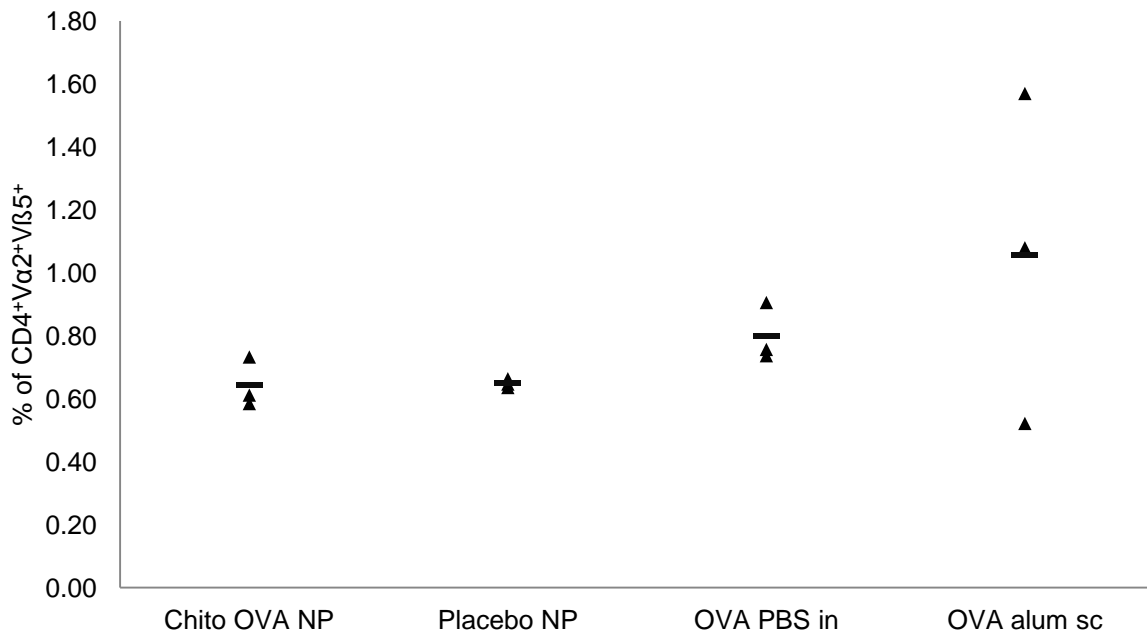


Figure 5.58 Percentage of CD4⁺ TG cells of the parent population from the mediastinal lymph node. Data from each animal (triangle) and the mean group values (black bar). No significant differences between the groups (One way ANOVA on ranks).

In sum, it has to be concluded that regarding the CD4⁺ TG cells the OVA containing Chitosan OVA NP formulation showed no better results compared to the Placebo NP formulation and thus the formulation has not triggered an antigen specific CD4⁺ immune response.

Regarding the total number and percentage of CD8⁺ TG cells in the mediastinal lymph node as illustrated in Figure 5.59 and Figure 5.60 things become more interesting. The number of CD8⁺ TG cells obtained from group 3 (OVA in PBS i.n.) is significantly higher than those of group 4 (OVA plus alum s.c.) and noticeably (but not statistically significant) higher than in group 1 and 2 (Chitosan OVA NP and Placebo NP).

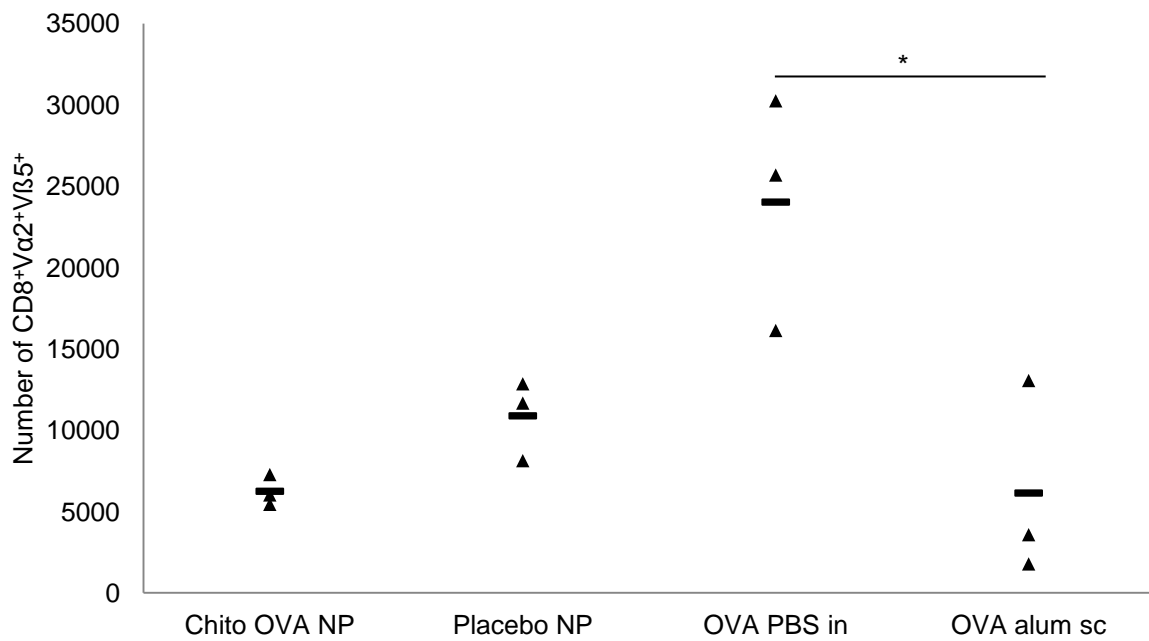


Figure 5.59 Total number of CD8⁺ TG cells from the mediastinal lymph node. Data from each animal (triangle) and the mean group values (black bar). (* $p \leq 0.05$; One way ANOVA).

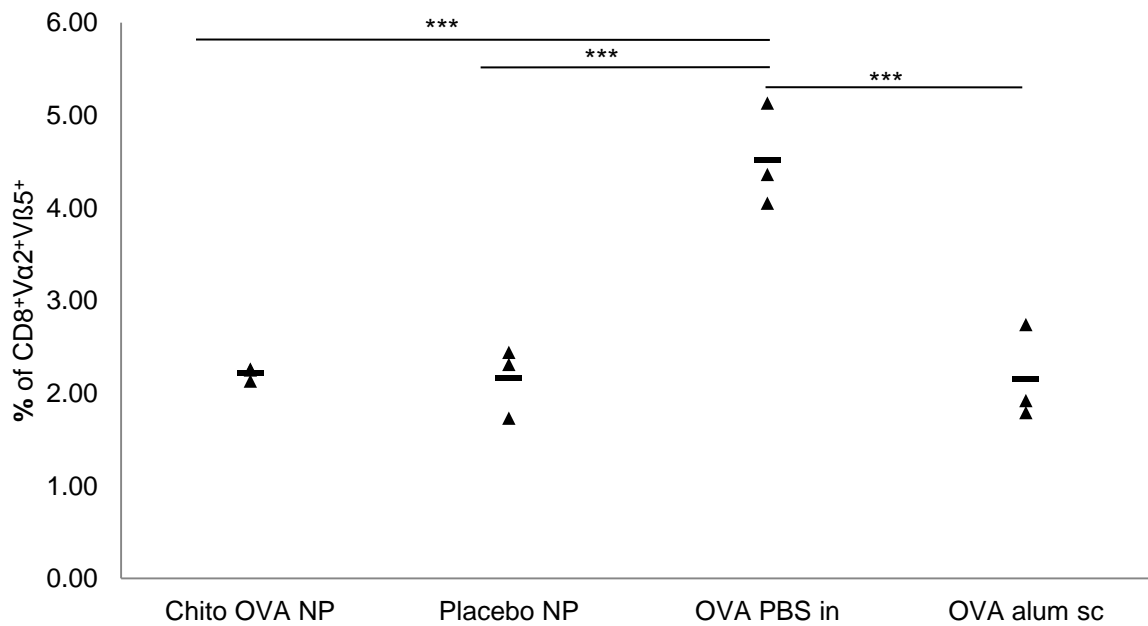


Figure 5.60 Percentage of CD8⁺ TG cells of the parent population from the mediastinal lymph node. Data from each animal (triangle) and the mean group values (black bar). (***) $p \leq 0.001$; One way ANOVA)

Looking at the percentage of CD8⁺ TG cells group 3 (OVA in PBS i.n.) showed statistically significant higher values compared to all the other groups. Regarding this observation one has to consider that parts of the mediastinal lymph nodes are located nearby the trachea and the lungs. It is likely that the liquid formulation partly flowed down the trachea into these regions after administration. Here, the formulation triggered an immune response which causes the higher values of CD8⁺ TG cells. That the same thing also happened with the dry powder is very unlikely and also not wanted. For the dry powder NiM formulations (Chitosan OVA NP, Placebo NP) it can be assumed that they remained inside the nasal cavity after administration.

5.6.7.2 FACS data obtained from the Cervical Lymph Nodes

At first, it has to be mentioned that regarding the cells obtained from the cervical lymph nodes no statistically significant differences between any of the groups that were compared was detected. Nevertheless, looking at the data of CD4⁺ TG cells (total number) shown in Figure 5.61 it can be seen that, this time, the variability within the groups 1 and 2 (Chitosan OVA NP, Placebo NP) was much higher than in group 3 and 4 (OVA in PBS i.n., OVA with alum s.c.). This high variability also led to slightly higher mean values, caused by, in fact, one outstanding high value in each of these two groups. This indicates that the formulation in principle has the ability to induce an immune response but the adjuvant activity was not strong enough and maybe the antigen concentration was also too low.

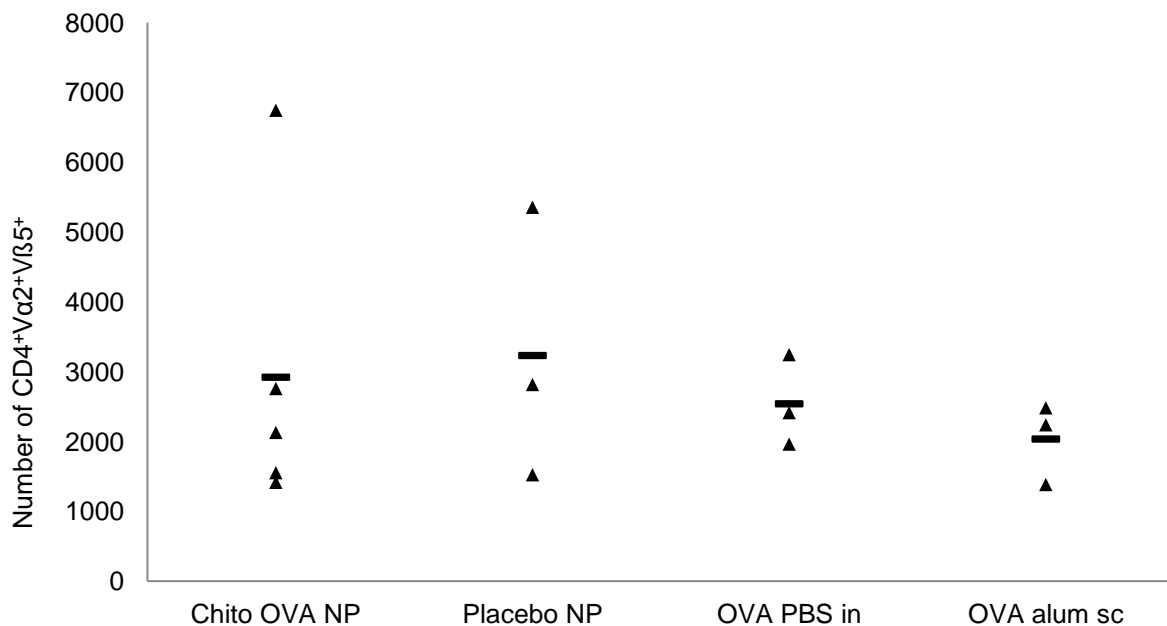


Figure 5.61 Total number of CD4⁺ TG cells from the cervical lymph nodes. Data from each animal (triangle) and the mean group values (black bar). No significant differences between the groups (One way ANOVA).

Regarding the percentage of CD4⁺ TG cells all values, except one animal in group 1 (Chitosan OVA NP), were on the same level and thus the mean values were. Variability within the groups is also quite the same (except group 1).

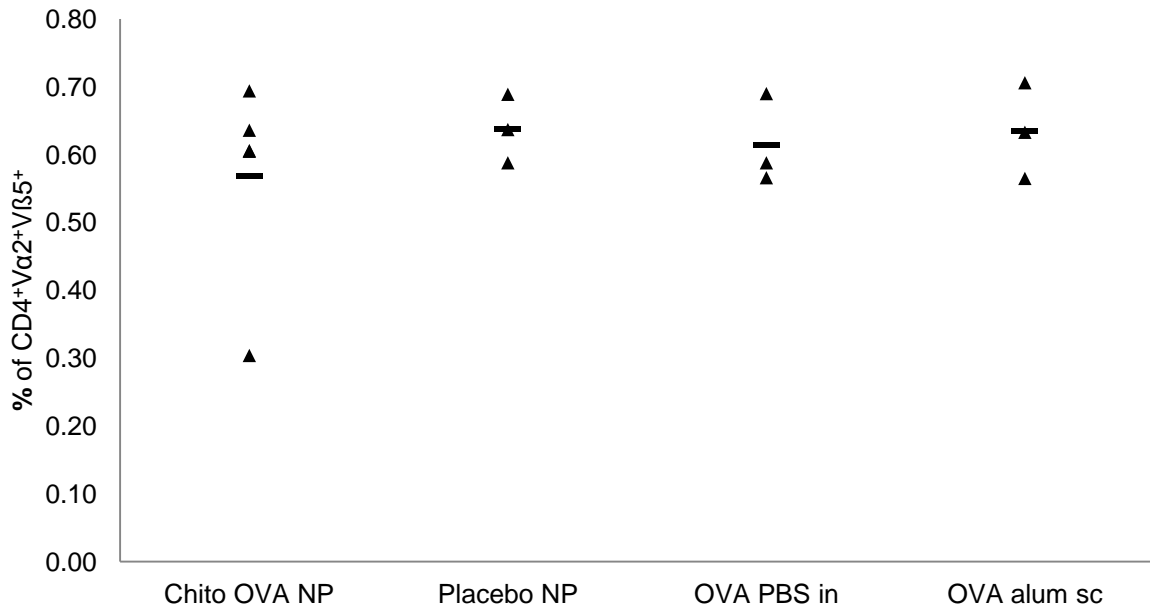


Figure 5.62 Percentage of CD4⁺ TG cells of the parent population from the cervical lymph nodes. Data from each animal (triangle) and the mean group values (black bar). No significant differences between the groups (One way ANOVA on ranks).

Looking at the number and percentage of CD8⁺ TG cells shown in Figure 5.63 and Figure 5.64 it can be seen that the mean values of group 1 and 2 (Chitosan OVA NP; Placebo NP) are slightly increased compared to those of groups 3 and 4 (OVA PBS i.n.; OVA alum s.c.). But as already seen regarding the cells obtained from the mediastinal lymph node the dry powder verum NiM formulation (group 1) showed no statistically significant higher value compared to the placebo formulation (group 2).

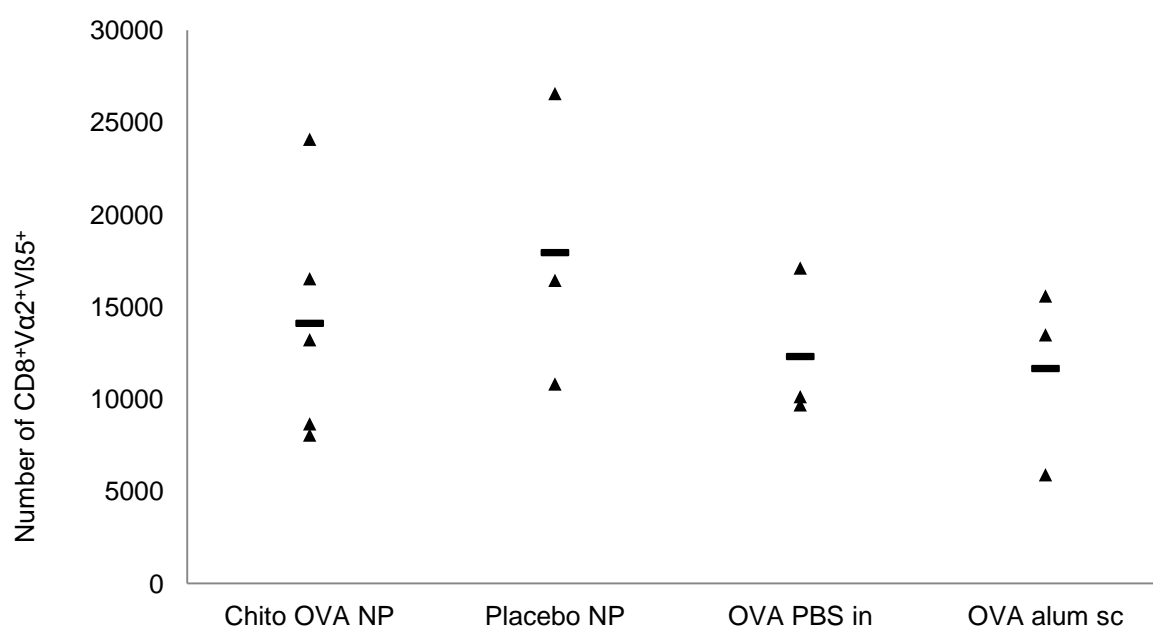


Figure 5.63 Total number of CD8⁺ TG cells from the cervical lymph nodes. Data from each animal (triangle) and the mean group values (black bar). No significant differences between the groups (One way ANOVA).

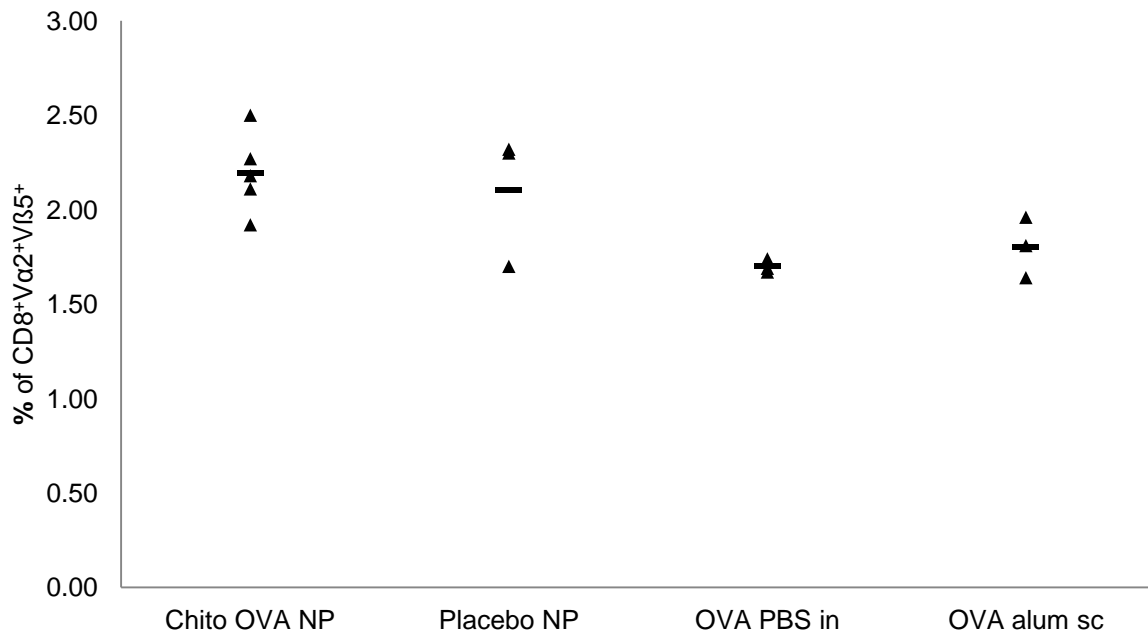


Figure 5.64 Percentages of CD8⁺ TG cells of the parent population from the cervical lymph nodes. Data from each Animal (triangle) and the mean group values (black bar). No significant differences between the groups (One way ANOVA).

In summary, it has to be noted that regarding the analysed CD4⁺ and CD8⁺ TG cells the dry powder Chitosan OVA NP formulation caused not a stronger immune response than the Placebo NP formulation. In none of the comparisons a statistically difference could be detected. Thus, it has to be concluded that no visible antigen specific immune response could be triggered. Only the intranasal administration of OVA in PBS led to significantly higher cell values regarding the percentages of CD8⁺ TG cell gained from the mediastinal lymph node. To improve the formulation adding a second adjuvant which is known to enhance cell-mediated immune response after intranasal administration (e.g. IL-12) (Okada et al., 1997) would be an interesting option. In addition, the amount of model antigen should be increased in order to induce a stronger immune response.

6 Summary

In this work, a dry powder nano-in-microparticle (NiM) vaccine formulation was developed by using a very gentle two-step-production method involving, first, an ionic gelation step to achieve primary nanoparticles followed by a spray drying step to gain the final dry powder vaccine formulation. The biopolymer chitosan was chosen as adjuvant and particle forming excipient because of its mucoadhesive and adjuvant properties. At first, different chitosan qualities were analysed with respect to their polymer properties like the molecular weight and the degree of deacetylation. Subsequently, an *in vivo* study (in cooperation with the University of Otago, Dunedin, New Zealand) was conducted in order to evaluate the adjuvant activity of three different chitosan qualities after s.c. administration. For this, two of the chitosans used were spray dried prior to the application and then administered as PBS soluble hydrochloride salts, the third quality was used as received and thus given as a PBS chitosan suspension. All three qualities were given together with the model antigen ovalbumin and also without it as placebo formulations. As a result of this study Chitosan from Sigma was identified as the chitosan with the highest adjuvant activity. Parallel to this study, a nanoparticle production method was developed. For this, chitosan was dissolved in acidic medium and then the bile salt derivative sodium deoxycholate was added under stirring to induce the gelation process. A method was developed to obtain nanoparticles with about 250 nm in diameter. Particles of this size are known to be taken up well by DCs specialised cells, called M-cells, which are located in the mucosal membranes. Particulate antigens induce both a strong systemic and also a local immune response on the mucosal membranes. The nanoparticles were combined with two model antigens, bovine serum albumin and ovalbumin, that were associated with the particles during the particle forming process. The particle forming process was further investigated regarding the relationship between the pH value of the chitosan solution and the resulting particle size as well as the antigen loading efficiency. These experiments were performed in order to enable the user to produce tailored particles in the different size ranges, if desired. In addition, the influence of the molecular weight of the polymer on the size of the

generated particles was analysed. After that, freeze and spray drying with different stabilising excipients were examined in order to transfer the nanosuspension into a dry powder formulation being capable for direct respiratory administration. Finally, it was found that adding a 10% mannitol solution to the nanosuspension followed by spray drying led to the best dry powder NiM formulation regarding handling and powder properties. Subsequently, protein stability in the final formulation was verified using SDS-PAGE and circular dichroism analysis. The results showed that the antigen (OVA) was not affected by the production process. The obtained powder was further analysed regarding its deposition profile inside the nasal cavity of adults and children using two nasal cast models and a nasal powder dispenser. In order to determine the respirable fraction the Twin Stage Glass Impinger with two dry powder inhalers were used. Obtained data showed that the nasal deposition of the NiM formulation inside the adults nasal cast model was satisfactory, while, due to the anatomy, the amount of NiM formulation deposited in the anterior regions of the child model was unacceptably high and thus the obtained deposition profile failed to match the desired one. Regarding the pulmonary delivery it was found that the produced powder showed a very high capsule and device retention. This problem was solved by adding 1% magnesium stearate to the spray dried powder and blending for 3 h. Nevertheless, the resulting respirable fraction remained little too low. Finally, a second *in vivo* as well as another *in vitro* study were performed. In these studies the produced NiM formulation was administered intranasally to mice and the immune response measured as expression of CD4⁺ and CD8⁺ transgenic (OVA specific) cells was analysed via flow cytometry. In addition, the cell toxicity and the cellular uptake of the NiM formulation were investigated. In these studies it was found that the NiM formulation was taken up by dendritic cells in a satisfactory extent of about 50%. Unfortunately, the magnitude of the immune response induced by the NiM formulation was rather modest and not significantly higher than those induced by the antigen-free placebo NiM formulation. Based on the obtained results, in future work it should be examined if a second adjuvant can be added to the existing formulation in order to increase the immune response. This new formulation should then be tested again in an *in vivo* study regarding

its immunological potential. In order to ensure to induce an appropriate immune response in further studies the amount of antigen in the formulation should also be increased to about 2%. But for this, the NiM formulation which was developed in this work is certainly a good basis for further development and optimisation.

7 Zusammenfassung der Arbeit

In der vorliegenden Arbeit wurde eine nano-in-mikropartikuläre pulverförmige Modelimpfformulierung entwickelt. Zur Herstellung wurde ein schonender zweistufiger Prozess bestehend aus einer ionischer Gelierung, um die primären Nanopartikel zu erhalten und anschließender Sprühtrocknung, um die finale Trockenpulverformulierung zu erhalten, eingesetzt. Das Biopolymer Chitosan wurde aufgrund seiner mukoadhäsiven und adjuvanten Eigenschaften als partikelformender Hilfsstoff und als Adjuvants eingesetzt. Zuerst wurden verschiedene Chitosanqualitäten bezüglich ihrer Polymereigenschaften wie dem Molekulargewicht und dem Deacetylierungsgrad untersucht. Anschließend wurde eine *in vivo* Studie (in Kooperation mit der Universität von Otago in Dunedin, Neuseeland) durchgeführt um das Adjuvantepotenzial von drei Chitosanen nach subkutaner Gabe zu ermitteln. Dazu wurden zwei der Chitosane vor der Gabe sprühgetrocknet und als lösliche Hydrochloride in PBS Puffer verabreicht. Das dritte Chitosan wurde als freie Base eingesetzt und als PBS-Chitosan Suspension verabreicht. Alle Chitosane wurden zusammen mit dem Modelantigen Ovalbumin und zusätzlich als Placebo-Formulierungen ohne Ovalbumin verabreicht. Das Ergebnis zeigte, dass das Chitosan von Sigma das höchste Adjuvantepotenzial besitzt. Parallel zu dieser Studie wurde eine Methode zur Herstellung von Nanopartikeln entwickelt. Dazu wurde das Chitosan in saurem Medium gelöst und mit dem Gallensalzderivat Natriumdesoxycholat unter Rühren ionisch geliert. Die Methode wurde so entwickelt, dass sie zu Nanopartikeln mit einem Durchmesser von um die 250 nm führte. Partikel dieser Größe werden gut von dendritischen Zellen und speziellen Zellen, sogenannten M-Zellen, die in den Schleimhäuten zu finden sind, aufgenommen. Partikuläre Antigene rufen daher sowohl eine starke systemische als auch eine lokale Immunantwort hervor,

wenn sie über die Schleimhäute aufgenommen werden. Die Nanopartikel wurden mit einem Modelprotein (BSA) und einem Modelantigen (OVA) kombiniert. Die Modellsbstanzten wurden während der ionischen Gelierung mit den Partikeln assoziiert. Der Gelierungprozess wurde dann genauer untersucht indem analysiert wurde, welchen Einfluss der pH Wert der Chitosanlösung auf die resultierende Partikelgröße und Beladungseffektivität hat. Diese Versuche helfen den Prozess besser zu verstehen um es anschließend zu ermöglichen Nanopartikel mit zuvor definierten Eigenschaften bezüglich Größe und Beladungseffektivität herzustellen. Zusätzlich wurde der Einfluss verschiedener Molekulargewicht auf die Partikelgröße untersucht. Anschließend wurden Gefriertrocknung und Sprühtrocknung, sowie verschiedene Hilfsstoffe getestet um die erhaltene Nanosuspension in ein trockenes Pulver zu überführen, welche dann direkt nasal oder pulmonal verabreicht werden kann. Es stellte sich heraus, dass die Zugabe einer 10%igen Mannitollösung zur Nanosuspension und anschließendes sprühtrocknen zu dem Pulver mit den besten Eigenschaften bezüglich Handling und Dispergierbarkeit führte. Anschließend wurde die finale Formulierung mit Hilfe von SDS-PAGE und Zirkular Dichroismus bezüglich der Proteinstabilität untersucht. Es zeigte sich, dass die Modellsbstanzten durch den Herstellungsprozess nicht geschädigt wurden. Des Weiteren wurde die Formulierung bezüglich des Depositionsprofils in der Nase untersucht. Dazu wurden zwei Nasenmodelle (erwachsener Mann; Junge, 5 Jahre) und eine Applikationshilfe zur nasalen Verabreichung von Pulvern verwendet. Zusätzlich wurde die respirable Fraktion bestimmt. Hierzu wurde ein zweistufiger Glas Impinger (TSI) zusammen mit zwei Trockenpulverinhalatoren verwendet. Das Depositionsprofil im Model des Mannes war zufriedenstellend, im Gegensatz zu dem im Jungen, wo aufgrund der Anatomie zu viel der Formulierung in den vorderen Teilen der Nase abgeschieden wurde. Bezüglich der respirablen Fraktion stellte sich heraus, dass ein Großteil der Formulierung in der Kapsel beziehungsweise den Inhalatoren zurück gehalten wurde. Durch die Zugabe von 1% Magnesiumstearat konnte dieses Problem gelöst werden, allerdings blieb die respirable Fraktion dennoch etwas zu gering. Zum Abschluss der Arbeit wurde noch eine weitere *in vivo* sowie eine *in vitro* Studie durchgeführt. In dieser Studie wurde Mäusen die finale Formulierung

nasal verabreicht. Die anschließende Immunantwort wurde als Expression von CD4⁺ und CD8⁺ antigenspezifischen (OVA) Zellen mittels Durchflusszytometrie gemessen. Zusätzlich wurde die Zelltoxizität und die Zellaufnahme der Formulierung untersucht. Die Aufnahme der Formulierung in dendritische Zellen war mit um die 50% zufriedenstellend. Leider war die von der Formulierung hervorgerufene Immunantwort eher moderat und nicht signifikant höher als die von der Placebo-Formulierung. Aufbauend auf der bisherigen Arbeit wäre der Einsatz eines zweiten Adjuvants eine interessante Weiterentwicklung der Formulierung. In dieser Formulierung sollte zusätzlich noch die Antigenkonzentration von 1% auf beispielweise 2% erhöht werden um zuverlässig eine Immunantwort hervorzurufen.

8 Appendix

8.1 List of Abbreviations

AD	Anno Domini
ANOVA	analysis of variance
APCs	antigen presenting cells
API	active pharmaceutical ingredient
BALT	bronchus-associated lymphoid tissue
BCA	bicinchoninic acid
BCG	Bacillus Calmette-Guérin
BCR	B cell receptors
BMDCs	bone marrow-derived dendritic cells
BSA	bovine serum albumin
CD	circular dichroism
CD4	cluster of differentiation 4
CD8	cluster of differentiation 8
CDC	Centre for Disease Control and Prevention
CD-retention	capsule and device retention
CFD	computational fluid dynamics
cIMDM	complete Iscove's modified Dulbecco's medium

CLDN 4	claudin-4
cm²	square centimetre
COPD	chronic obstructive pulmonary disease
D₂O	deuterium oxide
Da	Dalton
DCA	sodium deoxycholate
DCs	dendritic cells
DDA	degree of deacetylation
ddH₂O	in double distilled water
DMU	Delivered Mass Uniformity
DPIs	dry powder inhalers
DTT	dithiothreitol
e.g.	exempli gratia (for example)
FACS	fluorescence-activated cell sorting
FBS	foetal bovine serum
FITC	fluorescein isothiocyanate
FSC	forward scatter
GM-CSF	granulocyte macrophage colony stimulating factor
HCl	hydrochloric acid
H-NMR	H-nuclear magnetic resonance spectroscopy
HSA	human serum albumin
i.n.	intranasal
i.p.	intraperitoneal
IEP	isoelectric point
IFN-γ	interferon gamma
IgA	immunoglobulin A
IL-2	interleukin 2
IU	international unit
LAL	limulus amoebocyte lysate
LC₅₀	Lethal Concentration 50%
LCC	liquid-covered culture method
LE	loading efficiency
LN	lymph nodes
MALT	mucosa associated lymphoid tissue
M-cells	microfold cells

MEM	Minimum Essential Medium
MgSt	magnesium stearate
MHC	major histocompatibility complex
mL	millilitre
MPL	monophosphoryl lipid A
MRI	magnetic resonance imaging
MTT	3-(4,5-dimethylthiazol-2-yl)-2,5-diphenyltetrazolium bromide
M_w	weight-average molecular weight
MWCO	molecular weight cut-off
n.s.	not specified
NALT	nose-associated lymphoid tissue
NaOH	sodium hydroxide
NF	National Formulary
NGI	Next Generation Impactor
NiM	nano-in-microparticle
NK-cells	natural killer cells
OVA	ovalbumin
PBS	Phosphate buffered saline
PCCS	photon cross correlation spectroscopy
PCS	photon correlation spectroscopy
PDI	polydispersity index
Ph. Eur.	European Pharmacopoeia
PI	propidium iodide
pMDIs	pressurised metered dose inhalers
ppm	parts per million
PSD	particle size distribution
PTFE	Polytetrafluoroethylene
rcf	relative centrifugal force
rpm	revolutions per minute
s.c.	subcutaneous
SD	spray dried
sd	standard deviation
SDS-PAGE	Sodium dodecyl sulfate polyacrylamide gel electrophoresis
SEM	scanning electron microscope
sIgA	secretory IgA

SLS	static light scattering
SOI	site of injection
SSC	side scatter
TCR	T cells receptors
TEER	transepithelial electric resistance
TG	transgenic
Th1, 2	T helper 1, 2
TJ	tight junction
TM	throat and mouth piece adapter
TSI	Twin Stage Glass Impinger
TSP	deuterated sodium trimethylsilyl propionate
USP	United States Pharmacopeia
WHO	World Health Organisation
WIV	whole inactivated virus
WSC	water-soluble-protein-like-contaminates
x-ray CT	x-ray computed tomography

9 References

- Aiba (1992): Studies on chitosan: 4. Lysozymic hydrolysis of partially N-acetylated chitosans. In *International Journal of Biological Macromolecules* 14 (4), pp. 225–228.
- Alpar; Somavarapu; Atuah; Bramwell (2005): Biodegradable mucoadhesive particulates for nasal and pulmonary antigen and DNA delivery. Trends in Particulate Antigen and DNA Delivery Systems for Vaccines. In *Advanced Drug Delivery Reviews* 57 (3), pp. 411–430.
- Amidi; Mastrobattista; Jiskoot; Hennink (2010): Chitosan-based delivery systems for protein therapeutics and antigens. Chitosan-Based Formulations of Drugs, Imaging Agents and Biotherapeutics. In *Advanced Drug Delivery Reviews* 62 (1), pp. 59–82.
- Amidi; Romeijn; Borchard; Junginger; Hennink; Jiskoot (2006): Preparation and characterization of protein-loaded N-trimethyl chitosan nanoparticles as nasal delivery system. In *Journal of Controlled Release* 111 (1–2), pp. 107–116.
- Amorij; Huckriede; Wilschut; Frijlink; Hinrichs (2008): Development of Stable Influenza Vaccine Powder Formulations: Challenges and Possibilities. In *Pharmaceutical Research* 25 (6), pp. 1256–1273.
- Amorij; Kersten; Saluja; Tonnis; Hinrichs; Slütter et al. (2012): Towards tailored vaccine delivery: Needs, challenges and perspectives. In *Journal of Controlled Release* 161 (2), pp. 363–376.
- Amorij; Meulenaar; Hinrichs; Stegmann; Huckriede; Coenen; Frijlink (2007): Rational design of an influenza subunit vaccine powder with sugar glass technology: Preventing conformational changes of haemagglutinin during freezing and freeze-drying. In *Vaccine* 25 (35), pp. 6447–6457.
- Ansaldi; Bacilieri; Durando; Sticchi; Valle; Montomoli et al. (2008): Cross-protection by MF59™-adjuvanted influenza vaccine: Neutralizing and haemagglutination-inhibiting antibody activity against A(H3N2) drifted influenza viruses. In *Vaccine* 26 (12), pp. 1525–1529.
- Aranaz; Mengibar; Harris; Panos; Miralles; Acosta et al. (2009): Functional Characterization of Chitin and Chitosan. In *Current Chemical Biology* 3 (2), pp. 203–230.
- Aspden; Mason; Jones; Lowe; Skaugrud; Illum (1997): Chitosan as a nasal delivery system: The effect of chitosan solutions on in vitro and in vivo mucociliary transport rates in human turbinates and volunteers. In *Journal of Pharmaceutical Sciences* 86 (4), pp. 509–513.
- Bacon; Newman; Rankin; Pitcairn; Whiting (2012): Pulmonary and nasal deposition of ketorolac tromethamine solution (SPRIX) following intranasal administration. In *International Journal of Pharmaceutics* 431 (1–2), pp. 39–44.

- Baldrick (2010): The safety of chitosan as a pharmaceutical excipient. In *Regulatory Toxicology and Pharmacology* 56 (3), pp. 290–299.
- Bannister; Bannister (1974): Circular dichroism and protein structure. In *International Journal of Biochemistry* 5 (9–10), pp. 673–677.
- Barnden; Allison; Heath; Carbone (1998): Defective TCR expression in transgenic mice constructed using cDNA-based [agr]- and [bgr]-chain genes under the control of heterologous regulatory elements. In *Immunology and Cell Biology* 76 (1), pp. 34–40.
- Baudner; Giuliani; Verhoef; Rappuoli; Junginger; Giudice (2003): The concomitant use of the LTK63 mucosal adjuvant and of chitosan-based delivery system enhances the immunogenicity and efficacy of intranasally administered vaccines. In *Vaccine* 21 (25–26), pp. 3837–3844.
- Baxter; Dillon; Anthony Taylor; Roberts (1992): Improved method for i.r. determination of the degree of N-acetylation of chitosan. In *International Journal of Biological Macromolecules* 14 (3), pp. 166–169.
- Behara; Kippax; Larson; Morton; Stewart (2011): Kinetics of emitted mass—A study with three dry powder inhaler devices. In *Chemical Engineering Science* 66 (21), pp. 5284–5292.
- Behm (1997): The role of trehalose in the physiology of nematodes. In *International Journal for Parasitology* 27 (2), pp. 215–229.
- Bennett; Zeman; Jarabek (2007): Nasal Contribution to Breathing and Fine Particle Deposition in Children Versus Adults. In *Journal of Toxicology and Environmental Health, Part A* 71 (3), pp. 227–237.
- Berthold; Cremer; Kreuter (1996): Preparation and characterization of chitosan microspheres as drug carrier for prednisolone sodium phosphate as model for anti-inflammatory drugs. In *Journal of Controlled Release* 39 (1), pp. 17–25.
- Birch (1963): Trehaloses. In *Advances in Carbohydrate Chemistry* 18, pp. 201–225.
- Bivas-Benita; Ottenhoff; Junginger; Borchard (2005): Pulmonary DNA vaccination: Concepts, possibilities and perspectives. In *Journal of Controlled Release* 107 (1), pp. 1–29.
- Bloemendal; Jiskoot (2005): Circular Dichroism Spectroscopy. USA: AAPS Press.
- Bloom; Canning; Weston (2005): The Value of Vaccination. In *World Economics* 6 (3), pp. 15–39.
- Bonu; Rani; Baker (2003): The impact of the national polio immunization campaign on levels and equity in immunization coverage: evidence from rural North India. In *Social Science & Medicine* 57 (10), pp. 1807–1819.
- Boonsongrit; Mitrevej; Mueller (2006): Chitosan drug binding by ionic interaction. In *European Journal of Pharmaceutics and Biopharmaceutics* 62 (3), pp. 267–274.
- Borges; Cordeiro-da-Silva; Romeijn; Amidi; Sousa; Borchard; Junginger (2006): Uptake studies in rat Peyer's patches, cytotoxicity and release studies of alginate

- coated chitosan nanoparticles for mucosal vaccination. In *Journal of Controlled Release* 114 (3), pp. 348–358.
- Braun (1998): ¹H-NMR-Spektroskopie. In *CHEMKON* 5 (4), pp. 187–192.
- Bravo-Osuna; Vauthier; Farabollini; Palmieri; Ponchel (2007): Mucoadhesion mechanism of chitosan and thiolated chitosan-poly(isobutyl cyanoacrylate) core-shell nanoparticles. In *Biomaterials* 28 (13), pp. 2233–2243.
- Brugnerotto; Lizardi; Goycoolea; Argüelles-Monal; Desbrières; Rinaudo (2001): An infrared investigation in relation with chitin and chitosan characterization. In *Polymer* 42 (8), pp. 3569–3580.
- Bruner; St. Tolloczko (1901): Über die Auflösungsgeschwindigkeit fester Körper. In *Zeitschrift für anorganische Chemie* 28 (1), pp. 314–330.
- Cadete; Figueiredo; Lopes; Calado; Almeida; Gonçalves (2012): Development and characterization of a new plasmid delivery system based on chitosan–sodium deoxycholate nanoparticles. In *European Journal of Pharmaceutical Sciences* (45), p. 451.
- Cao (2008): Immunology in China: the past, present and future. In *Nature Immunology* 9 (4), pp. 339–342.
- Carter; He; Munson; Twigg; Gernert; Broom; Miller (1989): Three-dimensional structure of human serum albumin. In *Science* 244 (4909), pp. 1195–1198.
- CDC (2013): Guidelines for Vaccinating Pregnant Women. April 2013. Centre of Disease Control and Prevention.
- Chadwick; Kriegel; Amiji (2010): Nanotechnology solutions for mucosal immunization. Nanotechnology Solutions for Infectious Diseases in Developing Nations. In *Advanced Drug Delivery Reviews* 62 (4-5), pp. 394–407.
- Chang; Wu; Yang (1978): Circular dichroic analysis of protein conformation: Inclusion of the β -turns. In *Analytical Biochemistry* 91 (1), pp. 13–31.
- Cheng; Holmes; Gao; Guilmette; Li; Surakitbanharn; Rowlings (2001): Characterization of Nasal Spray Pumps and Deposition Pattern in a Replica of the Human Nasal Airway. In *Journal of aerosol medicine* 2 (14), pp. 267–280.
- Chung; Lee; Lee (2012): Mechanism of freeze-drying drug nanosuspensions. In *International Journal of Pharmaceutics* 437 (1–2), pp. 42–50.
- Cleland (1964): Dithiothreitol, a New Protective Reagent for SH Groups*. In *Biochemistry* 3 (4), pp. 480–482.
- Cocquyt; Baten; Simoens; van Broeck (2005): Anatomical localisation and histology of the ovine tonsils. In *Veterinary Immunology and Immunopathology* 107 (1–2), pp. 79–86.
- Colonna; Conti; Perugini; Pavanetto; Modena; Dorati et al. (2008): Ex vivo evaluation of prolidase loaded chitosan nanoparticles for the enzyme replacement therapy. In *European Journal of Pharmaceutics and Biopharmaceutics* 70 (1), pp. 58–65.

- Cormack; Valdivia; Falkow (1996): FACS-optimized mutants of the green fluorescent protein (GFP). In *Gene* 173 (1), pp. 33–38.
- Davis (2001): Nasal vaccines. In *Advanced Drug Delivery Reviews* 51 (1–3), pp. 21–42.
- Debord; Lefebvre; Guyot-Hermann; Hubert; Bouché; Cuyot (1987): Study of Different Crystalline forms of Mannitol: Comparative Behaviour under Compression. In *Drug Development and Industrial Pharmacy* 13 (9-11), pp. 1533–1546.
- Deli (2009): Potential use of tight junction modulators to reversibly open membranous barriers and improve drug delivery. Apical Junctional Complexes Part II. In *Biochimica et Biophysica Acta (BBA) - Biomembranes* 1788 (4), pp. 892–910.
- Deng; Cao; Wang (2009): Coacervation of Cationic Gemini Surfactant with Weakly Charged Anionic Polyacrylamide. In *Journal of Physical Chemistry B* 113 (28), pp. 9436–9440.
- Denizot; Lang (1986): Rapid colorimetric assay for cell growth and survival: Modifications to the tetrazolium dye procedure giving improved sensitivity and reliability. In *Journal of Immunological Methods* 89 (2), pp. 271–277.
- Dokoumetzidis; Macheras (2006): A century of dissolution research: From Noyes and Whitney to the Biopharmaceutics Classification System. In *International Journal of Pharmaceutics* 321 (1–2), pp. 1–11.
- Domard (1987): Determination of N-acetyl content in chitosan samples by c.d. measurements. In *International Journal of Biological Macromolecules* 9 (6), pp. 333–336.
- Domard; Rinaudo (1983): Preparation and characterization of fully deacetylated chitosan. In *International Journal of Biological Macromolecules* 5 (1), pp. 49–52.
- Donovan; Mapes (1976): A differential scanning calorimetric study of conversion of ovalbumin to S-ovalbumin in eggs. In *Journal of the Science of Food and Agriculture* 27 (2), pp. 197–204.
- Dupuis; Denis-Mize; LaBarbara; Peters; Charo; McDonald; Ott (2001): Immunization with the adjuvant MF59 induces macrophage trafficking and apoptosis. In *European Journal of Immunology* 31 (10), pp. 2910–2918.
- Dupuis; Murphy; Higgins; Ugozzoli; van Nest; Ott; McDonald (1998): Dendritic Cells Internalize Vaccine Adjuvant after Intramuscular Injection. In *Cellular Immunology* 186 (1), pp. 18–27.
- Dworetzky; Cohen; Mullin (2003): Prometheus in Gloucestershire: Edward Jenner, 1749-1823. In *Journal of Allergy and Clinical Immunology* 112 (4), pp. 810–814.
- Ehreth (2003): The global value of vaccination. In *Vaccine* 21 (7–8), pp. 596–600.
- European Directorate for the Quality of Medicines (Ed.) (2013): European Pharmacopoeia. 7.4. EDQM.
- Fairbairn (1958): Trehalose and Glucose in Helminths and other Invertebrates. In *Canadian Journal of Zoology* 36 (5), pp. 787–795.

- Fanali; Di Masi; Trezza; Marino; Fasano; Ascenzi (2012): Human serum albumin: From bench to bedside. In *Molecular Aspects of Medicine* 33 (3), pp. 209–290.
- Fan; Yan; Xu; Ni (2012): Formation mechanism of monodisperse, low molecular weight chitosan nanoparticles by ionic gelation technique. In *Colloids and Surfaces B: Biointerfaces* 90 (0), pp. 21–27.
- FDA (2002): Guidance for Industry Nasal Spray and Inhalation Solution, Suspension, and Spray Drug Products — Chemistry, Manufacturing, and Controls Documentation.
- Fotakis; Timbrell (2006): In vitro cytotoxicity assays: Comparison of LDH, neutral red, MTT and protein assay in hepatoma cell lines following exposure to cadmium chloride. In *Toxicology Letters* 160 (2), pp. 171–177.
- Franks (1998): Freeze-drying of bioproducts: putting principles into practice. In *European Journal of Pharmaceutics and Biopharmaceutics* 45 (3), pp. 221–229.
- Fujihashi; Kiyono (2009): Mucosal immunosenescence: new developments and vaccines to control infectious diseases. In *Trends in Immunology* 30 (7), pp. 334–343.
- Fujihashi; Koga; van Ginkel; Hagiwara; McGhee (2002): A dilemma for mucosal vaccination: efficacy versus toxicity using enterotoxin-based adjuvants. In *Vaccine* 20 (19–20), pp. 2431–2438.
- Gan; Wang (2007): Chitosan nanoparticle as protein delivery carrier—Systematic examination of fabrication conditions for efficient loading and release. In *Colloids and Surfaces B: Biointerfaces* 59 (1), pp. 24–34.
- Gaumet; Vargas; Gurny; Delie (2008): Nanoparticles for drug delivery: The need for precision in reporting particle size parameters. In *European Journal of Pharmaceutics and Biopharmaceutics* 69 (1), pp. 1–9.
- Geldart; Abdullah; Hassanpour; Nwoke; Wouters (2006): Characterization of powder flowability using measurement of angle of repose. In *China Particuology* 4 (3–4), pp. 104–107.
- Geller (2005): Comparing Clinical Features of the Nebulizer, Metered-Dose Inhaler, and Dry Powder Inhaler. In *Respiratory Care* 50 (10), pp. 1313–1322.
- Gettins (2002): Serpin Structure, Mechanism, and Function. In *Chemical Reviews* 102 (12), pp. 4751–4804.
- Glenny; Pope; Waddington; Wallace (1926): Immunological notes. XVII–XXIV. In *The Journal of Pathology and Bacteriology* 29 (1), pp. 31–40.
- Gordon; Moses; Silver; Flier; Carey (1985): Nasal absorption of insulin: enhancement by hydrophobic bile salts. In *Proc. Natl. Acad. Sci. U.S.A.* 82 (21), pp. 7419–7423.
- Gréco (2001): Key drivers behind the development of global vaccine market. In *Vaccine* 19 (13–14), pp. 1606–1610.
- Grenha; Grainger; Dailey; Seijo; Martin; Remuñán-López; Forbes (2007): Chitosan nanoparticles are compatible with respiratory epithelial cells in vitro. In *European Journal of Pharmaceutical Sciences* 31 (2), pp. 73–84.

- Griffin; Lynch M. J. (Eds.) (1972): Polyhydric alcohols. CRC Handbook of Food Additives. 2nd ed. 2 volumes. Cleveland: CRC Press (CRC Handbook of Food Additives, 1).
- Groot; Scott (2007): Immunogenicity of protein therapeutics. In *Trends in Immunology* 28 (11), pp. 482–490.
- Gross; Sepkowitz (1998): The myth of the medical breakthrough: Smallpox, vaccination, and Jenner reconsidered. In *International Journal of Infectious Diseases* 3 (1), pp. 54–60.
- Guilmette; Gagliano (1994): Construction of a Model of Human Nasal Airways Using In Vivo Morphometric Data. In *Annals of Occupational Hygiene* 38 (inhaled particles VII), pp. 69–75.
- Hagesaether (2011): Permeation modulating properties of natural polymers – Effect of molecular weight and mucus. In *International Journal of Pharmaceutics* 409 (1–2), pp. 150–155.
- Hänninen; Braakhuis; Heath; Harrison (2001): Mucosal Antigen Primes Diabetogenic Cytotoxic T-Lymphocytes Regardless of Dose or Delivery Route. In *Diabetes* 50 (4), pp. 771–775.
- Hansen; Nielsen; Berg (1989): Re-examination and further development of a precise and rapid dye method for measuring cell growth/cell kill. In *Journal of Immunological Methods* 119 (2), pp. 203–210.
- Helanto; Aarnikunnas; Weymarn; Airaksinen; Palva; Leisola (2005): Improved mannitol production by a random mutant of *Leuconostoc pseudomesenteroides*. In *Journal of Biotechnology* 116 (3), pp. 283–294.
- Henderson (2011): The eradication of smallpox – An overview of the past, present, and future. In *Vaccine* 29S (4), pp. D7.
- Herzenberg; Parks; Sahaf; Perez; Roederer; Herzenberg (2002): The History and Future of the Fluorescence Activated Cell Sorter and Flow Cytometry: A View from Stanford. In *Clinical Chemistry* 48 (10), pp. 1819–1827.
- Hickey; Martonen (1993): Behavior of Hygroscopic Pharmaceutical Aerosols and the Influence of Hydrophobic Additives. In *Pharmaceutical Research* 10 (1), pp. 1–7.
- Hirai; Odani; Nakajima (1991): Determination of degree of deacetylation of chitosan by ¹H NMR spectroscopy. In *Polymer Bulletin* 26 (1), pp. 87–94.
- Hirayama; Akashi; Furuya; Fukuhara (1990): Rapid confirmation and revision of the primary structure of bovine serum albumin by ESIMS and Frit-FAB LC/MS. In *Biochemical and Biophysical Research Communications* 173 (2), pp. 639–646.
- Holt; Schon-Hegrad; McMenamin (1990): Dendritic Cells in the Respiratory Tract. In *International Reviews of Immunology* 6 (2-3), pp. 139–149.
- Huang; Garmise; Crowder; Mar; Hwang; Hickey et al. (2004a): A novel dry powder influenza vaccine and intranasal delivery technology: induction of systemic and mucosal immune responses in rats. In *Vaccine* 23 (6), pp. 794–801.

- Huang; Khor; Lim (2004b): Uptake and Cytotoxicity of Chitosan Molecules and Nanoparticles: Effects of Molecular Weight and Degree of Deacetylation. In *Pharmaceutical Research* 21 (2), pp. 344–353.
- Huang; Kim; Dass (2004c): Probing three-dimensional structure of bovine serum albumin by chemical cross-linking and mass spectrometry. In *Journal of the American Society for Mass Spectrometry* 15 (8), pp. 1237-1247.
- Huang; Ma; Khor; Lim (2002): Uptake of FITC-Chitosan Nanoparticles by A549 Cells. In *Pharmaceutical Research* 19 (10), pp. 1488–1494.
- Hughes; Allen; Dorato; Wolff (1993): Effect of Delivery Devices on Nasal Deposition and Mucociliary Clearance in Rhesus Monkeys. In *Aerosol Science and Technology* 18 (3), pp. 241–249.
- Huntington; Stein (2001): Structure and properties of ovalbumin. In *Elucidation of Allergens in Food* 756 (1–2), pp. 189–198.
- Illum (1998): Chitosan and Its Use as a Pharmaceutical Excipient. In *Pharmaceutical Research* 15 (9), pp. 1326–1331.
- Illum; Jabbal-Gill; Hinchcliffe; Fisher; Davis (2001): Chitosan as a novel nasal delivery system for vaccines. In *Advanced Drug Delivery Reviews* 51 (1-3), pp. 81–96.
- Islam; Gladki (2008): Dry powder inhalers (DPIs)—A review of device reliability and innovation. In *International Journal of Pharmaceutics* 360 (1–2), pp. 1–11.
- Janeway (2002): Immunologie. 5th ed. Heidelberg: Spektrum Akademischer Verlag.
- Jung; Kamm; Breitenbach; Kaiserling; Xiao; Kissel (2000): Biodegradable nanoparticles for oral delivery of peptides: is there a role for polymers to affect mucosal uptake? In *European Journal of Pharmaceutics and Biopharmaceutics* 50 (1), pp. 147–160.
- Kac (1947): Random Walk and the Theory of Brownian Motion. In *The American Mathematical Monthly* 54 (7), pp. 369–391.
- Kadoya; Fujii; Izutsu; Yonemochi; Terada; Yomota; Kawanishi (2010): Freeze-drying of proteins with glass-forming oligosaccharide-derived sugar alcohols. In *International Journal of Pharmaceutics* 389 (1–2), pp. 107–113.
- Kang; Cho; Yoo (2009): Application of chitosan microspheres for nasal delivery of vaccines. In *Biotechnology Advances* 27 (6), pp. 857–865.
- Karlsson; Gustafsson; Cronholm; Möller (2009): Size-dependent toxicity of metal oxide particles—A comparison between nano- and micrometer size. In *Toxicology Letters* 188 (2), pp. 112–118.
- Kelly; Jess; Price (2005): How to study proteins by circular dichroism. In *Biochimica et Biophysica Acta (BBA) - Proteins and Proteomics* 1751 (2), pp. 119–139.
- Kieny; Excler; Girard (2004): Research and Development of New Vaccines Against Infectious Diseases. In *American Journal of Public Health* 94 (11), pp. 1931–1935.

- Kiyono; Fukuyama (2004): NALT- versus PEYER'S-patch-mediated mucosal immunity. In *Nature Reviews Immunology* 4 (9), pp. 699–710.
- Kotzé; Thanou; Lueßen; Boer; Verhoef; Junginger (1999): Effect of the degree of quaternization of N-trimethyl chitosan chloride on the permeability of intestinal epithelial cells (Caco-2). In *European Journal of Pharmaceutics and Biopharmaceutics* 47 (3), pp. 269–274.
- Kreuter (1991): Peroral administration of nanoparticles. In *Advanced Drug Delivery Reviews* 7 (1), pp. 71–86.
- Kumar; Majeti (2000): A review of chitin and chitosan applications. In *Reactive and Functional Polymers* 46 (1), pp. 1–27.
- Lambrecht; Kool; Am Willart; Hammad (2009): Mechanism of action of clinically approved adjuvants. In *Current Opinion in Immunology* 21, pp. 23–29.
- Langer; Balthasar; Vogel; Dinauer; Briesen; Schubert (2003): Optimization of the preparation process for human serum albumin (HSA) nanoparticles. In *International Journal of Pharmaceutics* 257 (1–2), pp. 169–180.
- Larsen; Hansen; Thygesen; Begtrup; Poulsen; Nielsen (2001): Adjuvant and immuno-suppressive effect of six monophthalates in a subcutaneous injection model with BALB/c mice. In *Toxicology* 169 (1), pp. 37–51.
- Larson; Cooper; Eskola; Katz; Ratzan (2011): Addressing the vaccine confidence gap. In *The Lancet* 378 (9790), pp. 526–535.
- Lavertu; Xia; Serreqi; Berrada; Rodrigues; Wang et al. (2003): A validated ¹H NMR method for the determination of the degree of deacetylation of chitosan. In *Journal of Pharmaceutical and Biomedical Analysis* 32 (6), pp. 1149–1158.
- Lawson; Norton; Clements (2011): Defending the mucosa: adjuvant and carrier formulations for mucosal immunity. In *Current Opinion in Immunology* 23, pp. 414–420.
- Le Roux (2012): Purification de la chitine par hydrolyse enzymatique à partir de coproduits de crevette *Penaeus vannamei*. Caractérisations des produits et optimisation du procédé. Thèse de Doctorat. Université de Nantes, Nantes.
- Lee (2002): Spray-Drying of Proteins. In: Rational Design of Stable Protein, Pharmaceutical Biotechnology, Vol. 13, pp. 135–158.
- Lenz (1834): Ueber die Bestimmung der Richtung der durch elektrodynamische Vertheilung erregten galvanischen Ströme. In *Annalen der Physik* 107 (31), pp. 483–494.
- Leuenberger (2002): Martin Physikalische Pharmazie. Pharmazeutisch angewandte physikalische-chemische Grundlagen. 4th ed. Stuttgart: Wissenschaftliche Verlagsgesellschaft mbH Stuttgart.
- LiCalsi; Christensen; Bennett; Phillips; Witham (1999): Dry powder inhalation as a potential delivery method for vaccines. In *Vaccine* 17 (13–14), pp. 1796–1803.
- Li; Dunn; Grandmaison; Goosen (1992): Applications and Properties of Chitosan. In *Journal of Bioactive and Compatible Polymers* 7 (4), pp. 370–397.

- Li; Inthavong; Tu (2012): Particle inhalation and deposition in a human nasal cavity from the external surrounding environment. In *Building and Environment* 47, pp. 32–39.
- Lindblad (2004): Aluminium adjuvants—in retrospect and prospect. In *Vaccine* 22 (27–28), pp. 3658–3668.
- Maa; Costantino; Nguyen; Hsu (1997): The Effect of Operating and Formulation Variables on the Morphology of Spray-Dried Protein Particles. In *Pharmaceutical Development and Technology* 2 (3), pp. 213–223.
- Makkee; Kieboom; van Bekkum (1985): Production Methods of D-Mannitol. In *Starch/Stärke* 37 (4), pp. 136–141.
- Malvern Instruments (2003): Zetasizer Nano Series. User Manual.
- Malvern Instruments (2011): Dynamic Light Scattering common terms defined. Edited by Malvern Instruments. Worcestershire, UK.
- Mao; Augsten; Mäder; Kissel (2007): Characterization of chitosan and its derivatives using asymmetrical flow field-flow-fractionation: A comparison with traditional methods. In *Journal of Pharmaceutical and Biomedical Analysis* 45 (5), pp. 736–741.
- Marcinkiewicz; Polewska; Knapczyk (1991): Immunoadjuvant properties of chitosan. In *Arch Immunol Ther Exp (Warsz)* 39 (1-2), pp. 127–132.
- Martin; Thongborisute; Takeuchi; Yamamoto; Kawashima; Alpar (2005): Cholesterol–bile salt vesicles as potential delivery vehicles for drug and vaccine delivery. In *International Journal of Pharmaceutics* 298 (2), pp. 339–343.
- Matthias; Robertson; Garrison; Newland; Nelson (2007): Freezing temperatures in the vaccine cold chain: A systematic literature review. In *Vaccine* 25 (20), pp. 3980–3986.
- Maury; Murphy; Kumar; Mauerer; Lee (2005): Spray-drying of proteins: effects of sorbitol and trehalose on aggregation and FT-IR amide I spectrum of an immunoglobulin G. In *European Journal of Pharmaceutics and Biopharmaceutics* 59 (2), pp. 251–261.
- Mausser; Pitman; Witt; Fernandez; Zurcher; Kung et al. (1993): Inhibitory Effect of the TRFK-5 Anti-IL-5 Antibody in a Guinea Pig Model of Asthma. In *American Review of Respiratory Disease* 148, pp. 1623–1627.
- McNeela; O'Connor; Jabbal-Gill; Illum; Davis; Pizza et al. (2000): A mucosal vaccine against diphtheria: formulation of cross reacting material (CRM197) of diphtheria toxin with chitosan enhances local and systemic antibody and Th2 responses following nasal delivery. In *Vaccine* 19 (9–10), pp. 1188–1198.
- McReynolds; O'Malley; Nisbet; Fothergill; Givol; Fields et al. (1978): Sequence of chicken ovalbumin mRNA. In *Nature* 273 (5665), pp. 723–728.
- Miletic; Schiffman; Miletic; Sattely-Miller (1996): Salivary IgA secretion rate in young and elderly persons. In *Physiology & Behavior* 60 (1), pp. 243–248.
- Mine (1995): Recent advances in the understanding of egg white protein functionality. In *Trends in Food Science & Technology* 6 (7), pp. 225–232.

- Mönckedieck (2013): In vitro and in vivo characterisation of particulate formulations for dry powder nasal vaccines. Diploma Thesis. Martin-Luther-University, Halle-Wittenberg.
- Mosmann (1983): Rapid colorimetric assay for cellular growth and survival: Application to proliferation and cytotoxicity assays. In *Journal of Immunological Methods* 65 (1–2), pp. 55–63.
- Murayama; Tomida (2004): Heat-Induced Secondary Structure and Conformation Change of Bovine Serum Albumin Investigated by Fourier Transform Infrared Spectroscopy. In *Biochemistry* 43 (36), pp. 11526–11532.
- Neutra; Kozlowski (2006): Mucosal vaccines: the promise and the challenge. In *Nature Reviews Immunology* 6 (2), pp. 148–158.
- Nguyen; Hisiger; Jolicoeur; Winnik; Buschmann (2009a): Fractionation and characterization of chitosan by analytical SEC and ^1H NMR after semi-preparative SEC. In *Carbohydrate Polymers* 75 (4), pp. 636–645.
- Nguyen; Winnik; Buschmann (2009b): Improved reproducibility in the determination of the molecular weight of chitosan by analytical size exclusion chromatography. In *Carbohydrate Polymers* 75 (3), pp. 528–533.
- Nisbet; Saundry; Moir; Fothergill; Fothergill (1981): The Complete Amino-Acid Sequence of Hen Ovalbumin. In *European Journal of Biochemistry* 115 (2), pp. 335–345.
- Okada; Sasaki; Ishii; Aoki; Yasuda; Nishioka et al. (1997): Intranasal immunization of a DNA vaccine with IL-12 γ and granulocyte-macrophage colony-stimulating factor (GM-CSF)-expressing plasmids in liposomes induces strong mucosal and cell-mediated immune responses against HIV-1 antigens. In *The Journal of Immunology* 159 (7), pp. 3638–3647.
- Omer; Salmon; Orenstein; deHart; Halsey (2009): Vaccine Refusal, Mandatory Immunization, and the Risks of Vaccine-Preventable Diseases. In *New England Journal of Medicine* 360 (19), pp. 1981–1988.
- Peng; Hidajat; Uddin (2004): Adsorption of bovine serum albumin on nanosized magnetic particles. In *Journal of Colloid and Interface Science* 271 (2), pp. 277–283.
- Pettini; Ciabattini; Pozzi; Medaglini (2009): Adoptive transfer of transgenic T cells to study mucosal adjuvants. In *Methods* 49 (4), pp. 340–345.
- Pillai; Paul; Sharma (2009): Chitin and chitosan polymers: Chemistry, solubility and fiber formation. In *Progress in Polymer Science* 34 (7), pp. 641–678.
- Prego; García; Torres; Alonso (2005): Transmucosal macromolecular drug delivery. In *Journal of Controlled Release* 101 (1–3), pp. 151–162.
- Qin; Li; Xiao; Liu; Zhu; Du (2006): Water-solubility of chitosan and its antimicrobial activity. In *Carbohydrate Polymers* 63 (3), pp. 367–374.
- Qun; Ajun (2006): Effects of molecular weight, degree of acetylation and ionic strength on surface tension of chitosan in dilute solution. In *Carbohydrate Polymers* 64 (1), pp. 29–36.

- Rauw; Gardin; Palya; Anbari; Gonze; Lemaire et al. (2010): The positive adjuvant effect of chitosan on antigen-specific cell-mediated immunity after chickens vaccination with live Newcastle disease vaccine. In *Veterinary Immunology and Immunopathology* 134 (3–4), pp. 249–258.
- Ribeiro; Schijns (2010): Immunology of Vaccine Adjuvants. In Gwyn Davies (Ed.): *Vaccine Adjuvants*, vol. 626: Humana Press (Methods in Molecular Biology), pp. 1–14.
- Richards; Krakowka; Dexter; Schmid; Wolterbeek; Waalkens-Berendsen et al. (2002): Trehalose: a review of properties, history of use and human tolerance, and results of multiple safety studies. In *Food and Chemical Toxicology* 40 (7), pp. 871–898.
- Riedel (2005): Edward Jenner and the history of smallpox and vaccination. In *BUMC Proceedings* 18, pp. 21–25.
- Rinaudo (2006): Chitin and chitosan: Properties and applications. In *Progress in Polymer Science* 31 (7), pp. 603–632.
- Rodbard; Chrambach (1970): Unified Theory for Gel Electrophoresis and Gel Filtration. In *Proceedings of the National Academy of Sciences* 65 (4), pp. 970–977.
- Rothschild; Oratz; Schreiber (1988): Serum albumin. In *Hepatology* 8 (2), pp. 385–401.
- Rücker; Neugebauer; Willems (2001): *Instrumentelle pharmazeutische Analytik*. 3rd ed. Stuttgart: Wissenschaftliche Verlagsgesellschaft mbH Stuttgart.
- Sakula (1982): Robert Koch: centenary of the discovery of the tubercle bacillus, 1882. In *Thorax* 37 (4), pp. 246–251.
- Saluja; Amorij; Kapteyn; Boer; Frijlink; Hinrichs (2010): A comparison between spray drying and spray freeze drying to produce an influenza subunit vaccine powder for inhalation. In *Journal of Controlled Release* 144 (2), pp. 127–133.
- Schuchat (2011): Human Vaccines and Their Importance to Public Health. In *Procedia in Vaccinology* 5, pp. 120–126.
- Shah; Dickens; Ward; Banaszek; George; Horodnik (2013): Design of Experiments to Optimize an In Vitro Cast to Predict Human Nasal Drug Deposition. In *Journal of aerosol medicine and pulmonary drug delivery* 28 (0).
- Sharma; Mukkur; Benson; Chen (2009): Pharmaceutical aspects of intranasal delivery of vaccines using particulate systems. In *Journal of Pharmaceutical Sciences* 98 (3), pp. 812–843.
- Shinichiro; Takatsuka; Hiroyuki (1981): Mechanisms for the enhancement of the nasal absorption of insulin by surfactants. In *International Journal of Pharmaceutics* 9 (2), pp. 173–184.
- Singh; O'Hagan (1999): Advances in vaccine adjuvants. In *Nature Biotechnology* 17 (11), pp. 1075–1081.
- Singh; O'Hagan (2002): Recent Advances in Vaccine Adjuvants. In *Pharmaceutical Research* 19 (6), pp. 715–728.

- Slater; Sawyer; Sträuli (1963): Studies on succinate-tetrazolium reductase systems: III. Points of coupling of four different tetrazolium salts III. Points of coupling of four different tetrazolium salts. In *Biochimica et Biophysica Acta* 77 (0), pp. 383–393.
- Slütter; Hagens; Jiskoot (2008): Rational design of nasal vaccines. In *Journal of Drug Targeting* 16 (1), pp. 1–17.
- Smith; Back (1965): Studies on ovalbumin. II. The formation and properties of S-Ovalbumin, a more stable form of Ovalbumin. In *Australian Journal of Biological Sciences* (18), pp. 365–377.
- Smith; Dornish; Wood (2005): Involvement of protein kinase C in chitosan glutamate-mediated tight junction disruption. In *Biomaterials* 26 (16), pp. 3269–3276.
- Smith; Krohn; Hermanson; Mallia; Gartner; Provenzano et al. (1985): Measurement of protein using bicinchoninic acid. In *Analytical Biochemistry* 150 (1), pp. 76–85.
- Soetaert (1990): Production of mannitol with *Leuconostoc mesenteroides*. In *Mededelingen van de Faculteit Landbouwwetenschappen, Rijksuniversiteit Gent 1990 Vol. 55 No. 55* (4), pp. 1549–1552.
- Sreerama; Woody (2000): Estimation of Protein Secondary Structure from Circular Dichroism Spectra: Comparison of CONTIN, SELCON, and CDSSTR Methods with an Expanded Reference Set. In *Analytical Biochemistry* 287 (2), pp. 252–260.
- Sreerama; Woody (2004): On the analysis of membrane protein circular dichroism spectra. In *Protein Science* 13 (1), pp. 100–112.
- Stanek (1957): Optical Rotation of the Isomeric Trehaloses. In *Nature* 179 (4550), pp. 97–98.
- Stentebjerg-Andersen; Nøtlevsen; Brodin; Nielsen (2011): Calu-3 cells grown under AIC and LCC conditions: Implications for dipeptide uptake and transepithelial transport of substances. In *European Journal of Pharmaceutics and Biopharmaceutics* 78 (1), pp. 19–26.
- Streefland; Chowdhury; Ramos-Jimenez (1999): Patterns of vaccination acceptance. In *Social Science & Medicine* 49 (12), pp. 1705–1716.
- Szmuk; Szmuk; Ezri (2005): Use of needle-free injection systems to alleviate needle phobia and pain at injection. In *Expert Review of Pharmacoeconomics and Outcomes Research* 5 (4), pp. 467–477.
- Tabata; Inoue; Ikada (1996): Size effect on systemic and mucosal immune responses induced by oral administration of biodegradable microspheres. In *Vaccine* 14 (17–18), pp. 1677–1685.
- Takeuchi; Thongborisute; Matsui; Sugihara; Yamamoto; Kawashima (2005): Novel mucoadhesion tests for polymers and polymer-coated particles to design optimal mucoadhesive drug delivery systems. In *Advanced Drug Delivery Reviews* 57 (11), pp. 1583–1594.

- Tay; Das; Stewart (2010): Magnesium stearate increases salbutamol sulphate dispersion: What is the mechanism? In *International Journal of Pharmaceutics* 383 (1–2), pp. 62–69.
- Thews; Mutschler; Vaupel (1999): Anatomie, Physiologie, Pathophysiologie des Menschen. 5th ed. Stuttgart: Wissenschaftliche Verlagsgesellschaft mbH Stuttgart.
- Thomas (1987): The determination of log normal particle size distributions by dynamic light scattering. In *Journal of Colloid and Interface Science* 117 (1), pp. 187–192.
- Tomljenovic; Shaw (2011): Aluminum Vaccine Adjuvants: Are they Safe? In *Current Medicinal Chemistry* 18 (17), pp. 2630–2637.
- Trivedi; Valerio; Slater (2003): Endotoxin content of standardized allergen vaccines. In *Journal of Allergy and Clinical Immunology* 111 (4), pp. 777–783.
- Trows (2012): Pulverformulierungen für die nasale Vakzinierung. Dissertation. Kiel University, Kiel.
- Twining (1984): Fluorescein isothiocyanate-labeled casein assay for proteolytic enzymes. In *Analytical Biochemistry* 143 (1), pp. 30–34.
- United States Pharmacopeial Convention (Ed.): USP–NF 36. United States Pharmacopeial Convention. Rockville, Maryland, USA.
- van den Broeck; Derore; Simoens (2006): Anatomy and nomenclature of murine lymph nodes: Descriptive study and nomenclatory standardization in BALB/cAnNCrl mice. In *Journal of Immunological Methods* 312 (1–2), pp. 12–19.
- van der Lubben; Verhoef; Borchard; Junginger (2001): Chitosan for mucosal vaccination. In *Advanced Drug Delivery Reviews* 52 (2), pp. 139–144.
- Vandenberg; Drolet; Scott; La Noüe (2001): Factors affecting protein release from alginate–chitosan coacervate microcapsules during production and gastric/intestinal simulation. In *Journal of Controlled Release* 77 (3), pp. 297–307.
- Vila; Sánchez; Tobío; Calvo; Alonso (2002): Design of biodegradable particles for protein delivery. In *Journal of Controlled Release* 78 (1–3), pp. 15–24.
- Vilella; Bayas; Diaz; Guinovart; Diez; Simó et al. (2004): The role of mobile phones in improving vaccination rates in travelers. In *Preventive Medicine* 38 (4), pp. 503–509.
- Vllasaliu; Exposito-Harris; Heras; Casettari; Garnett; Illum; Stolnik (2010): Tight junction modulation by chitosan nanoparticles: Comparison with chitosan solution. In *International Journal of Pharmaceutics* 400 (1–2), pp. 183–193.
- Vollmar; Zündorf; Dingermann (2013): Immunologie. Grundlagen und Wirkstoffe. 2nd ed. Stuttgart: Wissenschaftliche Verlagsgesellschaft mbH Stuttgart.
- Wang; Huang; Nakamura; Burchard; Hallett (2005): Molecular characterisation of soybean polysaccharides: an approach by size exclusion chromatography, dynamic and static light scattering methods. In *Carbohydrate Research* 340 (17), pp. 2637–2644.

- Wheatley; Dent; Wheeldon; Smith (1988): Nasal drug delivery: An in vitro characterization of transepithelial electrical properties and fluxes in the presence or absence of enhancers. In *Journal of Controlled Release* 8 (2), pp. 167–177.
- Wilson-Welder; Torres; Kipper; Mallapragada; Wannemuehler; Narasimhan (2009): Vaccine adjuvants: Current challenges and future approaches. In *Journal of Pharmaceutical Sciences* 98 (4), pp. 1278–1316.
- Winton; Wan; Cannell; Gruenert; Thompson; Garrod et al. (1998): Cell lines of pulmonary and non-pulmonary origin as tools to study the effects of house dust mite proteinases on the regulation of epithelial permeability. In *Clinical & Experimental Allergy* 28 (10), pp. 1273–1285.
- Wisselink; Weusthuis; Eggink; Hugenholtz; Grobбен (2002): Mannitol production by lactic acid bacteria: a review. In *International Dairy Journal* 12 (2–3), pp. 151–161.
- Witt; Röthele (1995): Laser Diffraction - unlimited? Edited by Sympatec GmbH. System-Partikel-Technik. Clausthal-Zellerfeld.
- Wolff; Flemming; Schmitz; Gröger; Müller-Goymann (2008): Protection of aluminum hydroxide during lyophilisation as an adjuvant for freeze-dried vaccines. In *Colloids and Surfaces A: Physicochemical and Engineering Aspects* 330 (2–3), pp. 116–126.
- Wu (2010): Correlations between the Rayleigh ratio and the wavelength for toluene and benzene. In *Chemical Physics* 367 (1), pp. 44–47.
- Xu; Du (2003): Effect of molecular structure of chitosan on protein delivery properties of chitosan nanoparticles. In *International Journal of Pharmaceutics* 250 (1), pp. 215–226.
- Yang; Hu; Fan; Shen (2008): Study on the binding of luteolin to bovine serum albumin. In *Spectrochimica Acta Part A: Molecular and Biomolecular Spectroscopy* 69 (2), pp. 432–436.
- Yeh; Hsu; Tseng; Lee; Sonjae; Ho; Sung (2011): Mechanism and consequence of chitosan-mediated reversible epithelial tight junction opening. In *Biomaterials* 32 (26), pp. 6164–6173.
- Zaharoff; Rogers; Hance; Schlom; Greiner (2007): Chitosan solution enhances both humoral and cell-mediated immune responses to subcutaneous vaccination. In *Vaccine* 25 (11), pp. 2085–2094.
- Zamankhan; Ahmadi; Wang; Hopke; Cheng; Su; Leonard (2006): Airflow and Deposition of Nano-Particles in a Human Nasal Cavity. In *Aerosol Science and Technology* 40 (6), pp. 463–476.
- Zeeman (1897): On the Influence of Magnetism on the Nature of the Light Emitted by a Substance. In *The Astrophysical Journal* 5, p. 332.

Hiermit erkläre ich gemäß §8 der Promotionsordnung der Mathematisch-Naturwissenschaftlichen Fakultät und Technischen Fakultät der Christian-Albrechts-Universität zu Kiel, dass ich die vorliegende Arbeit, abgesehen von der Beratung durch meinen Betreuer, selbstständig und ohne fremde Hilfe verfasst habe. Ich habe keine anderen als die angegebenen Quellen benutzt und die den benutzten Werken wörtlich oder inhaltlich entnommenen Stellen als solche kenntlich gemacht. Die Arbeit ist unter Einhaltung der Regeln guter wissenschaftlicher Praxis der Deutschen Forschungsgemeinschaft entstanden und wurde bei keiner anderen Universität zur Begutachtung eingereicht.

Simon-David Lennart Buske

Lebenslauf

Persönliche Daten

Name	Simon-David Lennart Buske
Geburtsdatum	22.11.1983
Geburtsort	Hamburg, Deutschland
Staatsangehörigkeit	deutsch

Schulbildung

1990-1994	Carl-Götze-Grundschule, Hamburg, Groß Borstel
1994-2003	Heilwig Gymnasium, Hamburg, Alsterdorf
2003	Allgemeine Hochschulreife

Hochschulstudium

10/2004 – 10/2008	Studium der Pharmazie Universität Hamburg
08/2006	1. Abschnitt der pharmazeutischen Prüfung
10/2008	2. Abschnitt der pharmazeutischen Prüfung

Praktische Ausbildung

11/2008 – 04/2009	Pfeil-Apotheke, Hamburg, Eimsbüttel
05/2009 – 10/2009	Beiersdorf AG, Hamburg, Eimsbüttel
12/2009	3. Abschnitt der pharmazeutischen Prüfung

Berufliche Tätigkeit

02/2010 – 03/2010	Wissenschaftlicher Mitarbeiter, Pharmatech GmbH, Kiel
03/2010 – 03/2014	Wissenschaftlicher Mitarbeiter am pharmazeutischen Institut der Christian- Albrechts-Universität zu Kiel.

Zum Abschluss möchte ich mich ganz herzlich bei meinem Doktorvater Herrn Prof. Hartwig Steckel und Frau Dr. Regina Scherließ für die Möglichkeit bedanken, dieses spannende und hoch aktuelle Thema, von Ihnen begleitet, dennoch frei und selbstständig bearbeitet haben zu dürfen.

Ich danke den Firmen RPC Formatech, Aptar Pharma und Boehringer Ingelheim für die Zurverfügungstellung der verwendeten nasalen Applikationshilfen beziehungsweise der beiden Nasenmodelle.

Desweiteren bedanke ich mich beim Organisationskomitee von NanoFormualtion 2011 und speziell bei Frau Dr. Helen Dutton (Universität Manchester) für die Prämierung eines Teils meiner Arbeit und dem damit verbundenen Reisestipendium für die oben genannte Konferenz in Singapur.

Frau Dr. Sabrina Trows danke ich für die vielen Tipps und Ratschläge, die mir, besonders zu Anfang meiner Arbeit, sehr geholfen haben mich schnell in das komplexe Thema einzufinden und so einige zeitraubende Fehler zu vermeiden, sowie für das aufmerksame Korrekturlesen der vorliegenden Arbeit.

Weiterer Dank gilt,

Herrn Dr. Ulrich Girreser für die enorme Hilfe, die er mir bei den ^1H -NMR und MS Messungen war;

Frau Ronja Wittmann, Herrn Eike Cordts, sowie Herrn Lars Wagenseil, Frau Julia Janke und Frau Dr. Wean Sin Cheow (National University of Singapore) für die Hilfe bei verschiedensten Fragestellungen;

Herrn Rüdiger Small für das Anfertigen verschiedener Abbildungen für diese Arbeit;

allen Kollegen mit denen ich zusammen die Studentenpraktika betreuen durfte, sowie Herrn Ankur Ajmera und nochmal Frau Dr. Scherließ für das aufmerksame vorab lesen der Arbeit.